Covid-19 statement

The global Covid-19 pandemic led to the closure of my department for approximately 4 months, and as a result, my thesis work was disturbed. Once the department reopened, social distancing restrictions on the number of people allowed to be in the same room at any one time meant that for more than 8 months, I could only have access to the departmental facilities including the laboratory on a part-time basis. I wound up working remotely from home in France for close to a year. Furthermore, we had to spend a few extra hours each week planning out people's use of the facilities to ensure compliance with Covid 19 safety restrictions in place and share routine tasks to optimise time usage.

In an effort to continue generating results while working from home, I started the bioinformatic investigations described in chapter 5 of this thesis. In the process, I had to learn a variety of techniques I did not have any experience with, so that progress was slower than it would have been on the experimental work I was planning to do in the lab. A major part of the experimental work that I was unable to complete due to Covid19 disruptions is an untargeted transposon bulk mutant screen (RB-TnSeq), which I have provided further details on in the appendix of this thesis.

THESIS

INVESTIGATING THE EFFECTS OF TEMPERATURE ON BACTERIAL PATHOGENS OF COMMON BEAN

2023

Julianna Isabelle Olivia Piat,

Under the supervision of Gail M. Preston, Leighton Pritchard, Nick J. Kruger

Table of contents

Covid-19 statement 1

Table of contents 3

0.0 Abstract 11

Chapter 1: Literature review 12

1.1 Common bean is economically important 12

1.2 The plant immune system 13

1.3 Temperature affects plant immunity 15

1.4 Three major bacterial pathogens of common bean 17

1.5 Introducing plant-pathogenic *Pseudomonas* 18

1.6 Introducing *P. syringae* pv *syringae* 18

1.7 Introducing *P. savastanoi* pv *phaseolicola* 19

1.8 Introducing *Xanthomonas axonopodis* pv *phaseoli* 19

1.9 Optimal temperature for bacterial growth of the PSSC 20

1.10 Disease occurrence in the field 22

1.11 Temperature affects pathogenicity factors in plant pathogenic *Pseudomonas* 22

1.12 Phaseolotoxin: a key phytotoxin produced by Pspph 23

1.13 Phytotoxins produced by Pss 25

1.14 Plants and reactive oxygen species 27

1.15 Bacterial strategies to tolerate ROS *in planta* 30

1.16 Enzymes involved in ROS detoxification by the plant pathogens 32

1.17 ROS response also affects virulence factor expression 33

1.18 Links between oxidative stress tolerance and temperature responses in bacteria 34

1.19 Metabolic responses of bacteria 34

1.20 Objectives 35

Chapter 2: Materials and Methods 38

2.1 Bacterial cultures 38

2.2 Plant growth conditions 40

2.3 Apoplast extraction 41

2.4 Infection assay 42

2.5 Oxidative stress assay 43

2.6 Plate reader data analysis 44

2.7 Transcriptome sample preparation 44

2.8 Transcriptome RNA extraction 45

2.9 Transcriptome RNA sequencing 46

2.10 Transcriptome data analysis 49

2.11 Field strain isolation and *in planta* phenotyping 50

2.12 Field strains genome sequencing 52

2.13 Bioinformatics analysis 54

2.14 Oxired quantification of reactive oxygen species 57

2.15 Viability assay 58

2.16 Hydrogen peroxide challenge on bacteria in biofilms 59

2.17 Motility assay: swimming 59

2.18 Motility assay: Swarming 60

Chapter 3: Characterisation of the effects of temperature and oxidative stress on bacterial pathogens of common bean 62

3.1 Introduction 62

3.1.1 Temperature affects bacterial growth rate 63

3.1.2 Discrepancy between expected and observed effects of temperature on bacterial virulence 63

3.1.4 Bacterial motility is affected by temperature 64

3.1.5 Temperature affects expression of the T3SS 64

3.1.6 Phytotoxin production is temperature-regulated 65

3.1.7 Plant pathogens are exposed to ROS during infection 66

3.1.8 Exposure to ROS leads to bacterial starvation 66

3.1.9 Objectives 67

3.2 Materials and methods 68

3.3 Results 68

3.3.1 Temperature affects virulence differently for Pspph and Pss 68

3.3.2 Temperature affects oxidative stress differently for Pspph and Pss 71

3.3.3 H_2O_2 stability does not differ at 21°C and 28°C 74

3.3.4 H_2O_2 kills Pss and Pspph 78

3.3.5 The temperature oxidative stress cross-talk is affected by medium composition 82

3.4 Discussion 83

3.4.1 Temperature affects oxidative stress tolerance but not detoxification 84

3.4.2 Medium composition affects the cross-talk between oxidative stress tolerance and temperature 85

3.4.3 Pss is more resilient to oxidative stress than Pspph 85

3.4.4 Oxidative stress and temperature responses interact differently in Pss and Pspph 86

3.4.5 Pss may become more prevalent in fields in the future 86

3.5 Conclusion 87

Chapter 4: Gene expression changes in response to oxidative stress and temperature 89

4.1 Introduction 89

4.1.1 Two contrasting *Pseudomonas* phytopathogens of common bean 89

4.1.2 Gene expression is tightly regulated 90

4.1.3 Limitations of transcriptional regulation 92

4.1.4 Gene candidates for differences between Pss and Pspph 93

4.1.5 Gene candidates for differences in oxidative stress tolerance 94

4.1.6 Gene candidates for differences in temperature range 95

4.1.7 Aims and rationale 96

4.2 Results 97

4.2.1 Hydrogen peroxide treatment is responsible for more variation between transcriptomes than temperature 97

4.2.2 A mixture of up and downregulated genes in response to temperature 102

4.2.3 Genes involved in transmembrane transport, protein folding and metabolism biosynthesis are responsive to temperature and oxidative stress 102

4.2.4 Orthologues do not all share the same transcriptional responses to environmental cues..... 105

4.2.5 Phaseolotoxin genes are thermoregulated in Pspph 1302A 110

4.2.6 Catalase and superoxide dismutase genes are thermoregulated in both strains 110

4.2.7 Iron scavenging and metabolism 111

4.2.8 Master regulator RpoS is only differentially expressed in Pss B728a and not in Pspph 1302A 112

4.2.9 Expression of exopolysaccharides is temperature and oxidative stress responsive 112

4.3 Discussion..... 113

4.3.1 Differences in methodology may be responsible for differences in temperature responses with published datasets 113

4.3.2 Transcriptional responses of B728a to H_2O_2 are more consistent with published transcriptomic studies than 1302A 115

4.3.3 The role of iron in temperature and oxidative stress response remains elusive 117

4.3.4 Master regulator RpoS potentially plays different roles in Pss B728a and Pspph 1302A 120

4.3.5 Phaseolotoxin expression is thermoregulated in Pspph 1302A *in vitro* 121

4.3.6 Differences in catalase and superoxide dismutase expression may be involved in the cross-talk between temperature and oxidative stress responses in Pss and Pspph 122

4.3.7 Glucose metabolism is likely important for H_2O_2 tolerance 124

4.3.8 Avirulence factor HopAB1 is thermoregulated and may contribute to temperature-based differences in virulence 124

4.3.9 Motility is important for stress responses in both strains 125

4.3.10 Challenges in comparing the oxidative stress responses of different strains 126

4.4 Conclusions 127

Chapter 5: Bioinformatic investigations of the genetic and genomic basis of pathogenicity of common bean pathogens 128

5.1 Introduction 128

5.1.1 Taxonomic changes in the plant-pathogenic *Pseudomonas* 128

5.1.2 Defining pathogenicity 129

5.1.3 The role of T3SS effectors 130

5.1.4 Effector set determines the race structure of Pspph 130

5.1.5 The ever-changing effector nomenclature 131

5.1.6 Approaches to predict effector sets 132

5.1.7 Beyond pathogenicity 133

5.1.8 Aims and objectives 134

5.2 Results 135

5.2.1 Twenty-four newly sequenced Pspph genomes 135

5.2.2 262 *Pseudomonas savastanoi* candidates genomes 136

5.2.3 *Pseudomonas savastanoi* is a monophyletic clade 138

5.2.4 Phylogenetic structure dependence 139

5.2.5 Effector nomenclature in NCBI is inconsistent and unreliable 143

5.2.6 Linking the genome to the phenotype 147

5.3 Discussion 150

5.3.1 *Pseudomonas* classification is constantly evolving 150

5.3.2 Refining bioinformatic approaches to T3SS effector identification 151

5.3.3 Multiple independent evolutions of race 6 152

5.3.4 Thermoregulated and Oxidative stress responsive T3SS effectors 153

5.3.5 AvrB4 may be accessory to Pspph virulence 154

5.3.6 HopF1 and HopF3 are required for race 1 phenotype 154

5.3.7 Vertical transmission is more important in determining race structure of Pspph than horizontal transmission 155

5.4 Conclusions 156

6.0 General discussion 157

7.0 Acknowledgments 160

8.0 References 161

Supplementary material 176

Appendix 245

RB-TnSeq Optimisation 245

Introduction 245

Background 245

Protocol 247

Optimisation and discussion 257

Appendix references 259

0.0 Abstract

Common bean is a staple crop throughout the World, but production is threatened by a number of pathogens. Two major bacterial pathogens of common bean, *Pseudomonas savastanoi* pv. *phaseolicola* (Pspph) and *P. syringae* pv. *syringae* (Pss) currently infect bean fields in South-Africa. However, Pss incidence is higher at warmer temperatures whilst Pspph incidence is higher at cooler temperature, suggesting that temperature affects bacterial virulence. We were able to successfully replicate this *in vivo* in controlled conditions and found that temperature indeed affects Pss and Pspph differentially. Pss is more virulent at 28°C while Pspph is more virulent at 21°C. Interestingly, Pss is also more H_2O_2 tolerant at 28°C than at 21°C and Pspph is more tolerant at 21°C *in vitro*. We established a transcriptomic screen to determine which genes may be involved in the three-way interaction between temperature, oxidative stress response and virulence in Pss and Pspph. In doing so, we identified some key candidate genes for future work, including some type 3 secretion system effectors. Furthermore, we generated 24 new genome sequences for Pspph, confirmed that this pathovar is monophyletic, and built a pipeline to determine the canonical set of effectors. Altogether, this thesis paves the way to an improved understanding of the effects of abiotic environmental conditions on bacterial pathogenesis, in particular temperature, an understudied factor in plant pathology.

Chapter 1: Literature review

Beans are a major crop worldwide and among the most important sources of protein in many parts of Africa, in particular for subsistence farmers. However, bacterial diseases of beans are common and threaten yields. Interestingly, the severity of bacterial diseases of common bean is dependent on temperature conditions although it is not documented why that is the case (Fourie, 2002). In this thesis, we aim to improve our understanding of temperature effects on plant disease development and outcome by looking at the bean-*Pseudomonas* pathosystem. Phytopathogenic *Pseudomonas* are often used as robust model organisms for plant pathology (Arnold et al., 2011, Feil et al., 2005), and all evidence in the literature points towards relatively large effects of temperature on this pathogen. This thesis has four main themes that will be introduced in this introduction: i) characterising the impact of temperature on bacterial pathogens of bean, ii) studying the cross-talk between temperature response and oxidative stress tolerance in those pathogens, iii) characterising gene expression changes involved in the temperature and oxidative stress response, and iv) determining which factors contribute to enhanced virulence in modern isolates infecting beans. In this introductory chapter, I will introduce the major bacterial pathogens of bean and discuss what is already known about their temperature dependence. This will be followed by a review of our current understanding of the effect of temperature on plant immunity. Finally, I will describe how ROS acts as an antimicrobial factor during plant-bacteria interactions and why it is of particular relevance to our research.

1.1 Common bean is economically important

Phaseolus vulgaris or common bean is widely grown through the world, and is an important source of proteins in many cultures. It is estimated that over 30 million tonnes of dry bean and 24 million tonnes of

green bean were produced worldwide in 2018 (FAO, 2019), of which the majority is *Phaseolus vulgaris*, although these numbers probably also include some other *Vignia* and *Phaseolus spp* that are also labelled as “dry beans” for commercial purposes (FAO, 2019). Africa and the Americas produce two thirds of the world’s dry bean (Myers and Kmiecik, 2017). Common bean is a member of the legume family so it is able to enter a symbiotic relationship with rhizobia bacteria to fix atmospheric nitrogen (Laguerre et al., 2001). It is therefore an excellent crop, fast-growing and requiring less fertilizer input than cereals though yields per hectare are still sub-optimal in fields in Africa compared to the crops’ potential (Belachew et al., 2022). It can take as little as 60 days to get produce from seed under favourable conditions (Myers and Kmiecik, 2017). Despite its economic value and practicality, common bean is relatively understudied compared to other crops: in the last 5 years, 1099 papers were published with titles containing the scientific name for common bean; in comparison, there were 3320 *Arabidopsis thaliana* papers, 2381 *Zea mays* (maize) papers, 1140 *Solanum lycopersicum* (tomato), and 1265 *Glycine max* (soybean) papers in the same time period (Web of Science). We suspect that this is in part because it is difficult to transform (Hnatuszko-Konka et al., 2019). Half of legume grains consumed worldwide are common bean, making *Phaseolus vulgaris* the most commonly consumed legume (Broughton et al., 2003). Common bean is a warm weather crop, doing best in temperatures ranging from 15 to 30°C (De Ron et al., 2016).

1.2 The plant immune system

We saw that temperature affects bacterial disease severity in bean. The plant host is not a silent participant and disease development and severity is partly under the control of the plant immune system. Plants have evolved two strategies to detect and respond to pathogens in a model commonly referred to as the zig-zag model (Figure 1.1) (Jones and Dangl, 2006). The first of these strategies relies on the recognition of conserved microbial molecular patterns (called pathogen-associated molecular

patterns or PAMPs for short, although they are not specific to pathogens) such as flagellin (a component of the bacterial flagellum) by receptor proteins on the surface of the host cell and elicit PAMP-triggered immunity (PTI) (Jones and Dangl, 2006). During PTI, there is a rapid oxidative burst (Torres and Dangl, 2005). The cells surrounding the pathogen release large amounts of reactive oxygen species or ROS and other antimicrobial compounds, thereby inhibiting pathogen growth by causing oxidative stress (Fones and Preston, 2012). ROS also plays a role in signal transduction to the rest of the plant to induce plant-wide defences (Sewelam et al., 2016). If the pathogen is unable to overcome PTI, the interaction comes to an end and the plant is considered a non-host of this pathogen (Waite et al., 2017). In order to overcome PTI, pathogens produce inhibitors of plant immunity called effectors and secrete them using the type 3 effector secretion system (T3SS) (Chisholm et al., 2006). In turn, resistant plant hosts rely on the second immune strategy which involves intracellular perception of these effectors, eliciting effector-triggered immunity (ETI) (Jones and Dangl, 2006). The genes encoding the plant receptors capable of recognising effectors are called Resistance or R genes (Chisholm et al., 2006). During ETI, a qualitatively stronger and faster ROS burst occurs and is often accompanied by a form of localized cell death called the hypersensitive response (HR) in the plant cells surrounding the pathogen (Dodds and Rathjen, 2010). As a more specific but also more robust pathogen resistance, ETI is typically what the breeding programmes aim to achieve (Jones and Dangl 2006). Successful pathogens are able to suppress PTI while evading ETI or suppressing ETI (Figure 1.1). In recent years, it has become increasingly apparent that PTI and ETI are not discrete processes. For instance, there is significant overlap in the protein components involved in PTI and ETI and components of PTI are required for HR, a response typically exclusive of ETI (Yuan et al., 2021). Furthermore, ETI is not only triggered in response to interaction with pathogens, but also with commensals and even symbionts such as rhizobia (Yang et al., 2010). Plants and pathogens are in constant arms races in which multiple effectors and recognition mechanisms are involved (Ngou et al., 2022b), so that the overall picture is more complex than a simple zig-zag model of plant pathology and

this model is now considered somewhat simplistic (Ngou et al., 2022a). This is why a better understanding of pathosystems is important. In particular, environmental factors are often overlooked in favour of classic resistance traits (Preston, 2017). Indeed, external factors, such as environmental conditions can have drastic but somewhat stochastic effects on the outcome of plant-pathogen interaction. For instance, *Xanthomonas* infection on common bean is known to be more severe after a storm (Saettler, 1989), as the leaves get damaged, creating openings for the pathogen to enter and colonise the host.

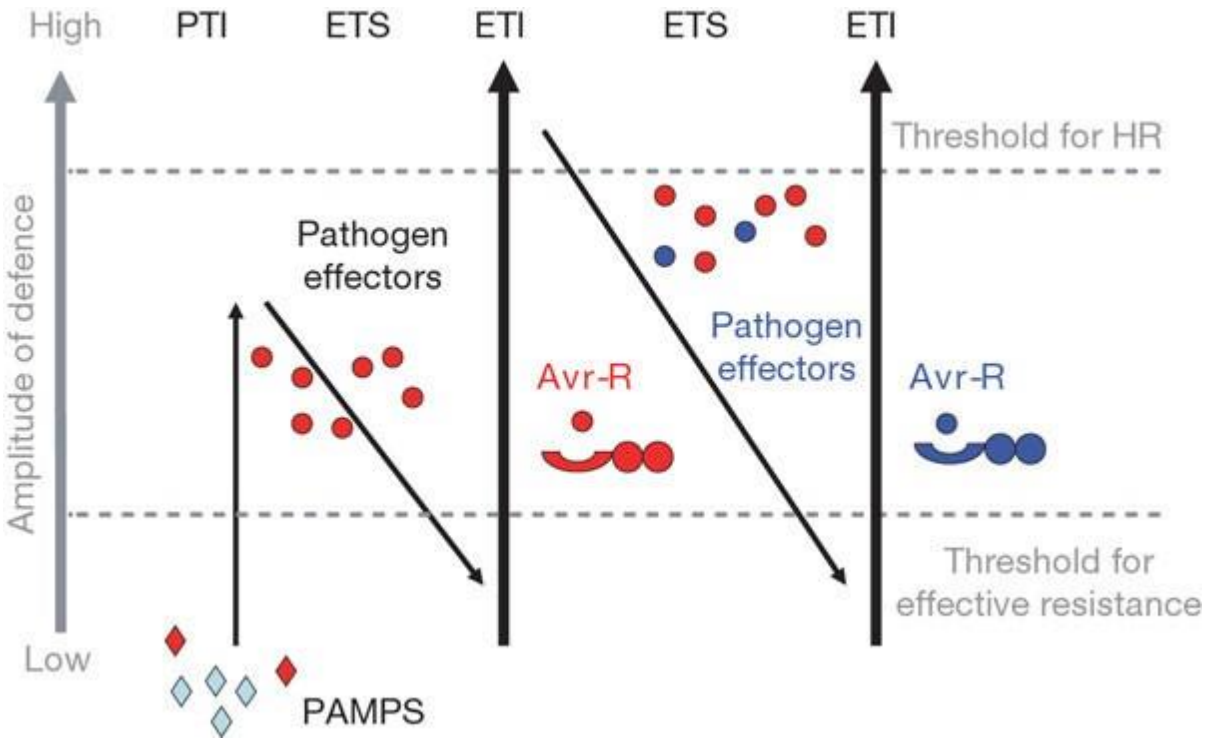


Figure 1.1: Schematic representation of the zig zag model of plant-pathogen interactions. PTI is the represented in the first phase, and ETI is in the second phase, leading to the hypersensitive response HR. (reproduced from Jones and Dangl, 2006)

1.3 Temperature affects plant immunity

It has been documented that for many plants, immune responses are tuned down at higher temperatures (Hua, 2013). Arabidopsis for instance is more sensitive to Pto DC3000 at elevated temperatures (30°C compared to 23°C). However, it is not entirely clear whether this is due to the effect of temperature on host or pathogen, as this increase in disease susceptibility has also been suggested to be due to increased effector translocation by the pathogen (Huot et al., 2017). Different plant immune defence mechanisms may also be differentially affected by temperature. For example, Arabidopsis preferentially activate ETI signalling at 10-23°C and PTI signalling at 23-32°C (Cheng et al., 2013). Multiple R genes have been described to have a temperature threshold above which they are not able to defend the host e.g. RPS4 -mediated defence against *P. syringae* is suppressed at 28°C (Hua, 2013). However, it is not clear whether this generalisable to other pathosystems as some plants show the opposite pattern: for instance, Xa7-mediated resistance in rice has been reported to function better at high temperature (35 vs 29°C daytime temperatures) (Cohen et al., 2017). Some have found that high temperatures do not affect ETI signalling but instead inhibit programmed cell death associated with the hypersensitive response (Menna et al., 2015). Less controversial is the impact of temperature on salicylic and abscisic acid signalling pathways as they are generally disturbed at elevated temperatures (Hua, 2013). To our knowledge, no study has examined the effect of temperature on defence responses in bean to bacteria specifically. Bean resistance to root nematode is stable at temperatures ranging 24 to 32°C (Sydenham et al., 1997), but elevated temperatures (35°C vs 20°C) lead to increased viral load in susceptible cultivars (Meziadi et al., 2021). While temperatures between 28°C and 32°C may be stressful for Arabidopsis, which grows in temperate climate zones, beans may not be stressed until they experience temperatures above 36°C. At 38°C, increased expression of immune-linked genes was observed in bean (Alvarado-Gutierrez et al., 2008). Similarly, chitinase (involved in immune defence against fungi) gene expression is induced at 42°C in bean (Margispinheiro et al., 1994). This range of responses displayed by bean in response to a variety of stressors suggests that within moderate

temperature ranges, temperature effects on pathogens may be more important than effects on host resistance.

1.4 Three major bacterial pathogens of common bean

Common blight *Xanthomonas axonopodis* pv *phaseoli* (Xap), halo blight *Pseudomonas savastanoi* pv *phaseolicola* (Pspph) and brown spot *Pseudomonas syringae* pv *syringae* (Pss) are the three main bacterial pathogens that have a significant impact on bean production in sub-Saharan Africa (Figure 1.2). All three colonise the apoplast but can also reside in contaminated beans, and have been observed to co-infect the same host during the growing season (Fourie, 2002).

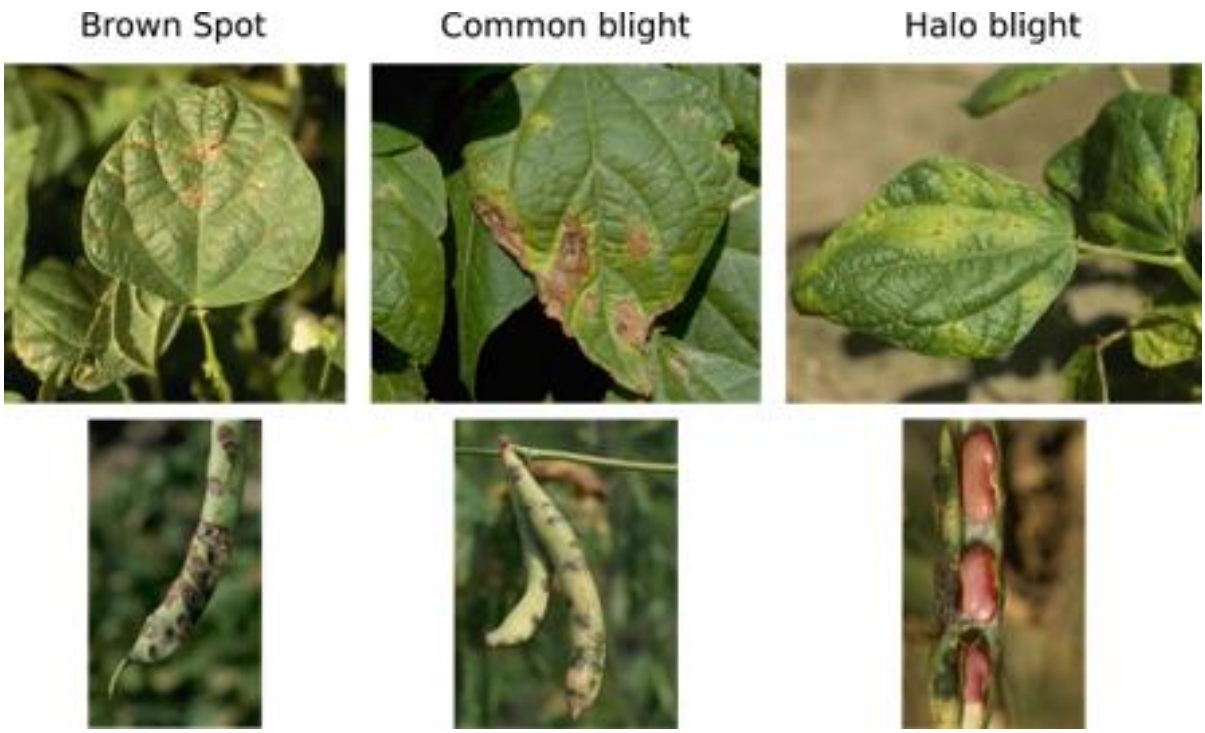


Figure 1.2: Symptoms of bacterial diseases of bean brown spot, common blight and halo blight, on leaflets and bean pods. (Courtesy of Howard F. Schwartz, Colorado State University, Bugwood.org)

1.5 Introducing plant-pathogenic *Pseudomonas*

Pseudomonas is a clade of gram-negative aerobic bacteria which encompasses plant-pathogens, human pathogens, and plant commensals (Kersters et al., 1996). *Pseudomonas savastanoi* used to be part of the *Pseudomonas syringae* clade but has been reclassified as a separate species more recently. From here on out, we refer to *Pseudomonas savastanoi* and *syringae* combined as the *Pseudomonas syringae species complex* (PSCC for short) as they share a number of features. They are hemi-biotrophic pathogens – infection begins in living plant tissues followed by a second phase of bacterial growth which happens in dead tissue (Lindeberg et al., 2009). Members of the *Pseudomonas syringae species complex* are commonly found in the environment, and infect their host by entering through wounds and the stomata. The PSSC was organised in pathovars based on the host range of the strains (Morris et al., 2019). Host range varies widely between members of the PSSC and is determined by a number of factors and thus pathovars are not necessarily monophyletic. Now while pathovars are still used, phylogroups are also used to subclassify members of the PSSC (Berge et al., 2014). Phylogroups are grouped together based on similarity of their genomic DNA. *Pseudomonas syringae* pv*. syringae* is part of phylogroup 2d and *Pseudomonas savastanoi* pv. *phaseolicola* belongs to phylogroup 3 (Parkinson et al., 2011). Despite belonging to different phylogroups, Pss and Pspph are relatively closely related as phylogroup 2 and 3 are the most closely related to one another in the PSSC (Berge et al., 2014). As genetically related strains with an overlapping host range and with published annotated genomes, Pss and Pspph make for a robust pathosystem for studying temperature effects on disease development.

1.6 Introducing *P. syringae* pv *syringae*

P. syringae pathovar *syringae* (Pss), commonly known as brown spot, is a generalist pathogen with a broad host range. It is able to infect over 180 host plant species (Muedi et al., 2015) including economically important crops belonging to the cabbage, solanacea and legume families (Morris et al., 2019), and has a pronounced epiphytic stage of growth (Feil et al., 2005). Pss is often seed-borne in bean. Infections start with water-soaked lesions which get progressively larger as the infection progresses and eventually turn brown, sunken and necrotic. In young pods, Pss leads to cessation of growth at the site of infection (Muedi et al., 2015). Pss can cause substantial losses in bean, up to 55% in South Africa (Serfontein, 1994).

1.7 Introducing *P. savastanoi* pv *phaseolicola*

In contrast with Pss, Pspph is a poorer epiphyte and a more specialised pathogen: it is only able to infect common bean and a few other members of the legume family (Arnold et al., 2011). Pspph has been recognised as a model system for plant pathology, due to the extensive research that has been done since the 1970s and the diversity of effector set that this pathovar displays (Arnold et al., 2011). Halo blight owes its colloquial name to the symptomatic chlorotic lesions it causes on bean leaves which form a halo around the water-soaked site of infection (Fourie, 1998). Pspph can also be seed-borne. It can cause losses in yield of up to 43% in the US (Arnold et al., 2011).

1.8 Introducing *Xanthomonas axonopodis* pv *phaseoli*

Xanthomonas axonopodis pv *phaseoli* (Xap), previously known as *Xanthomonas campestris* pv *phaseoli,* commonly referred to as common blight, is the third major bacterial pathogen of common bean. While

not a member of the PSSC like Pss and Pspph, it is also a gram-negative aerobic bacterium with a hemi-biotrophic lifestyle (Akhavan et al., 2013). It is able to infect beans and a few other legumes such as *Vigna* spp. and common pea (Chen et al., 2021). There are two supopulations of Xap: fuscan and non-fuscan. Fuscous are identified as producing a brown pigment, an intermediate in the tyrosine catabolic pathway (Health, 2014). Fuscous strains tend to be more aggressive than non-fuscous strains during infection (Opio et al., 1996, Chan and Goodwin, 1999). Infected leaves typically display water soaking within 4 to 10 days of infection before spots become larger and necrotic (Akhavan et al., 2013). Other plant parts become sunken and turn brown and necrotic at later stages of the disease (Chen et al., 2021). These symptoms are similar to brow spot (caused by Pss) and so these two bacterial diseases can sometimes be confused (Fourie, 2002). In the US, yield losses of legumes due to Xap are estimated to range between 20 and 40% (Wallen and Jackson, 1975).

1.9 Optimal temperature for bacterial growth of the PSSC

The optimal temperature for growth of plant pathogenic *Pseudomonas* under non-limiting conditions, is typically between 25-30°C but *P. syringae* pv *syringae* is able to survive outside of this range (Morris et al., 2008). In the case of *Pseudomonas syringae* and *savastanoi*, optimal growth *in vitro* is generally assumed to be 28°C – e.g. in (Hockett et al., 2013). Whilst this has not been formally tested in Pspph or Pss, there is evidence in other pathovars that this may not be the case (table 1.1). For instance *P. savastanoi* pv *glycinea* (previously *P. syringae*) strain PG4180 can grow at temperatures upwards of 35°C and optimal temperature for doubling rate in LB was recorded to be 30.7°C (Keith et al., 1999) . A panel of uncharacterised *Pseudomonas syringae* (likely pathovar *syringae* and/or *morsprunorum*) was shown to have an optimal doubling rate at 26°C, whilst a representative P. *syringae* (unnamed but very likely pv *syringae*) was estimated to have a temperature optimum of 28°C with a doubling time of 1.27 h but

overall doubling rates did not significantly differ in the range 23-33°C (Young et al., 1977). Whilst the optimum temperature is up for debate and likely differs between pathovars and strains, it is unequivocal that bacterial growth rate is substantially affected by temperature.

Table 1.1: Published data on Optimal Temperature for Growth of Plant-pathogenic *Pseudomonas*

Species	Pathovar	Strain	Medium	Optimal temperature	Doubling rate	Reference
P. syringae	spp (presumed *syringae* or *morsprunorum*)	520, 3023, 3674, 3677	YP	26°C (based on mean of four isolates)	1.30h +/- 0.27 (based on mean of four isolates)	(Young et al., 1977)
P. syringae	spp (presumed *syringae* or *morsprunorum*)	?	YP	28°C	1.27h	(Young et al., 1977)
P. savastanoi	*glycinea*	PG4180	LB	30.7°C		(Keith et al., 1999)
P. savastanoi	*glycinea*	PG4180	MG	14/30°C	ND	(Palmer and Bender, 1993)
Pseudomonas	spp	1W, 9AW, 9BW, 10AW, 10CW, 29W, 39W, 44W, 51W, Lz4W	? YDC?	20 better than 10 or 30°C	ND	(Shivaji et al., 1989)
P. savastanoi	*glycinea*	PG4180.N9	HSC	28 better than 18°C	5h	(Budde et al., 1998)
P. syringae	spp	Lz4W	Antarctic bacterial medium	22°C	ND	(Pavankumar et al., 2021)
P. savastanoi	*phaseolicola*	1321	Medium reference in foreign journal I can't access	27°C	ND	(Nuske and Fritsche, 1989)
P. syringae	*syringae*	3556	*In planta* (lilac leaf)	18-19.5°C	ND	(Young, 1991)

1.10 Disease occurrence in the field

Common bean is an annual crop that is typically either sown in March/April in frost-free areas in Southern Africa for harvests as early as September, or November/December in frost-prone areas. At some latitudes, two harvests are possible every year and a second sowing happens in September (Wortmann and Allen, 1994). Halo blight infection occurs early in the growing season and is favoured by low temperatures (23-28°C) and cool nights (15-16°C) (Fourie, 2002, Arnold et al., 2011). Common blight and brown spot occur later in the season at warmer temperatures (respectively 28-32°C and 27-29°C) (Muedi et al., 2015, Wallen and Jackson, 1975, Saettler, 1989, Fourie, 2002). These three bacterial pathogens infect the same host species and can even coinfect the same individuals but seem to favour different temperature ranges. Therefore, this seems to be independent of the host response to environmental cues. This raises the question: Does temperature affect bacterial pathogenicity?

1.11 Temperature affects pathogenicity factors in plant pathogenic *Pseudomonas*

Temperature can affect the expression of pathogenicity and virulence mechanisms in *P. syringae* and *savastanoi*. Effects of temperature on virulence factor production have already been well-characterised in the literature. All three pathogens use the type 3 secretion system T3SS to deliver effectors into host cells to suppress plant immunity (Hueck, 1998). The T3SS has been documented to be regulated by temperature in multiple pathovars of *Pseudomonas syringae*, both transcriptionally (McCraw and Preston, 2014, Huot et al., 2017, Hockett et al., 2013) and post-translationally (effector translocation) (Huot et al., 2017). Members of the PSSC Pgy PG4180 and Pto DC3000 have been shown to have

increased T3SS transcription at low temperatures compared to higher temperatures (Ullrich et al., 2000, McCraw and Preston, 2014). However, a microarray study comparing the gene expression of Pspph NPS3121 at 18 and 28°C found that the T3SS is downregulated at low temperatures while oxidative stress responses and motility are upregulated (Arvizu-Gomez et al., 2013). Interestingly, an RNAseq study looking specifically at Pss B728a found a similar pattern: the transcription of 18 T3SS genes was induced by warm temperatures (30°C), and none were cold (20°C) induced, while most genes involved in motility were downregulated at the warmer temperature (Hockett et al., 2013).

Another part of the array of virulence factors produced by the *Pseudomonas syringae* species complex are phytotoxins, and these have also been established as temperature-dependent (Bender et al., 1999). Thought to be mainly involved in virulence, phytotoxins also display antimicrobial activities (Bender et al., 1999). One of the best documented phytotoxins is coronatine, a phytotoxin produced by various members of the PSSC (Bender et al., 1999). Coronatine is only produced at temperatures below 28°C, with a peak around 18°C (Ullrich et al., 2000). This temperature-dependence has been shown to be linked to a two-component regulatory system affecting transcription (Ullrich et al., 1995). The genes involved in biosynthesis of coronatine have not been found in isolates of Pss or Pspph but these have access to other phytotoxins that are also temperature-regulated (Bender et al., 1999).

1.12 Phaseolotoxin: a key phytotoxin produced by Pspph

Pspph produces phaseolotoxin, the phytotoxin responsible for the characteristic chlorosis of photosynthetic tissue that led to the name ‘halo blight’ (Patil et al., 1991). Interestingly, phaseolotoxin is a broad-spectrum antibiotic as it works by inhibiting the enzyme (ornithine carbamoyl transferase OCTase) responsible for the biosynthesis of arginine and polyamines in plants and in bacteria

(Aguilera et al., 2007). Phaseolotoxin itself is a reversible inhibitor (Langley et al., 2000), but *in planta*, it is converted to p-sorn (figure 1.3) which is an irreversible inhibitor of OCTase (Bender et al., 1999). Pspph is resistant to its own toxin because it has an OCTase resistant to phaseolotoxin ArgK, which unlike the conserved OCTase ArgD is not sensitive to inhibition by phaseolotoxin (Rowley et al., 2000). The resistant argK gene is part of the phaseolotoxin gene cluster (pht cluster) which is required for phaseolotoxin production in Pspph (Aguilera et al., 2007). The pht cluster is organised so that *argK* transcriptional regulation is linked to the other genes in the cluster (Figure 1.3). As a result, ArgK is only produced under conditions inducive to phaseolotoxin production (Aguilera et al., 2012). At least one other locus outside of the cluster seems to be required for phaseolotoxin production, a putative nonribosomal peptide synthase (Aguilera et al., 2012), but overall presence of this genetic island is indicative of the genetic capability of an organism to produce phaseolotoxin. Phaseolotoxin production has been described in another pathovar of *Pseudomonas syringae*, the kiwifruit pathogen *P. syringae* pv *actinidiae (Murillo et al., 2011)*. There is not much information available on the importance of phaseolotoxin for virulence but it has been described that when the phaseolotoxin resistant enzyme ArgK was introduced into non-host tobacco, it improved resistance to Pspph (Delafuentemartinez et al., 1992).

Phaseolotoxin is maximally produced at temperatures between 18 and 20°C, while production is abolished at 28°C and above (Aguilera et al., 2007). The genetic components required for thermoregulation of the pht cluster are not yet fully uncovered. So far, all regulatory mechanisms described act at the transcriptional level, but it is not possible to exclude the possibility that post-transcriptional regulation is also happening in response to temperature and other environmental factors. The evidence suggests that some of the genes of the pht cluster are involved in regulation of the cluster, indicative of a feedback loop (Aguilera et al., 2012, Gonzalez-Villanueva et al., 2014). Furthermore, a 485bp long thermoregulatory TRR motif of the interpromoter region of argK and

the phtA, B and C genes seems to be at least partly responsible for the thermoregulation of transcription. Indeed, when the region is modified to be present in multiple repeat copies, phaseolotoxin is produced as usual at 18°C, but inhibition at 28°C is only partial (Rowley et al., 2000, Rowley et al., 1993). Common regulators of virulence factors - GacS, GacA, and IHF - are also described to be regulators of the phaseolotoxin cluster (Aguilera et al., 2017). Phaseolotoxin production is also induced by activation of OxyR, a transcriptional regulator involved in oxidative stress responses (Hernandez-Morales et al., 2018, Arvizu-Gomez et al., 2022).

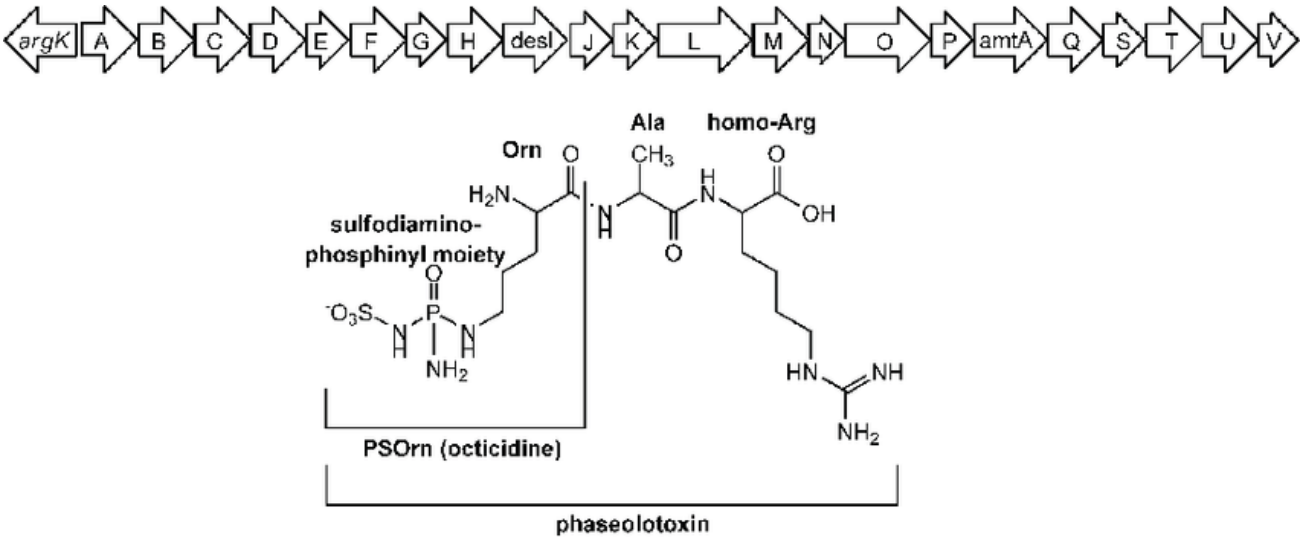


Figure 1.3: Structure of phaseolotoxin and phaseolotoxin cluster organisation. There are 23 genes in the cluster including the gene encoding the phaseolotoxin-insensitive OCTase argK (reproduced from Gross and Loper, 2009)

1.13 Phytotoxins produced by Pss

Pss does not produce phaseolotoxin, but it does produce another phytotoxin, syringomycin and the related syringopeptins, which altogether are referred to as “syringotoxin” (Bender et al., 1999). These

small lipodepsipeptides disrupt cell membranes, resulting in cell lysis (Gross and Loper, 2009). Syringotoxin production is also documented to be temperature-regulated (Sinden et al., 1971, Hockett et al., 2013). Syringomycin may be involved in competition between strains *in planta* as it exhibits broad-range antibiotic activities (Sinden et al., 1971). The biosynthesis cluster for syringomycin comprises six genes with structural functions (syrB1, syrB2, syrC, syrE and syrP), three genes with regulatory functions (syrF, syrG and salA), and syrD with secretory functions (Figure 1.4). In Pss B728a, the syringomycin and syringopeptin biosynthesis clusters are located on a large 180 kb pathogenicity island which also encodes genes for biosynthesis of siderophore, antibiotic resistance, and a degenerate locus for phaseolotoxin biosynthesis (Gross and Loper, 2009). Both halo blight and brown spot are described to also produce bacteriocins (also called tailocins) - modified phages that are toxic to other bacteria (Vidaver et al., 1972, Hockett et al., 2013).

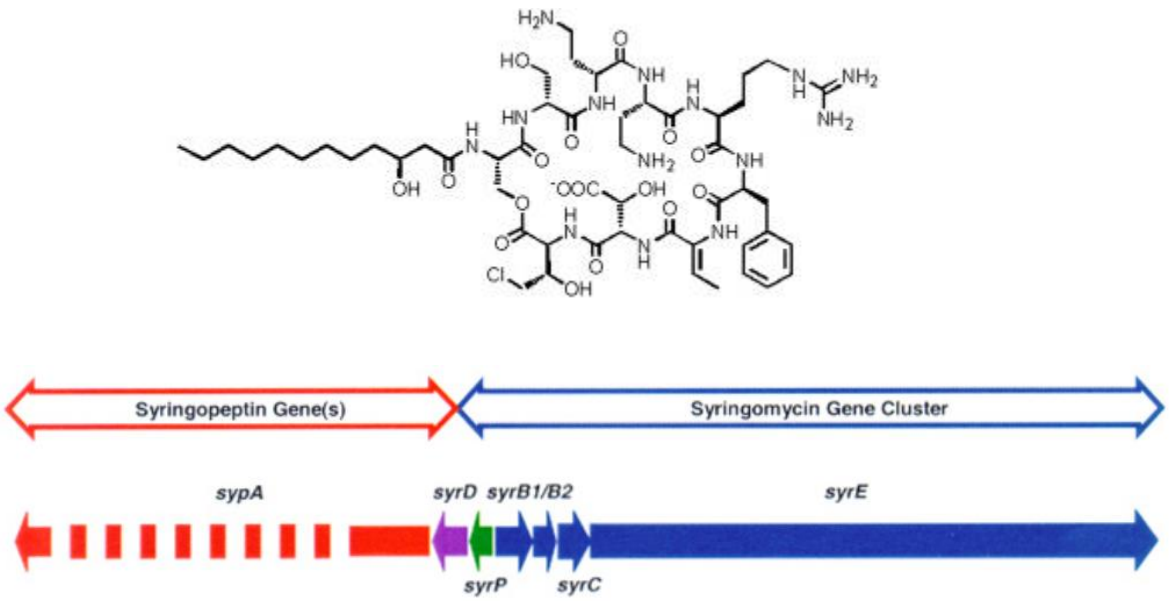


Figure 1.4: Structure of syringomycin, and biosynthesis cluster of syringomycin (in blue) and syringopeptin (in red). The biosynthesis cluster covers a 43kb stretch in the genome of Pss (reproduced from Scholz-Schroeder et al., 2001, Singh et al., 2007)

Altogether, there is ample data on the effects of temperature on virulence factors, especially on phytotoxins, and it is still an active area of research. However, we predict that the temperature response of bacterial pathogens of beans is the result of a complex cross-talk between multiple interacting factors, including but not restricted to virulence. Some of those other factors are understudied in comparison to virulence factors, as little is known for instance about temperature-mediated changes in metabolism, nutrition, and stress tolerance.

1.14 Plants and reactive oxygen species

While the effect of temperature on bacterial virulence factors is relatively well-documented, we also need to consider the effect of temperature on bacterial stress tolerance, of which a key example is oxidative stress. Plants ubiquitously rely on reactive oxygen species (ROS) for defence against pathogens (Doke, 1985, Fang, 2011). Reactive oxygen species serve as antimicrobial compounds and as signalling molecules in plants (Sewelam et al., 2016). While ROS is produced passively as a result of physiological stress, production is substantially increased in response to both abiotic and biotic stress (Torres and Dangl, 2005) 2005).

Upon pathogen recognition (PTI), a first ROS phase occurs: a low amplitude production of ROS mostly generated by plasma membrane Rboh NADPH oxidases and cell wall peroxidases (Figure 1.5). The latter generates hydrogen peroxide while oxidases produce superoxide which is rapidly converted to H_2O_2 either spontaneously or by the plants's superoxide dismutases. Thus, hydrogen peroxide is likely the dominant form of ROS that bacteria experience during initial colonisation of the plant apoplast. Following this initial phase, a second ROS phase happens during ETI, with a high ROS amplitude (Torres et al., 2006). ROS is generated in many compartments of plant cells, including but not restricted to chloroplasts, mitochondria and peroxisomes. In particular, the chloroplastic photosystems PSII and PSI are primary generators of

singlet oxygen and superoxide respectively (Lu and Yao, 2018). Intracellular hydrogen peroxide can cross the plasma membrane into the extracellular space either by free diffusion or through aquaporins (Lu and Yao, 2018).

ROS are also used to create subcellular polarised barriers at infection sites, as cationic peroxidases and bacteria (Xap) were found to colocalise together with other components of the papillae in bean – the papilla is a nub-like structure that is formed between the plasma membrane and plant cell wall during plant immunity - (Brown et al., 1998). Both ROS phases are required for plant defence against pathogens and opportunistic micro-organisms. In common bean, ROS based defences are essential to defense against Pspph (Diaz-Valle et al., 2019, Nowogorska and Patykowski, 2015). Hydrogen peroxide and ROS also act as signalling molecules *in planta* (Figure 1.5). Hydrogen peroxide mediates ABA-induced stomatal closure against pathogen entry, and ROS interact with the jasmonate signalling pathway (Barna et al., 2012). Calcium metabolism is intimately related to ROS signalling: calcium influx upon pathogen recognition is required for ROS production and other components of plant immunity (Torres et al., 2006).

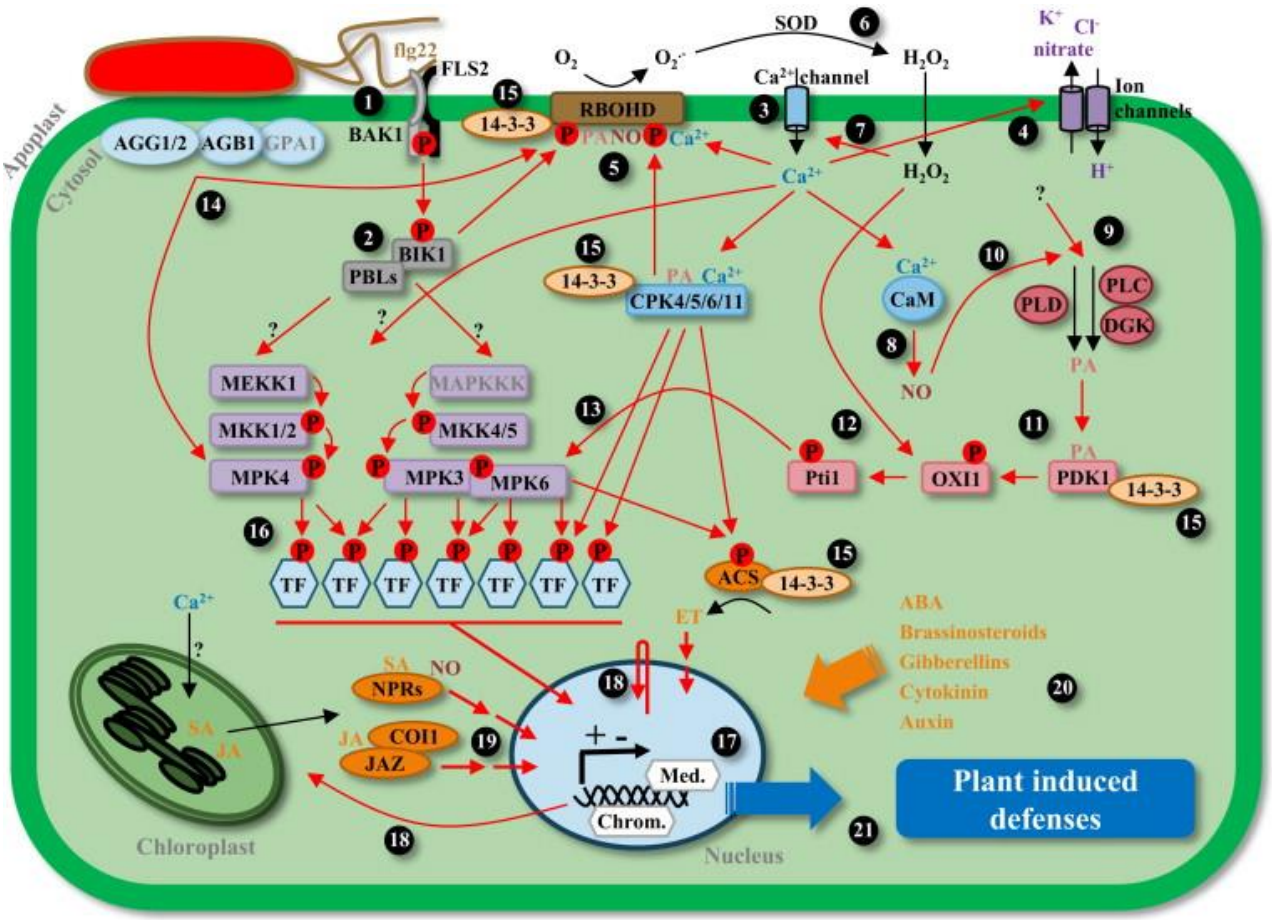


Figure 1.5: ROS as a signaling molecule in plants. Flg22 perception by FLS2 induces rapid immune receptor complex formation at the plasma membrane and phosphorylations of the actors (1). BIK1 is quickly phosphorylated and released from the complex (2). A Calcium burst occurs (~30 s to 2 min) and reaches a peak at around 4–6 min (3). This leads to an extracellular alkalinization (~1 min) and a depolarization of the plasma membrane (1–3 min) (4). A ROS burst then rapidly occurs (~2–3 min) via RBOHD and peaks at around 10–14 min (5). RBOHD produces O2.– in the apoplast, which is converted into H_2O_2 by superoxide dismutases (SOD) (6). H_2O_2 can enter the cytosol and the different organelles of the cell and is capable of inducing cytosolic Ca2+ elevations (7). Ca2+-induced calmodulin (CaM) leads to synthesis of nitric oxides NO, which can regulate NPR1 and RBOHD via cysteine S-nitrosylation (8). Phosphatidic acid (PA) production is rapidly induced (already at 2 min) (9). NO production is partly required for PA generation (10). PA can modulate the activity of RBOHD. PA activates OXI1 (11), and H_2O_2 can activate Pti1 kinases in an OXI1-dependent way (12). Pti1 kinases then may regulate MAPKs (13). AGB1, AGG1, and AGG2 G proteins are partly required for ROS burst (14). 14-3-3 proteins modulate the activity of RBOHD (15). MAPK modules are activated in a few minutes and phosphorylate a large spectrum of substrates such as ACS isoforms, leading to ET synthesis, and transcription factors (TFs) (16). These participate in the regulation of thousands of genes (17). First changes include notably genes involved in phytohorme signaling: salicylic acid SA, jasmonic acid JA, and ethylene ET; as well as synthesis of antimicrobial compounds and transcription regulatory factors (18). SA, JA, and ET signaling pathways in turn also regulate gene expression (19). Crosstalks also occur with other phytohormones (20). This complex signaling network finally leads to the implementation of plant-induced defenses, such as the production and secretion of antimicrobial compounds and the generation of toxic ROS (21). Black

arrows denote enzymatic pathways or transport, and red arrows denote regulation (direct or indirect activation/inhibition). Question marks indicate unidentified or unclear events. (Figure reproduced from Bigeard et al., 2015)

1.15 Bacterial strategies to tolerate ROS *in planta*

P. syringae has distinctively high levels of ROS tolerance relative to non-pathogenic plant-associated pseudomonads (Klotz and Hutcheson, 1992). While bacterial pathogens typically secrete effectors to tune down plant immunity and therefore reduce ROS levels in their environment, they still experience oxidative stress *in planta*, as evidenced by the in-planta transcriptional induction of various ROS-sensing mediators such as AlgU (Markel et al., 2016, Wang et al., 2022). Furthermore, *P. syringae* mutants lacking ROS response genes OxyR (Ishiga and Ichinose, 2016) or ppGpp (Chatnaparat et al., 2015) are impaired in growth *in planta*. ROS are stressful to bacteria because they cause cellular damage. In particular, their oxidative power may attack heme groups, FeS_4 clusters and thiol groups rendering many key enzymes inactive. They can also cause lipid peroxidation and damage proteins. As a result, if present in sufficient levels, ROS can inhibit pathogen growth and even kill cells (Fones and Preston, 2012). The ability to tolerate high levels of ROS is likely to be important to plant pathogenic pseudomonads.

There are four main strategies to tolerate oxidative stress: exclusion, export, inactivation, and modification of the target of the toxin (Fones and Preston, 2012). Pathogens can rely on their extracellular matrix to absorb oxidative damage before the ROS reach more important bacterial structures. Extracellular polysaccharides (EPS) such as alginate and levan, but also polyesters such as PHA have been shown to have a role in protecting the pathogen from both abiotic and biotic stresses. Indeed, EPS production is upregulated in the presence of reactive oxygen species in Pss (Keith and Bender, 1999). Polyamines also serve as ROS scavengers (Stewart et al., 2018), and they are produced both intracellularly

and extracellularly by *P. syringae* during infection (Vilas et al., 2018). The export strategy relies on the transport of reactive oxygen species outside of the bacterial intracellular space (Fones and Preston, 2012). Modification of the target of ROS can take various forms but a common one is mutation of cysteine residues in sensitive proteins and enzymes (Fones and Preston, 2012). Cysteine is sensitive to oxidation because of its sulfur group which is required for protein folding and in turn enzyme activity (Deng et al., 2013, Rhee et al., 2000). Once the damage has occurred, bacteria can repair oxidised proteins at a cost (Gennaris et al., 2015), or need to replace them. Finally and probably the most studied strategy for oxidative stress tolerance is inactivation of the toxin. This can be achieved by production of antioxidant in the extracellular space, the periplasm and the intracellular space. The antioxidants can be small molecules such as glutathione (Masip et al., 2006) or larger enzymes. There are three main antioxidant enzymes: catalase, superoxide dismutase and peroxidase. Catalases and peroxidases induce the transformation of hydrogen peroxide into water. Superoxide dismutases catalyse the conversion of superoxide into oxygen (Figure 1.7). Iron nutrient status is also likely important, as Fe(II) is involved in the Fenton reaction that generates destructive hydroxyl radicals from H_2O_2 (Fones and Preston, 2012) (Fones and Preston 2012). Bacteria can sequester their iron to reduce the risk of a Fenton reaction (Fones and Preston, 2012). Similarly, sulfate metabolism is important as sulfur is a key component of cysteine, allowing cysteine disulphide bond formation, a conformation crucial for redox sensing (Poole, 2015). Interestingly, glutathione is composed of cysteine residues and also acts as a regulator of disulphide bond formation (Masip et al., 2006).

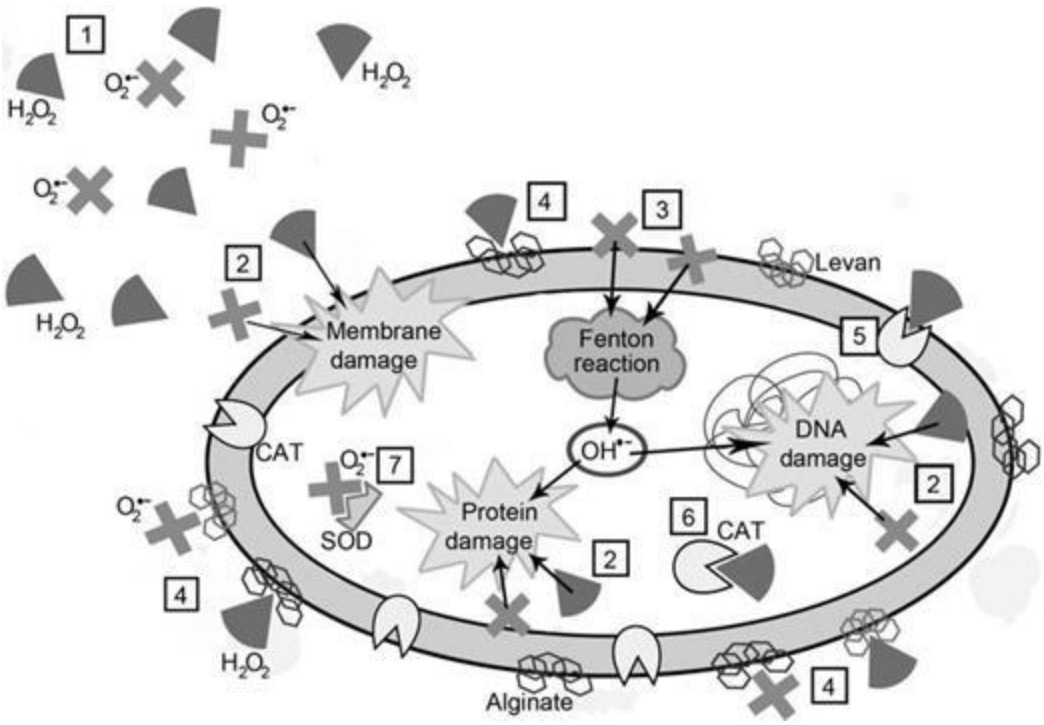


Figure 1.7: Summary of interactions between host-secreted ROS during infection and bacterial ROS tolerance mechanisms . ROS, including H_2O_2 and $O\cdot^{-}_2$, are produced at the plasma membrane of plant cells following detection of a pathogen (1). These cause damage to bacterial protein, DNA and membranes (2). $O\cdot^{-}_2$ can also participate in Fenton reactions, resulting in the generation of highly reactive $OH^{\cdot}-$ radicals, causing further damage (3). Bacterial defences include extracellular polysaccharides (e.g. levan and alginate) (4) and periplasmic catalase (represented by triangles) (5), which can neutralize ROS prior to their entering the bacterial cell. Once inside the cell, ROS may be detoxified by cytoplasmic catalase (represented by triangles) (6) and superoxide dismutases SOD (7). (Figure reproduced from Fones and Preston, 2012)

1.16 Enzymes involved in ROS detoxification by the plant pathogens

The genome of Pspph encodes five catalases including a manganese containing catalase and a catalase-peroxidase HPI KatG. Pss has access to five including a Mn-containing catalase and a catalase-peroxidase HPII KatE (Feil et al., 2005, Joardar et al., 2005). Pspph has 8-9 peroxidase genes, three of which encode glutathione peroxidases. Pss has 10 peroxidases in its genome, including four glutathione peroxidases. Both Pss and Pspph genomes encode three superoxide dismutases: SodA, SodB and SodC, which have either a copper-zinc or an iron cofactor. There are also other genes predicted to be involved in oxidative

stress tolerance that these pathogens have access to: peroxiredoxin, organic hydroperoxide resistance protein, osmotically inducible proteins, and hydroperoxide reductases (Winsor et al., 2016). Work in Pss has already shown that the *sod* genes are important for oxidative stress response as the double mutant *sodAsodB* is more sensitive to paraquat (a herbicide which generates oxidative stress in cells) than the wild type, however the double mutant is still able to infect its host and induce brown spot symptoms *in planta* (Kim et al., 1999). Catalase mutants in *Pseudomonas syringae pv tomato* DC3000 are more sensitive to hydrogen peroxide stress, and the triple catalse *katB/E/G* mutant is compromised in virulence in the tomato host (Guo et al., 2012), indicative that tolerance to hydrogen peroxide is important to pathogenicity of *Pseudomonas syringae*.

1.17 ROS response also affects virulence factor expression

The expression of key virulence factors in *P. syringae* and *savastanoi* has also been linked to oxidative stress. For instance the oxidative stress master regulator OxyR is transcriptionally regulated in response to both ROS presence and temperature and induces the expression of phytotoxin biosynthesis genes and other virulence-related genes in Pspph (Arvizu-Gomez et al., 2022). It has even been described that thermoregulation of the *pht* cluster is abolished in 1mM hydrogen peroxide (Hernandez-Morales et al., 2018). However, these results are to be taken with caution. The authors do not find that a higher level of H_2O_2 applied leads to a significant increase in intracellular ROS. Despite this, they find that only two of the five *pht* genes tested are upregulated at 2.5mM while all five are upregulated at 1mM. In *P. syringae*, AlgU is responsible for the activation of oxidative stress responses but it also regulates genes encoding components of the Hrp type III secretion system, and the HrpL and HrpRS transcription regulators (Markel et al., 2016). Altogether these studies strongly suggest that oxidative stress responses, and virulence are intimately inter-connected and that temperature may also be involved.

1.18 Links between oxidative stress tolerance and temperature responses in bacteria

There is little information available on the effect of temperature on oxidative stress resilience mechanisms but we do know that Pspph NPS3121 catalase expression is upregulated at 18°C (Arvizu-Gomez et al. 2013). No significant differences were found in B728a (Hockett, Burch, and Lindow 2013). However, it has long been hypothesised that cold temperatures cause oxidative stress in cells. This has not been described for *Pseudomonas syringae*, but in other micro-organisms, even non-freezing temperatures ca. 10-20°C below the optimal temperature for the microbe have been described to cause oxidative stress (Garcia-Rios, Ramos-Alonso, and Guillamon 2016, Smirnova, Zakirova, and Oktyabrskii 2001).

1.19 Metabolic responses of bacteria

We do not have clear candidate temperature-responsive metabolic pathways yet, but there is more data on how oxidative stress affects metabolism. Remodelling metabolism to promote extracellular polysaccharides (EPS) and polyamine biosynthesis is one of the strategies employed by members of the PSSC in response to oxidative stress (Vilas et al., 2018, Keith and Bender, 1999). Furthermore, preliminary data from studies on Pto DC3000 suggests that certain metabolic enzymes from central metabolism are particularly sensitive to cysteine oxidation (Morimoto, Preston and van der Hoorn, unpublished). One in particular stands out: the cobalamin-independent methionine synthase. Methionine is an amino acid central to metabolism in bacteria. It is the only amino acid that contains a thioether, and as such is necessary for the production of all molecules requiring this molecular pattern

(Ferla and Patrick, 2014). *Pseudomonas* typically can rely on two different enzymes to synthesise methionine: the cobalamin dependent MetH and the cobalamin independent synthase MetE. *E. coli* has been found to be methionine deficient in minimal medium when exposed to transient oxidative stress. This has been linked to the cobalamin independent methionine synthase MetE. Oxidation of cysteine residue 645 is predicted to inactivate the enzyme, causing methionine auxotrophy (Hondorp and Matthews, 2004). MetE seems to be one of the proteins most susceptible to oxidative damage in *E. coli*, along with citrate synthase GltA, serine hydroxymethyltransferase GlyA and others (Leichert and Jakob, 2004). Phytopathogenic *Pseudomonas* heavily rely on MetE *in planta* as cobalamin requires a cobalt cofactor and cobalt resources *in planta* are severely limiting. Indeed, metE has been found to be upregulated *in planta* in another bacterial phytopathogen, *Ralstonia solanacearum* (Plener et al., 2012). Not much is known about these enzymes' temperature response. Pss strain B728a was found to express *metE* at similar levels at 20 and 30°C *in planta*, but did not express *metH* in either treatments (Hockett et al., 2013). Additionally, regeneration of NADPH pool appears to be important for *Pseudomonas putida* in the face of sublethal oxidative stress, and this has been linked to modified fluxes through the glycolytic and gluconeogenesis pathways (Nikel et al., 2021).

1.20 Objectives

Throughout this section, we have highlighted the key research that has prompted this project. Bacteria are important pathogens of beans but show temperature dependence in disease severity. Therefore, it is important to understand the reasons for this temperature dependence, both in terms of disease control and in understanding how climate change may affect agriculture in the future. We already know that temperature can affect plant immunity, but this may not be an important explanatory factor here, as bean is relatively heat tolerant. An alternative explanation would be that temperature could affect

bacterial virulence gene expression and mechanisms – and there is some evidence for this. One explanation that has not been explored in depth is whether plant pathogenic bacteria show temperature-dependent differences in stress tolerance and one of the most important stressors during plant-bacteria interactions is ROS. In this thesis, we aim to improve our understanding of temperature effects on plant disease development and outcome in the model pathogens Pspph and Pss. These pathogens are robust model organisms for plant pathology, and all evidence in the literature points towards relatively large effects of temperature, particularly for Pspph. Most of our available knowledge comes from a very limited number of well-characterised strains, and it is important to consider that phenotypic variation with respect to these traits may exist between related strains, both in the field and due to adaptation to the laboratory environment. The overarching aim of this project is improving our understanding of environmental effects on bacterial infections.

This project can be divided into four separate objectives:

i) Characterising the impact of temperature on Pss and Pspph

ii) Studying the cross-talk between temperature response and oxidative stress tolerance in Pspph,

iii) Characterising gene expression changes involved in the temperature and oxidative stress response

iv) Determining which factors may contribute to enhanced virulence in modern isolates of Pspph that have been newly genome-sequenced.

In chapter 3, I confirm observations from the field that have indicated that Pspph and Pss show differences in infection at different temperatures and find that *in vitro* oxidative stress tolerance appears to correlate with temperature responses for these pathogens. In chapter 4, we use transcriptomics to explore how temperature and ROS affect two model bacteria that show differences in

ROS tolerance at different temperatures. Finally, in chapter 5, we sequence modern halo blight isolates, determine their relatedness to other Pspph and build the foundations of a pipeline to identify the canonical set of Pspph effectors.

Chapter 2: Materials and Methods

2.1 Bacterial cultures

Unless otherwise stated, *Pseudomonas* cultures were typically grown in Luria Broth (LB) (Bertani, 1951), King's B (KB) (King et al., 1954), M9-glucose (Miller, 1972) or Mannitol-Glutamate (MG) (Keane et al., 1970) medium (Table 1.1), and incubated overnight in a Stuart orbital incubator S1500 or an Innova 4230 refrigerated incubator shaker at 220 rpm, 28°C. When needed, the medium was solidified with 1.2% agar, and resulting plates were incubated in a Sanyo static incubator MIR153 set at 28°C. *E. coli* cultures were typically grown in Luria Broth at 37°C in a Benchmark incu shaker 10LR or Innova 4230 refrigerated incubator shaker at 220rpm or on LB plates incubated at 37°C in a Gallenkamp cooled static incubator. All media were prepared using sterile milliQ (Elga Purelab Ultra) and when pH needed to be adjusted, it was measured using either the Fisher Scientific accumet AE150 or the Jenway 3540 pH and conductivity meter, which we assume give the same result given they are regularly calibrated.

Table 2.1: Medium recipes

1L KB broth:

- 20g Bacto™ proteose peptone #3 (Gibco, ThermoFisher Scientific)
- 1.5g K_2HPO_4
- 24ml 50% glycerol
- (+/- 12g agar)

Adjust to pH 7 with HCl/KOH

Autoclave

- 10ml 1M $MgSo_4$

1L MG broth:

- 10g mannitol
- 2g glutamate
- 0.5g KH_2PO_4
- 0.2g NaCl
- 0.2g $MgSo_4$
- (+/- 12g agar)

Adjust to pH 7 with HCl/KOH

Autoclave

1L LB broth:

- 10g tryptone
- 5g yeast extract
- 10g NaCl
- (+/- 12g agar)

Autoclave

1L MgCl2 (infiltration) buffer:

- 4g $MgCl_2$
- 4g MES pH 5.6

Adjust to pH 5.6 with KOH if needed

Autoclave

1L M9 medium:

- M9 salts:
- 6g Na_2HPO_4
- 3g KH_2PO_4
- 0.5g NaCl
- 1g NH_4Cl
- (+/- 12g agar)

Autoclave

- 0.1ml 1M $CaCl_2$
- 2ml 1M $MgSO_4$
- 20ml 20% glucose

2.2 Plant growth conditions

Phaseolus vulgaris (common bean) seeds of either the cultivar Canadian Wonder or TenderGreen (Kings Seeds Direct) were surface sterilised by bathing them in 70% ethanol for 1 min before thorough rinsing with ultrapure water. These were then germinated on soaked paper towels in petri dishes for 3-5 days until roots appeared. Germinated seeds were then transferred to 10x10 cm pots filled with a mixture of compost and vermiculite (volume ratio 4:1), with a single seed per pot. Pots were placed in trays covered by a transparent plastic cover to increase moisture, and these were placed in a greenhouse set at 22°C supplemented with artificial LEDs to a minimum of 12h light exposure (uncontrolled humidity). The plastic covers were removed once the cotyledons started to appear, typically after 5 days. Plants older than 10 days were given the support of a wooden cane, along which they were encouraged to

twine to prevent stem breakage. Plants were typically used between 7 and 30 days post germination depending on the experiment. Plants were always used before they reached the flowering and senescence stage.

2.3 Apoplast extraction

Plants were grown as described above. Because of seasonal variation in light availability, plants used were of slightly different ages but always had 3-4 sets of true leaves when harvested (and had no flowers). On the day of the apoplast extraction, plants were generously watered and left to transpire for 15-30 min. Then, leaves were carefully cut off the plant, cleaned of soil with ice cold water, patted dry with paper towels and weighed. They were then submerged in icy ultra pure water. A vacuum (Ashcroft Thomas Vacuum Pump model no. 2522C-02) was applied to allow water infiltration into the leaf apoplast – a vacuum had to be applied twice to maximise infiltration. Infiltrated leaves were then patted dry, and weighed again. The difference in weight was used to infer the infiltration volume of the extracted apoplast which in turn determines how diluted the apoplastic fluid is compared to in leaf (O'Leary et al., 2014). Leaves were then placed in centrifuge tubes and centrifuged at 1500xg for 10min at 4°C, minimum acceleration (Beckman Coulter Allegra X-15R centrifuge). The liquid at the bottom of the tube was collected and immediately frozen in liquid nitrogen. If the liquid had a brown or green tint, it was discarded because this is suggestive of cytoplasmic concentration: only clear apoplastic fluid (with a slight tinge of yellow green due to oxidation) was kept. The apoplastic fluid was then stored at -20°C until needed. When using the stored apoplast, it was defrosted gently on ice and used within a couple of hours to reduce oxidation.

2.4 Infection assay

Tendergreen bean plants were surface-sterilised, germinated and potted as described above. Once the cotyledons emerged, the plastic cover was removed and plants were transferred to a climate chamber (Percival model E -75L1) with strict conditions: 21 or 28°C, 70% relative humidity, 16h daylight, 8h lights off, lights turned on at 10am and turned off at 2am. A HOBO data logger (Onset) was used to monitor the real time climate condition during the infection assay and validate readings by the climate chamber itself. Plants were allowed to adapt to the new conditions for 4 days, after which their cotyledons were fully extended and the first true leaves were emerging. At 10am on the day of inoculation, plants were watered in excess to allow stomatal aperture. After 30min, cotyledons were syringe-infiltrated with bacterial suspension in $MgCl_2$ infiltration buffer or sterile $MgCl_2$ (see Table 2.1 for recipe). Areas surrounding the mid vein were mostly homogenously infiltrated.

The bacterial suspensions were made by picking and transferring bacteria from a trio of colonies from an LB-agar plate incubated at 28°C for 2 days into 15 ml sterile LB medium supplemented with 100µg/ml nitrofurantoin. The 15 ml were divided into 3 aliquots of 5 ml in 50 ml falcon tubes and incubated overnight at 28°C, 220rpm (New Brunswick Innova 4230 refrigerated incubator shaker). The saturated culture was then pelleted in a centrifuge (Beckman Coulter Allegra X-15R) at 3000xg rcf, room temperature, for 3 min. The supernatant was discarded and the pellet was resuspended in milliQ for washing. Centrifugation and washing was repeated another two times. Finally, the pellet was resuspended in $MgCl_2$ infiltration buffer and the OD_{600} was measured with the JenWay 7200 visible spectrum spectrophotometer using a VWR semi-micro cuvette. Bacterial suspensions were adjusted to OD 0.001 and were used to infiltrate plants with a needleless 10ml syringe within a two hour window. For each plant, a minimum of three inoculation zones were made (1 for each strain and a water control) on a maximum of two leaves (paired together) of the same age, and no more than 6 inoculation zones

were made on a single plant to prevent cross-contamination of inoculation zones. After infection, the plants were allowed to dry off back in their climate chambers at the temperature of interest. Then a first timepoint (at approximately 3-4hpi) was taken: leaf disks of 1 cm in diameter were bored out using a metal leaf borer. For each biological sample, 3 leaf disks from 3 different leaves were combined, and 3 biological samples were taken for each strain at each temperature and for each timepoint. Leaf disks were homogenised by placing them in sterile Eppendorf tubes with 800 µl sterile $MgCl_2$ and 3 stainless steel beads 3.2mm in diameter (Thistle) per tube, and placing the tubes in a tissue-lyser (Qiagen Tissuelyser II) at max speed for 3-4 round of 3min until the liquid was homogenous and green. The homogenate was then serial diluted with an electronic multichannel pipettor: 20µl homogenate into 180µl 10mM infiltration buffer $MgCl_2$ to final volume 200µl (i.e. 10x dilution), repeated serially 7 times. 10µl of each dilution was plated on LB-agar (LBA) plates supplemented with 100µg/ml nitrofurantoin. Plates were left to dry under a flow hood before incubating at 28°C for approximately 30 hours. Colonies were then counted and this data was recorded as bacterial load. Another two timepoints were taken, respectively 2 and 3 days post inoculation with the same set-up. This experiment was repeated independently three times.

2.5 Oxidative stress assay

Bacterial cultures were grown overnight from a single colony on an LB-agar plate inoculated into 5 ml LB in 50 ml falcon tubes at 28°C in shaking incubator (New Brunswick Innova 4230 refrigerated incubator shaker) at 220rpm. They were then pelleted at 3000xg for 3 min, washed in 10ml milliQ, pelleted again and resuspended in liquid cultures of interest (MG and KB). The OD_{600} was adjusted to OD 0.1 and 145µl of culture or sterile medium for the blanks was added to each well of a 96 wells plate. The 96 wells plates were incubated in the New Brunswick Innova 4230 refrigerated incubator shaker set to the

temperature of interest (21/28°C) and OD_{-600} was recorded every hour in a Tecan Infinite M200 plate reader. After 4h of growth, 5µl of 30X H_2O_2 stocks were added to wells to induce oxidative stress, and a corresponding 5µl of milliQ in the control wells. The final concentration of H_2O_2 reached is recorded in each figure, but it ranged from 0 to 150mM depending on the strain and the medium. The 96 well plates were then incubated again at the temperature of interest and OD_{600} was recorded every hour for another 4h. Finally, the 96-well plate was left to incubate overnight and a final timepoint of OD_{600} was recorded the next morning, 24h after the cultures started growing in a 96-well plate.

2.6 Plate reader data analysis

Unless otherwise stated, most datasets were reformatted and analysed using excel and R (using the R-studio interface). R packages tidyverse (Wickham et al., 2019), ggplot2 (Wickham, 2009) and their dependencies were typically used. Scripts can be found on github at https://github.com/JuliannaPiat/Thesis_figures .

2.7 Transcriptome sample preparation

Glycerol stocks of Pspph 1302A and Pss B728a were streaked on LBA plates supplemented with 100 µg/ml nitrofurantoin and left to incubate for 2 days at 28°C. A single colony for each strain was then grown in 10 ml LB in a 50 ml falcon tube overnight at 28°C in a shaking incubator (220 rpm, Innova 4230 refrigerated incubator shaker). The next day, the cell cultures were pelleted down in a centrifuge set at 3000xg rcf at room temperature (22°C) for 3min. The supernatant was discarded, cultures were resuspended in 10ml milliQ. This process was repeated another two times. The pellet was then

resuspended in MG medium, and each bacterial culture was adjusted to an OD_{600} of 0.1. Aliquots of 5ml of these cultures in MG in 50ml falcon tubes were incubated at the temperatures of interest (21 vs 28°C) in a shaking incubator (220rpm, Innova 4230 refrigerated incubator shaker) for 4h so that they were in early log phase. 50µl of 100X concentrated H_2O_2 stock diluted in milliQ water or just milliQ water was added to each culture. The final H_2O_2 concentrations were: 20mM for 1302A and 80mM for B728a. These were then allowed to incubate for another 30min before 10ml of RNAlater reagent (Invitrogen) was added to stabilise the RNA content. The tubes were then centrifuged at 3000xg rcf for 10min at 4°C. The supernatant was carefully removed and the pellet was flash frozen in liquid nitrogen and stored at -80°C until RNA extraction.

2.8 Transcriptome RNA extraction

Frozen pellets were resuspended in 600µl lysis buffer RLT plus from the RNeasy plus mini extraction kit (Qiagen) supplemented with 10ul/ml β-mercaptoethanol according to the manufacturer's instructions. This mixture was then vortexed for 1min, and then first loaded through a gDNA column to remove the bulk of the genomic DNA. The runoff was then mixed with 600µl of 70% ethanol and loaded onto a RNA spin column. After centrifuging for 1min at 9000xg rcf on a benchtop centrifuge (Fisher Scientific accuSpin Micro17) the runoff was discarded and the column was treated with 80µl DNAse I in buffer (RNAse-free DNAse kit, Qiagen) according to the manufacturer's specifications. The DNAse treated column was incubated for 20 min at 28°C and then the column was washed as per the manufacturer's recommendations. Finally, the RNA was eluted from the column with 50µl 37°C ultra pure DEPC-treated water into a fresh nuclease-free eppendorf tube. The eluate was then treated with Turbo DNAse (Turbo DNA-free kit, Invitrogen) according to the company's instructions: 1.5µl Turbo DNAse was added to each sample as well as the required buffer, and samples were incubated at 37°C for 20min, before another

1.5µl DNAse was added and a second incubation period at 37°C for 30min. The DNAse was then inactivated with 0.2 volume of deactivation beads incubated in the samples for 5min and centrifuged at 17000xg rcf, RT. The supernatant was transferred to a new nuclease-free Eppendorf tube. The concentration and purity of the RNA was checked using a Nanodrop spectrophotometer and the Qubit's RNA and DNA HS quantification kit. The levels of DNA and protein contaminants were still too high so the Turbo DNAse treatment was repeated. The RNA was purified from the resulting mixture using the RNeasy plus kit. For this clean-up step, fresh columns were used with an extra washing step with RPE buffer for a total of 3 washes instead of 2. Furthermore, I incubated the samples in RW1 wash buffer for 5min instead of centrifuging straight away. To counter the potential reduction of RNA concentration from this second step, RNA was eluted in a lower volume than in the first round - volume 35µl. RNA was then quantified using the Qubit and Nanodrop, the levels of protein and DNA contamination were also measured by the Nanodrop (ThermoScientific Nanodrop One) and the Qubit (Invitrogen Qubit 4 Fluorometer) (see table 2.3). Samples were then frozen and stored at -80°C until they were sent for sequencing. As per the sequencing company's requirements, only samples which had A260/280 and A260/230 ratios above 2, more than 500 ng RNA total and ≥ 6.0 RNA integrity number were sent for sequencing. To check that the DNA had been removed from the samples, a sample that had fit these readings on the nanodrop and Qubit and could have been sent for sequencing was treated with RNAse and then loaded onto an agarose ethidium bromide gel to double check for DNA contamination. No DNA bands were detected in the sample even though 8µl were loaded. This together with the Nanodrop and Qubit readings, confirmed that sample quality was high enough for sequencing.

2.9 Transcriptome RNA sequencing

A total of 34 samples were sent to Novogene on dry ice for sample QC and sequencing: 24 samples and 10 extra substitute samples. Two samples failed the QC check (j9 and j14) and were thus replaced by their corresponding substitute. The 24 samples (table 2.2) were then sequenced by the company.

Table 2.2: RNA samples specifications.

Sample Name	Species Latin Name	Strain	H2o2 level (mM)	Temperature (°C)	Concentration (ng/ul)	Total amount RNA (ug)	A260/A280	A260/A230	Integrity value	QC Results	Nucleic Acid ID
j2	*Pseudomonas syringae*	B728a	0	21C	62	1.364	2.097	2.297	9	Pass	FKRN220179391-1A
j5	*Pseudomonas savastanoi*	1302a	0	28C	75	1.95	2.037	1.74	6.8	Pass	FKRN220179394-1A
j6	*Pseudomonas syringae*	B728a	80	28C	62	1.612	2.069	2.058	8.8	Pass	FKRN220179395-1A
j10	*Pseudomonas syringae*	B728a	0	28C	90	1.98	2.085	2.157	9.2	Pass	FKRN220179399-1A
j11	*Pseudomonas syringae*	B728a	80	21C	64	1.472	2.084	1.706	9.1	Pass	FKRN220179400-1A
j12	*Pseudomonas syringae*	B728a	80	28C	68	1.564	2.107	2.23	9.1	Pass	FKRN220179401-1A
j13	*Pseudomonas savastanoi*	1302a	20	28C	52	1.56	2.102	2.554	7.1	Pass	FKRN220179402-1A
j15	*Pseudomonas savastanoi*	1302a	20	21C	46	1.288	2.1	2.083	7.6	Pass	FKRN220179404-1A
j17	*Pseudomonas syringae*	B728a	0	28C	195	4.875	2.099	2.221	9.5	Pass	FKRN220179406-1A
j18	*Pseudomonas savastanoi*	1302a	0	28C	56	1.568	2.002	1.658	7.7	Pass	FKRN220179407-1A
j19	*Pseudomonas savastanoi*	1302a	20	21C	94	2.632	2.012	1.687	8.3	Pass	FKRN220179408-1A
j20	*Pseudomonas syringae*	B728a	0	21C	162	4.374	2.108	2.569	9.8	Pass	FKRN220179409-1A
j21	*Pseudomonas savastanoi*	1302a	20	28C	83	2.324	2.112	2.097	7.8	Pass	FKRN220179410-1A
j22	*Pseudomonas syringae*	B728a	80	21C	178	4.628	2.126	2.399	9.3	Pass	FKRN220179411-1A
j24	*Pseudomonas syringae*	B728a	80	28C	182	4.55	2.115	2.515	9.5	Pass	FKRN220179413-1A
j25	*Pseudomonas savastanoi*	1302a	0	21C	91	2.639	2.096	2.547	8.8	Pass	FKRN220179414-1A
j26	*Pseudomonas syringae*	B728a	0	21C	78	2.262	2.089	2.429	9.6	Pass	FKRN220179415-1A
j27	*Pseudomonas savastanoi*	1302a	0	21C	107	3.317	2.093	2.564	8.9	Pass	FKRN220179416-1A
j28	*Pseudomonas syringae*	B728a	80	21C	43	1.075	1.806	0.981	9.4	Pass	FKRN220179417-1A
j29	*Pseudomonas savastanoi*	1302a	20	21C	83	2.075	2.099	2.572	9	Pass	FKRN220179418-1A
j30	*Pseudomonas syringae*	B728a	0	28C	109	2.834	2.103	2.562	9.8	Pass	FKRN220179419-1A
j31	*Pseudomonas savastanoi*	1302a	0	28C	47	1.175	1.881	1.118	7.9	Pass	FKRN220179420-1A
j32	*Pseudomonas savastanoi*	1302a	0	21C	92	2.668	2.113	2.169	8.7	Pass	FKRN220179421-1A
j34	*Pseudomonas savastanoi*	1302a	20	28C	92	2.3	2.149	2.13	8.1	Pass	FKRN220179423-1A

Library preparation and paired-end sequencing 250bp Illumina sequencing was performed by the company according to their company policy: Ribosomal RNA was removed using the Illumina Ribo-Zero Plus rRNA Depletion Kit, followed by ethanol precipitation. The remaining RNA was then fragmented and the first strand cDNA was synthesized using random hexamer primers. During the second strand cDNA synthesis, dUTPs were replaced with dTTPs in the reaction buffer. The sequencing library was made using Novogene's NGS Stranded RNA Library Prep Set (PT044) which includes end-repair, A-tailing, adapter ligation, size selection USER enzyme digestion, amplification and purification. For this library, the size selection was between 250 and 300bp. Finally, pooled Illumina sequencing was performed on this library.

2.10 Transcriptome data analysis

RNA sequencing data was first processed using kallisto version 0.48.0 (Bray et al., 2016). Details of the code used can be found in github, link to the repository here: https://github.com/JuliannaPiat/Psy_RNAseq_screen . K-mers derived from reads were pseudo-aligned to their genomic sequence (1302A assembly GCF_001294025.1 and B728a assembly GCA_000012245.1 respectively) and the TPM (transcripts per million) was recorded. This quantified data was analysed and graphed using DeSeq2 version 1.36.0 (Love et al., 2014) from Bioconductor 3.15 on R version 4.2.1. DeSeq2 was used to calculate the log2 fold change (L2FC) between treatments and the L2FC was used as the quantitative measure of gene expression change for the rest of the data analysis. DeSeq2 also calculated the corresponding P-value associated with the L2FC, and this P-value adjusted to reduce false discovery rate using the Benjamini-Hochberg Procedure was the P-value used for determining significance. Genome and Proteome annotations from NCBI, KEGG and Pseudomonas.com were used to

identify transcripts by locus name. In the case of Pspph 1302A, annotations from Pspph 1448A were mostly used because 1448A is the reference genome for Pspph in these databases. A list of orthologues shared by Pspph 1448A and B728a was obtained from Pseudomonas.com and used as the reference for orthologue pairs when comparing gene expression between our strains. A PCA analysis was conducted for the transcriptome datasets for each strains, using R's base function prcomp. The data was centered around the origin and transformed with a variance stabilising transformation vst (DeSeq2) prior to PC calculations to meet the assumptions of the PCA.

2.11 Field strain isolation and *in planta* phenotyping

Deidre Fourie and Felix Homma isolated strains from bean fields in various South African locations (figure 5.4) in 2017-2018 following the methodology published in (Fourie, 1998). Mature leaves of bean plants (*Phaseolus vulgaris* multiple cultivars) with halo blight symptoms were collected from fields. Prior to isolation, pods and leaves were rinsed under running tap water for 10 min and then surface sterilized by soaking material for 3 min in 3.5% sodium hypochlorite and rinsing it twice in sterile water for 1 min each. Bacteria were isolated using the method of (Hildebrand, 1988) and streaked onto King's B medium. After incubation for 48 hr, fluorescent colonies were selected and purified on King's B medium by a series of single colony transfers.

Following their isolation, the strains were inoculated onto healthy plants following methodology published in (Fourie, 1998). The race, systemic infections and local infection scores are recorded 10 dpi.

Local infection score:

1. red-brown necrotic reaction in the area of maximum inoculation either side of the leaf midrib (highly resistant)

2. red-brown necrotic reaction with a trace of water-soaking (resistant)
3. some necrosis but more extensive water-soaking largely confined to the area of maximum inoculation (slightly susceptible)
4. small water-soaked lesions (< 1mm diameter) distributed at random over the leaf undersurface (susceptible)
5. large water-soaked lesions (1-3 mm diameter) distributed at random over the leaf undersurface (fully susceptible)

Systemic infection classification:

A) typical halo blight symptoms on trifoliate leaf (necrosis with surrounding halo of chlorosis)
B) chlorosis that covers whole trifoliate leafs and wrinkled surface, no water soaking, no necrosis on leaves other than the directly inoculated ones
C) stunted growth, full chlorosis of trifoliate leaves and water soaking. C) is dominant over A) and B) and leads to death of the host plant
D) red colour on veins and internodes, high level of systemic infection

P. savastanoi pv. *phaseolicola* is organised in races according to which *P. vulgaris* cultivars the strain is able to infect without causing HR. In order to determine the race of the field isolates, the strains were inoculated onto the following cultivars: Canadian Wonder, A52, TenderGreen, Red Mexican, A53, A43 and Guatemala. Strains that successfully infected all 7 cultivars were classified as race 6 (no race-specific resistance in *P. vulgaris*) (see figure 2.1).

	Race								
Cultivars	1	2	3	4	5	6	7	8	9
Canadian Wonder	+	+	+	+	+	+	+	+	+
ZAA54 (A52)	+	+	+	+	-	+	+	+	+
TenderGreen	+	+	-	-	+	+	+	+	+
Red Mexican UI3	-	+	+	+	-	+	-	+	-
1072	+	-	+	-	-	+	-	+	+
ZAA55 (A53)	+	+	-	-	-	+	+	+	+
ZAA12 (A43)	+	-	-	-	-	+	-	-	-
Guatemala 196-B	-	+	-	-	-	+	-	+	-

Figure 2.1: Race structure classification of *Pseudomonas savastanoi* pv *phaseolicola* (adapted from (Taylor et al., 1996)). A plus sign denotes compatible interaction, a minus sign denotes incompatible infection.

2.12 Field strains genome sequencing

A subset of 24 strains (see table 2.3) were selected from the panel of strains isolated by Deidre Fourie's team to be sequenced. The genomic DNA was extracted using Qiagen's DNA extraction kit following the manufacturer's recommendations but replacing the elution buffer with ultra pure water warmed to 50°C. The genomic DNA was quantified using a Nanodrop spectrophotometer and then sent to the MicrobesNG sequencing company for whole genome sequencing (Illumina sequencing 2x250bp, 30x coverage).

Table 2.3: List of field isolates sequenced in this study

Strain name	Isolation Location	Isolation date	Isolation Cultivar	race	Sequencing date	reference
Pspph isolate 6.1	Middelburg, South-Africa	18/01/2018	Black Wonder	8	2021	this study
Pspph isolate 43.2	Vaalharts, South-Africa	27/02/2017	ND, Phaseolus vulgaris	6	2021	this study
Pspph isolate 91.1.2	Cedara, South-Africa	15/02/2018	ND, Phaseolus vulgaris	6	2021	this study
Pspph isolate 92.3	Cedara, South-Africa	15/02/2018	ND, Phaseolus vulgaris	6	2021	this study
Pspph isolate 33.1	Middelburg, South-Africa	18/01/2018	Colorado del Pais	1	2021	this study
Pspph isolate 4.1	Middelburg, South-Africa	18/01/2018	Kabuku	1	2021	this study
Pspph isolate 12.2.1	Middelburg, South-Africa	18/01/2018	PI209815	1	2021	this study
Pspph isolate 51.1.1	Middelburg, South-Africa	31/01/2018	AC Calmont	1	2021	this study
Pspph isolate 80.2.2	Petrus Steyn, South-Africa	13/02/2018	Pan9292	8	2021	this study
Pspph isolate 81.1	Petrus Steyn, South-Africa	13/02/2018	Sedeberg	8	2021	this study
Pspph isolate 69.1	Sarclet, South-Africa	13/02/2018	Pan9292	6	2021	this study
Pspph isolate 46.3.3	Middelburg, South-Africa	31/01/2018	ND, Phaseolus vulgaris	6	2021	this study
Pspph isolate 61.2	Vaalharts, South-Africa	27/02/2017	PIC-273	6	2021	this study
Pspph isolate 67.2	Sarclet, South-Africa	13/02/2018	ND, Phaseolus vulgaris	6	2021	this study
Pspph isolate 47.1.2	Middelburg, South-Africa	31/01/2018	ND, Phaseolus vulgaris	6	2021	this study
Pspph isolate 47.3.2	Middelburg, South-Africa	31/01/2018	ND, Phaseolus vulgaris	6	2021	this study
Pspph isolate 18.2	Middelburg, South-Africa	18/01/2018	Kablanketi	6	2021	this study
Pspph isolate 18.3	Middelburg, South-Africa	18/01/2018	Kablanketi	6	2021	this study
Pspph isolate 24.1	Middelburg, South-Africa	18/01/2018	Lushala	6	2021	this study
Pspph isolate 2.2	Middelburg, South-Africa	18/01/2018	Sodan	6	2021	this study
Pspph isolate 2.3	Middelburg, South-Africa	18/01/2018	Sodan	6	2021	this study
Pspph isolate 3.1	Middelburg, South-Africa	18/01/2018	Maalasa	6	2021	this study
Pspph isolate 10.2	Middelburg, South-Africa	18/01/2018	Blush	6	2021	this study
Pspph isolate 97.2.2	Warden, South-Africa	16/02/2018	ND, Phaseolus vulgaris	6	2021	this study

2.13 Bioinformatics analysis

Pseudomonas savastanoi and related genomes were obtained from the NCBI database on the 20th January 2022. All the genomes labelled as "Pseudomonas" available at NCBI were downloaded and a total of 29056 genomes were run through Pyani version 0.3.0a0 (Pritchard et al., 2016) to calculate the ANI score (average nucleotide identity) using the whole genome. Accessions with more than 95% identity and 50% coverage with our reference genome Pspph 1302A were retained as *Pseudomonas savastanoi* candidates and the others were dropped from further analysis with the exception with a few strains chosen as model outgroups.

As proof of concept, a first phylogeny was built of the *Pseudomonas* as whole, including the 24 newly sequenced South African strains, 11 model strains representative of Pspph, and 19 outgroup reference strains (see the full list in figure 5.1) chosen to be representative of the diversity of the *Pseudomonas* clade. In order to build a phylogenetic tree of this panel, an alignment was necessary. To streamline computation, the genomes were run through prodigal (v.2.6.3) to predict proteomes. The generated proteomes were analysed using OrthoFinder version 2.5.4 (Emms and Kelly, 2019, Emms and Kelly, 2015) to identify single copy orthologues shared by all strains. These orthologue sequences (henceforth referred to as "the core genome") were concatenated and aligned using MAFFT version 7.313 (Katoh et al., 2002). The alignments were then threaded back onto the known coding sequences from the genomes using T-COFFEE v.12.00 (Notredame et al., 2000). These were then used to reconstruct phylogeny with RAxML v8.2 (Stamatakis, 2014) to generate a maximum likelihood tree with 100 bootstraps. A partition was used to ensure a separate evolutionary/substitution model was fitted for each individual coding sequence. Having confirmed that this generated phylogenetic tree was consistent

with previously published phylogenies of *Pseudomonas*, we modified this pipeline in order to better resolve the intraspecific phylogeny of Pspph.

A total of 294 strains were used for a second, more detailed phylogenetic tree, including 262 *Pseudomonas savastanoi* candidates identified previously, all 24 newly sequenced South African strains and 8 representative outgroup strains that were chosen from the original set for their relative closeness to the Pspph strains in the first phylogeny built: *P. syringae pv syringae* B728a, *P. syringae pv aptata* P21, *P. syringae pv mellea* ICMP5711, *P. syringae pv amygdali* ATCC11528, *P. syringae pv meliae* N6801, *P. syringae pv maculicola* KN91, *P. savastanoi pv savastanoi* NCBP3335 and ICMP13519. In order to build a phylogenetic tree of this panel, an alignment was necessary. To streamline computation, the genomes were run through prodigal (v.2.6.3) to predict proteomes. The generated proteomes were analysed using OrthoFinder version 2.5.4 (Emms and Kelly, 2019, Emms and Kelly, 2015) to identify single copy orthologues shared by all 294 strains. These orthologue sequences (henceforth referred to as "the core genome") were concatenated and aligned using MAFFT version 7.313 (Katoh et al., 2002). A total of over 200 000 sites were taken forward for phylogenetic reconstruction. The alignments were then threaded back onto the known coding sequences from the genomes using T-COFFEE v.12.00 (Notredame et al., 2000). These were then used with RAxML v8.2 (Stamatakis, 2014) to generate a maximum likelihood tree with 100 bootstraps. . A partition was used to ensure a separate evolutionary/substitution model was fitted for each individual coding sequence. Due to the size of the dataset used, inference of complete ancestral recombination was prohibitively difficult, and we expect that there are essentially no loci unaffected by recombination in this set (Sakoparnig et al., 2021) so that sites of recombination could not be excluded from the analysis. In the case of the first, smaller tree, the diversity of strains used means that this is a deep-rooting tree. As such, recombination cannot be inferred as recent evolutionary history is a prerequisite for inference tools (Croucher et al., 2015). As a result, neither of these

phylogenetic trees are reconstructions of clonal phylogeny, but instead largely reflect population structure and distributions of recombination rates amongst lineages.

The code used in this pipeline to compute the ANI score, alignments and draw the phylogenetic trees is available on github at https://github.com/JuliannaPiat/WGS_Phylogenetic_Tree_2022.

Identification of T3SS effectors and classification based on their effector family was mostly done in python version 3.10.6 and bash. The set of scripts is available on github, under this repository: https://github.com/JuliannaPiat/find_effectors . All effector protein sequences available at NCBI with the descriptor “Pseudomonas” and “T3SS effector” were downloaded on 09/12/22. The descriptors for these sequences were mined with a regex search for known effector names (eg. HopQ, AvrPPhB etc) and annotated sequences were preliminarily grouped together by annotated effector family as determined from the sequence description string. Sequences from each effector family were aligned using MAFFT version 7.313 and run through HMMER version 3.1b2 (hmmer.org) to build a HMMER profile. The training set (effectors already assigned an effector family) were queried against their own HMMER profile to define the threshold value for membership as the smallest bit score value obtained for each set. The rest of the effectors (those which had no recognizable effector family name in the description string) were then queried against the HMMER profiles, and sequences with a bit score higher than the previously defined threshold value were moved to the corresponding effector family group. A new expanded HMMER profile was then built using these newly expanded groups for each effector family. To identify T3SS effectors in the newly sequenced South African strains, we used prodigal to predict their proteome and then queried protein sequences against each effector family HMMER profile using the threshold bit score for each profile to determine effector family membership. Finally a heatmap of effectors detected in each strain of interest was built by calculating distance matrices using clustal omega (clustalo) version 1.2.4 (Sievers and Higgins, 2018, Sievers et al., 2011) and rendering a visual representation of the distance matrix using seaborn v.0.11.1 (Waskom, 2021).

I also determined if orthologues of the phaseolotoxin cluster were present in the same genomic conformation (i.e. syntenously) in the same set of strains using FlaGs (Saha et al., 2021).

2.14 Oxired quantification of reactive oxygen species

In order to quantify reactive oxygen species *in vitro*, we used a fluorometric and colorimetric dye, amplex red (previously called oxired). The dye was used as part of the Amplex Red Hydrogen Peroxide/Peroxidase assay kit from Invitrogen, following manufacturer's instructions. Samples of interest containing hydrogen peroxide (which was added exogenously so we knew what the starting hydrogen peroxide concentrations were) were transferred to a black 96 well plate (Costar) and each sample was diluted 1/10 (5µl in total of 50µl) serially in the kit's buffer until the predicted hydrogen peroxide levels were in range of up to twice the amplex red quantification threshold (between 0.1µM and 5µM). Adding the dye reagent mix led to a final ½ dilution (50µl in total of 100µl) and the fluorescence and absorbance at 560nm was immediately recorded in a Tecan Infinite M200 plate reader after mixing by pipetting. If the signal was low (similar to the water control), the dye was added to the next dilution down (10x more concentrated), I mixed by pipetting and recorded the fluorescence and absorbance again. This is because we expect that hydrogen peroxide gets degraded very quickly in some samples, and therefore the predicted hydrogen concentration is often overestimated. The reason that we do not use the dye on all dilutions for all treatments is due to the high cost of the dye, and the need for speed as the dye is photosensitive and susceptible to air oxidation. Every time a new batch of dye-reagent mix was made, a calibration curve was built anew, by recording fluorescence and absorbance of the dye in the absence of hydrogen peroxide, and in three concentrations (0.1µM, 1µM and 5µM) of hydrogen peroxide in ultra pure water. This calibration curve together with the dilution coefficient was used to estimate the level of reactive oxygen species in samples in standard units (mM).

2.15 Viability assay

Pspph 1302A and Pss B728a were streaked from glycerol stock onto LBA plates and grown for 2 days at 28°C. From these plates, a single colony for each strain was picked and transferred to 5ml LB in a 50ml falcon tube which was incubated overnight at 28°C in a shaking incubator. The culture was centrifuged at 3500xg for 3min, the supernatant was discarded and the pellet was resuspended in 10ml milliQ. The centrifugation was repeated and the supernatant was again discarded. Then the washed pellet was resuspended in the medium of interest (MG or KB), and the OD_{600} was adjusted to 0.1. 145µl of bacterial culture per well was transferred to a clear Corning 96 well plate (flat-bottom, low evaporation lid). There were three replicates (so three wells) for each strain, each medium and each H_2O_2 treatment (including the water control). The plate with the lid on was then incubated at the temperature of interest (28°C or 21°C) for 4h in a shaking incubator. After 4h of growth, the OD_{600nm} was recorded and 5µl 30x concentrated H_2O_2 to reach the desired concentration was added to each well, or 5µl of milliQ for the water control. Cultures were then swiftly mixed by pipetting and samples were then serially diluted 7 times. For each dilution, 20µl of culture/upper dilution was added to 180µl milliQ (so a 1/10 dilution) and mixed by pipetting 80µl up and down 25 times. Fresh tips were used for each new dilution. To ensure speed, a maximum of 12 samples were done simultaneously, the maximum capacity of our multichannel pipette. 20µl of each dilution and each sample was dropped on LBA plates and left to dry (approximately 10-30min). These LBA plates were then incubated at 28°C for ca. 24-36h until colonies were big enough to count. Colony count was only recorded when colonies could be distinguished from each other without doubt. The number of live and viable bacteria was then calculated from the colony count and the dilution factor.

2.16 Hydrogen peroxide challenge on bacteria in biofilms

Glycerol stocks of Pspph 1302A and Pss B728a were streaked on LBA plates and left to incubate for 2 days at 28°C. A single colony for each strain was then grown in 10 ml LB in a 50 ml falcon tube overnight at 28°C in a shaking incubator (220 rpm, Innova 4230 refrigerated incubator shaker). The next day, the cell cultures were pelleted down in a centrifuge set at 3500xg rcf at room temperature (22°C) for 3min. The supernatant was discarded and the remaining pellet was resuspended in 10ml milliQ. The mixture was centrifuged again at 3500xg for 3min and the supernatant was discarded again. The pellet was then resuspended in the medium of interest (KB or MG), and each bacterial culture was adjusted to an OD_{600} of 1. 300ul of the resulting bacterial culture was evenly applied to sterile petri dishes (n=3) filled with either set KB-agar or set MG-agar using a flat spreader until the plate was dry. A piece of round dry sterile filter paper with a 1cm radius was placed in the center of each inoculated plate. 200µl of hydrogen peroxide solution at concentration of interest (9.8M or 980mM) or milliQ was dripped directly onto the filter paper so that the filter paper was soaked with the solution. The plates were then stacked with the lid still on the top (unlike usual) to keep the filter paper from moving or falling off. To prevent dehydration of the plates, they were double-coated in plastic film before being transferred to a static incubator set at the temperature of interest (21°C or 28°C). The incubator was covered so that the plates were not exposed to light. Plates were incubated for 48h before the diameter of the inhibition zone lacking bacterial growth was recorded.

2.17 Motility assay: swimming

Pspph 1302A and Pss B728a were streaked from glycerol stock onto LBA plates and grown for 2 days at 28°C. From these plates, a single colony for each strain was picked and transferred to 5ml LB in a 50ml

falcon tube which was incubated overnight at 28°C in a shaking incubator. Separately, soft agar plates were made by making KB medium with 0.25% agar instead of the usual 1.2%. These plates were kept unstacked and unflipped with their lid on top and left to dry overnight under a plastic film. The next morning, the overnight culture was centrifuged at 3500xg for 3min at room temperature, the supernatant was discarded and the pellet was resuspended in 10ml 10mM KPO_4 solution. The centrifugation was repeated and the supernatant was again discarded. Then the washed pellet was resuspended in 10mM KPO_4, and the absorbance was adjusted to OD_{600}=1. A sterile (autoclaved) toothpick was dipped in the bacterial inoculum and immediately stabbed in the centre of a soft agar plate. This was done on three plates for each strain and each temperature. The plates were then wrapped in plastic film and incubated in a dark static incubator for 48h at the temperature of interest (28°C or 21°C). The diameter of bacterial swimming was recorded and pictures of each plate were taken.

2.18 Motility assay: Swarming

Pspph 1302A and Pss B728a were streaked from glycerol stock onto LBA plates and grown for 2 days at 28°C. From these plates, a single colony for each strain was picked and transferred to 5ml LB in a 50ml falcon tube which was incubated overnight at 28°C in a shaking incubator. Separately, soft agar plates were made by making KB medium with 0.4% agar. These plates were kept unstacked and unflipped with their lid on top and left to dry overnight under a plastic film. The next morning, the overnight culture was centrifuged at 3500xg for 3min at room temperature, the supernatant was discarded and the pellet was resuspended in 10ml 10mM KPO_4 solution. The centrifugation was repeated and the supernatant was again discarded. Then the washed pellet was resuspended in 10mM KPO_4, and the OD was adjusted to OD_{600}=1. Each plate was inoculated by pipetting 5µl of bacterial culture in the centre. This was done on three plates for each strain and each temperature. The plates were then wrapped in plastic film and

incubated in a dark static incubator for 24h at the temperature of interest (28°C or 21°C). The diameter of bacterial swarming was recorded and pictures of each plate were taken.

Chapter 3: Characterisation of the effects of temperature and oxidative stress on bacterial pathogens of common bean

3.1 Introduction

An understanding of bacterial diseases of plants is key to tackling the current food security crisis, as bacterial and other plant pathogens cause substantial yield loss yearly. In the case of common bean, yield loss due to bacterial diseases is not well-recorded because records typically group all dry beans together, which include species other than *Phaseolus vulgaris*, and excludes some varieties of common bean such as French/green beans (FAO, 2019). However, the information available suggests that yield loss caused by bacterial diseases are substantial worldwide and can vary drastically vary depending on the weather that year (Muedi et al., 2015, Fourie, 2002). For instance, common blight caused by *Xanthomonas axonopodis* pathovar *phaseoli* (Xap) is estimated to cause 10-40% yield loss on susceptible cultivars in Ethiopia but it becomes more destructive when it is exposed to extended periods of humid warm weather (Degu et al., 2020). Brown spot caused by *Pseudomonas syringae* pv. *syringae* (Pss) is also more severe in this weather in South Africa. By opposition, halo blight caused by *Pseudomonas savastanoi* pv *phaseolicola* (Pspph) is favoured by cool temperatures and humid weather (Fourie, 2002). This raises the question: how does temperature affect bacterial virulence?

In this study, we focused our work on Pspph and Pss because they appear to be affected differently by environmental conditions but are nevertheless close relatives, both belonging to the plant-pathogenic *Pseudomonas* clade (Gardan et al., 1999). Furthermore, they have been documented to frequently co-infect plants (Fourie, 2002). Finally, plant-pathogenic *Pseudomonas* are well-studied model organisms

with pre-existing genomic data (Arnold et al., 2011, Feil et al., 2005) and they are easy to maintain in lab conditions unlike Xap. Altogether, these elements make them an ideal model pair for comparison to study the effect of temperature on bacterial plant pathogens.

3.1.1 Temperature affects bacterial growth rate

As described in the general introduction, temperature has a substantial effect on growth rate of Pss and Pspph. While the optimum temperature for growth *in vitro* of members of the PSSC is generally assumed to be 28°C, it is still unclear if this is the case for Pss and Pspph, and if this temperature optimum extends to *in planta* conditions. This gap in the literature highlights how understudied temperature is as a factor affecting phytopathogens. From the literature available, we can approximate that Pss and Pspph should grow faster at 28°C than at 21°C.

3.1.2 Discrepancy between expected and observed effects of temperature on bacterial virulence

Assuming 28°C is close to the optimum temperature for our strains, we should expect to find that our pathogens grow faster and are therefore more virulent at this temperature. However, this pattern does not hold true in reality: halo blight incidence is higher at colder temperatures than 28°C and more severe following cool nights (15-16°C), while brown spot starts to appear when day-time temperatures reach 28°C and above in fields in South Africa (Fourie, 2002). This is particularly striking because these two strains are closely related. This indicates that temperature effects on growth rate are not solely responsible for the observed difference in disease development.

Please note however, that environmental temperatures are not necessarily reflective of temperatures experienced by the bacteria *in planta*. Indeed, the plant host regulates its internal temperature to

escape lethal temperatures. For example, in gerbera flowers grown under greenhouse conditions, leaf temperature increases with ambient temperature until a certain threshold point at which the plant appears to keep the leaves at temperatures below 30°C presumably via stomatal air exchanges (Ganguly and Bauri, 2014). Whilst internal temperature regulation by the plant is complex and multifactorial (Inamullah and Isoda, 2005), this suggests that in moderate temperature ranges, we can approximate that the bacteria experience warmer temperatures when the ambient air is warmer. What is the available evidence that they respond to this cue?

3.1.4 Bacterial motility is affected by temperature

An often overlooked aspect of bacterial pathogenicity is motility. Flagellum-based motility is important to colonisation of the leaf for Pspph in bean leaves (Panopoulos and Schroth, 1974). Similarly, hypermotility (rapid swarming-like movement) is beneficial to Pss B728a virulence on bean leaves (Quinones et al., 2005). Interestingly, motility is also temperature-regulated in Pss B728a: swarming motility is suppressed between 28°C and 30°C (Hockett et al., 2013). Motility is co-regulated with quorum sensing and alginate production and has been shown to be important for tolerance to stressors such as hydrogen peroxide (Quinones et al., 2005). Genes involved in motility were also downregulated at 28°C compared to at 18°C in Pspph NS3121 (Arvizu-Gomez et al., 2013). However, motility is not the only trait known to be important for bacterial virulence *in planta*.

3.1.5 Temperature affects expression of the T3SS

The Type 3 secretion system (T3SS) of bacteria is responsible for secretion of most effectors required for virulence *in planta* and is therefore a key aspect of phytopathogenicity. Furthermore, plant pathogen's response to environmental cues such as temperature, presence of antimicrobials and nutrient availability

is known to be integrated to promote pathogenicity and survival in the apoplastic space through the hrp regulon - the pool of coregulated virulence factors in *Pseudomonas* spp - (Xiao et al., 1992). Indeed, a study comparing the transcriptome of Pspph NPS3121 *in vitro* at 18 and 28°C found that the T3SS is downregulated at the lower temperature (Arvizu-Gomez et al., 2013). In Pss B728a, 18 T3SS genes were transcriptionally induced by warm temperatures (30°C), and none were cold (20°C) induced *in vitro* (Hockett et al., 2013). Nevertheless, the exact mechanism underlying this response is still undescribed. A better studied case is temperature-regulation of phytotoxin production.

3.1.6 Phytotoxin production is temperature-regulated

Phytotoxins are small molecules produced by a pathogen to increase its own pathogenicity or virulence. Of these, phaseolotoxin is one of the most striking examples of temperature being the major factor regulating gene expression. Indeed, phaseolotoxin is only produced by Pspph at temperatures below 28°C, with a peak of production at 18°C-20°C (Bender et al., 1999, Aguilera et al., 2017). This regulation has been strongly suggested to be due to a temperature responsive element (TRR) in the regulon of the phaseolotoxin gene cluster (Rowley et al., 1993, Rowley et al., 2000). It is particularly interesting because phaseolotoxin is responsible for the halo-like chlorotic lesions that gave Pspph the name of halo blight. Indeed, phaseolotoxin inhibits (irreversibly *in planta*) an enzyme of the urea cycle, thus leading to chloroplast death (Chen et al., 2015, Langley et al., 2000). Phaseolotoxin being preferentially produced at cooler temperatures would certainly contribute to Pspph's higher virulence at those temperatures. However, syringomycin and syringopeptin, the phytotoxins that Pss predominantly produces are similarly more abundant at 20°C than at 28/30°C (Hockett et al., 2013, Sinden et al., 1971). Given that Pss severity is worse in warm weather, this indicates that phytotoxin thermoregulation cannot alone explain temperature effects on bacterial virulence and disease severity. Furthermore, it is not clear

whether this temperature regulation of phaseolotoxin production is a cause or a consequence of Pspph's preference for cooler weather. Furthermore, phaseolotoxin and syringopeptin/syringomycin exhibit broad range toxicity (Sinden et al., 1971). It has been hypothesised that these phytotoxins play a broader role, not just as plant immunity inhibitors but also as antimicrobial agents (Sinden et al., 1971) against other microorganisms associated with the plant host: epiphytes, endophytes, and fellow pathogens so their regulation may be made more complicated by this dual function.

3.1.7 Plant pathogens are exposed to ROS during infection

Upon detection of pathogens, all plants display basal immunity. A key component of this is the production of reactive oxygen species (ROS): mainly hydrogen peroxide H_2O_2 and superoxides. ROS accumulation is lethal or inhibitory to bacteria growth (Van Acker and Coenye, 2017). Downtuning of plant immunity, detection, evasion and ROS detoxifying are all common strategies that plant pathogens take to avoid this (Fones and Preston, 2012). As a result, reactive oxygen species are central to plant-pathogen interactions. Interestingly, while Pspph transcription of T3SS elements is downregulated at low temperatures (18°C) and therefore may not contribute to the enhanced virulence of Pspph *in planta* at those temperatures, oxidative stress responses and motility are upregulated in Pspph at 18°C (Arvizu-Gomez et al., 2013). We therefore hypothesised that oxidative stress tolerance is a contributing factor to temperature effects on bacterial diseases of common bean and tested this hypothesis in this chapter.

3.1.8 Exposure to ROS leads to bacterial starvation

The production of reactive oxygen species ROS is central to plant immunity (Jones and Dangl, 2006, Camejo et al., 2016), but they are also involved in more general stress signalling responses of plants

(Baxter et al., 2014, Torres and Dangl, 2005). As described in the general introduction, reactive oxygen species are inhibitory to bacterial growth. This is in part because ROS inactivate enzymes necessary for bacterial metabolism, such as for instance methionine synthase (Hondorp and Matthews, 2004) (Deng et al., 2013). As a result, oxidative stress often leads to bacterial starvation (Noctor et al., 2015). Because the bacteria are not able to process the nutrients at hand, they experience starvation despite the apparent availability of nutrients. Plants will also actively sequester specific nutrients that are needed for basal bacterial metabolism as part of their immune response. One such contentious nutrient is iron. Indeed, iron is a cofactor required for many enzymatic reactions, but it is often limiting in the apoplastic space where plant pathogenic *Pseudomonas* reside – plants sequester the iron in their vacuole and plastids (Franza and Expert, 2013). As a result, these bacteria often secrete siderophores – molecules that scavenge iron – during infection (Aznar et al., 2015). They also are prone to secreting siderophores and producing ROS when they undergo iron starvation (Cornelis and Matthijs, 2002). Pspph and Pss may have different temperature optima associated with their ability to scavenge for, transport and metabolise host nutrients or to tolerate stress in the host environment. It is common for organisms to display environmental stress tolerance trade-offs (Kissoudis et al., 2014). We therefore hypothesised that nutrient starvation may affect temperature response of these bacteria and tested the contribution of medium richness in this chapter.

3.1.9 Objectives

It has been observed that bacterial disease development and severity in beans is affected by temperature. The fact that disease development of Pspph is more severe at cooler temperatures unlike Pss infection suggests that the plant is not solely responsible for the temperature effects we observe in fields. In this chapter, we confirm that temperature affects the bacterial pathogens directly *in planta*

and *in vitro*. We hypothesised that this may be a result of a cross-talk between temperature and oxidative stress responses. We decided to test our hypotheses and determine how temperature affects bacterial virulence, and test if phytotoxins, oxidative stress tolerance and/or nutrient availability play a role in the temperature response.

3.2 Materials and methods

See chapter 2

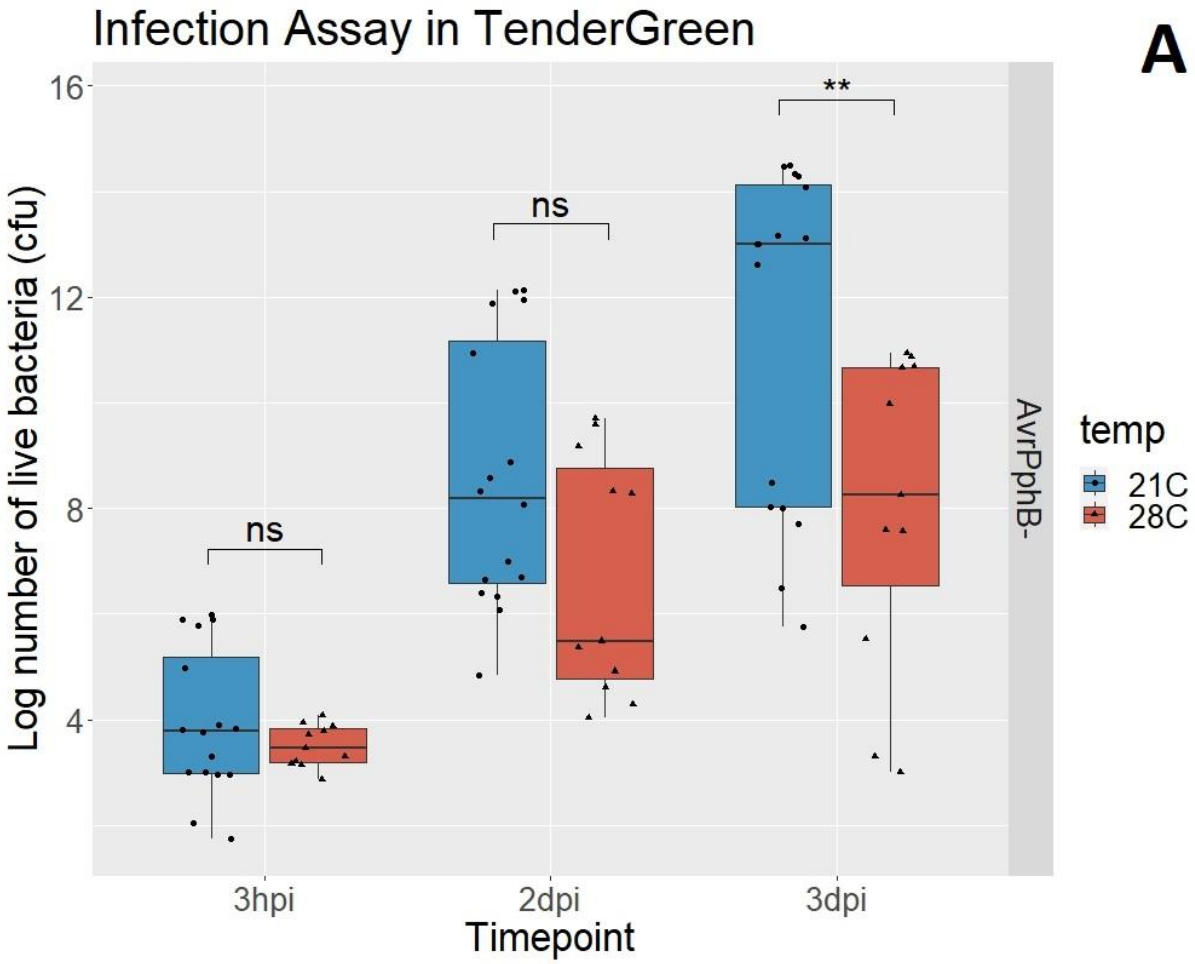
3.3 Results

3.3.1 Temperature affects virulence differently for Pspph and Pss

As established above, there is published evidence that bacterial pathogens of common beans are affected by temperature in the field. Our first question was: does this temperature effect also occur in controlled lab conditions ? Furthermore, we needed to establish whether temperature itself, or one of the coinciding environmental factors (such as seasonal changes in light intensity, humidity, rainfall…) were responsible for the observations. To do so, we infected common bean with the pathogens of interest at two different temperatures : 21°C (low) and 28°C (high) in fixed conditions. These temperatures were chosen as being representative of seasonal temperatures, non-stressful to the plants as long as sufficient water is provided, but still substantially different. The high temperature is also considered the optimum temperature for plant pathogenic *Pseudomonas* growth *in vitro*. We chose strain B728a as the representative for Pss as it is ubiquitously considered the model strain for this pathovar. We chose 1302A as the Pspph representative after testing various other Pspph model strains, as we had access to some constructs of 1302A in our lab. Plants were germinated and grown in the same greenhouse settings until their cotyledons emerged, at which point they were split into two groups and

moved to controlled climate chambers set to either temperature of interest. Relative humidity, light intensity and watering were controlled to be constant and similar in both groups. Humidity is affected by temperature as warmer air can hold more water, so absolute humidity was always a little higher at the warmer temperature around the time of watering, but otherwise, conditions were kept relatively constant, in order to minimise confounding effects and isolate the effects of temperature alone on the pathogen-plant interaction.

After three days of incubation in the chambers, plant leaves were infected with the pathogens. We chose the *Phaseolus vulgaris* cultivar TenderGreen for its robust and healthy growth in lab conditions. Furthermore, this could allow us to examine virulence and ETI in the same cultivar by using strains of 1302A that possess or lack AvrPphB – one of the Pspph effector which triggers ETI in this cultivar. We confirmed that the AvrPphB- mutant of 1302A does not behave differently from the wild type in the face of oxidative stress and temperature (supplementary figure S1). For comparison, we used the wild type B728a strain of Pss. Following infection, plants were incubated at their respective temperature treatment and sampled over the course of 3 days. We conducted a colony count, and infection load was determined from these values. While both strains are able to grow *in planta* at both temperatures – since bacterial load increases over time - Pspph count at 3 days post-infection (dpi) is significantly higher at 21 than at 28°C. In contrast, Pss count is significantly lower at 21 compared to 28°C at 3dpi (figure 3.1). No substantial difference in plant growth or symptom development was observed between plants grown at the two different temperatures. This indicates that temperature directly affects bacterial load. This is not to say that other factors such as humidity and light regime do not have an impact, but that temperature is a deciding factor in its own right. However, this raises the question : does temperature affect bacterial virulence directly or does this effect arise from phenotypic differences of the plant host response?


Infection Assay in TenderGreen
A
Log number of live bacteria (cfu)
16
12
8
4
ns
ns
**
3hpi
2dpi
3dpi
Timepoint
AvrPphB-
temp
21C
28C

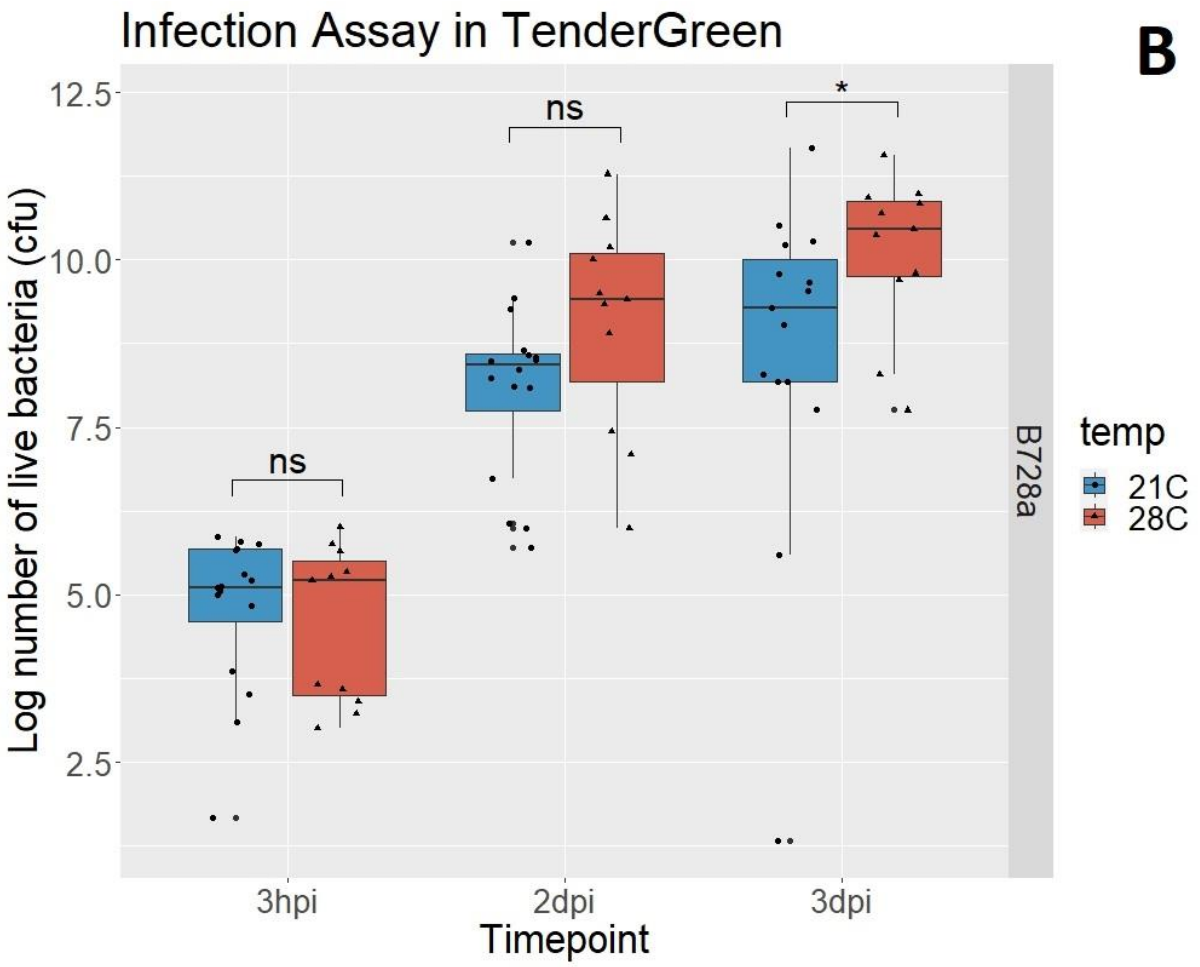
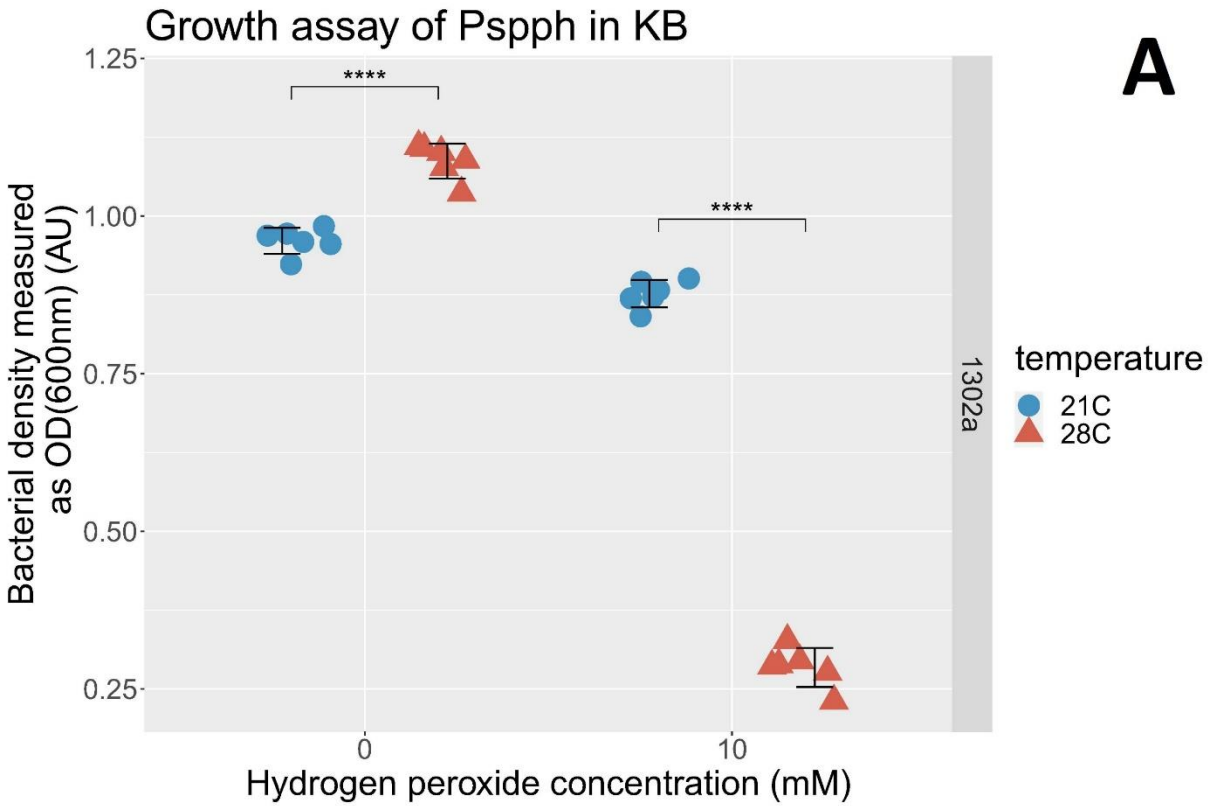


Figure 3.1: Temperature affects virulence *in planta*.
Pspph strain 1302A AvrPphB- and Pss strain B728a were inoculated onto leaves of plants 1 week old plants that were conditioned at 21°C (represented in blue and with circles) and 28°C (represented in red and with triangles) in controlled climate chambers. Leaf disks were then sampled at 3hpi, 2dpi and 3dpi, and colony-forming unit numbers per cm² were calculated. Data was plotted using ggplot, boxplots display the median, interquartile range, minimum and maximum values. Significantly different values are marked with asterisks (linear model with random effect of experimental ID, combined results from N=5 experiments, n=2-4 replicates per experiment for a minimum of 11 replicates per treatment, *= P-value < 0.05, **= P-value<0.01, ***=P-value<0.001, ns = P-value > 0.05).

A) Bacterial load of 1302A on Tendergreen
B) Bacterial load of B728a on Tendergreen

3.3.2 Temperature affects oxidative stress differently for Pspph and Pss

We decided to determine if some classic phytopathogenic traits are affected by temperature. A prime candidate for this is oxidative stress response: production of reactive oxygen species (ROS) is central to plant immunity. In order to answer this question, I grew bacteria *in vitro*, exposing them to increasing concentrations of hydrogen peroxide and incubating them at low and high temperatures. If temperature does not affect oxidative stress response, we would expect that bacterial growth in the face of ROS challenge is similar at both temperatures if not higher at 28°C. This is not the case so we can reject this null hypothesis: Pspph bacterial density after 20h of growth in 5mM H_2O_2 is not significantly different from the water control at 21°C, whereas it is significantly lower at 28°C (figure 3.2A). Bacterial density in 10mM H_2O_2 is also three times higher at 21°C than at 28°C (Figure 3.2A). This is strongly indicative of an effect of temperature on bacterial tolerance/resistance/resilience to oxidative stress. This suggests that Pspph copes with oxidative stress better at lower temperatures. On the other hand, Pss appears to display better ROS tolerance at the higher temperature: Pss density after 20h of growth in 60mM H_2O_2 is significantly lower than the water control at 21°C but is not significantly different at 28°C (Figure 3.2B). Furthermore, bacterial density of Pss in 80mM H_2O_2 at 28°C is over six times the bacterial density at 21°C (Figure 3.2B). Note that Pss is much more tolerant of H_2O_2 than Pspph is. Much higher concentrations of H_2O_2 had to be used on Pss to find the threshold where growth is impaired. Note that we are infering differences in bacterial sensitivity to hydrogen peroxide based on small differences in optical density, especially in the case of Pss B728a. This is a technical limitation associated with using optical density. Altogether, these results suggest that temperature does affect bacterial phytopathogens directly, more specifically by affecting their oxidative stress responses. The fact that the direction of the temperature crosstalk with oxidative stress is opposite in Pss and Pspph is indicative that this is not due to differences in H_2O_2 stability at different temperatures. We further confirmed this by quantifying levels of H_2O_2 in solution in the absence of bacteria. Similar levels of H_2O_2 could be detected at 21 and 28°C in the first 30min of incubation in the absence of bacteria (Figure 3.3).


Growth assay of Pspph in KB
A
Bacterial density measured as OD(600nm) (AU)
1.25
1.00
0.75
0.50
0.25
****
****
0
10
Hydrogen peroxide concentration (mM)
1302a
temperature
21C
28C

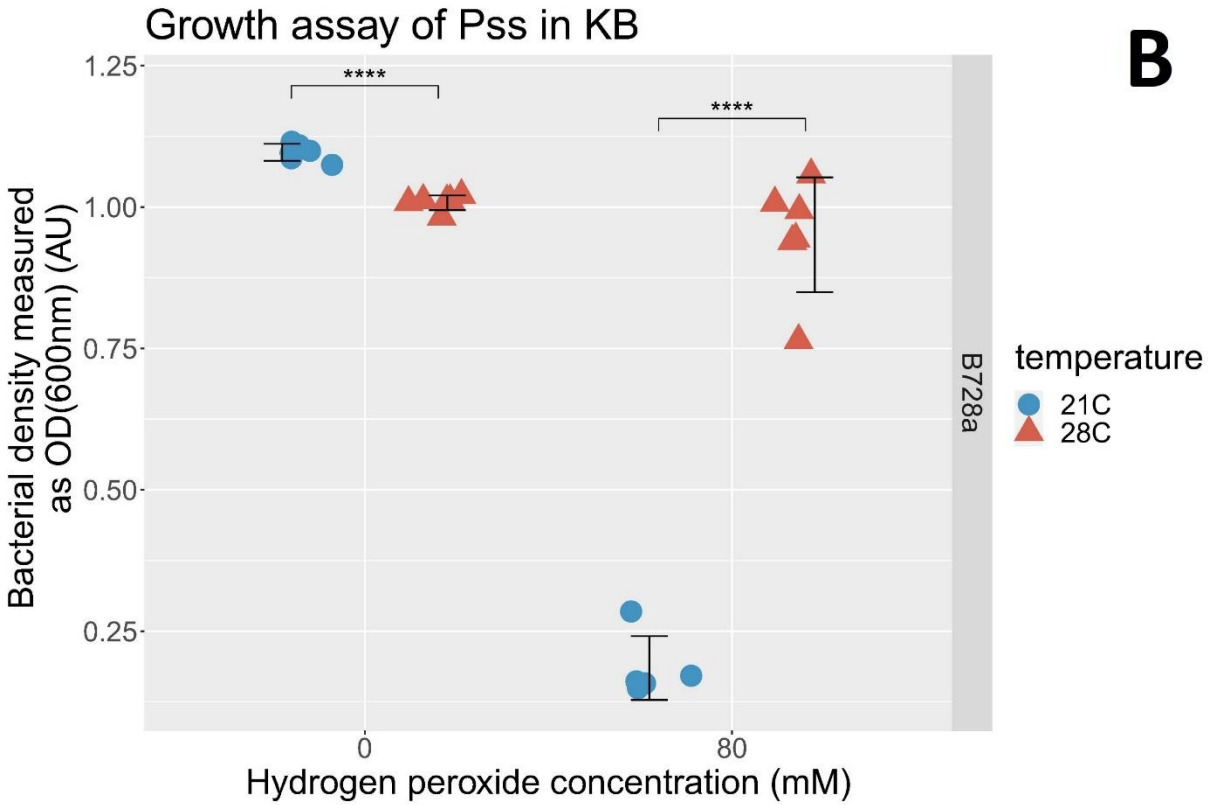
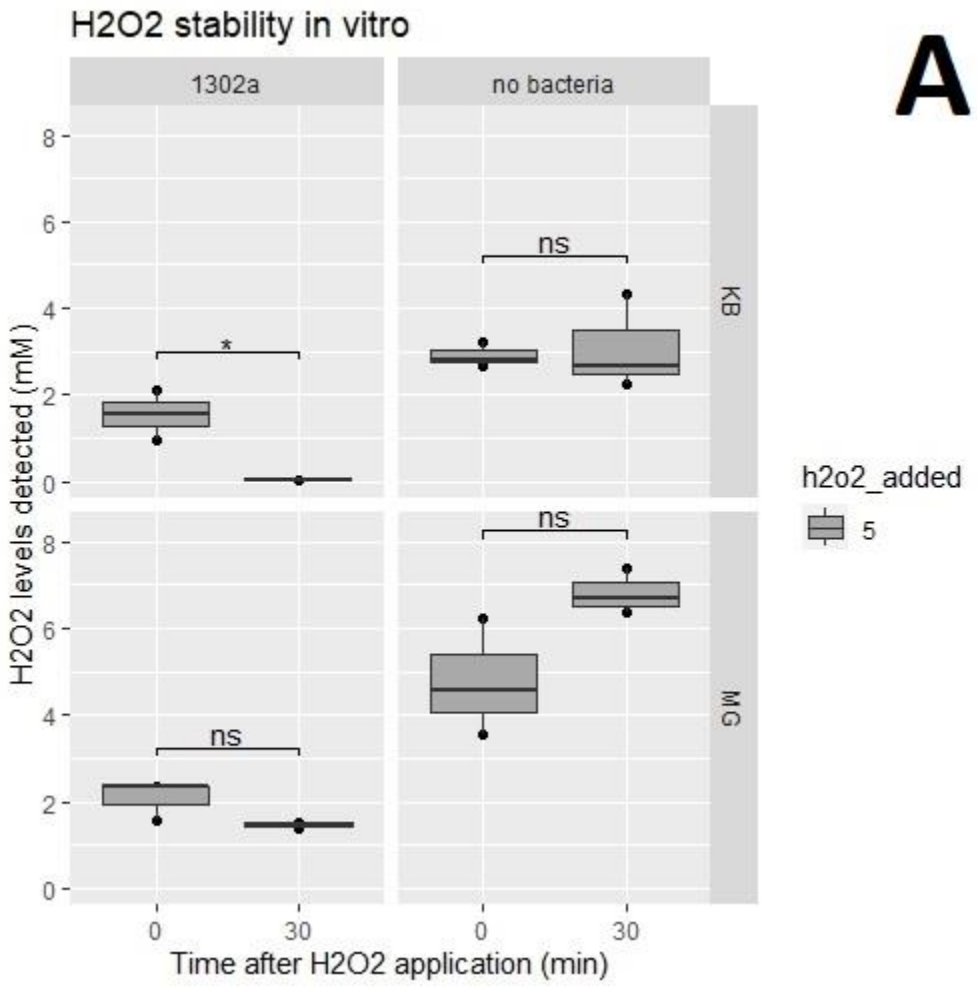

Growth assay of Pss in KB
B
Bacterial density measured as OD(600nm) (AU)
1.25
1.00
0.75
0.50
0.25
****
****
0
80
Hydrogen peroxide concentration (mM)
B728a
temperature
21C
28C

Figure 3.2: Temperature affects oxidative stress tolerance.
Pss strain B728a and Pspph strain 1302A cultures were grown in KB medium for 4h in an incubator set to either 21°C (represented in blue with circles) or 28°C (represented in red with triangles) until they reached the early log growth phase. Varying concentrations of H_2O_2 (10mM for Pspph, 80mM for Pss) or water was added to the cultures, and the cultures were put back in the incubators to grow at the temperature of interest for another 20h. At the 24h mark, the OD_{600} of each culture was recorded and blanked over sterile medium. These values were plotted individually as points, with each point representing a biological replicate, n=6, and standard deviation represented by the error bars. A Tukey post-hoc test following an Anova determined P-values of differences between the means of each treatment at 21°C and 28°C (*= P-value < 0.05, **= P-value<0.01, ***=P-value<0.001, ****=P-value<0.0001, ns = P-value > 0.05). This experiment was repeated twice for each temperature and strain. This figure is representative of those replicates.
A) Pspph tolerance to H_2O_2 is higher at 21°C. Pspph was exposed to H_2O_2 concentrations of 0mM (water) and 10mM.
B) Pss tolerance to H_2O_2 is higher at 28°C. Pss is more H_2O_2 tolerant than Pspph. Pss was exposed to H2O2 concentrations of 0mM (water) and 80mM, a level eight times higher than used on Pspph because no significant growth effects are observed at 20mM and below in KB medium for this strain. Because the level of H_2O_2 is quite high and KB medium is a viscous medium containing glycerol, the oxygen released during H_2O_2 degradation can form bubbles in the cultures which can in turn affect the OD_{600} detected by the spectrophotometer, hence the larger standard deviations in this graph compared to figure 3.2A.

3.3.3 H_2O_2 stability does not differ at 21°C and 28°C

Furthermore, hydrogen peroxide disappears from the solution in the presence of bacteria within a couple of hours. Within the first thirty minutes, H_2O_2 levels have already decreased below the detection threshold of our assay. Hydrogen peroxide is detectable twice as long in the absence of bacteria (Pspph or Pss) (Figure 3.3). This rapid degradation in the presence of bacteria suggests that the bacteria produce ROS scavengers in culture even before experiencing ROS stress. Alternatively or additionally, direct oxidation of bacterial structures by ROS means that it disappears from the culture faster in the presence of the said bacterial structures. We actually find that ROS degradation in bacterial cultures is due to the presence of a factor in the medium (potentially secreted by the bacteria) which can be inactivated by boiling (figure 3.4). This supports the first hypothesis as the primary mechanism for ROS degradation. Consistent with this, H_2O_2 degradation is more advanced in the presence of Pss than in the presence of Pspph (Figure 3.3). This may be partially due to the small differences in growth rate

between those two strains but this is also suggestive of a stronger ROS response from Pss which would correlate with its greater hydrogen peroxide tolerance/resilience/resistance.



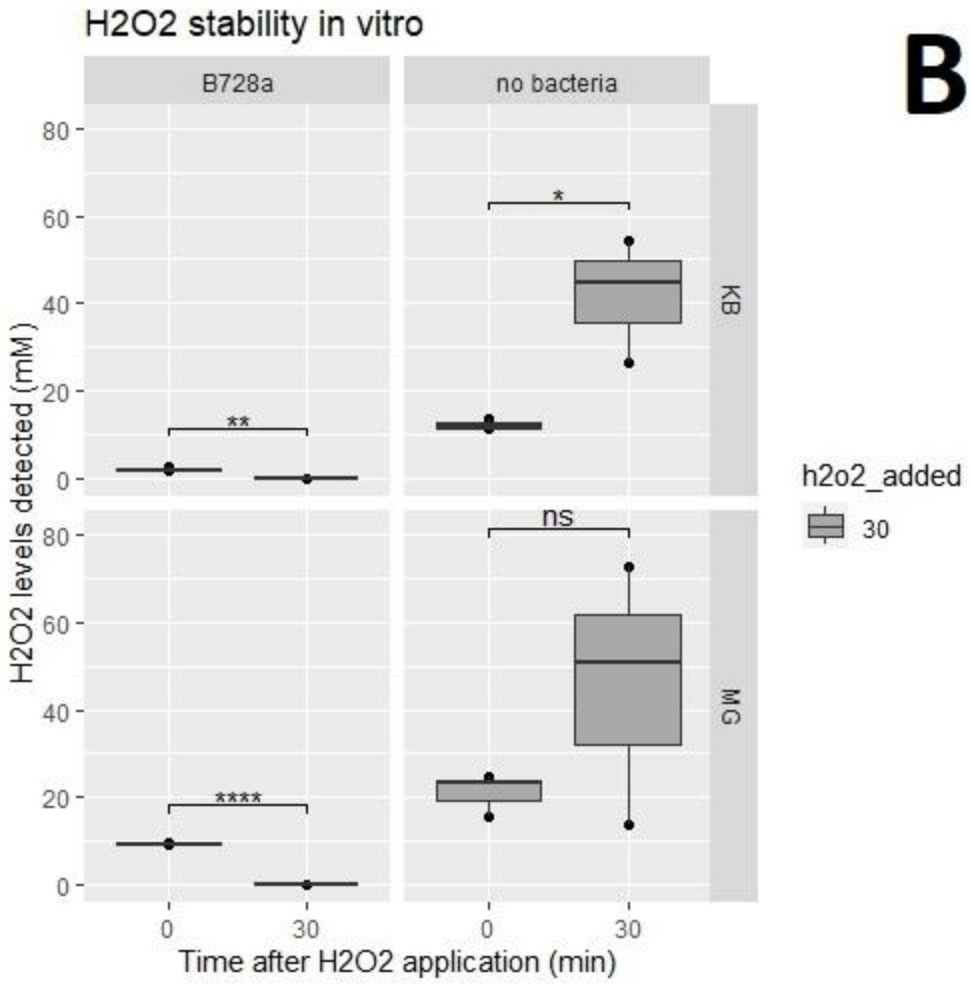


Figure 3.3: H_2O_2 disappears from bacterial cultures rapidly
Bacterial cultures were grown in King's B (KB) and MG media for 4h until they reached early log phase. Cultures were then inoculated with O-30mM H_2O_2. An amplex red kit was used at various timepoints after addition of H_2O_2 to measure the levels of H_2O_2 remaining in culture. The amplex red reagent is only able to detect a medium range of H_2O_2 concentrations, so serial dilutions had to be done to reach the detection threshold. Separately, a dose response curve was done in each medium to allow quantification of H_2O_2 concentration in mM. The figures above show the levels of H_2O_2 as expected before dilution. A combination of an Anova and Tukey Post-Hoc Test was used to calculate P-values of differences between the means (n=3 replicates per treatment, *= P-value < 0.05, **= P-value<0.01, ***=P-value<0.001, ****=P-value<0.0001, ns = P-value > 0.05). The data is represented by a standard boxplot displaying the median, interquartile range, minimum and maximum values. The same assay was also performed on sterile medium without bacterial cultures to control for natural H_2O_2 decay. This experiment was repeated once, and the data is representative of findings.
A) H_2O_2 persistence in the presence and absence of Pspph strain 1302A.
B) H_2O_2 persistence in the presence and absence of Pss strain B728a.

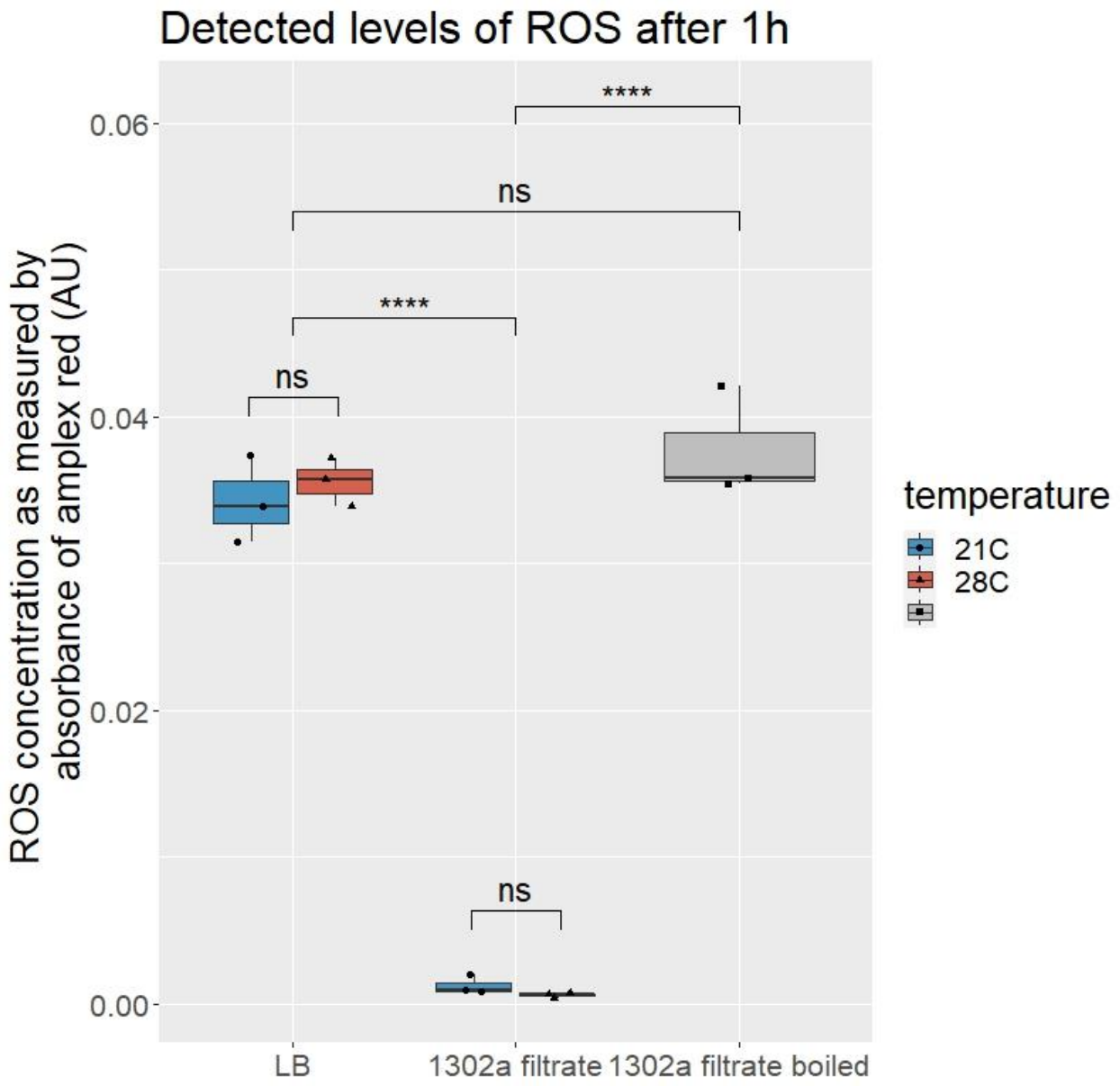
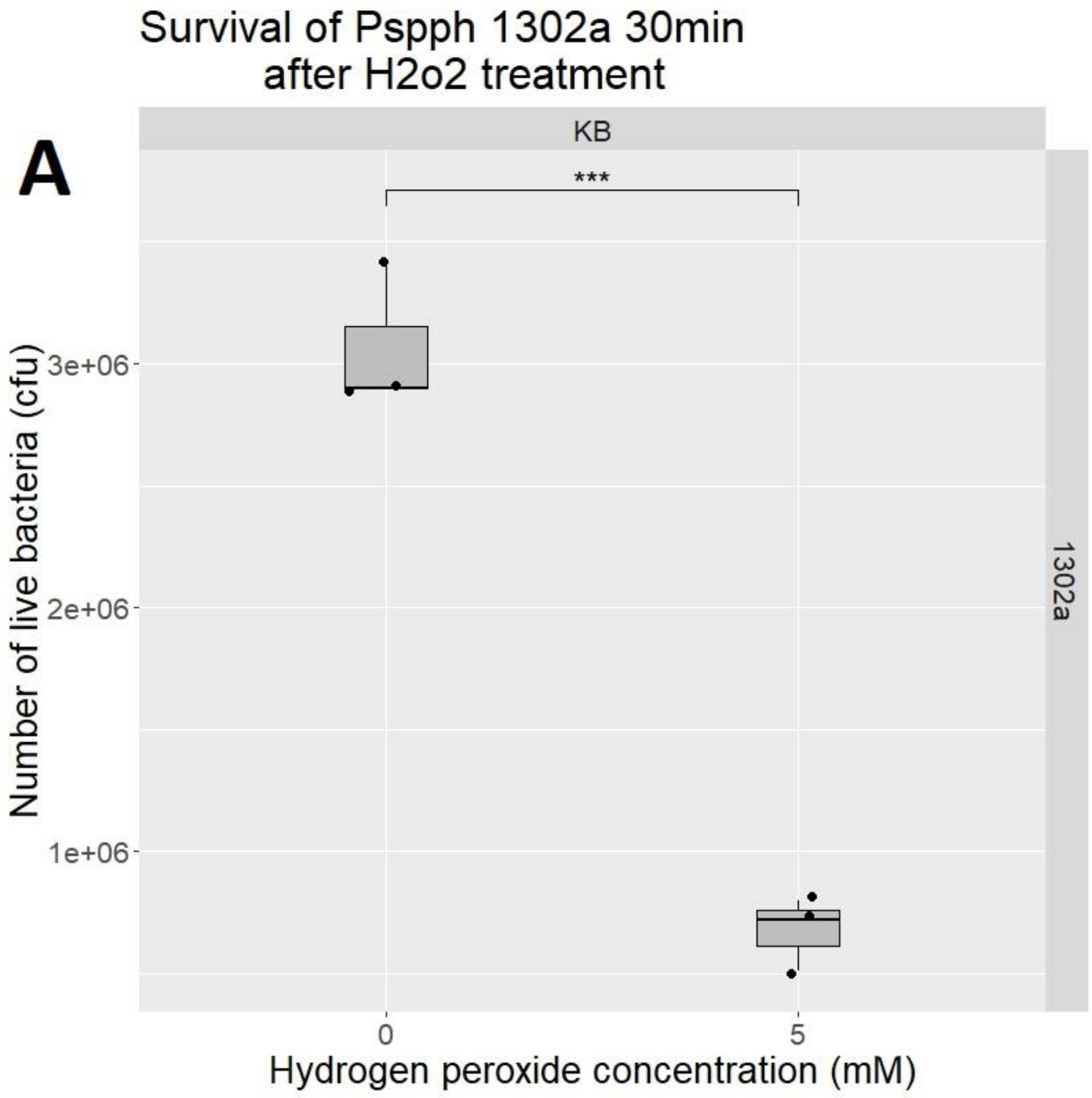


Figure 3.4: H_2O_2 is degraded by a factor that can be inactivated by boiling. This factor is not responsible for differences in oxidative stress tolerance of Pspph at different temperatures.
Sterile medium was incubated and bacteria were grown in LB for 4h. After 1h, samples were collected. Three culture samples were filtered through a 2um filter to remove bacteria ("1302a filtrate"), and three were filtered and boiled at 95C for 10min before addition of 1uM H_2O_2 at the temperatures of interest ("1302a filtrate boiled"). ROS levels were quantified using the amplex red reagent. A combination of an Anova and Tukey Post-Hoc Test was used to calculate P-values of differences between the means (n=3, *= P-value < 0.05, **= P-value<0.01, ***=P-value<0.001, ****=P-value<0.0001, ns = P-value > 0.05). Detected levels of H_2O_2 at 21 and at 28C are not statistically significant in sterile medium (LB) and in the bacterial filtrate. Levels of H_2O_2 detected in boiled filtrate are not statistically different than in sterile medium but they are statistically higher than levels detected in raw filtrate. Data is represented as individual data points (circles at 21°C, triangles at 28°C) and by a standard Boxplot displaying the median, interquartile range, minimum and maximum values (Blue at 21°C, Red at 28°C).

3.3.4 H_2O_2 kills Pss and Pspph

The transient nature of reactive oxygen species stress applied to bacterial cultures *in vitro* suggested that hydrogen peroxide was not inhibiting growth but instead was causing apparent lags in bacterial growth curves by killing a portion of our population, effectively reducing bacterial density without lowering the OD600 (Figure 3.6). We tested this by plating serial dilutions of reactive oxygen species exposed bacterial cultures and comparing them with water treated cultures which were at the same starting OD. If we find that they differ in colony count, this means that indeed, H_2O_2 kills bacterial cells even though this is not picked up by the spectrophotometer and not reflected by the OD600. Pspph 1302A cultures exposed to five millimolar hydrogen peroxide had significantly lower colony counts than the water control by a factor of approximately 3 (Figure 3.5A). This was also the case for Pss B728a in 50 millimolar H_2O_2 (Figure 3.5B). These results confirm that despite their differences, both strains experience a level of mortality in the presence of H_2O_2 from which they recover once H_2O_2 levels recede. Over two thirds of the Pspph bacteria were killed by 5mM H_2O_2 while 2/5ths of the Pss died following exposure to 30mM H_2O_2, once again confirming that Pss is more resilient than Pspph to oxidative stress.


Survival of Pspph 1302a 30min
after H2o2 treatment
A
KB
***
3e+06
2e+06
1e+06
Number of live bacteria (cfu)
1302a
0
5
Hydrogen peroxide concentration (mM)

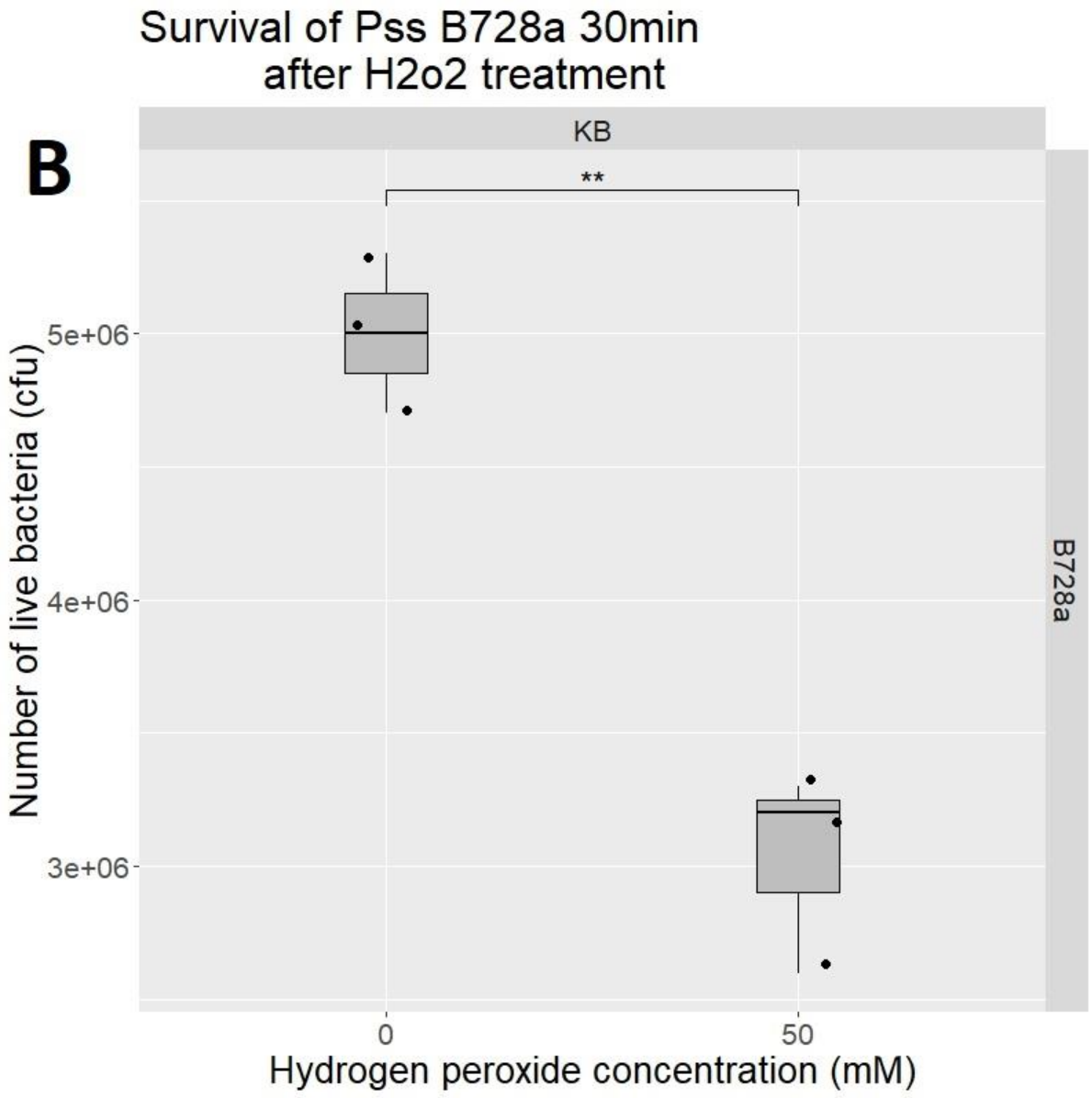


Figure 3.5: H_2O_2 kills bacterial cells within the span of thirty minutes.
Bacterial cultures were grown in KB at 28°C to log-phase before they were inoculated with H_2O_2 or water. Serial dilutions were taken after 30 minutes, and all dilutions were plated onto LBA. The number of colony-forming units was recorded and the number of live bacteria in culture was calculated using these values and the dilution factor.
A) Survival of Pspph strain 1302A in 0 vs 5mM H_2O_2.
B) Survival of Pss strain B728a in 0 vs 50mM H_2O_2.
Data is represented by individual data points for each biological replicate (n=3), and standard boxplots displaying the median, interquartile range, minimum and maximum values. A Tukey HSD test following an ANOVA determined the adjusted P-values for comparison of the means. ns = non-significant; * = P-value below 0.05, ** = P-value below 0.01, *** = P-value below 0.001.

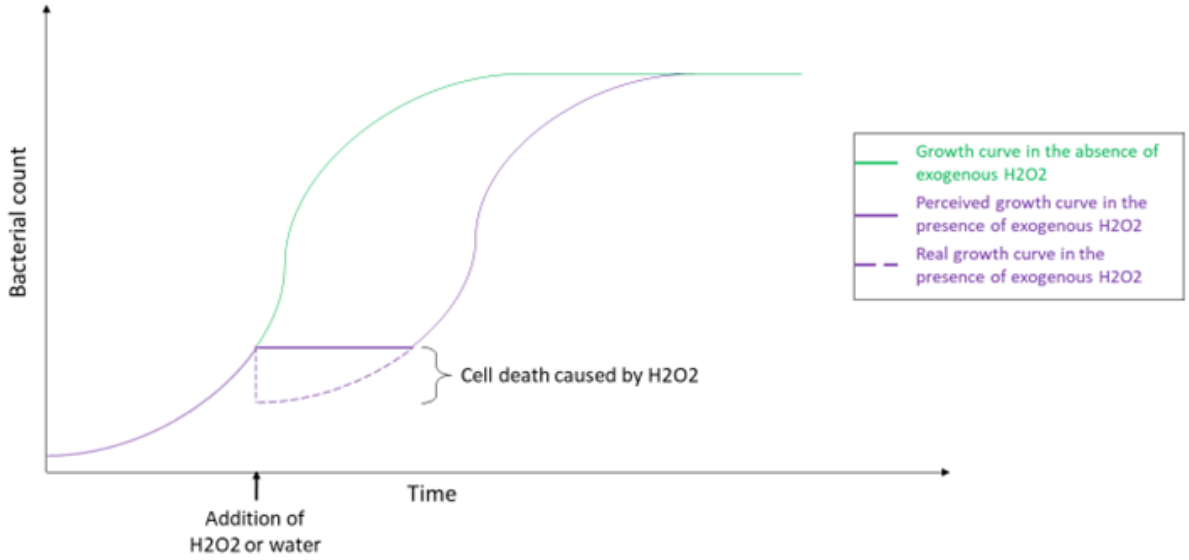


Figure 3.6: Model of bacterial response to H_2O_2. In green, the growth curve in the absence of exogenous H_2O_2. In purple the perceived growth curve in the presence of exogenous H_2O_2, as measured by a spectrophotometer recording OD_{600}. Dashed in purple, the hypothetical real growth curve in the presence of exogenous H_2O_2. The drop in bacterial cell numbers is not recorded by the spectrophotometer which does not measure live cell count but absorbance.

Bacteria growing in a biofilm on agar plates made of the same media as in the planktonic experiments were exposed to previously established relevant concentrations of H_2O_2 as H_2O_2 tolerance in biofilms is much higher for most bacteria. We find that for 1302A, the inhibition zone is slightly smaller at 21 degrees Celsius than at 28 degrees Celsius although this is not statistically significant (table 3.2). Interestingly, the medium composition seems to affect this.

Table 3.2: Similar ROS-temperature pattern observed in bacterial biofilms

Strain	Medium	H_2O_2 treatment (M)	diameter (cm) at 21°C	diameter (cm) at 28°C
B728a	King's B	9.8	4.4 +/- 0.3	4.0 +/- 0.4
B728a	King's B	0.0	0.0 +/- 0.0	0.0 +/- 0.0
1302A	King's B	9.8	6.0 +/- 0.2	6.2 +/- 0.2
1302A	King's B	0.0	0.0 +/- 0.0	0.0 +/- 0.0

Strain	Medium	H_2O_2 treatment (M)	diameter (cm) at 21°C	diameter (cm) at 28°C
B728a	MG	9.8	4.3 +/- 0.1	4.6 +/- 0.3
B728a	MG	0.0	0.0 +/- 0.0	0.0 +/- 0.0
1302A	MG	9.8	6.2 +/- 0.3	6.8 +/- 0.3
1302A	MG	0.0	0.0 +/- 0.0	0.0 +/- 0.0

High density (OD_{600}=1) cultures of Pspph 1302A and Pss B728a were resuspended in water and streaked onto KBA plates. Once dry, a filter paper disk was applied in the centre and soaked with 200µl 30% H_2O_2 (9.8M) or water. Plates were then incubated for 24h at 21/28°C. Inhibition zones surrounding the disk are zones where H_2O_2 concentration was lethal. Inhibition zone diameters are recorded for each treatment and strain (n=3), and the mean and standard deviation are reported in this table. Differences in diameter between temperature treatments are not statistically significant (Tukey on ANOVA).

3.3.5 The temperature oxidative stress cross-talk is affected by medium composition

Oxidative stress and temperature are intimately linked in driving bacterial growth. Interestingly, this cross-talk seems to be affected by the nutritional composition of the bacterial environment. We had originally studied this crosstalk in two different media: a rich medium King's B for optimal growth rate, and a minimal medium inducive of the type 3 secretion system (mannitol glutamate) to replicate *in vivo* conditions more faithfully. We found that oxidative stress tolerance/resilience/resistance was drastically affected by the medium. Both strains are generally more tolerant/resilient/resistant to H_2O_2 in the richer medium KB (figure 3.7). It is still unclear whether this is due to bacteria recovering more quickly in richer medium or to some regulatory effects, but we have confirmed this is not due to direct reduction of oxidative stress by the medium. Indeed, H_2O_2 stability in sterile medium is not significantly different between KB and MG media (figure 3.3). ROS are inhibitors of bacterial growth because they oxidise cysteine residues, thereby inactivating various metabolic enzymes and leading to bacterial starvation. We hypothesise that the richer medium compensates for nutrient starvation, allowing bacteria exposed to H_2O_2 to resume growth and recover faster and more efficiently.

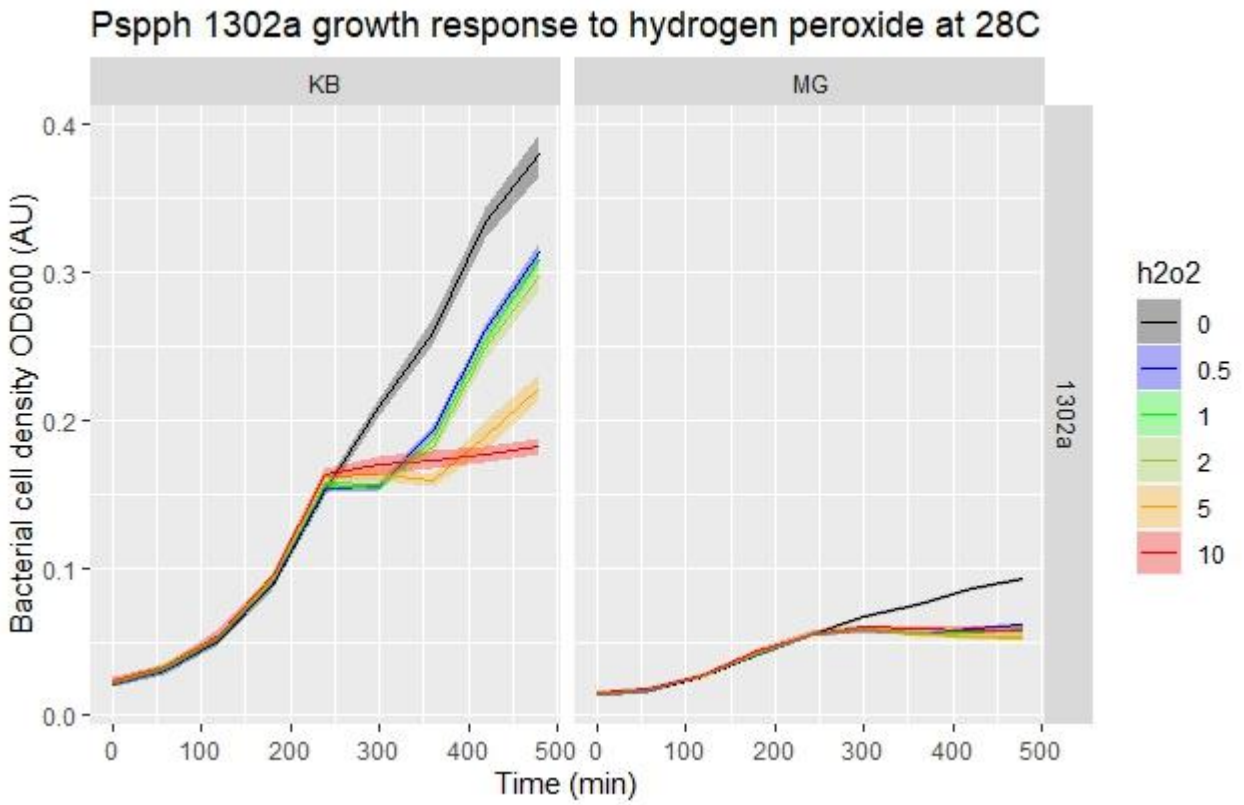


Figure 3.7: Medium composition/richness may affect temperature-oxidative stress cross-talk.
Early log-phase cultures (4h or 240min of growth) of 1302A were grown in KB and MG media at 28°C with 0-15mM H_2O_2 for 4h. The mean of the measured OD_{600} over time (n=6) is plotted as a growth curve, with a ribbon spanning two standard deviations. The OD_{600} is blanked over the OD_{600} recorded for sterile medium. Growth is slower and the plateau is at a lower OD in MG compared to the rich medium KB in the water control. However, concentrations of H_2O_2 that are fully inhibitory (no growth from addition of H_2O_2 onwards) in MG are not in KB: while delayed, growth resumes in KB before the 8hpi mark. This is indicative that medium richness affects oxidative stress resilience. This data is representative of N=3 independent replicate experiments.

3.4 Discussion

There is ample evidence that plants respond to temperature in a variety of ways: of special interest for plant pathology are stomatal aperture, apoplastic nutrient content, hormone signalling and stress responses (Hua, 2013, Miura and Tada, 2014). There is however not as much literature on temperature effects on bacterial pathogens. Literature on non-phytopathogenic bacteria suggest that bacterial growth rate, metabolism and stress response are affected by temperature (Gadgil et al., 2005, Humair et

al., 2009). We set out to determine if and how temperature affects bacterial pathogens of common bean. Consistent with previous in field observations of disease development and severity in South Africa (Fourie, 2002, Goss, 1940), we find that Pspph virulence is higher at cooler temperatures (21°C) whilst Pss virulence is higher at warmer temperatures (28°C). This is an important finding as disease recording of halo blight in the fields often relies on disease being symptomatic but halo blight's characteristic halo light chlorotic lesions are caused by phaseolotoxin, a phytotoxin that is well-known to only to be expressed at cooler temperatures. We show that Pspph virulence in terms of bacterial multiplication *in planta* is indeed higher at cooler temperatures, and that is not just that the symptoms are attenuated above 28°C.

3.4.1 Temperature affects oxidative stress tolerance but not detoxification

Furthermore, this temperature preference extends to these pathogens' oxidative stress tolerance *in vitro*. Indeed, Pspph tolerates H_2O_2 stress better at cooler temperatures whereas Pss H_2O_2 tolerance is higher at warmer temperatures in KB medium. It will be interesting to determine exactly how oxidative stress ties in with temperature responses but we were able to exclude a couple of options. We find that H_2O_2 stability is minimally affected if at all by temperature and so is not responsible for our phenotype. Furthermore, we show that while H_2O_2 is quickly degraded by a secreted molecule (likely an enzyme such as a catalase) in *in vitro* bacterial cultures, this molecule is unlikely to be responsible for the phenotype either as it seems to not be affected by temperature – the secreted factor is just as efficient at removing H_2O_2 from solution at 21°C and at 28°C, with trace amounts of H_2O_2 undetectable 1h after exogenous application of H_2O_2.

3.4.2 Medium composition affects the cross-talk between oxidative stress tolerance and temperature

Finally, we find that oxidative stress tolerance is reduced in minimal medium (MG) compared to rich medium (KB), and nutrient availability affects the cross-talk between temperature and ROS response in Pss. This is consistent with what we know of H_2O_2 toxicity – H_2O_2 and other ROS inactivate metabolic enzymes leading to nutrient imbalances and starvation, so a richer medium would alleviate this issue. We do not currently know why medium richness/composition affects the temperature-oxidative stress response cross-talk, but we hypothesise that this is potentially due to temperature effects on enzyme catalytic rates and/or temperature effects on transcription and translation of metabolic genes. Indeed, in the non-pathogenic *Pseudomonas fluorescens* CHA0, the master oxidative stress regulator RpoS has been shown to be transcriptionally regulated in response to temperature: the expression of RpoS was significantly lower at 35°C than at 30°C (Humair et al., 2009). We investigate this further in chapter 4 of this thesis. Another factor that may be involved in this crosstalk is phaseolotoxin: indeed, phaseolotoxin production is not only temperature sensitive but also responsive to oxidative stress through OxyR regulation (Hernandez-Morales et al., 2018).

3.4.3 Pss is more resilient to oxidative stress than Pspph

We observe that Pss is substantially more resilient to oxidative stress than Pspph and that this is in part linked to Pss's greater ability to degrade H_2O_2 and to recover population numbers quickly. The lifecycle of a typical *Pseudomonas* bacterium can be quite varied: environmental/aerosol, epiphytic, plant pathogenic and occasionally saprophytic (Morris et al., 2008). Furthermore, plant-pathogenic *Pseudomonas* are hemibiotrophs: pathogens capable of infecting and scavenging nutrients from both

live and dead plant tissues. Pss can be exposed to a wide range of environment, including cloud dwelling in the upper atmosphere because of its ice nucleation ability. So it is not surprising that it responds differentially to an array of cues including temperature, ROS and nutrient availability, and that these responses are integrated and cross-talk with one another. It is likely that the frequent cycling of Pss through the water cycle (Morris et al., 2008) is responsible for its enhanced ROS tolerance, as the higher atmosphere is highly oxidising due to increased incidence of ozone.

3.4.4 Oxidative stress and temperature responses interact differently in Pss and Pspph

These results are consistent with the literature that was previously suggesting that oxidative stress response correlates with temperature response. However, the available data was mostly transcriptomic (Arvizu-Gomez et al., 2013, Hockett et al., 2013). We find that temperature directly affects oxidative stress tolerance of a bacterial plant pathogen and that this correlates to temperature effects on virulence. Importantly, we show this effect with biologically relevant moderate temperature differences (21 – 28°C, a 7°C difference). The few papers that look at temperature effects on plant diseases sometimes use unusually large temperatures that are close to lethal range for the plant host and for the pathogens e.g. 25 vs 39°C in pepper-*Ralstonia* interaction (Noman et al., 2018). This is a significant advancement as although temperature has long been known and described to have large effects on plants, temperature is less studied than other co-inciding factors such as humidity and seasonality. Our work suggests that temperature can also have significant and substantial effects on bacterial phytopathogens irrespective of host responses.

3.4.5 Pss may become more prevalent in fields in the future

Furthermore, many have hypothesised that rising temperatures due to climate change will lead to increased incidence of crop diseases and higher plant mortality (Velasquez et al., 2018). While this is likely to be the case in many crops, our work suggests that temperature rises may also lead to shifts in the types of diseases that occur in the field. In our case, Pss would likely benefit from increasing temperatures and become more prevalent even earlier in the season than usual whilst Pspph may become less prevalent. Alternatively, Pspph may become more common and severe in areas that typically overwinter their bean plants. Common bean is an annual crop that is typically either sown in March/April in frost-free areas in Southern Africa for harvests as early as September, or November/December in frost-prone areas. At some latitudes, two harvests are possible every year and a second sowing happens in September (Wortmann and Allen, 1994). We expect that changes in climate may not only affect disease incidence and severity, but also the composition of the plant pathogen pool in South Africa.

If we had more time and resources, field testing of temperature effects on disease development would have been interesting albeit challenging because coinciding factors cannot be easily controlled. We hope that our work will encourage other research teams to look more closely at the temperature response of their model plant pathogen.

3.5 Conclusion

There is ample evidence in the literature that disease development in the field is affected by temperature, and that temperature has large effects on bacterial phenotype. In this chapter, we show that this holds true for *Pseudomonas* pathogens of common bean in controlled lab conditions. We were able to replicate the observed temperature effects on pathogen virulence *in planta*, and we found a three-way interaction between temperature, oxidative stress response and nutrient status to be involved. While oxidative stress is transient, it can lead to bacterial cell death as part of plant immunity,

so our finding that H_2O_2 tolerance/resilience is affected by temperature in both Pss and Pspph, and that these two strains differ in this cross-talk suggests a potential avenue of research for understanding temperature effects on bacterial diseases. We study this cross-talk in more detail via a transcriptomics screen in chapter 4 of this thesis.

Chapter 4: Gene expression changes in response to oxidative stress and temperature

4.1 Introduction

4.1.1 Two contrasting *Pseudomonas* phytopathogens of common bean

Common bean is susceptible to a range of bacterial diseases which are detrimental to crop yield. Of those, two members of the PSSC are of particular interest: the causal agents of brown spot, *P. syringae* pv. *syringae* (Pss), and halo blight, *P. savastanoi* pv. *phaseolicola* (Pspph). They are of special interest due to their status as a model species in the research field (Arnold et al., 2011), and the severity of the infection they cause in bean fields (Fourie, 2002). Furthermore, these strains are related but quite different in their characteristics, so that comparing them provides insight into the different ways that a pathogen can achieve reproductive success on common bean:

- Host range: Pss is a generalist pathogen, able to infect over 180 species of plants (Muedi et al., 2015). On the other hand, Pspph is more specialised, only able to infect a selection of legume hosts (Arnold et al., 2011). Furthermore, whilst Pspph is organised in 9 races based on which cultivars a strain is able to infect (Fourie, 1998), there is limited genetic resistance to Pss to be found in the bean germplasm: some cultivars appear more resilient to Pss infection, but ultimately environmental conditions determine the severity of the infection (Muedi et al., 2015).
- Ecology: Pss is an exceptional epiphyte (Feil et al., 2005) but is also known to be able to survive and thrive outside of the plant sphere - it can be found alive in harsh environments such as clouds (Morris et al., 2008). Pspph is generally regarded as having an exclusive plant-associated

lifecycle consisting of an epiphytic and endophytic phase (Marques and Samson, 2016). Both can be seed-transmitted (Arnold et al., 2011, Fourie, 2002).

- Resilience to stress: as previously described in chapter 3, Pss is highly tolerant to oxidative stress. It is able to withstand upwards of 100mM H_2O_2 in liquid synthetic medium, and even higher levels in biofilms. Pspph on the other hand is more susceptible to H_2O_2 stress though still showing higher levels of tolerance (up to 20mM H_2O_2) than some other members of the PSSC such as *P. syringae* pv. *tomato* (Feil et al., 2005).
- Temperature range: Pss and Pspph are present throughout the growing season of common bean in South Africa, but their impact varies with temperature changes: Pspph infections appear first when daytime temperatures are cooler (below 28°C) and are most severe following cool nights (15-16°C). Then, when temperatures are warmer (above 28°C), Pss is more prevalent (Fourie, 2002). We showed in chapter 3 that this is not just a seasonality effect but that these pathogens indeed have different temperature ranges: Pspph is more virulent on bean at 21°C than at 28°C whilst Pss is the opposite, it is more virulent at 28°C than at 21°C.

In this chapter, our aim was to identify candidate genes responsible for the temperature-oxidative stress-virulence cross-talk affecting Pss and Pspph differentially. We were particularly interested in genes that were upregulated at 28°C in Pss, upregulated at 21°C in Pspph, differentially expressed in Pss and Pspph, and showing large changes in expression in response to any treatment.

4.1.2 Gene expression is tightly regulated

What makes these two pathogens so different despite their phylogenetic relatedness? One of the main ways that organisms adapt to their environment and achieve reproductive success is by regulation of gene expression. Only by fine-tuning which genes are expressed and at what level dynamically in response to current conditions, can a plant pathogen be successful as they are exposed to a range of

conditions, both inside and outside of the plant host (Yu et al., 2013). Their environment changes both on temporal scale but also on physical scale – for example, the epiphytic environment is very different from the environment inside the plant host (Marques and Samson, 2016). Gene expression is often regulated by means of signalling cascades: a receptor spanning the bacterial membrane binds to or is modified by a trigger (e.g. oxidation of the oxidative stress regulator OxyR by H_2O_2) which induces conformation changes leading to the release or activation of a signalling molecule or post-translational modification of an interacting protein, which directly or indirectly leads to activation of a transcriptional regulator which then binds to the promoter region of a specific genomic region, allowing transcription of the gene into mRNA and then translation into protein . There are many variations of this: for example, depending on the case, a regulator may block the DNA polymerase from accessing the DNA therefore inhibiting rather than promoting gene expression. Some transcriptional regulators promote or inhibit the expression of many other transcriptional regulators and therefore have quite large impacts on the organism's phenotype. Such transcriptional regulators are called master regulators. They are particularly interesting because they allow for co-regulation of gene expression: the expression of certain genes can be intimately linked in this way. In the case of temperature responses, not much is known about the mechanisms by which bacteria sense temperature and adjust gene expression in response. However, there is some evidence that specific thermoregulatory regions TRR in the promoter regions are involved in Pspph (Rowley et al., 1993, Rowley et al., 2000). Membrane fluidity changes also appear to be used by bacteria to sense temperature. For instance, this is the case for thermoregulation of coronatine biosynthesis in *P. savastanoi* pv*. glycinea*. In this PSSC strain, the phytotoxin coronatine is only produced at temperatures below 28°C, with a peak in production at 18°C (Bender et al., 1999). This thermoregulation is achieved at the transcriptional level by a two-component system consisting of the membrane bound histidine protein kinase CorS and the response regulators CorR and CorP. CorR only binds the promoter region of the coronatine biosynthesis cluster in the presence of CorS and at

permissive temperature (18°C) (Wang et al., 1999). CorS is membrane bound with the exception of its N-terminus which hangs off the membrane into the cytoplasmic space and contains the catalytic site required for interaction with CorR. There is evidence suggesting that at 28°C, the catalytic H-box of the protein kinase becomes a transmembrane domain as a result of changes in membrane fluidity thereby disallowing the activation of coronatine synthesis transcription (Braun et al., 2007). Interestingly, a few transcription factors have been shown to regulate membrane fluidity in response to temperature-induced changes to membrane fluidity in a feedback loop (e.g. DesK-DeskR in *Bacillus subtilis*) (Mansilla and de Mendoza, 2005). Two-component systems are often used by bacteria to respond to a variety of environmental changes such as osmolarity, pH, light, and even host factors (Stock et al., 2000) so we expect they may also play a role in Pss and Pspph response to temperature and the cross-talk between temperature and oxidative stress responses.

Transcriptional regulators can also affect transcription and folding of small non-coding RNAs, which in turn have important roles in post-transcriptional regulation. Of special notice, the small RNAs *rsmZ* and *rsmX1-5* are thermoregulated (more expressed at 28°C than at 18°C in Pspph 1448A) and in turn affect phaseolotoxin gene synthesis as well as the rest of the GacA/GacS system (Ramirez-Zapata et al., 2020). Overexpression of the small RNA *rsmY* which is encoded in the aforementioned TRR regions (Rowley et al., 2000) leads to biosynthesis of phaseolotoxin at non-permissive temperatures in Pspph NPS3121 (Valverde et al., 2003). The GacA/GacS system is not only required for phaseolotoxin production, it also affects other virulence genes by modulating the expression of the master transcriptional regulator *hrpL* which regulates many aspects of the T3SS in *Pseudomonas* (Liu et al., 2021).

4.1.3 Limitations of transcriptional regulation

Transcriptional regulation is not the only way that organisms regulate their phenotype: mRNA translation into protein is known to be subjected to tight regulation and RNA turnover also acts to regulate mRNA abundance, e.g. polyadenylation of mRNA reducing RNA stability in bacteria mediated by PcnB in response to various factors (Maes et al., 2017). Furthermore, even once translated into a protein, many enzymes and proteins need to be activated e.g. by phosphorylation so that their activity is tightly regulated as well (Stock et al., 1989). Whilst transcription of a gene does not necessarily lead to a phenotype, gene expression changes are still very informative in the ways that an organism senses and responds to its environment. Assuming that at least some of the differences in virulence and oxidative stress tolerance at different temperatures observed between Pss and Pspph are due to gene expression changes, what are our candidate genes?

4.1.4 Gene candidates for differences between Pss and Pspph

As previously described, Pss and Pspph are both capable of epiphytic growth outside of a plant host. However, Pss is the superior epiphyte. It has been found alive in a variety of water-cycle ecosystems, including clouds (Morris et al., 2008). In fact, this epiphytic lifestage is potentially part of the virulence strategy of this bacterium. Outside of the plant host, Pss produces ice-nucleation compounds. Frozen water on leaves creates tears in the tissue which are potential entry points for a variety of bacteria including Pss, which protects itself from frost injury by producing an antifreeze compound (Feil et al., 2005). Pss has access to a large arsenal of strategies that enhance its success outside of a plant host. These include surfactant production, chemotaxis, enhanced flagellum-based motility and biofilm formation (Yu et al., 2013). We do not yet know all the adaptations that make Pss a better epiphyte than other members of the *Pseudomonas syringae* species complex, but it is largely assumed that the

mechanisms described above, as well as a generalised high level of resilience to stress -in particular oxidative stress- are important (Feil et al., 2005).

4.1.5 Gene candidates for differences in oxidative stress tolerance

Mechanisms to detoxify and tolerate reactive oxygen species are important for all organisms, but particularly so for plant pathogens as the plant produces ROS as part of its immune defences (Guo et al., 2012, Fones and Preston, 2012, Camejo et al., 2016). ROS cause cell stress by damaging lipids, nucleic acids and proteins and inactivating enzymes. Symptoms of ROS stress include nutrient starvation, redox imbalance and cell death (Ezraty et al., 2017, Noctor et al., 2015). To prevent this, bacteria adopt a three-way strategy:

- 1. Evasion: suppression of plant immunity (e.g. by secreting T3SS effectors) (Oh et al., 2010), exclusion of ROS from the intracellular space (e.g. buffering by the extracellular matrix (Fones and Preston, 2012))
- 2. Detoxifying: production of ROS scavengers and antioxidants (e.g. catalase, superoxide dismutase, glutathione etc…) and secretion of these molecules into the periplasmic and extracellular space (Guo et al., 2012, Klotz and Hutcheson, 1992, Nowogorska and Patykowski, 2015)
- 3. Repair: detection of protein, nucleic acid and lipid damage and repair or replacement (Ezraty et al., 2017)

Pss and Pspph share many ROS coping strategies. To the best of our knowledge, the differing capacity of Pss and Pspph to tolerate H_2O_2 has never been formally tested for this pair of pathogens. Looking at their genomes, they both encode 5 catalase genes (Guo et al., 2012), superoxide dismutase and the DNA repair and antioxidant machinery (Feil et al., 2005, Joardar et al., 2005). It is possible that their

differences lie in the regulation of the expression of genes important to oxidative stress response rather than their gene pool. Previous transcriptomic studies of other gram-negative bacteria indicate that genes involved in the SOS and stringent response (Khakimova et al., 2013), DNA repair systems, sulfur transport and antioxidant systems are upregulated while genes involved in general (primary) metabolism, fatty acid biosynthesis and nucleic acid synthesis are transiently downregulated in the presence of non-lethal levels of H_2O_2 in synthetic medium in *P. aeruginosa* (Nizer et al., 2021) and *E. coli* (Roth et al., 2022). Interestingly, the involvement of iron metabolism is more controversial, as conflicting results have been documented independently (Nizer et al., 2021). This is likely a result of differences in experimental set-up as we demonstrated in chapter 3 that oxidative stress responses are multifactorial.

4.1.6 Gene candidates for differences in temperature range

It is very difficult to determine factors responsible for a species' temperature range because temperature often coincides with other factors such as humidity, light intensity, season etc. As a result, temperature is still vastly understudied compared to other abiotic factors. Nevertheless, it has been previously found to have drastic effects on members of the *Pseudomonas* genus. For instance, phytotoxin production in some strains of Pspph is largely controlled by temperature. Phaseolotoxin is only synthesised at temperatures below 30°C, with a peak in production around 20°C (Patil et al., 1991). A microarray screen of Pspph strain NPS3121 in synthetic medium confirmed that regulation of phaseolotoxin biosynthetic genes happens at a transcriptional level (Arvizu-Gomez et al., 2013), and found that an array of additional genes were also transcriptionally regulated in response to temperature. Genes involved in phytotoxin (phaseolotoxin) production, non-ribosomal synthesis, type VI secretion, membrane synthesis, motility, oxidative stress response and iron metabolism were upregulated at 18°C compared to 28°C, whilst genes involved in alginate synthesis, plant-pathogen

interaction, type IV secretion system, heat shock proteins and nucleic acid biosynthesis were downregulated at 18°C (Arvizu-Gomez et al., 2013).

Pss infection is more severe on bean plants at warmer temperatures above 28°C (Fourie, 2002). However, it appears that genes involved in polysaccharide synthesis and regulation, phage, IS elements, type VI secretion, chemosensing and chemotaxis, translation, flagellar synthesis, motility, phytotoxin synthesis and transport are downregulated in Pss strain B728a grown in synthetic medium at 30°C compared to 20°C. Genes linked to transcriptional regulation, chaperone heat-shock proteins, and quaternary ammonium compound metabolism and transport were found to be upregulated at the warmer temperature (Hockett et al., 2013). A large portion of these are potential candidates for the cross-talk between oxidative stress, virulence and temperature in our strains of interest. For example, phaseolotoxin synthesis has been shown to be induced in response to oxidative stress as well as by temperatures below 28°C (Arvizu-Gomez et al., 2022). On the other hand, while polysaccharide synthesis is expected to increase H_2O_2 tolerance (Fones and Preston, 2012), it is downregulated at 30°C in Pss B728a (Hockett et al., 2013) so EPS is unlikely to contribute to the enhanced H_2O_2 tolerance of Pss at 28°C.

4.1.7 Aims and rationale

In the previous chapter, we identified a cross-talk between oxidative stress tolerance and temperature. We demonstrated that Pss exhibits higher H_2O_2 tolerance at 28°C than at 21°C whilst in contrast Pspph exhibits lower H_2O_2 tolerance at 28°C than at 21°C. We hypothesised that this may be the reason why Pss virulence is higher at 28°C than at 21°C *in planta* while Pspph virulence is higher at 21°C than at 28°C. In this chapter, we aimed to identify key candidate genes that could mechanistically explain our findings. We also aim to determine why Pss and Pspph exhibit these differences despite being phylogenetically

related and infecting the same host plant (bean). To achieve this, we perform a transcriptomic screen of the gene expression changes of Pss and Pspph at 21°C and at 28°C, in the absence and presence of H_2O_2 *in vitro*.

4.2 Results

4.2.1 Hydrogen peroxide treatment is responsible for more variation between transcriptomes than temperature

We grew Pspph 1302A in MG medium in early-log phase at 21°C and 28°C and challenged it with 20mM H_2O_2 or the corresponding volume of water. Similarly, we grew Pss B728a in MG medium in early-log phase at 21°C and 28°C and challenged them with 80mM H_2O_2 or the corresponding volume of water. We chose MG medium because it more closely resembles the apoplast compared to the rich medium KB and we had tested strains for oxidative stress tolerance in both media. The H_2O_2 concentrations were chosen based on those previous experiments to be sufficiently large to affect bacterial growth *in vitro* without being lethal. Thirty minutes later (a time frame used by various other bacterial transcriptomic papers (Hockett et al., 2013)), samples were collected and RNA was purified and sent for sequencing. Looking at the distance map of the sample transcriptomes, biological replicates (n=3) from the same treatment appear to cluster together with one exception, sample j34 (Figure 4.1). The PCA plot also clusters samples according to their treatment and further supports the observation that j34 is an outlier (Figure 4.2). As a result, we excluded j34 from the rest of our analyses. While the samples cluster by both temperature and oxidative stress treatment, the samples also cluster by oxidative stress across both temperatures, indicating a common response.

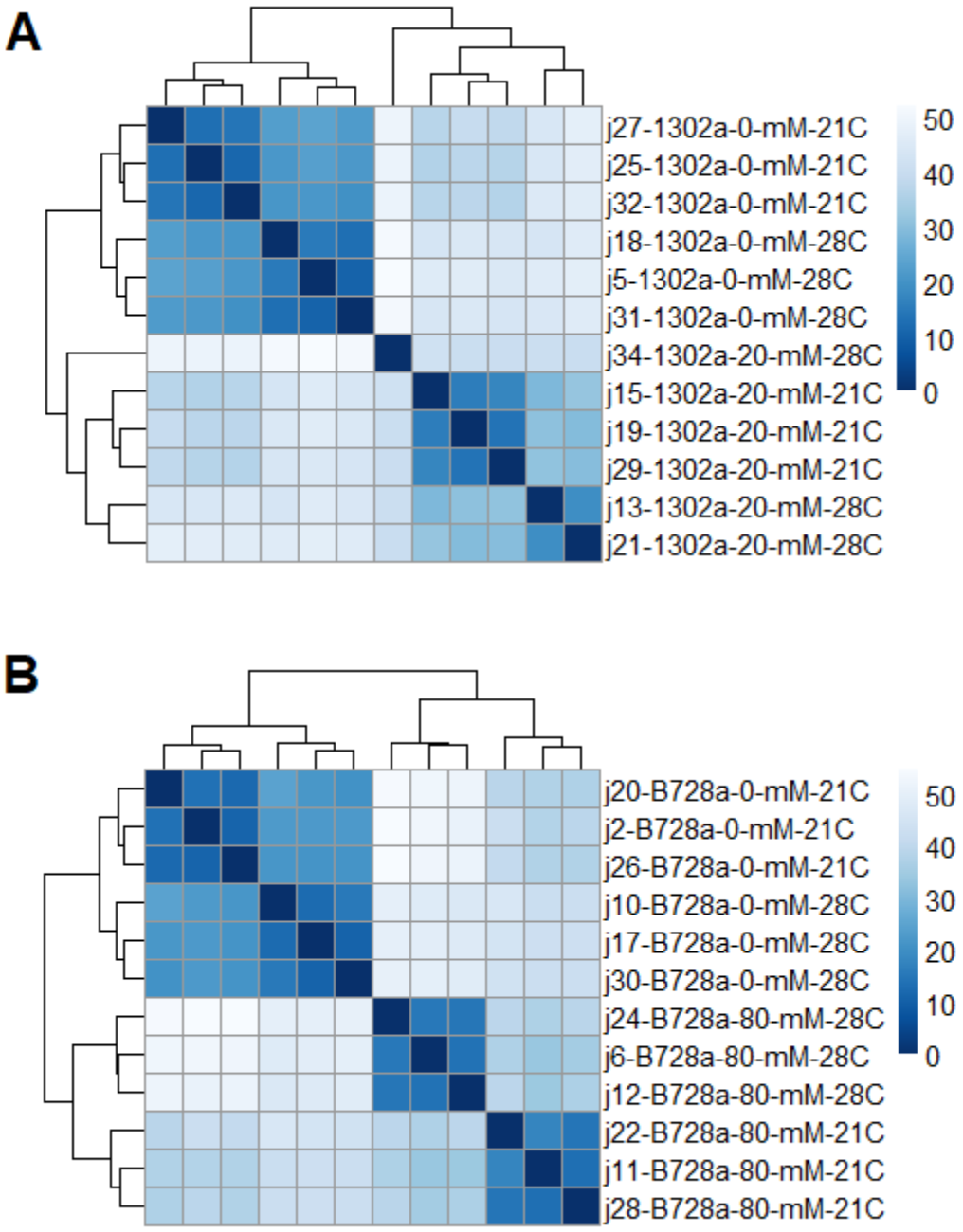


Figure 4.1: Euclidean distance matrix of the transcriptomes of A) 1302A and B) B728a samples. Samples are labelled by sample ID (e.g. j27), strain name, concentration of hydrogen peroxide used (in mM) and temperature. Euclidean distance is represented in blue, the darker the blue, the smaller the distance, indicating that the samples are similar to each other. The 1302A samples cluster together by treatment with the exception of the outlier sample j34. The B728a samples cluster together by treatment.

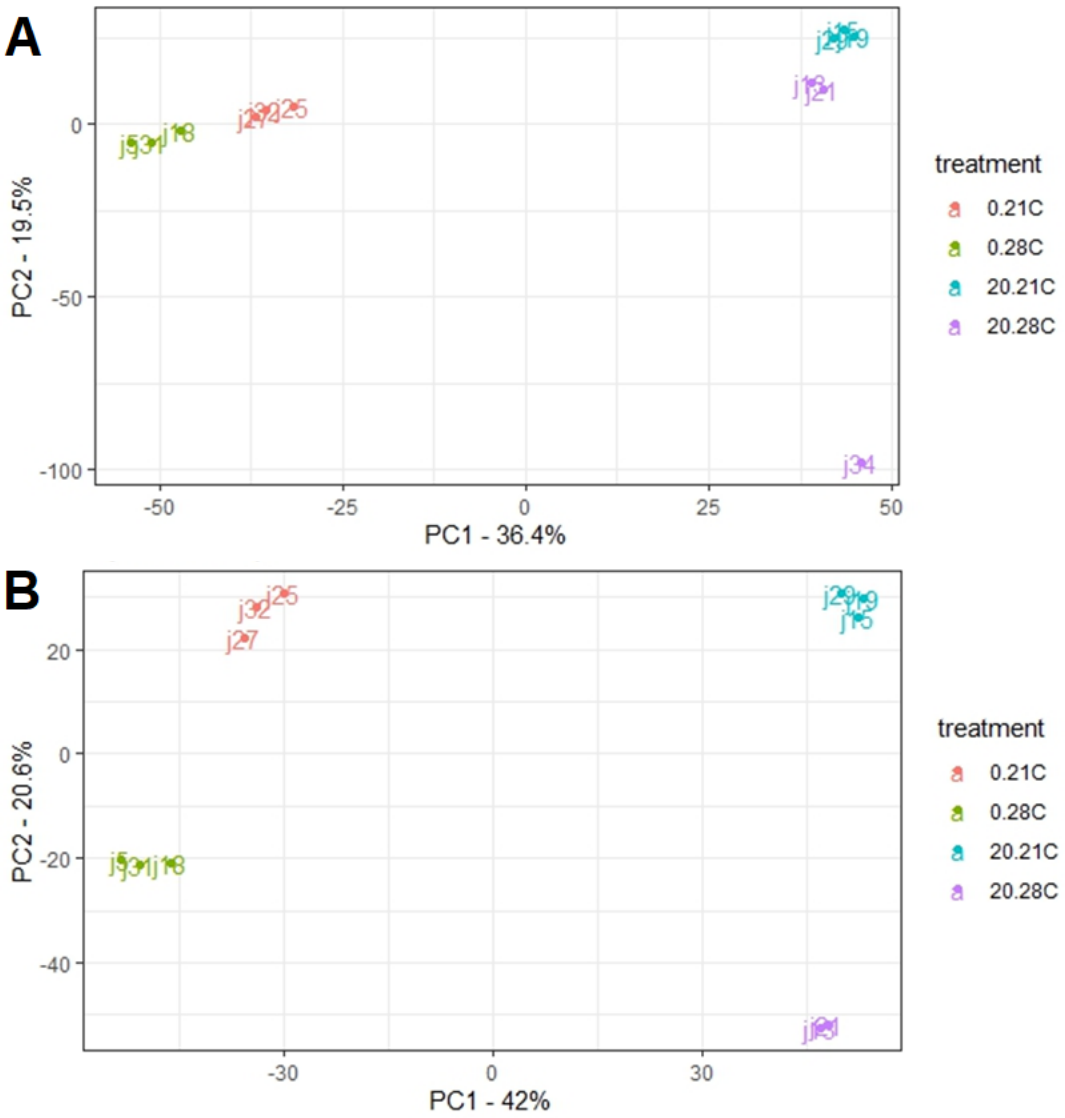


Figure 4.2: Principal component analysis plot of 1302A samples A) with and B) without outlier sample j34. Values of principal component 1 (PC1) are plotted along the x-axis. Values of principal component 2 (PC2) are plotted along the y axis. Each dot represents a unique sample and is labelled with its sample ID (e.g. j27). Dots and labels are colour-coded by treatment: coral for water control samples incubated at 21°C, green for water control samples incubated at 28°C, blue for hydrogen peroxide treated (20mM) samples incubated at 21°C and lilac for hydrogen peroxide treated (20mM) samples incubated at 28°C. PCA plot using prcomp, centred data on vsd transformed data. PC1 accounts for 36.4% of the variation in the data, but increases to 42% when the outlier j34 is excluded from the analysis. PC2 accounts for 19.5% of the variation in the data in plot A and 20.6% in plot B.

The PCA analysis also revealed that the largest source of variation in our samples' transcriptome was linked to the presence or absence of H_2O_2 (PR1 = 42% for the 1302A samples, and PR1= 40.5% for the

B728a samples), whilst temperature was second, being responsible for the second largest source of variation (PR2= 20.6% for the 1302A samples, and PR2= 27.6% for the B728a samples) (Fig4.2 and 4.4). This is consistent with our volcano plot, showing that the largest gene expression changes (highest absolute values of log2 fold change) were in response to H_2O_2 and not temperature (Fig 4.3).

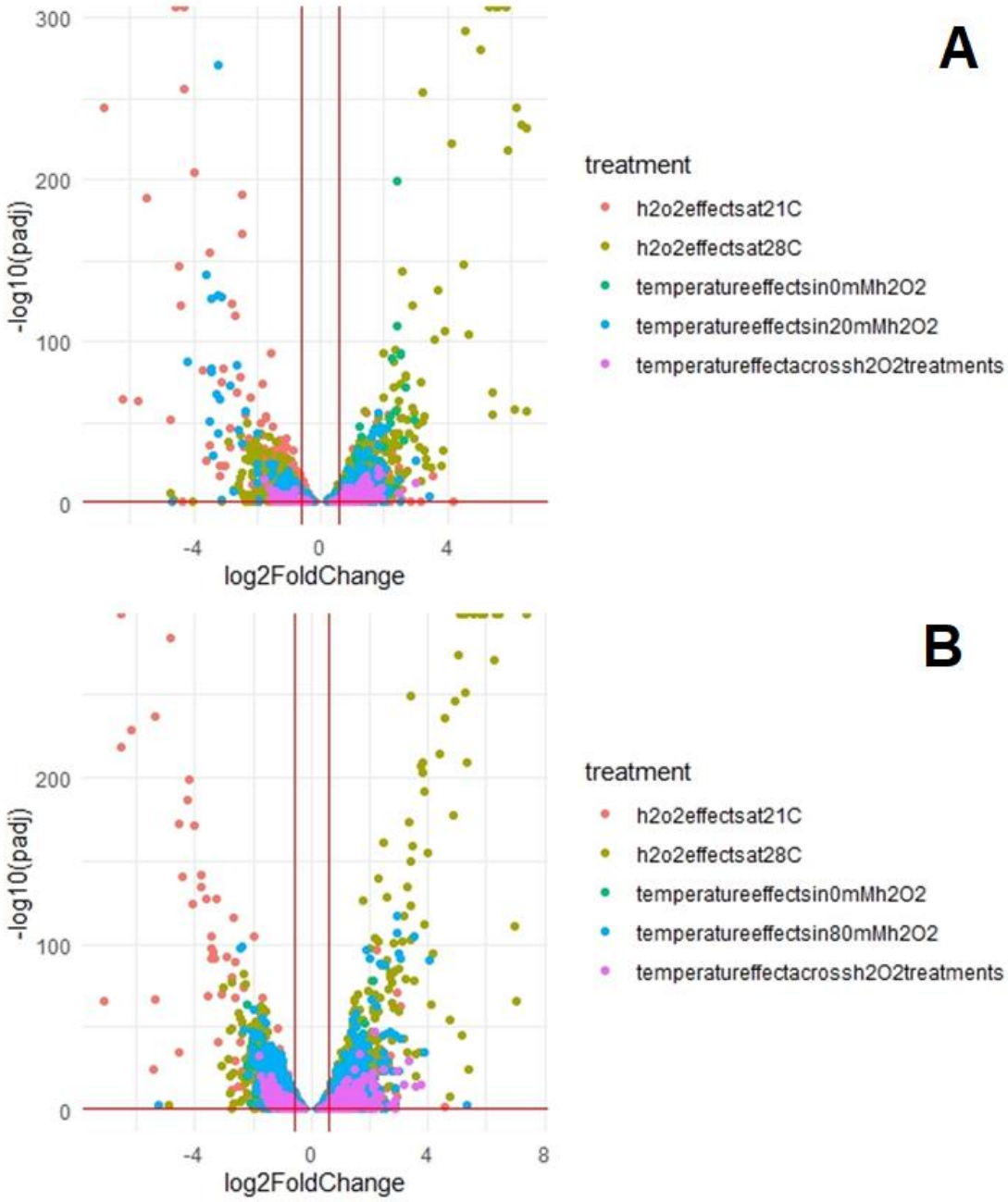


Figure 4.3: Differential gene expression in response to temperature and H_2O_2 in 1302A (A) and B728a (B). Volcano plot of fold change in expression (log2) against P-value adjusted for multiple testing (Bonferroni correction) (log10). The red lines delimit arbitrary threshold values that are used to eliminate less significant results. The thresholds used are P-value < 0.05 and log2foldchange > 0.4 or < -0.4. Each dot represents a gene. Dots are colour-coded by treatment: coral for changes in gene expression induced by Hydrogen peroxide challenge in samples incubated at 21°C; lime green for changes in gene expression induced by hydrogen peroxide challenge in samples incubated at 28°C; forest green for changes in gene expression at 28 vs 21°C in the absence of hydrogen peroxide, blue for changes in gene expression at 28 vs 21°C in the presence of hydrogen peroxide, purple for temperature effects on gene expression across hydrogen peroxide treatment (interaction term).

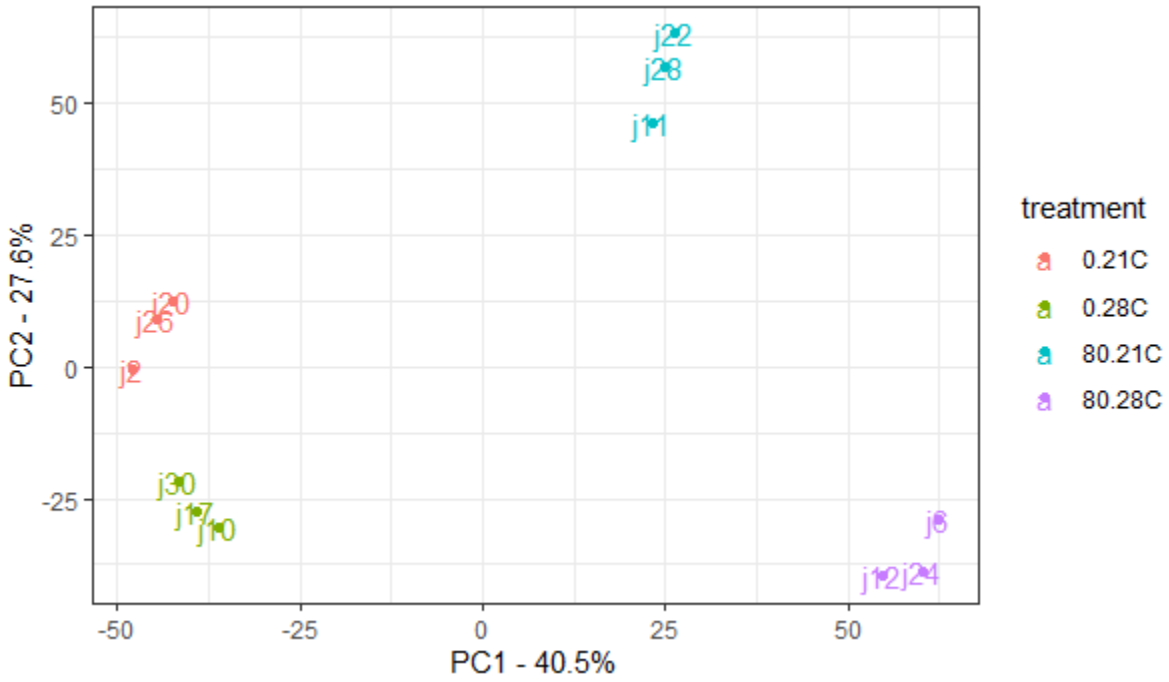


Figure 4.4: B728a samples cluster together by treatment in the PCA landscape. Values of principal component 1 (PC1) are plotted along the x-axis. Values of principal component 2 (PC2) are plotted along the y axis. Each dot represents a unique sample and is labelled with its sample ID (e.g. j27). Dots and labels are colour-coded by treatment: coral for water control samples incubated at 21°C, green for water control samples incubated at 28°C, blue for hydrogen peroxide treated (80mM) samples incubated at 21°C and lilac for hydrogen peroxide treated (80mM) samples incubated at 28°C. The largest amount of variation – 40% - (PC1) appears to be linked to presence/absence of 80mM H_2O_2, and the second largest amount of variation -27% - in the data (PC2) seems to be linked to temperature. PCA plot using prcomp, centred data on vsd transformed data.

4.2.2 A mixture of up and downregulated genes in response to temperature

We identified 1137 genes (20% of ORFs) in 1302A that are more expressed and 1031 genes (19%) that are less expressed in the presence of H_2O_2 than in the absence of H_2O_2 (adjusted P-value <0.05) at 28°C. At 21°C, we observe similar numbers: 1319 (24% of ORFs) are upregulated in presence vs absence of H_2O_2, 1109 (20%) are downregulated (supplementary table S3). Of those genes that appear to be differentially expressed in response to H_2O_2, 94 show opposite patterns of regulation at 21°C and 28°C and may therefore be involved in the temperature- H_2O_2 cross-talk response. In addition, we identify 406 (7.3% of ORFs) genes with higher and 328 genes (6%) with lower expression levels (adjusted P-value <0.05) at 21 than at 28°C in the presence of 20mM H_2O_2. In the absence of H_2O_2, 527 genes (9.5%) are more expressed at 28°C than at 21°C, while 666 genes (12%) are more expressed at 21°C than at 28°C.

In B728a, we identified 1433 upregulated genes (28% of ORFs) and 1349 downregulated genes (adjusted P-value <0.05) in the presence vs absence of H_2O_2 at 28°C. At 21°C, 1319 genes (26% of ORFs) are upregulated and 1208 (23%) are downregulated in the presence vs absence of H_2O_2 (table S3). On the other side, 467 B728a genes are upregulated (9% of ORFs) and 500 genes (10%) are downregulated at 28°C vs 21°C in the absence of H_2O_2. In the presence of H_2O_2, 1093 genes (21% of ORFs) are more expressed at 28°C than at 21°C whilst 1272 genes (25%) are more expressed at 21°C than at 28°C.

4.2.3 Genes involved in transmembrane transport, protein folding and metabolism biosynthesis are responsive to temperature and oxidative stress

In order to obtain a functional profile of the set of genes responsive to temperature and oxidative stress, we performed a Gene Ontology (GO) Term Enrichment Analysis (GOTEA). GO terms associated with

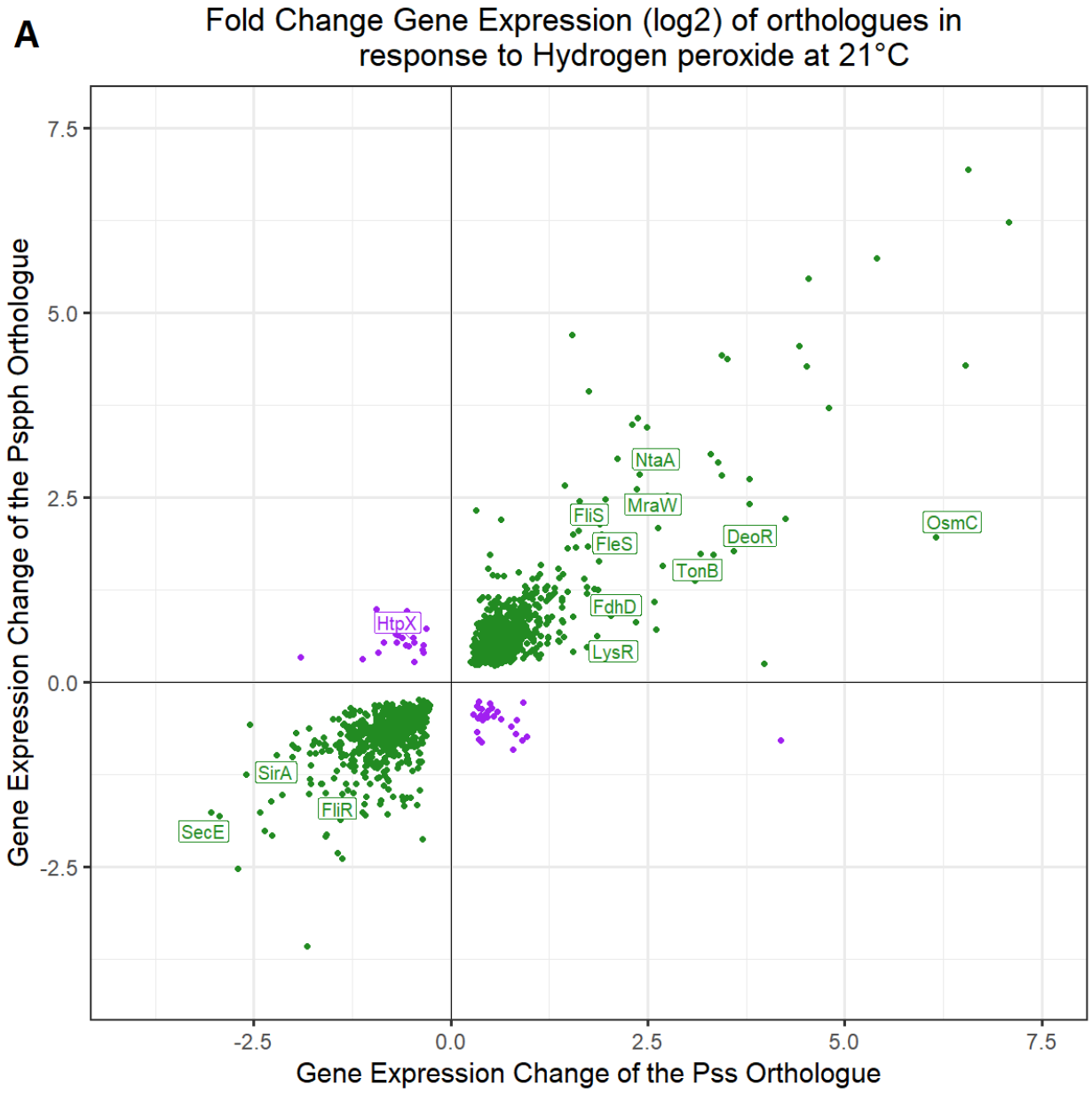
response to oxidative stress, bacterial motility, transmembrane transport, iron scavenging, metabolic biosynthesis, catabolism, gene expression remodelling and protein folding were found to be enriched among differentially expressed genes in 1302A and B728a (table 4.1). Hydrogen peroxide treatment strongly correlated with enrichment of genes involved in oxidative stress response as well as motility and catabolism in both strains. Thermoregulated genes were associated with transmembrane transport, protein folding and metabolic biosynthesis.

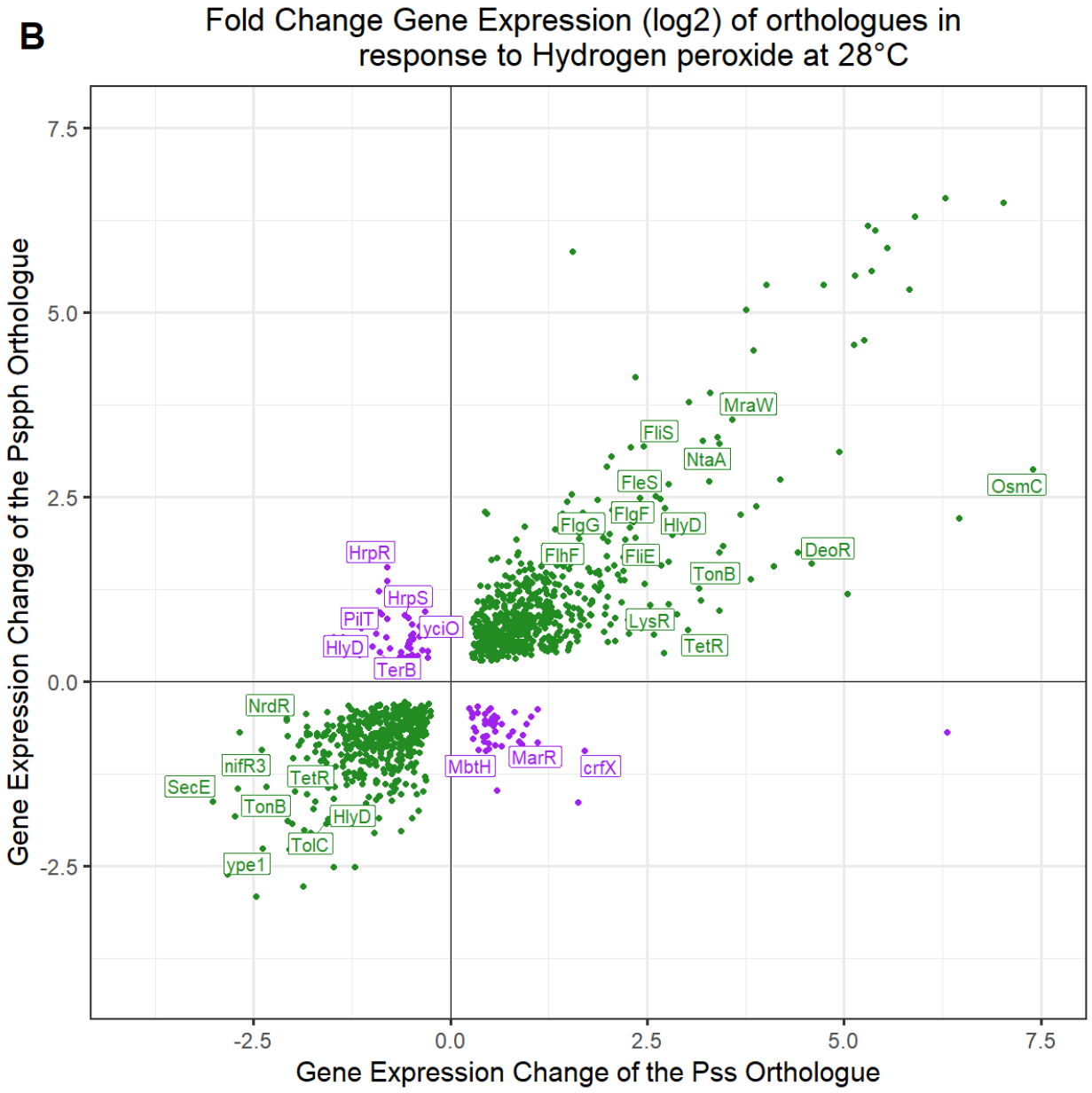
Table 4.1: Gene Ontology (GO) term enrichment analysis using GO annotations for Pspph 1302A (in green) and Pss B728a (in purple). A “y” indicates that genes associated with the GO-term described in each row were significantly enriched amongst genes with statistically significantly changes in expression (Bonferroni adjusted P-value < 0.05) for the treatment displayed in the column. “ns” indicates that there was no significant enrichment. “NA” indicates that this GO term was not found in this strain.

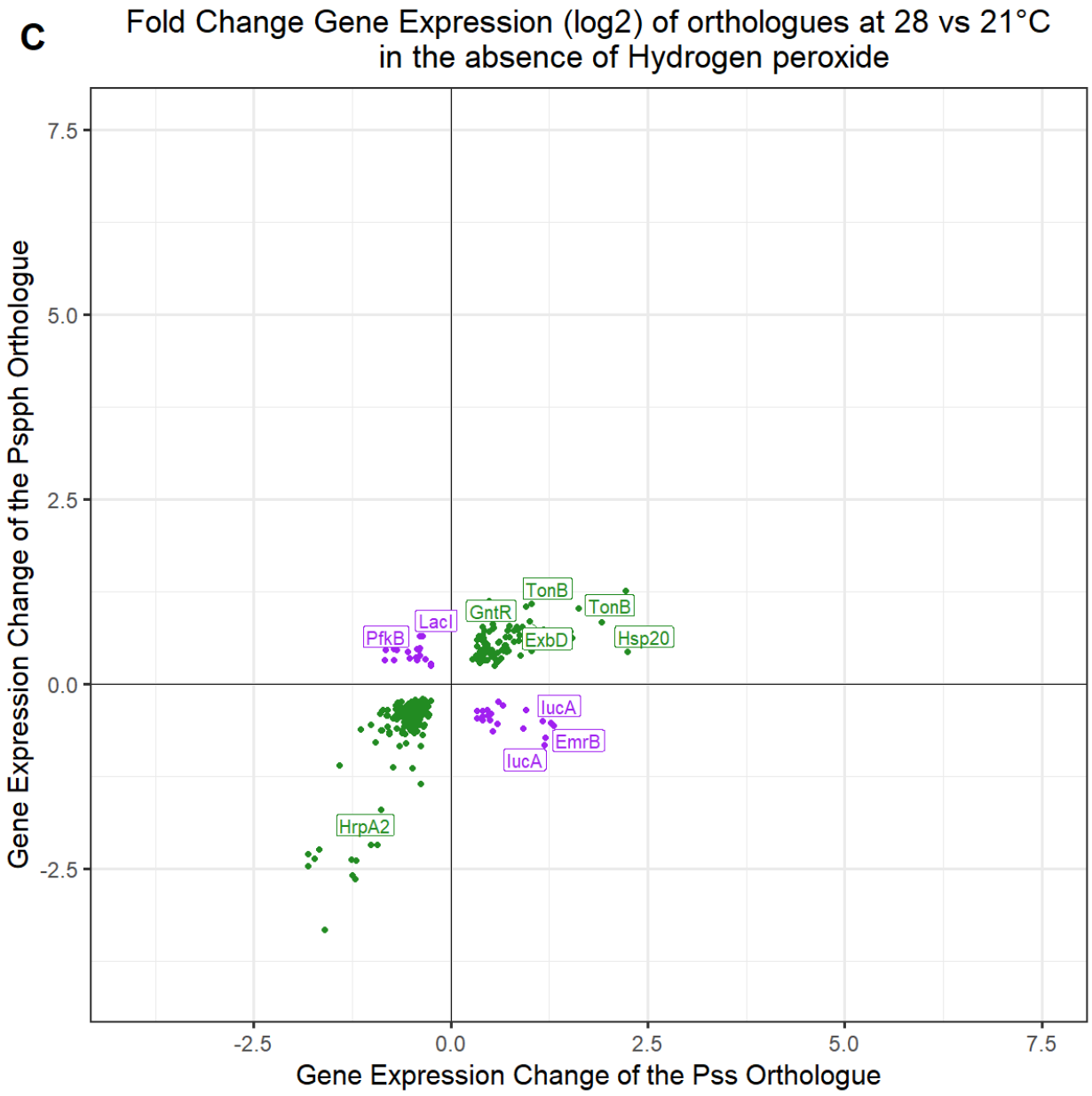
	1302A					B728a				
	Oxidative stress responsive		Thermoregulated genes		Interaction	Oxidative stress responsive		Thermoregulated genes		Interaction
	at 21°C	at 28°C	"- H2o2"	"+ H2o2"		at 21°C	at 28°C	"- H2o2"	"+ H2o2"	
Response to stress										
Catalase activity (GO:0004096)	y	y	ns	y	y	y	y	ns	ns	ns
Response to oxidative stress (GO:0006979)	y	y	ns	y	y	y	y	ns	ns	ns
Detoxification (GO:0098754)	y	y	ns	ns	y	ns	y	ns	ns	ns
Reactive oxygen species metabolic process (GO:0072593)	y	y	ns	ns	ns	y	y	ns	ns	ns
Bacterial motility										
Bacterial type flagellum assembly (GO:0044780)	y	y	ns	y	y	NA	NA	NA	NA	NA
Bacterial type flagellum (GO:0009288)	NA	NA	NA	NA	NA	y	y	ns	y	ns
Bacterial type flagellum basal body (GO:0009425)	ns	y	ns	y	y	ns	y	ns	y	y
Bacterial type flagellum basal body rod (GO:0030694)	y	y	ns	ns	y	y	y	ns	ns	y
Bacterial type flagellum-dependent cell motility (GO:0071973)	y	y	ns	y	y	y	y	ns	ns	y
Chemotaxis (GO:0006935)	ns	y	y	y	y	ns	y	ns	ns	y
Transmembrane transport										
Export from cell (GO:0140352)	ns	y	ns	ns	y	NA	NA	NA	NA	NA
Inorganic anion transmembrane transport (GO:0098661)	ns	y	y	y	y	ns	y	y	y	y
Transmembrane signalling receptor activity (GO:0004888)	ns	ns	y	y	y	ns	y	ns	ns	y
Transmembrane transporter complex (GO:1902495)	ns	ns	y	ns	y	NA	NA	NA	NA	NA
Iron / Metal ions										
Iron-sulfur cluster assembly (GO:0016226)	ns	ns	ns	y	y	ns	ns	ns	y	y
Transition metal ion binding (GO:0046914)	NA	NA	NA	NA	NA	y	ns	ns	y	y
Heme binding (GO:0020037)	NA	NA	NA	NA	NA	y	y	ns	ns	ns
4Fe-4S cluster binding (GO:0051539)	y	ns	ns	ns	ns	y	y	ns	ns	ns
Sulfate transport (GO:0008272)	ns	y	ns	y	y	ns	y	y	y	y
Metabolic Biosynthesis										
Arginine biosynthetic process (GO:0006526)	ns	ns	y	y	ns	ns	ns	ns	y	ns
Polyamine biosynthetic process (GO:0006596)	ns	y	y	y	ns	ns	ns	y	y	ns
Secondary metabolite biosynthetic process (GO:0044550)	y	ns	ns	y	ns	y	ns	ns	ns	ns
Metabolic Catabolism										
Cellular catabolic process (GO:0044248)	y	y	ns	ns	ns	ns	y	ns	ns	ns
Amino acid catabolic process (GO:0009063)	y	y	y	ns	ns	ns	y	ns	ns	ns
Aromatic compound catabolic process (GO:0019439)	y	y	ns	ns	ns	NA	NA	NA	NA	NA
Gene expression remodelling										
Transcription factor binding (GO:0008134)	ns	ns	ns	y	y	NA	NA	NA	NA	NA
DNA-templated transcription (GO:0006351)	NA	NA	NA	NA	NA	y	y	ns	ns	ns
Negative regulation of DNA-templated transcription (GO:0045892)	NA	NA	NA	NA	NA	y	y	ns	y	ns
Translation (GO:0006412)	y	ns	y	ns	ns	y	ns	y	y	ns
Structural constituent of chromatin (GO:0030527)	ns	y	y	y	y	NA	NA	NA	NA	NA
Protein folding										
Protein folding (GO:0006457)	ns	ns	y	ns	ns	ns	y	y	ns	ns
Protein folding chaperone (GO:0044183)	ns	ns	y	ns	ns	ns	y	y	ns	ns

4.2.4 Orthologues do not all share the same transcriptional responses to environmental cues

We used orthology sets collated at Pseudomonas.com (Winsor et al., 2016) to pair genes from Pss and Pspph together as orthologues. In the rare event that a gene had multiple orthologues, the first one in the list was used to prevent personal biases in data interpretation. We then compared expression changes of the orthologues in the different treatments. We identified a number of orthologue pairs which display opposite patterns of expression change in the two strains in the same treatment (figure 4.5). For instance, the following genes are more expressed at 28°C than at 21°C in Pspph but are less expressed at 28°C than at 21°C in Pss: *pfkB* and *lacI* (figure 4.5C).


A
Fold Change Gene Expression (log2) of orthologues in response to Hydrogen peroxide at 21°C
Gene Expression Change of the Pspph Orthologue
Gene Expression Change of the Pss Orthologue
7.5
5.0
2.5
0.0
-2.5
-2.5
0.0
2.5
5.0
7.5
NtaA
MraW
FliS
FleS
DeoR
TonB
OsmC
FdhD
LysR
HtpX
SirA
FliR
SecE


B
Fold Change Gene Expression (log2) of orthologues in response to Hydrogen peroxide at 28°C
Gene Expression Change of the Pspph Orthologue
Gene Expression Change of the Pss Orthologue
7.5
5.0
2.5
0.0
-2.5
-2.5
0.0
2.5
5.0
7.5
MraW
FliS
NtaA
FleS
OsmC
FlgF
FlgG
HlyD
DeoR
HrpR
FlhF
FliE
TonB
HrpS
PilT
yciO
LysR
HlyD
TetR
TerB
NrdR
nifR3
MbtH
MarR
crfX
SecE
TetR
TonB
HlyD
TolC
ype1


c
Fold Change Gene Expression (log2) of orthologues at 28 vs 21°C
in the absence of Hydrogen peroxide
Gene Expression Change of the Pspph Orthologue
Gene Expression Change of the Pss Orthologue
7.5
5.0
2.5
0.0
-2.5
-2.5
0.0
2.5
5.0
7.5
TonB
TonB
GntR
LacI
PfkB
ExbD
Hsp20
IucA
EmrB
IucA
HrpA2

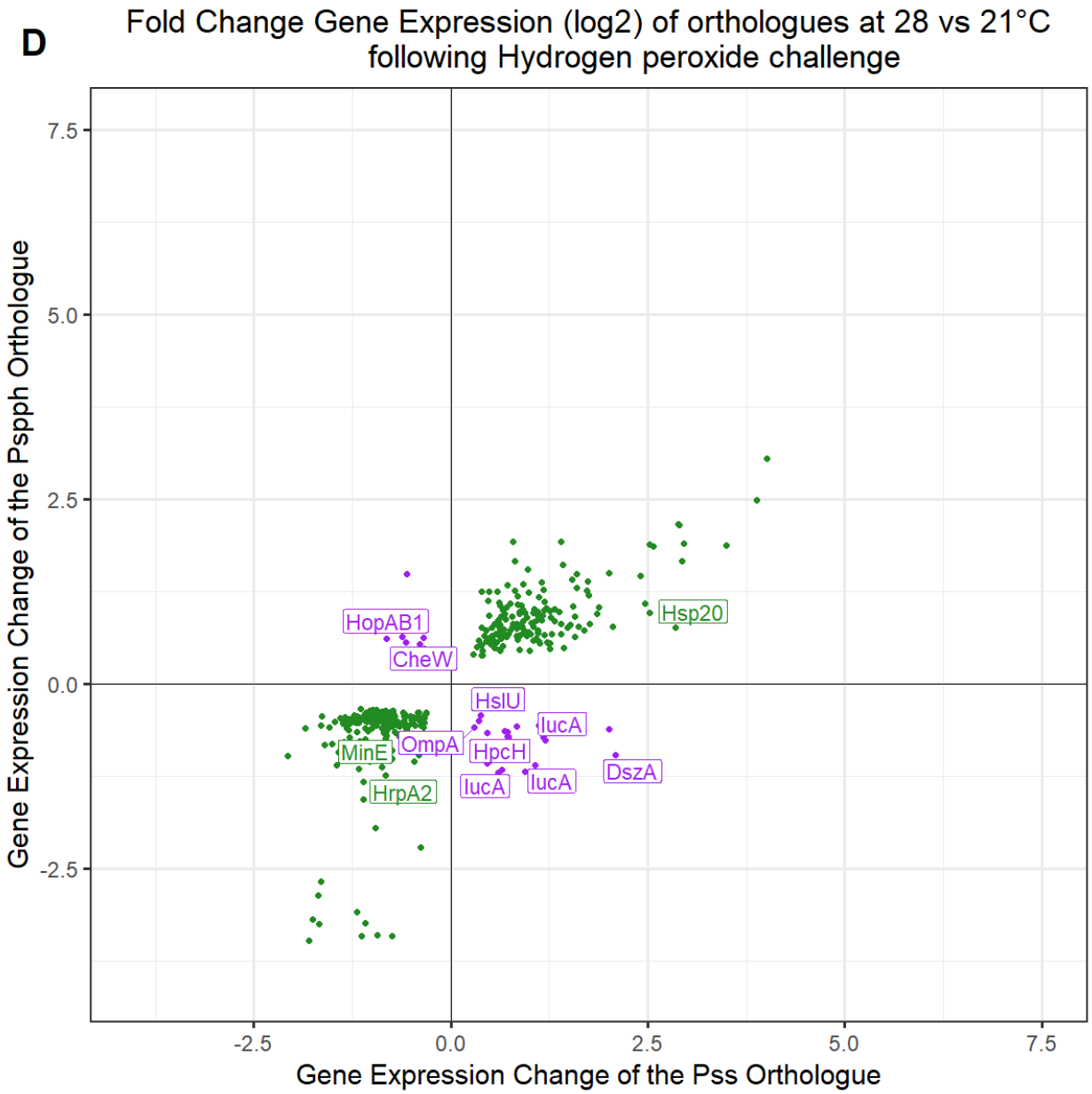


Figure 4.5: Fold change (log2) gene expression of orthologous genes between Pss (x-axis) and Pspph (y-axis) in different treatment combinations:

A) Challenged with H_2O_2 vs water control, at 21°C
B) Challenged with H_2O_2 vs water control, at 28°C
C) 21°C vs 28°C, in absence of H_2O_2
D) 21°C vs 28°C, in presence of H_2O_2

Each orthologue pair was determined from published database lists (available at Pseudomonas.com). In the event of a gene having multiple orthologues in the other strain, we kept only the first orthologue pair in the list. We only depict pairs with significant changes in expression in both strains (adjusted P-value <0.05, Bonferroni correction). Orthologues with opposite patterns of expression in the two strains are depicted in purple and the others are depicted in green. Where a common name was available (e.g. *osmC*), dots were labelled accordingly using R package ggrepel.

4.2.5 Phaseolotoxin genes are thermoregulated in Pspph 1302A

The majority of the genes that form the phaseolotoxin gene cluster had low levels of expression: expression ranged from a base mean of 27 to 5906 counts. Indeed, the cluster averaged a base mean of 416 (for comparison, the average base mean for the whole genome is 950).

Nonetheless, approximately half of the genes that belong to the phaseolotoxin cluster displayed statistically significant changes in expression in response to hydrogen peroxide and temperature treatment while the other half were not statistically significantly different (Adjusted P-value >0.05). Of the former set, all were more expressed at 21°C than at 28°C (L2FC ranging from -0.45 to -1.33) with the exception of the transposase bordering the cluster (L2FC = 0.71). Hydrogen peroxide treatment induced expression of a majority of the phaseolotoxin genes both at 21°C (9 genes with statistically significant positive L2FC) and 28°C (10 genes with statistically significant positive L2FC) (L2FC ranging from 0.40 to 1.62) with few exceptions at the margins of the cluster (supplementary table S3).

We were unable to detect *argK* expression in this assay in any treatment. This is significant because ArgK is responsible for the bacterial resistance to phaseolotoxin (Aguilera et al., 2012).

4.2.6 Catalase and superoxide dismutase genes are thermoregulated in both strains

Genes encoding catalases and superoxide dismutases were of special interest in this experiment as they are known to be regulated by oxidative stress (Fones and Preston, 2012). Catalase genes *katA, katB, katE* and *katG* display expression induced by hydrogen peroxide at both temperatures in B728a.

Furthermore, *katB, katE* and *katG* are significantly more expressed at 28°C than at 21°C in the presence of hydrogen peroxide in this strain (supplementary table S3).

In the case of 1302A, the expression of catalase genes *katA, katB* and *katG* is induced by hydrogen peroxide, and they are also more expressed at 28 than at 21°C in the presence of hydrogen peroxide ($P<0.05$). Interestingly*, katB* and *katG* are more expressed at 21 than at 28°C in the absence of hydrogen peroxide.

Superoxide dismutase *sodB* is the only superoxide dismutase gene significantly induced by hydrogen peroxide in 1302A, and it also shows a moderate increase in expression at 21 compared to 28°C in 1302A while the other two *sod* genes are not significantly differentially expressed. Conversely, in B728a, all three sod genes: *sodA, sodB* and *sodC* display expression induced by hydrogen peroxide treatment. Of those*, sodA* is more expressed at 28 than at 21°C while the others do not display significant thermoregulation (supplementary table S3).

4.2.7 Iron scavenging and metabolism

Iron metabolism and in particular siderophore gene expression has been previously linked to both oxidative stress (Salunkhe et al., 2005, Palma et al., 2004) and temperature responses (Hockett et al., 2013) in *Pseudomonas*. As such, they are of special interest in this assay. In both Pss and Pspph, there are a mixture of upregulated and downregulated iron-related genes at different temperatures, including genes encoding metal ion transporters, siderophores, and iron co-factors (supplementary table S3). Of special interest are the trio of genes responsible for siderophore achromobactin synthesis: *acsA* (PSPPH_2756/Psyr_2589), *acsC* (PSPPH_2754/ Psyr_2587) and *acsD* (PSPPH_2751/Psyr_2584) (labelled by their alternative protein name “LucA” in figure 4.5). These are more expressed at 28 than at 21°C in

B728a and more expressed at 21 than at 28°C in 1302A (supplementary table S3). The expression of all three genes is also induced by hydrogen peroxide stress in both strains.

4.2.8 Master regulator RpoS is only differentially expressed in Pss B728a and not in Pspph 1302A

The stationary phase transition master regulator RpoS is an interesting case because its gene expression is relatively unchanged in all treatments in Pspph 1302A but that is not the case in Pss B728a. In Pss B728a, *rpoS* expression is more expressed at 21°C in the presence of H_2O_2 (supplementary table S3).

4.2.9 Expression of exopolysaccharides is temperature and oxidative stress responsive

Pseudomonas typically produce a number of exopolysaccharides (EPS) including levan and alginate, which play a role in biofilm formation, adhesion to host surfaces and resistance to antimicrobial compounds such as ROS (Keith and Bender, 1999). Consistent with this, we find that most genes belonging to the alginate biosynthesis operon are activated in response to hydrogen peroxide stress in both strains in our transcriptomic screen (supplementary table S3). This appears to be independent of temperature in both strains with the exception of *algJ* which is more expressed at 28 than at 21°C in B728a. Interestingly, levan expression is induced by hydrogen peroxide and is significantly more expressed at 21 than at 28°C in both strains (supplementary table S3). This is potentially indicative of a role of EPS in the cross-talk between oxidative stress responses and temperature.

4.3 Discussion

In this chapter, we performed a transcriptomic screen of the gene expression changes of Pss and Pspph at 21°C and at 28°C, in the absence and presence of H_2O_2 *in vitro* in order to identify candidate genes responsible for the temperature-oxidative stress-virulence cross-talk affecting Pss and Pspph differentially. We were therefore particularly interested in genes that were upregulated at 28°C in Pss, upregulated at 21°C in Pspph, differentially expressed in Pss and Pspph and showing large changes in expression in response to any treatment.

4.3.1 Differences in methodology may be responsible for differences in temperature responses with published datasets

Our assay identifies fewer candidate genes involved in temperature response than previously available literature. For instance, Hockett et al (2013) found 1446 thermoregulated genes in B728a (for comparison we find 967 thermoregulated B728a genes in the absence of H_2O_2) using a similar methodology to us (RNAseq, 3 bio reps, adjusted P-value =< 0.05, comparison 20°C vs 30°C, KB medium). An important difference is that Hockett et al. (2003) used the rich medium KB, whereas we grew our bacteria in the nutritionally poor minimal medium MG. This is not only significant for carbon availability but also affects iron and other nutrients. The minimal medium MG has notably low levels of iron (table 2.1). Of the thermoregulated genes they identified, Hockett et al (2003) found that 1107 are more expressed at 30°C than at 20°C, and 338 are more expressed at 20°C than at 30°C. They determined that genes involved in polysaccharide synthesis and regulation, phage and IS elements, type IV secretion, chemosensing and chemotaxis, translation, flagella synthesis and motility, phytotoxin synthesis and transport were generally repressed at 30°C compared to 20°C. They also found that genes associated with transcriptional regulation, quaternary ammonium compound metabolism and transport, chaperone/heat shock proteins are generally upregulated at 30°C compared to 20°C. Consistent with

their findings, we determined through Gene ontology (GO) term enrichment analysis (GOTEA) that genes involved in chemosensing and chemotaxis (particularly iron scavenging), flagella synthesis and motility, gene expression remodelling and phytotoxin synthesis and transport were thermoregulated in B728a and 1302A (supplementary table S1 and S2). We also identified a number of chaperones and heatshock proteins amongst thermoregulated genes such as *htpX, grpE*, *hsp20, hsp70* and *hsp90* (supplementary table S3). We found that KEGG terms associated with lipopolysaccharide biosynthesis, T3SS and bacterial secretion systems are enriched among genes that are more expressed at 21C than at 28°C in B728a (supplementary table S7) which is consistent with Hockett's observations. However, we did not identify a particular link with phage and IS elements, or quaternary ammonium compound metabolism in our dataset. Instead, we found that sulfur metabolism genes are more expressed at 28 than at 21°C, while genes associated with amino acid biosynthesis, secondary metabolite biosynthesis, plant pathogen interactions, RNA degradation, and protein export are more expressed at 21 than at 28°C in this strain (supplementary table S7).

Results for 1302A are not dissimilar from those described for B728a in the previous paragraph, with a few notable exceptions which are of special interest to this study: KEGG terms associated with plant-pathogen interactions are more expressed at 21C in B728a whereas they are more expressed at 28°C in 1302A; glycine, serine and threonine metabolism genes are more expressed at 28°C in B728a and at 21°C in 1302A. Furthermore, we also find that genes involved in biofilm formation, flagellar assembly and bacterial chemotaxis (KEGG database) are generally more expressed at 28°C in 1302A (supplementary table S8).

Discrepancies between our findings despite similar setups (RNAseq), treatments (20/21°C vs 30/28°C) and genetic material (the same Pss strain B728a albeit from different glycerol stocks) are not entirely

surprising considering how multifactorial bacterial transcription regulation is. In particular, we suspect the difference in medium plays a large role in the differences observed. Indeed, Hockett et al. (2003) used the rich medium KB, whereas we grew our bacteria in the nutritionally poor minimal medium MG. We had already observed that medium composition has large effects on oxidative stress – temperature response cross-talk in chapter 3, so we expect that this is the case here. It is also possible that differences in data collection, annotation and analysis have led to some discrepancies. This experiment serves to highlight the variability of responses Pss B728a can display in response to changes in temperature.

4.3.2 Transcriptional responses of B728a to H_2O_2 are more consistent with published transcriptomic studies than 1302A

Transcriptomic studies of *P. aeruginosa* exposed to varying levels of exogenous ROS found that genes involved in protective mechanisms such as detoxifying enzymes (catalase, glutathione peroxidase, superoxide dismutases), DNA repair mechanisms, heat shock proteins, transport of sulfur-containing compounds and bacterial virulence genes were upregulated in response to ROS. They also generally found that genes involved in primary metabolism processes, energy metabolism, ribosomal biogenesis, purine and pyrimidine synthesis, fatty acid synthesis, polyamine and carbon metabolism were typically downregulated in response to challenge by a variety of ROS, including but not restricted to H_2O_2. Iron homeostasis related genes were upregulated in log phase but downregulated in stationary phase in response to sublethal levels of H_2O_2 (Nizer et al., 2021). In spite of the relatively different experimental setups (different species, human pathogen vs plant pathogen, different ROS/ different H_2O_2 levels), we found relatively similar functional groups of genes were upregulated in response to H_2O_2 in our experiment.

In 1302A: We found that genes associated with ROS detoxification and sulfur metabolism were generally upregulated in response to hydrogen peroxide (supplementary table S1 and S8). In contrast with the transcriptome from the *P. aeruginosa* study described above, we did not find that suppressed genes were associated with any particular function. Additionally, genes activated during hydrogen peroxide treatment were also associated with flagellar assembly (supplementary table S1).

In B728a: We find that genes associated with ROS detoxification, sulfur metabolism, virulence and iron metabolism are generally upregulated in the presence of hydrogen peroxide (supplementary table S2 and S7) which is consistent with the transcriptome results for *P. aeruginosa*. In contrast with the *P. aeruginosa* transcriptome described above, suppressed genes were associated with only a few cellular processes, namely lipopolysaccharide biosynthesis and bacterial secretion systems. Additionally, genes activated during hydrogen peroxide treatment were also associated with flagellar assembly and glutathione metabolism (supplementary table S2 and S7). This is to be expected as glutathione metabolism has previously been linked to redox processes and oxidative stress tolerance in *Pseudomonas* (Saninjuk et al., 2019, Wongsaroj et al., 2018).

Furthermore, genes associated with primary metabolism including carbon metabolism, the TCA cycle and glucose (glycolysis) metabolism, is actually upregulated in response to H_2O_2 challenge in Pss B728a, alongside genes involved in other metabolic processes such as fatty acid degradation and metabolism (at both temperatures); amino acid biosynthesis – including cysteine metabolism -, secondary metabolite biosynthesis, lipoic acid metabolism, sulfur metabolism (at 21°C); and lipopolysaccharide biosynthesis (at 28°C) (supplementary table S7). The upregulation of genes involved in fatty acid degradation at 28°C in the presence of H_2O_2 and at no other treatment in Pss B728a is particularly interesting because it suggests that the plasma membrane is getting recycled and modified in response to the new environmental conditions. Considering that temperature-mediated phytotoxin gene expression regulation is dependent on membrane fluidity (Braun et al., 2007), this further supports the

assumption that bacteria are actively responding to temperature, and that this may play a role in the cross-talk between temperature and oxidative stress response.

In the case of 1302A, genes involved in primary metabolism including carbon metabolism and the TCA cycle, were upregulated in response to H_2O_2 challenge alongside genes involved in other cellular processes such secondary metabolite biosynthesis, lipoic acid metabolism and sulfur metabolism (at both temperatures); amino acid biosynthesis (at 21°C); and one carbon pool by folate and chemotaxis (at 28°C) (supplementary table S8).

The activation of many metabolic pathways in both Pspph 1302A and Pss B728a in the face of ROS stress is in disagreement with published *P. aeruginosa* transcriptomic results. This may be a result of differences in data annotation and analysis but we suspect that differences in genetic material (*P. aeruginosa* is a relatively distant relative of Pss and Pspph despite being in the same genus) and treatment conditions play an important part. In particular, some *P. aeruginosa* transcriptomic studies used high levels of ROS that are potentially lethal to *P. aeruginosa* (eg. 10mM H_2O_2 by (Salunkhe et al., 2005)) and all use different media from our experiment (media more adapted to *P. aeruginosa* presumably) -LB for (Salunkhe et al., 2005, Chang et al., 2005) and Tryptic Soy medium for (Palma et al., 2004). These two media are both relatively rich and salty media unlike the minimal medium MG which we used in this experiment. This is likely to play a major part in the differences observed as minimal media require bacteria to be able to synthesise a wide range of metabolites whereas in rich media they can obtain metabolites from the medium.

4.3.3 The role of iron in temperature and oxidative stress response remains elusive

As described previously in this chapter, genes associated with iron metabolism and transport have been implicated in bacterial responses to temperature (Hockett et al., 2013, Arvizu-Gomez et al., 2013) and oxidative stress (Kim and Park, 2014, Salunkhe et al., 2005, Palma et al., 2004) so we were interested to determine expression changes of these genes in our dataset. Looking more closely at the fur regulon in B728a, we observe that iron-sulfur cluster operon genes, including *iscR, iscS, iscU,* and *iscA* are strongly expressed in response to hydrogen peroxide treatment and are generally more expressed at 28 than at 21°C. Conversely, the iron transporter genes *efeM* and *efeO* are induced by hydrogen peroxide challenge but are generally more expressed at 21 than at 28°C in this strain (supplementary table S3), and heme-related genes do not show particularly strong patterns of expression changes, with the exception of suppression of expression of iron exporters *ccmA, ccmB* and *ccmD* in hydrogen peroxide treatments.

In 1302A, the iron-sulfur cluster operon genes *iscS, iscU* and *iscR* are strongly expressed in response to hydrogen peroxide and are generally more expressed at 28 than at 21°C in the presence of hydrogen peroxide, in similar fashion to B728a. Gene expression of Iron transporters *efeB, efeM* and *efeO* is not significantly affected by hydrogen peroxide treatment but they are more expressed at 21 than at 28°C in 1302A which is a similar pattern to the one observed in B728a. Heme-related genes do not show particularly strong patterns of expression changes in this strain (supplementary table S3).

Considering that sulfur metabolism was found to be upregulated in both strains (supplementary table S7 and S8), it appears that iron-sulfur clusters are important for oxidative stress tolerance in Pspph 1302A and Pss B728a which is consistent with published literature on iron-sulfur clusters (Blanc et al., 2014, Deng et al., 2013). Iron-sulfur clusters are particularly sensitive to oxidation by hydrogen peroxide and other ROS (Blanc et al., 2014) which inactivates housekeeping enzymes such as glutamate synthase that contain these clusters, and regeneration of iron-sulfur clusters is necessary for bacterial survival and growth in the face of hydrogen peroxide stress (Deng et al., 2013). Additionally, these results may be part of a larger broad transcriptional response. Indeed, IscR has been documented to be required for

hydrogen peroxide tolerance in a mutant assay in *P. aeruginosa* (Choi et al., 2007), and is a master transcriptional regulator involved in transcriptional regulation of genes associated with iron-sulfur cluster biosynthesis but also iron homeostasis, resistance to oxidants, and pathogenicity in *Pseudomonas aeruginosa* (Saninjuk et al., 2019*)*. Note that glutathione also contain sulfur, and glutathione production is typically associated with oxidative stress tolerance in bacteria (Masip et al., 2006).

Interestingly, genes involved in production of iron-scavenging siderophores displayed differential of expression following hydrogen peroxide challenge in both strains. *Pseudomonas syringae* is known to produce two different siderophores, pyoverdine and achromobactin (Cornelis and Matthijs, 2002). The induction of pyoverdine biosynthesis by oxidative stress was expected as it was well-established in the literature for other *Pseudomonas* strains (Yu et al., 2014, Nizer et al., 2021) but this was not the case in either strain. Instead, the pyoverdine gene *pvdM* was suppressed in the presence of hydrogen peroxide (supplementary table S3). This may be a result of the nutritionally poor medium we chose as pyoverdine production is notably energetically expensive for bacteria (Griffin et al., 2004). Contrary to pyoverdine, achromobactin genes were induced in response to hydrogen peroxide treatment at both temperatures in B728a, but specifically at 21°C in 1302A.

More surprising was the temperature-responsive expression of achromobactin biosynthesis genes. They displays opposite patterns of thermoregulation in the two strains: more expressed at 21°C in 1302A but more expressed at 28°C in B728a (supplementary table S3).

Achromobactin synthesis requires AcsD, AcsA and AcsC in Pss B728a (Berti and Thomas, 2009). To the best of our knowledge, there is no published evidence of thermoregulation of achromobactin in B728a. Achromobactin synthesis has been demonstrated in Pspph 1448A, where it was shown to be temperature-regulated (Owen and Ackerley, 2011). They found that achromobactin was produced in

larger quantities at 22C than at 28°C in mutants incapable of producing the more efficient siderophore pyoverdine. However, achromobactin mutants retained virulence on beans irrespective of temperature suggesting achromobactin may not be a main factor affecting virulence of Pspph at different temperatures.

Nevertheless, this suggests that achromobactin could contribute to the greater hydrogen peroxide tolerance of Pspph 1302A tolerance at 21°C. Testing achromobactin mutants *in vitro* and in temperature-controlled virulence assays *in planta* would be interesting to determine achromobactin's contribution to the phenotype described in chapter 3.

Altogether, this suggests that iron plays a diversity of role in bacterial fitness and expression patterns of iron-related genes are multi-factorial. This is consistent with other published transcriptomes which find equivocal patterns of expression depending on bacterial growth phase, species, and environmental conditions (Franza and Expert, 2013, Palma et al., 2004, Salunkhe et al., 2005).

4.3.4 Master regulator RpoS potentially plays different roles in Pss B728a and Pspph 1302A

The gene encoding the stationary phase transition master transcription factor RpoS is one of the rare examples in our study of a gene displaying little to no expression change in response to treatment in one strain (1302A) but significant expression changes in another strain (B728a). This regulator is also interesting because it is more expressed at 21°C during hydrogen peroxide challenge in Pss B728a, which may be indicative that B728a is experiencing higher oxidative stress levels at 21 than at 28°C suggesting that RpoS may be involved in the oxidative stress-temperature response cross-talk demonstrated in chapter 3.

Previous studies suggest that RpoS is likely to be important for recovering from oxidative stress and is involved in general stress acclimation (Fasnacht and Polacek, 2021). Fine-tuning of *rpoS* expression in B728a could lead to higher H_2O_2 tolerance and thus could explain the higher oxidative stress tolerance of B728a. Indeed, mistranslation of proteins (a common side-effect of ROS toxicity) leads to the induction of *rpoS* in *E. coli* although the exact mechanism by which this happens is still elusive (Battesti et al., 2011). However, it is known that the small RNA *dsrA* is required for the protective effects of RpoS against H_2O_2 (Fasnacht and Polacek, 2021). Interestingly, *rpoS* is part of a larger regulon which includes the catalase gene *katE* and the peroxidase gene *osmC* (Fasnacht and Polacek, 2021) but they did not share the same expression patterns as *rpoS* in Pss B728a in our study.

4.3.5 Phaseolotoxin expression is thermoregulated in Pspph 1302A *in vitro*

Phaseolotoxin was of special interest during this project because the cluster encoding phaseolotoxin biosynthesis is well-established in the literature as subject to thermoregulation (Bender et al., 1999). Indeed, Arvizu-Gomez et al (2013) find that most of the phaseolotoxin genes are significantly more expressed at 18°C than at 28°C in Pspph NPS3121, and we identify a similar pattern in Pspph 1302A, although expression levels were generally low for the whole cluster in our dataset. The experimental conditions (synthetic medium) were likely not conducive to activation of phaseolotoxin expression in Pspph 1302A but we also suspect that this specific strain of Pspph is a poor producer of phaseolotoxin even *in planta*. Indeed, we rarely observe the characteristic chlorotic lesions on bean leaves caused by phaseolotoxin following infection with 1302A (personal statement) and we were unable to get 1302A to produce phaseolotoxin on an agar plate assay specifically designed for induction of phaseolotoxin synthesis whereas other Pspph strains showed chlorotic lesions and phaseolotoxin synthesis

(supplementary figure S2). It would be interesting to compare phaseolotoxin production *in planta* by different isolates of Pspph to determine if phaseolotoxin is truly important for *in planta* infection by Pspph. Isolates of Pspph lacking at least parts of the phaseolotoxin gene cluster were found to be infecting bean fields successfully (Rico et al., 2003) so we expect that phaseolotoxin is an accessory virulence mechanism. In our transcriptomic assay, we find that phaseolotoxin gene expression is highest at 21°C in the presence of hydrogen peroxide, but it is generally induced by hydrogen peroxide challenge regardless of temperature. This is consistent with previously published literature indicating that oxidative stress can override thermoregulation of phaseolotoxin expression (Arvizu-Gomez et al., 2022). Altogether, this means that phaseolotoxin is unlikely to be the main factor contributing to the higher oxidative stress tolerance and virulence of Pspph 1302A at 21°C compared to 28°C.

Pss B728a does not produce phaseolotoxin but instead can produce phytotoxins syringomycin and syringopeptin. Members of the *syr* operon were either not differentially expressed in response to temperature changes or showed higher expression levels at 21 than at 28°C (supplementary table S3). A number of *syr* genes were more expressed in response to oxidative stress. These results are consistent with published literature (Bender et al., 1999, Hockett et al., 2013). This suggests that syringo-toxins may not contribute to the enhanced virulence of B728a at 28°C.

4.3.6 Differences in catalase and superoxide dismutase expression may be involved in the cross-talk between temperature and oxidative stress responses in Pss and Pspph

We determined that the expression of several catalases was induced by hydrogen peroxide challenge at both temperatures in both strains, a finding consistent with the well-established role of catalases in detoxifying ROS (Fones and Preston, 2012).

Interestingly, catalase gene expression is also temperature-responsive: *katB*, *E* and *G* in B728a, and *katA*, *B* and *G* in 1302A are more expressed at 28 than at 21°C. This is surprising because as we demonstrate in chapter 3, 1302A exhibits a higher tolerance to hydrogen peroxide at 21°C than at 28°C. We found that *katB* and *katG* were more expressed at 21°C in the absence of hydrogen peroxide, so perhaps, this tolerance is in part due to the larger amount of catalase produced before hydrogen peroxide challenge which would protect cells pre-emptively.

Transcriptional regulation of catalase gene expression in response to temperature is less documented but our findings are generally consistent with the little information available. Indeed, Arvizu-Gomez et al (2013) determined that *katB* expression is higher at 18°C than at 28°C in Pspph strain NPS3121.

Superoxide dismutase expression patterns in our datasets are more consistent with our observations from chapter 3. Indeed, we found that expression of all three *sod* genes was activated during hydrogen peroxide challenge in B728a, whereas only *sodB* expression was activated in 1302A. This is consistent with the higher ROS tolerance of B728a described in chapter 3. Furthermore, we found that *sodB* showed a moderate increase in expression at 21 compared to 28°C in 1302A whereas *sodA* was more expressed at 28 than at 21°C in B728a. While we challenged our bacteria with hydrogen peroxide and not superoxide radicals in this assay, hydrogen peroxide can spontaneously generate superoxide radicals via the Fenton reaction if it is not detoxified by catalases or quenched by antioxidants. As a result, superoxide dismutases are likely to play a role in oxidative stress responses during hydrogen peroxide challenge. Indeed, induction of sod gene expression in response to hydrogen peroxide has been documented in other *Pseudomonas*. For instance, *sodB* (Salunkhe et al., 2005) and *sodM* (Palma et al., 2004) expression were shown to increase in response to hydrogen peroxide treatment in *P. aeruginosa*.

Temperature-mediated changes in *sod* expression were moderate so it seems unlikely that superoxide dismutase gene expression changes are the main factor responsible for the difference in oxidative stress

tolerance at different temperature between Pss and Pspph, but they may certainly be a contributing factor. To our knowledge, this is the first report of thermoregulation of superoxide dismutase gene expression in plant-pathogenic *Pseudomonas*.

4.3.7 Glucose metabolism is likely important for H_2O_2 tolerance

TCA cycle and glucose metabolism genes were enriched amongst genes with significant changes in expression in response to hydrogen peroxide for both strains in our assay. Our dataset is consistent with previous findings that glucose metabolism is important to oxidative stress tolerance: switching to glucose degradation from gluconeogenesis allows bacteria to replenish cysteine pools faster by producing NADPH in excess in *Pseudomonas putida* (Nikel et al 2021). Indeed, Pseudomonads process glucose and produces NADPH via the EDEMP cycle. Antioxidant enzymes are coupled to NADPH as a redox cofactor and therefore production of reducing equivalents is important for oxidative stress tolerance (Dolan et al., 2020). Taken together with the fact that we observe a general trend towards glucose metabolism, cofactor production, sulfur metabolism, it is not far-fetched to conclude that these traits are intimately linked together as part of the bacterial oxidative response in Pss and Pspph.

4.3.8 Avirulence factor HopAB1 is thermoregulated and may contribute to temperature-based differences in virulence

HopAB1 (alternative name AvrPtoB) is a T3SS effector involved in virulence and hypersensitive response mediation during infection. It is found in numerous members of the PSSC including our two strains of interest (Sarris et al., 2011). *hopAB1* was more expressed at 21 than at 28°C in H_2O_2 in B728a, while it is more expressed at 28°C in the same condition in 1302A. This difference may be due in part to

differences in genomic location: *hopAB1* is located on the large plasmid in Pspph whereas it is chromosomal in Pss (Joardar et al., 2005, Feil et al., 2005). This is interesting because oxidative stress is known to affect plasmid supercoiling (Weinstein-Fischer et al., 2000) which can in turn affect gene expression.

Interestingly, overexpression of *hopAB1* has been shown to cause a reduction of Pph 1448A bacterial growth *in planta* (on *P. vulgaris* cultivar Canadian Wonder), but no significant growth difference was observed in synthetic medium (Macho et al., 2012). Furthermore, our findings are consistent with another temperature expression assay: *hopAB1* is downregulated at 18°C (vs 28°C) in Pspph NPS3121 (Arvizu-Gomez et al., 2013).The greater expression of *hopAB1* at 28°C in Pspph 1302A may lead to a reduction in virulence at that temperature, which is consistent with our results from chapter 3. A proteomic or mutant screen *in planta* would be required to test this.

To the best of our knowledge, thermoregulation of *hopAB1* expression has not been described in Pss B728a prior to this study. The role of HopAB1 during infection is largely host-dependent: HopAB1 is a virulence factor in *N. benthamiana* but elicits a slow cell death (HR) in *P. vulgaris* (Vinatzer et al., 2006, Sarris et al., 2011). Suppressed expression of *hopAB1* at 28°C could potentially contribute to the greater virulence of B728a at this temperature. Infection assays of *hopAB1* knock-out mutants *in planta* would help decipher whether HopAB1 is required for virulence at specific temperatures in this strain.

4.3.9 Motility is important for stress responses in both strains

Genes associated with flagellum-based motility GO terms were found to be enriched amongst differentially expressed genes in our assay in both strains. Both strains displayed induced expression of most flagellum genes – most notably *fliD, flgD, flgG* and *flgK* – in response to challenge by hydrogen

peroxide. Moderate changes in expression in response to temperature were observed in both strains but only in the presence of hydrogen peroxide. *fliC* (encoding flagellin), *fliD* and *flgE* were more expressed at 21 than 28°C in B728a and *fliD* was more expressed at 21°C in 1302A. These results corroborate Hockett et al's (2013) findings that motility is suppressed at higher temperatures in Pss B728a. Flagellum-based motility has been linked to oxidative stress avoidance in other *Pseudomonas* strains (Venero et al., 2019). This suggests that enhanced motility is a general stress response and this potentially means that hydrogen peroxide is more stressful to B728a at 21°C whereas 1302A experiences more oxidative stress at 28°C, which is consistent with our findings from chapter 3. To formally test this, hyperreactive cysteine profiling (Deng et al., 2013) or analysis of the oxidation status of an oxidative stress biosensor such as roGFP (Knoke et al., 2023) at the two temperatures could allow us to determine how much stress the bacteria are experiencing in terms of protein oxidation as opposed to simply the amount of hydrogen peroxide exogenously applied.

4.3.10 Challenges in comparing the oxidative stress responses of different strains

Throughout this chapter, we have highlighted genes that were differentially expressed in response to temperature and oxidative stress in Pss and Pspph and compared our findings with previously published transcriptomic data looking at other Gram-negative bacteria in similar but not identical setups. We find discrepancies between our data and others' and have attributed this to differences in medium composition, growth phase, strain, timing and data analsysis, but it is also possible that these strains are just not experiencing the same level of oxidative stress as the bacteria in our assay. A key component of our analysis was the comparison between Pss B728a and Pspph 1302A as they appeared to have distinct virulence and oxidative stress responses to different temperatures. However, it is difficult to know for certain whether the gene expression differences we observe in H_2O_2 are comparable for these two

strains. Indeed, they display different levels of H_2O_2 tolerance, and so we aimed to achieve a similar level of H_2O_2 rather than a consistent molecular level of H_2O_2. Nevertheless, it is difficult to ascertain that the H_2O_2 levels chosen for each strain are equivalent in terms of oxidative stress / challenge to the bacteria. A hyper-reactive cysteine profiling approach would help decipher this. In the future, ROS stress reporters such as roGFP which are starting to be used in members of the PSSC (Matern et al., 2015) will be useful to further validate the H_2O_2 levels chosen.

4.4 Conclusions

In this chapter, we investigated the transcriptional responses displayed in response to temperature and oxidative stress by Pspph and compared and contrasted these with those of Pss. We found that more genes were transcriptionally regulated in response to oxidative stress than temperature change but temperature is still an important factor affecting gene transcription. This transcriptomic screen has yielded many interesting candidate genes for temperature responses of plant-pathogenic *Pseudomonas*, including the achromobactin, alginate and levan biosynthesis operon, and highlighted how variable transcriptomes can be depending on the environmental conditions.

Chapter 5: Bioinformatic investigations of the genetic and genomic basis of pathogenicity of common bean pathogens

5.1 Introduction

Halo blight causes substantial damage in fields in South-Africa and other bean growing regions of the world (Fourie, 2002). However, halo blight can be more or less severe depending on multiple factors such as host cultivar, environmental conditions and temperature (as seen in chapters 3 and 4). Interestingly, there is strain-specific variation in pathogenicity and virulence in the causal agent of halo blight, *Pseudomonas savastanoi* pv *phaseolicola* (Thakur et al., 2016, Joardar et al., 2005, Arnold et al., 2011) so that Pspph strains are organised in races (Taylor et al., 1996). As we have been using Pspph 1302A as a model organism for this phytopathogen species we were interested in determining how genetically similar this strain is to modern field isolates currently infecting bean plants in South African farms and to identify differences in effector set that could in turn potentially affect Pspph strains response to temperature *in planta*. In this chapter, we sequenced 24 new strains and defined their phylogenetic relationship with lab model strains such as 1302A. We then built a pipeline to determine the effector set of each strain, a pipeline which we then tested with our genomic dataset.

5.1.1 Taxonomic changes in the plant-pathogenic *Pseudomonas*

With the advent of new sequencing technologies making sequencing bacterial genomes relatively inexpensive, we now have access to a large collection of sequenced genomes of the *Pseudomonas* genus. Insights into genomes have led to large taxonomic shifts, and many species have been subdivided

and renamed as a result. *Pseudomonas savastanoi* is no exception: previously known as a collection of *Pseudomonas syringae* pathovars, it was deemed genetically distant enough from the rest of the *Pseudomonas syringae* to be its own species (Gomila et al., 2017). Halo blight was thus reclassified as *Pseudomonas savastanoi pv. phaseolicola* (this is not the first time it has been renamed, Pspph was previously known as *Pseudomonas syringae* pv *phaseolicol*a, previously *Pseudomonas medicaginis* f.sp *phaseolicola*, previously *Pseudomonas phaseolicola*) (Arnold et al., 2011). Altogether, these changes occurred within a short time frame and this can be confusing as Pspph strains are often still labelled "*Pseudomonas syringae*".

Furthermore, species classification of isolates from fields is rendered difficult because of the inherent diversity of phenotypes that this bacterial clade is able to display. Whilst halo blight is typically recognised via the chlorotic lesions that it induces in plants by producing phaseolotoxin, it is not uncommon for Pspph strains to lack parts of the phaseolotoxin gene cluster and therefore to not cause the characteristic symptoms to be found infecting common bean fields (Rico et al., 2003, Jose et al., 2010). This makes genome sequencing a more reliable approach to species classification than the traditional symptom characterisation.

5.1.2 Defining pathogenicity

For a pathogen such as Pspph to successfully colonise and cause disease on a host, it has to fit a number of criteria:

- ability to survive in the host environment
- ability to withstand/tolerate general host defences
- ability to modulate the host to its advantage
- ability to suppress or evade PTI
- absence of any factor that will trigger ETI OR ability to suppress ETI

These criteria are interconnected and dependent on both the host and the pathogenic strain. Effector set governs two of those criteria: avoidance and suppression of plant immunity.

5.1.3 The role of T3SS effectors

Plants naturally have defence mechanisms to protect themselves against pathogen attack. Pathogens belonging to the PSSC use effectors in order to successfully colonise, infect and reproduce inside the plant. These effectors include proteins and molecules secreted by the Type 3 secretion system that suppress PTI but can also improve pathogen virulence for example by promoting the release of nutrients or by making the apoplastic space a less harsh environment for bacterial growth (Zumaquero et al., 2010). These effectors are genetically encoded and can be conserved but they are not part of a pathogen species' core genome (Laflamme et al., 2020). Indeed, some host cultivars have adapted to recognise the effectors and trigger a stronger immune response which renders the pathogens that have this effector unable to colonise the host (Waite et al., 2017). In order to exhibit pathogenicity on a host, they need a specific minimal set of effectors that are sufficient to suppress PTI without eliciting ETI. ETI is a force driving the loss and gain of new effectors in the pathogenic genetic pool (McMullan et al., 2015). Thus, no single isolate of Pspph is representative of the species interaction with the plant host. Looking at a panel of isolates is important to understand the adaptive dynamics leading to disease development.

5.1.4 Effector set determines the race structure of Pspph

Unlike the generalist pathogen Pss which is known to be able to infect over 180 species of plants (Muedi et al., 2015), Pspph is a specialised pathogen of common bean and a few other related legume species

(Arnold et al., 2011). Traditionally, Pspph strains were categorised into races depending on which cultivars of common bean they are able to successfully infect. We now know that a pathogenic strain's ability to infect a specific cultivar and not another one is largely due to its effector set. As a result, the race structure of Pspph is directly linked to its effector pool. For instance, the T3SS effector AvrPphB is responsible for the inability of Pspph race 3 and race 4 to infect cultivars with resistance gene R3 (Jenner et al., 1991). With new cultivars and breeds of bean emerging, the number of Pspph races had to be expanded from 6 to 9 (Figure 2.1). Race 6 is now the group of strains that are able to infect all known economically important bean cultivars. Similarly, our expanded knowledge of effector functions led to the reclassification and renaming of most of the *Pseudomonas* effectors (supplementary table S4).

5.1.5 The ever-changing effector nomenclature

Pathovars of the PSSC interact with their plant hosts by injecting Hrp outer protein (Hop) effector proteins into plant cells using the type III secretion system (T3SS). The rapid increase in genomic data available led to the discovery of many new effectors. However, this meant that multiple names were being assigned to the same Hop, while some unrelated Hops were designated by the same alphabetic character (Lindeberg et al., 2005). This led to the reclassification of most of the *Pseudomonas* effectors to better reflect phylogenetic relatedness (list of old and new names in supplementary table S4). T3SS effectors are now organized in families by the alphabetic characters, which are subdivided in subgroups numerically (Lindeberg et al., 2005). The need for subgroups arose with our expanded understanding of effector structure and function. However, not all databases were updated to follow this unified nomenclature, and to this day people still use old nomenclatures out of habit and convenience. For instance effector HopAR1 is still often referred to as AvrPphB without mention of the name HopAR1 (for instance in (Carter et al., 2019, Jayaraman et al., 2021)). The name AvrPphB was given because it makes

strains of Pspph avirulent on some bean cultivars such as cultivar TenderGreen and this is how it was identified. In fact, in the original paper that identified this effector, it was called AvrPph3 (Jenner et al., 1991).

5.1.6 Approaches to predict effector sets

As T3SS effectors are genetically encoded, a pathogen's set of effectors can be investigated using both empirical and comparative bioinformatic approaches. Previous papers have attempted to determine the effector set of members of the PSSC using an array of methodologies with different advantages and limitations. Many papers focusing on *P. savastanoi pv phaseolicola* predicted effectors by looking for specific T3SS associated regulatory elements. For example, Vencato et al (2006) looked for a *hrp* box motif in the promoter region which is needed for regulation of gene expression by HrpL, a master regulator of the T3SS. They identified 27 high probability candidate effectors in Pspph, 8 more than the 19 T3SS effectors identified the year prior by *in vivo* assays (Vencato et al., 2006). While this approach can be very powerful, not all effectors are under the control of the HrpL regulon and not all genes regulated by HrpL are T3SS-secreted effectors (Lam et al., 2014). As T3SS effectors are secreted, specific patters in the N-terminus can be used to identify effectors. Using the COOH-terminus as a marker for T3SS secretion, Guttman et al predicted 38 effectors in Pspph, including 15 previously undescribed (Guttman et al., 2002). N-terminus amino acid motifs are helpful but they are only present in ca. 50% of effectors in *Ralstonia*, another gram negative bacterial plant pathogen (Wang et al., 2011), so it is not unlikely that only a portion of Pspph effectors would be accurately predicted using this approach . The main advantage of this method is that it can predict novel effectors that have never been described before since it is not bound to the protein sequence and therefore does not require prior knowledge of said effector. Other approaches rely heavily on known effectors and what we know of their sequence

and structure. For instance, Laflamme et al (2020) used a bulk blast approach to identify effectors in the PSSC. They first downloaded all protein sequences annotated with “type III effector” OR “type III helper” OR “type III chaperone” AND “*Pseudomonas syringae*” and categorised the ones unassigned to an effector family (10 340 sequences) by blasting them against the ones that were assigned to a family (a set of 8848 sequences) and retaining only reciprocal blast hits with a named sequence with an E-value below 1e-24. They then blasted 494 PSSC genomes against this custom effector database and assigned matching sequences their top hit as long as the E-value for the match was below 1e-24. While this cutoff value is described as ‘strict’ by the authors, they did not justify further why this value was chosen and they did not state whether this was tested against a holdout set. Using this approach, they annotated a total of 14 613 T3SS effectors. They then proceeded to validate these annotations by means of a large mutant screen (Laflamme et al., 2020). A good way to circumvent limitations of each methodology is using a combination of approaches including *in vivo* assays, and this was indeed done by many (Guttman et al., 2002, Laflamme et al., 2020, Vencato et al., 2006).

5.1.7 Beyond pathogenicity

Even given a specific set of effectors, the outcome of a plant-pathogen interaction is not as straight-forward as successful infection or host resistance. Indeed, there is a range of outcomes that are typically recorded as disease. There are variations:

- temporally, a pathogen may be able to cause disease for a short amount of time before succumbing to the host defences or may survive in the host long enough to infect the next generation

- spatially: a pathogen may be able to successfully colonise one organ of a plant but not other organs, and in some cases, the pathogen may spread and colonise the whole plant in a phenomenon called 'systemic' infection
- quantitatively: a pathogen may cause more or less severe symptoms, reach different bacterial loads etc…

These variations in infection are not only dependent on the host and the pathogen's genetic potential but also on environmental effects such as the climate at the time of infection. As such, it is particularly difficult to determine which factors are required for pathogenicity, and differentiate them from accessory virulence genes i.e. genes that contribute to pathogen success in the host but are not essential. Phaseolotoxin is a prime example illustrating this challenge. Halo blight is typically recognised by the halo-like chlorotic lesion caused by phaseolotoxin. As a result, phaseolotoxin production would appear to be essential to pathogenicity. However, phaseolotoxin is not produced by the pathogen at temperatures above 28°C and only causes halo symptoms in photosynthetic tissues (Bender et al., 1999) so that successful infection by Pspph may not be recorded as halo blight or may be recorded as host resistance. In fact, Pspph strains lacking phaseolotoxin production altogether can be very successful pathogens of common bean in fields (Rico et al., 2003, Jose et al., 2010). Phaseolotoxin is therefore an accessory virulence factor. This is why genomic approaches are very helpful in helping us decipher the role of virulence factors.

5.1.8 Aims and objectives

In this chapter, we generate new genomic data from modern field isolates which have well characterised race, systemic infection capacity and virulence *in planta*, and build a pipeline to identify all Pspph genomes available. We then infer an accurate phylogeny. We then build a pipeline to identify all

effectors in Pspph. In doing so, we were aiming to i) determine which effectors are part of the core genome of Pspph and ii) identify effectors which may be associated with certain races and certain traits such as systemic infection capacity.

5.2 Results

5.2.1 Twenty-four newly sequenced Pspph genomes

Many of the strains that we commonly research are historical (e.g. the representative Pspph strain 1302A was isolated in 1984). In order to gain a better understanding of the genetic pool currently able to successfully infect bean fields, we sequenced the genomes of 24 new strains isolated from 6 different locations in South Africa (table 5.1) between 2017 and 2018 and combined them with the newly sequenced genome of another 8 strains from this set from Felix Homma so altogether we have a set of 32 sequenced modern isolates (table 5.1). We selected these specific 24 strains out of the hundreds collected by the Fourie lab based on a set of criteria: i) all strains were isolated relatively recently (not before 2017), ii) strains were phenotyped for race, systemic infection and local infection score, iii) strains were from as many different races as possible, iv) strains were from a range of locations in South Africa, v) strains had a diversity of infection scores (described in section 2.11). Comparing the genomes of these strains to that of a panel representing the full breadth of *Pseudomonas* diversity as well as the common lab strains should allow us to have a better understanding of the genetic potential of the clade to cause infection, respond to environmental conditions and evade immunity.

5.2.2 262 *Pseudomonas savastanoi* candidates genomes

In order to accurately identify and select all genomes belonging to the *Pseudomonas savastanoi* clade, we first downloaded all genomes available on NCBI named “Pseudomonas” (all fields in NCBI search) and we then ran pyani to calculate genome-wide average nucleotide identity as a measure of relatedness to our representative isolate 1302A. We also ran the newly sequenced South African isolates through this pipeline to ensure they were indeed *Pseudomonas savastanoi* as expected. All 24 isolates did indeed belong to the *Pseudomonas savastanoi* clade. From the downloaded 29 056 “Pseudomonas” genomes from NCBI (downloaded in 2020), 262 were *Pseudomonas savastanoi* candidates as they displayed >95% identity and >50% coverage (Hugouvieux-Cotte-Pattat et al., 2021) with Pspph 1302A. Of those, 242 had a homologue of at least one of the phaseolotoxin cluster genes (>70% identity and >50% coverage). This set of 262 strains together with the 24 South-African isolates was chosen to be taken forward for comparative genomic analysis (supplementary table S5).

Table 5.1: List of newly-sequenced strains

Strain name	Isolation Location	Isolation date	Isolation Cultivar	race	Sequencing date	reference
Pspph isolate 6.1	Middelburg, South-Africa	18/01/2018	Black Wonder	8	2021	this study
Pspph isolate 43.2	Vaalharts, South-Africa	27/02/2017	ND, *Phaseolus vulgaris*	6	2021	this study
Pspph isolate 91.1.2	Cedara, South-Africa	15/02/2018	ND, *Phaseolus vulgaris*	6	2021	this study
Pspph isolate 92.3	Cedara, South-Africa	15/02/2018	ND, *Phaseolus vulgaris*	6	2021	this study
Pspph isolate 33.1	Middelburg, South-Africa	18/01/2018	Colorado del Pais	1	2021	this study
Pspph isolate 4.1	Middelburg, South-Africa	18/01/2018	Kabuku	1	2021	this study
Pspph isolate 12.2.1	Middelburg, South-Africa	18/01/2018	PI209815	1	2021	this study
Pspph isolate 51.1.1	Middelburg, South-Africa	31/01/2018	AC Calmont	1	2021	this study
Pspph isolate 80.2.2	Petrus Steyn, South-Africa	13/02/2018	Pan9292	8	2021	this study
Pspph isolate 81.1	Petrus Steyn, South-Africa	13/02/2018	Sedeberg	8	2021	this study
Pspph isolate 69.1	Sarclet, South-Africa	13/02/2018	Pan9292	6	2021	this study
Pspph isolate 46.3.3	Middelburg, South-Africa	31/01/2018	ND, *Phaseolus vulgaris*	6	2021	this study
Pspph isolate 61.2	Vaalharts, South-Africa	27/02/2017	PIC-273	6	2021	this study
Pspph isolate 67.2	Sarclet, South-Africa	13/02/2018	ND, *Phaseolus vulgaris*	6	2021	this study
Pspph isolate 47.1.2	Middelburg, South-Africa	31/01/2018	ND, *Phaseolus vulgaris*	6	2021	this study
Pspph isolate 47.3.2	Middelburg, South-Africa	31/01/2018	ND, *Phaseolus vulgaris*	6	2021	this study
Pspph isolate 18.2	Middelburg, South-Africa	18/01/2018	Kablanketi	6	2021	this study
Pspph isolate 18.3	Middelburg, South-Africa	18/01/2018	Kablanketi	6	2021	this study
Pspph isolate 24.1	Middelburg, South-Africa	18/01/2018	Lushala	6	2021	this study
Pspph isolate 2.2	Middelburg, South-Africa	18/01/2018	Sodan	6	2021	this study
Pspph isolate 2.3	Middelburg, South-Africa	18/01/2018	Sodan	6	2021	this study
Pspph isolate 3.1	Middelburg, South-Africa	18/01/2018	Maalasa	6	2021	this study
Pspph isolate 10.2	Middelburg, South-Africa	18/01/2018	Blush	6	2021	this study
Pspph isolate 97.2.2	Warden, South-Africa	16/02/2018	ND, *Phaseolus vulgaris*	6	2021	this study
Pspph 1302a	Ethiopia	1984	ND, *Phaseolus vulgaris*	4	2015	Thakur et al, 2016
Pss B728a	Wisconsin, US	1987	ND, *Phaseolus vulgaris*	NA	2005	Feil et al, 2005

5.2.3 *Pseudomonas savastanoi* is a monophyletic clade

Once we had established which strains are probable *Pseudomonas savastanoi* strains, we were then interested in determining how related they are to each other. To do so we built a first phylogenetic tree with common model *Pseudomonas* strains as outgroups (figure 5.1). The clade structure is consistent with previous findings and supports the reclassification of *Pseudomonas savastanoi* as a separate species. *Pseudomonas syringae* appears to be paraphyletic but *Pseudomonas savastanoi* is strictly monophyletic in this phylogenetic tree. In fact, this tree was not able to resolve the *P. savastanoi* strains into clades because of how closely related they are to each other. This is in part because of our methodology: we extracted the single copy orthologues that are shared between all the strains – including the outgroups –, i.e. the core genome, and used their alignment to build a phylogenetic tree. The inclusion of many clearly distinct and relatively distant outgroup genomes such as *Pseudomonas putida* reduced the number of orthologues in the core genome which in turn reduced resolution power.

To improve resolution within *P. savastanoi*, we decided to recalculate the tree using a smaller set of more closely related outgroup strains and a larger set of the *Pseudomonas savastanoi* pv. *phaseolicola* strains (figure 5.2). This new tree was able to resolve the structure of the Pspph a little better though due to limited genetic variation within the group, the branch lengths are quite short. The Pspph strains cluster together (100/100 bootstraps) and are most closely related to *P. savastanoi* pv *glycinea* which also cluster as a monophyletic clade (100/100 bootstraps). This strongly suggests that the Pspph are closely related to each other.

5.2.4 Phylogenetic structure dependence

Interestingly, the Pspph clade structure seems to correlate somewhat with race structure but not location of isolation (figure 5.2 and table 5.1). For instance, some South-African strains (51.1.1, 4.1, 12.2.1 and 33.1) cluster more closely with Pph strain ICMP2740 – a strain that was isolated in Canada in ca. 1985 (Thakur et al., 2016)- than with other strains originating from the same location in South-Africa (figure 5.2 and 5.3). Coincidentally, this specific subset of South-African strains all belong to race 1. ICMP2740's race is unknown but we predict it may also belong to race 1. Similarly, strains 81.1 and 80.2.2 cluster more closely to each other than other strains and they are both race 8. Adding another layer of complexity, the next closest strain Pspph 2709a does not belong to the same race.

Furthermore, some strains have unusually long branches (e.g. GCF_000143005.1 and GCF_003413065.1) compared to the majority of the Pspph in our set. Looking further into this, it seems that these genome sequences may be tainted with environmental / contaminant DNA which is artificially inflating the genetic distance since the genome size in these strains is larger than the other Pspph strains. Since building this tree (in 2020), NCBI has increased their sequence quality standards and the affected sequences have been suppressed (in 2022). Altogether, this suggests that despite displaying a range of phenotypes (different systemic infection scores, oxidative stress tolerance, race etc) the Pspph are a monophyletic group with low intraspecifc genetic variation in their core genome.

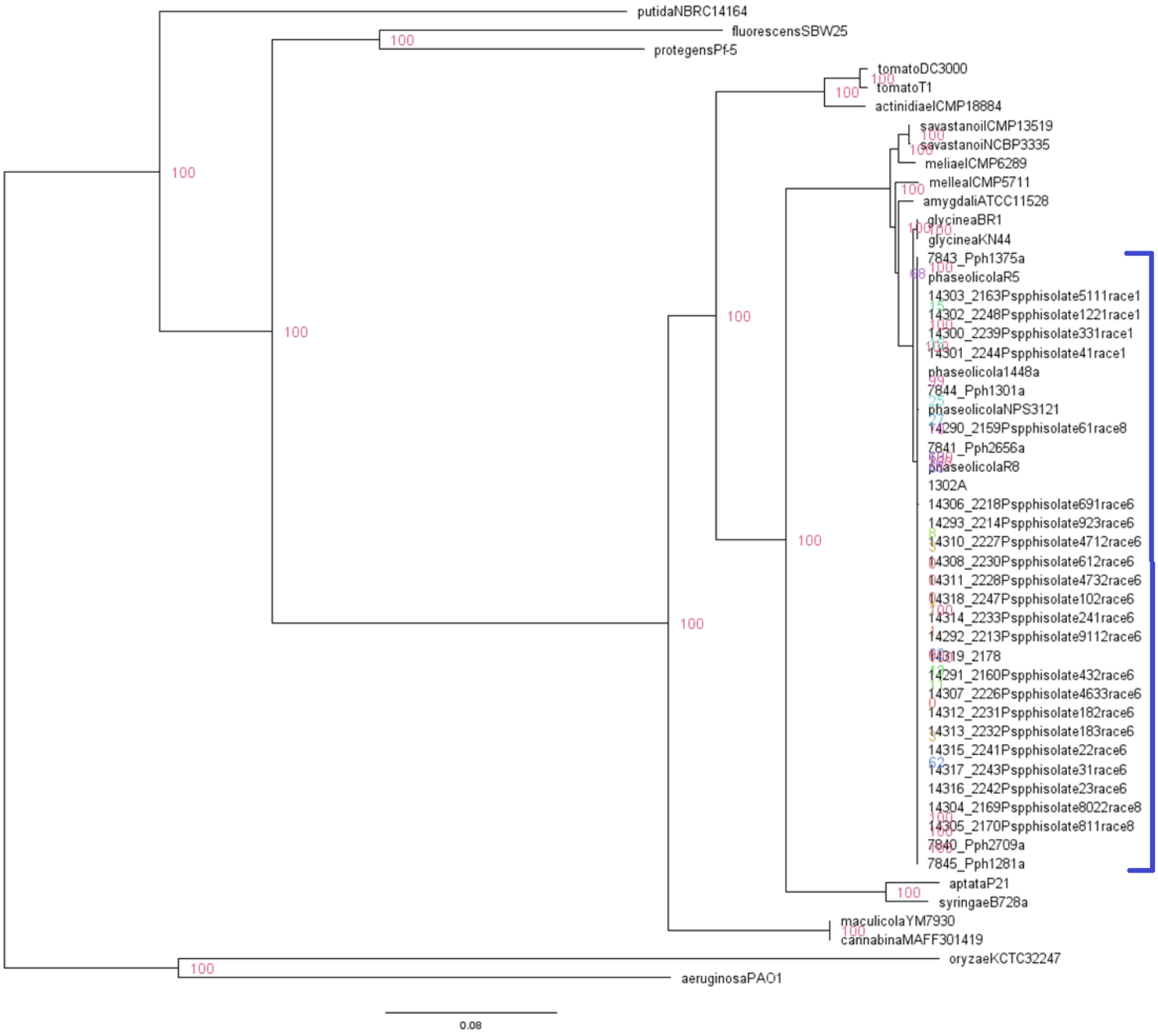


Figure 5.1: The Pspph form a monophyletic clade and are most closely related to *P. savastanoi pv. glycinea*. Maximum likelihood tree of the core genome of *Pseudomonas savastanoi* (Pspph are all in the blue section) and related strains (100 bootstraps). Bootstrap values for each node are displayed, bootstraps of 100 are in red, bootstrap values above 50 are purple and bootstrap values below 50 are green. The only bootstrap values below 100 in this tree are found within the Pspph indicating that this tree achieves poor resolution of the Pspph intraspecific phylogeny. The scale bar at the bottom refers to a phylogenetic distance of 0.08 nucleotide substitutions per site. putida = *Pseudomonas putida*, fluorescens = *P. fluorescens* , protegens = *P. protegens*, tomato = *P. syringae pv. tomato*, actinidiae = *P. syringae pv. actinidiae*, savastanoi = *P. savastanoi pv. savastanoi*, meliae = *P. syringae* pv *meliae*, mellea = *P. syringae* pv *mellea*, amygdali = *P. savastanoi* pv *amygdali*, glycinea = *P. savastanoi* pv *glycinea*,

phaseolicola/Pph = Pspph = *P. savastanoi pv phaseolicola*, aptata = *P. syringae* pv *aptata*, syringae = *P. syringae pv syringae*, maculicola = *P. syringae pv maculicola*, cannabina = *P. cannabina*, oryzae = *P. coronafasciens pv oryzae*, aeruginosa = *P. aeruginosa.*

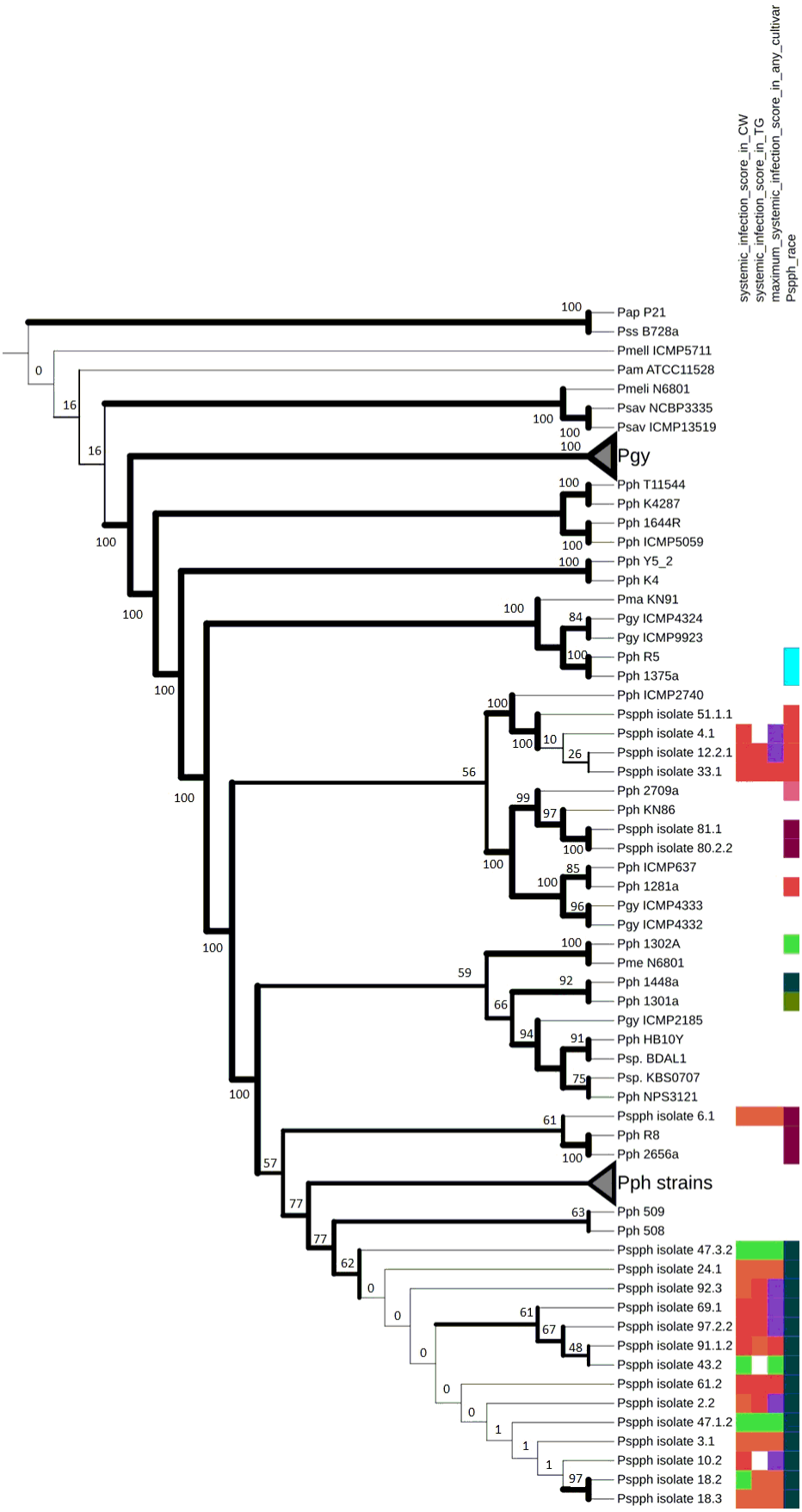

systemic_infection_score_in_CW
systemic_infection_score_in_TG
maximum_systemic_infection_score_in_any_cultivar
Pspph_race
Pap P21
Pss B728a
Pmell ICMP5711
Pam ATCC11528
Pmeli N6801
Psav NCBP3335
Psav ICMP13519
Pgy
Pph T11544
Pph K4287
Pph 1644R
Pph ICMP5059
Pph Y5_2
Pph K4
Pma KN91
Pgy ICMP4324
Pgy ICMP9923
Pph R5
Pph 1375a
Pph ICMP2740
Pspph isolate 51.1.1
Pspph isolate 4.1
Pspph isolate 12.2.1
Pspph isolate 33.1
Pph 2709a
Pph KN86
Pspph isolate 81.1
Pspph isolate 80.2.2
Pph ICMP637
Pph 1281a
Pgy ICMP4333
Pgy ICMP4332
Pph 1302A
Pme N6801
Pph 1448a
Pph 1301a
Pgy ICMP2185
Pph HB10Y
Psp. BDAL1
Psp. KBS0707
Pph NPS3121
Pspph isolate 6.1
Pph R8
Pph 2656a
Pph strains
Pph 509
Pph 508
Pspph isolate 47.3.2
Pspph isolate 24.1
Pspph isolate 92.3
Pspph isolate 69.1
Pspph isolate 97.2.2
Pspph isolate 91.1.2
Pspph isolate 43.2
Pspph isolate 61.2
Pspph isolate 2.2
Pspph isolate 47.1.2
Pspph isolate 3.1
Pspph isolate 10.2
Pspph isolate 18.2
Pspph isolate 18.3

Figure 5.2: Maximum likelihood tree of the full core genome (ca. 200 000 nucleotide sites) of *Pseudomononas savastanoi* (100 bootstraps). Branch boldness is representative of bootstrap values, and bootstrap values are displayed on the left of their relevant node. Two columns of colour-coded tiles display systemic infection scores in *P. vulgaris* cultivars TenderGreen and Canadian Xonder respectively: A is green, B is orange, C is red, D is purple with purple being the most aggressive and green the least (see chapter 2 for full description). The last column of colour-coded tiles is for race: race 1 is red, race 2 is orange, race 3 is kaki green, race 4 is grass green, race 5 is turquoise, race 6 is navy blue, race 7 is purple, race 8 is maroon, race 9 is pink. When the race is not known or not applicable (not a Pspph), no tile appears. Some monophyletic clades containing large numbers of strains of lower interest for this project are collapsed (triangle) for readability. Pgy = *P. savastanoi* pv *glycinea; Psav = P. savastanoi pv savastanoi; Pam = P. savastanoi* pv *amygdali ; Pmel = P. syringae* pv *mellea; Pma = P. syringae* pv *maculicola; Pap = P. syringae* pv *aptata; Pme = P. syringae* pv *meliae; Pph = Pspph = P. savastanoi pv phaseolicola*

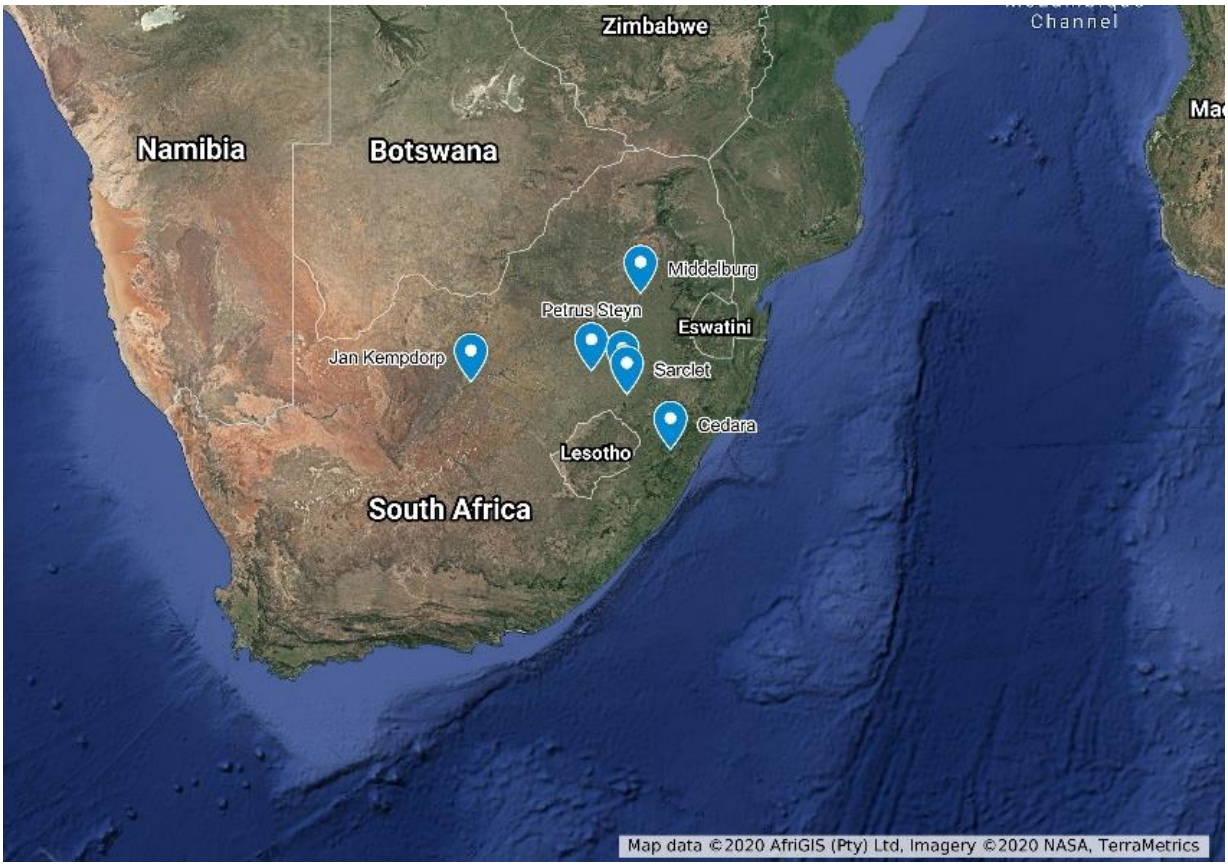


Figure 5.3: Location of sites in South-Africa at which Pspph were isolated.

5.2.5 Effector nomenclature in NCBI is inconsistent and unreliable

Now that we have established the phylogenetic background of these newly acquired strains that are currently affecting bean fields in South Africa, we can determine their effector set in order to attempt to

identify candidate effectors that may be involved in their ability to infect modern bean cultivars – this could be due to their presence or their absence as previously discussed. To do so we needed to determine the canonical set of effectors that Pspph has access to. This is obviously limited by our knowledge of effectors but fortunately, plant-pathogenic *Pseudomonas* are better studied than many other plant pathogens (Baltrus et al., 2017, Feil et al., 2005, Arnold et al., 2011). However, as previously discussed, effector nomenclature has been changed in the past, and effector sequences are not always labelled appropriately. For instance, many effector sequences (orthologous with known effectors described in the literature) are labelled as uncharacterised T3SS proteins (NCBI), presumably from an untargeted genome annotation software.

To deal with these issues, we built a pipeline to organise *Pseudomonas* candidate effectors, filter out mislabelled and/or incomplete/low-quality/"partial" sequences, and classify effectors into each of their families. We followed the effector family definition from Guttman et al (list in supplementary table S4). This allowed us to build a profile for each effector family (using HMMer), which we then used to identify effectors in our South African genomes. Presence/absence of a representative of a specific effector family is recorded. Presence is defined as a HMMer match with a threshold value above the self-search value. Because of the need for at least 3 representative sequences to build a HMMer profile, we were only able to perform this analysis for effector families which had 3 or more representative sequences (labelled as part of effector family) in the database.

We were unfortunately not able to test our pipeline with a hold-out set due to low effector numbers. A hold-out set is a portion of labelled data that is held out of the data sets used for training (in this case to build the profile) and is then used to test accuracy of the model.

Assuming that our false negative / positive rate is not too high, we can compare the effector set of each strain (figure 5.4) to their phylogenetic position in the phylogenetic tree of the Pspph (figure 5.2). Doing

so, we identify 33 effector families which are either specifically present in only a subset of Pspph strains or have different numbers of representatives in different Pspph strains (eg. HopAF1, HopAZ1…). However, the sensitivity of our methodology is insufficient to detect some effectors that are known to be present, such as for instance AvrPphB in Pspph 1302A and therefore needs optimisation.

Looking back at the cluster of race 1 strains: ICMP2740, 33.1, 4.1, 51.1.1 and 12.2.1 the effector search yielded some interesting results. Indeed, these four strains share an identical effector set according to our analysis except for one effector family: AvrB4. Our HMMer search yielded no significant match in Pph 33.1, Pph 12.2.1 or ICMP2740 but one significant match in both Pph 4.1 and 51.1.1 (figure 5.4). This is interesting because AvrB4 is described to have two members present in Pph 1448A in the literature, AvrB4-1 and AvrB4-2 and these two contribute to virulence in bean plants, and are functionally redundant to each other (Zumaquero et al., 2010). As you can see in figure 5.4, our analysis did not find more than 1 match for AvrB4 in Pspph 1448A or in any other strain for that matter. The race 1 South-African strains are the only South-African strains we sequenced that have a significant match for effector families HopF1 and HopF3.

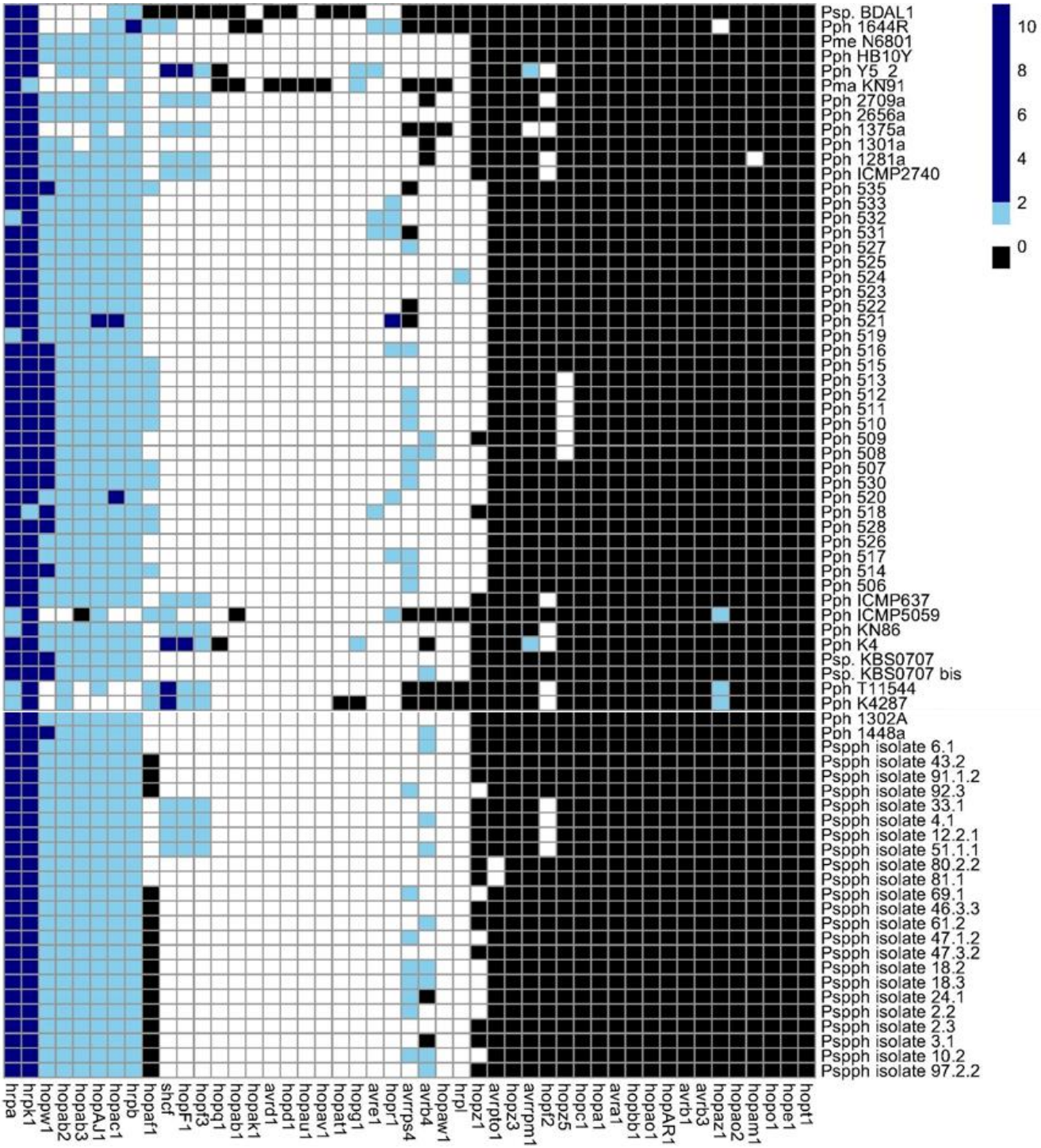


Figure 5.4: Heatmap of detected effector families by HMMer profiling in selected *Pseudomonas* strains. Threshold values for membership to an effector family were determined by testing the training set (effectors already assigned to an effector family) against its HMMer profile and keeping the smallest bit score value for each set. The rest of the effectors (which had no recognizable effector family name) were then queried against these HMMER profiles, and sequences with a bit score higher than this threshold value were moved to their effector family group. The colour code is representative of the number of matches found for each : black = no match for effector in the proteome, white = potential match(es) for effector in the proteome but not sufficiently supported by statistical test (HMMer score

above self-search score), sky blue = 1 match in the proteome, dark blue = more than 1 protein match in the proteome. *Psp. = Pseudomonas sp. ; Psav = P. savastanoi pv savastanoi ; Pam = P. savastanoi* pv *amygdali ; Pme = P. syringae* pv *mellea; Pma = P. syringae* pv *maculicola; Pap = P. syringae* pv *aptata; Pmeli = P. syringae* pv *meliae; Pph = Pspph = P. savastanoi pv phaseolicola; Pss = P. syringae pv syringae*

5.2.6 Linking the genome to the phenotype

Effector set, whilst important is not the only factor determining the pathogen's ability to infect plants. We phenotyped some traits that are typically important to Pspph virulence in a subset of the South-African strains: oxidative stress tolerance, and cross-talk with temperature, motility, phaseolotoxin production (Marcella Cross, Megan Beattie, Julianna Piat, unpublished), systemic and local infection ability (Felix Homma, Deidre Fourie, unpublished) (Table 5.2). We observed that apart from race type, none of these traits appear to be strongly linked to the phylogenetic structure of our strains:

- Pph 91.1.2 , 81.1 and 2.3 did not produce phaseolotoxin *in vitro*, but they do not cluster together. In fact, they cluster more closely with other strains that displayed robust phaseolotoxin production *in vitro*. For instance, 80.2.2 is a phaseolotoxin producer and clusters with isolate Pph 81.1 which does not (table 5.2). These strains share a race-typing however, they both belong to race 8. Thus phaseolotoxin production (*in vitro*) does not appear to be linked to phylogeny. Note that our phaseolotoxin assay is indirect (measuring antagonism with a bacterium) and further testing would need to be done to confirm that the strains do not produce phaseolotoxin. We did confirm independently that these strains had a full phaseolotoxin gene cluster.
- All the South-African strains belonging to race 6 cluster closely together independent of their systemic infection score. Indeed, Pph 47.3.2 displays low systemic infection aggression (score A in all cultivars), but clusters with systemic infection aggressive Pph 92.3, 69.1 and 97.2.2 (up to

score D in some cultivars, see chapter 2 for details) (figure 5.2). Thus, a strain's capacity for systemic infection does not appear to be tied to its phylogenetic history.

- There is little statistically significant difference in mortality to H_2O_2 between strains, and the few differences are not reflected in the phylogeny. For instance, isolates Pph 12.2.1 and 51.1.1 cluster closely but display somewhat different H_2O_2 tolerance levels, with 51.1.1 being more tolerant at both temperatures in MG medium, but less tolerant than 12.2.1 in KB medium (table 5.2). This suggests that oxidative stress tolerance variation in Pspph is not related to phylogeny.
- Phylogenetically close strains do not appear to show the same level of motility. For instance, 80.2.2 displays higher swarming capacity at both 21°C and 28°C than 81.1 (table 5.2) which is its closest kin according to the tree.

Table 5.2: Phenotype of South-African strains

Strain name	Isolated from	H2O2 mortality on plate at 21°C (cm) (MG+3/MG+30% / KB+3 / KB+30%)	H2O2 mortality on plate at 28°C (cm) (MG+3/MG+30 % / KB+3 / KB+30%)	Pht inhibition of E. coli growth (cm)	Swimming at 21°C (0.25% agar) (cm)	Swimming at 28°C (cm)	Swarming at 21°C (0.4% agar) (cm)	Swarming at 28°C (cm)	Race	Systemic infection score	Local infection score
Pph 33.1	Colorado del Pais in Middelburg			5.5					1	B, C	1, 3, 4
Pph 4.1	Kabuku in Middelburg	3.6/5.1/3.3/5	3.7/5/3.6/4.8	5	3	3	6	5	1	A, B, C, D	1 to 5
Pph 12.2.1	PI209815 in Middelburg	4.3/5.8/3.2/4.6	4/5.7/3.2/4.8						1	B,C,D	1 to 4
Pph 51.1.1	AC Calmont in Middelburg	3.4/5.1/3.7/5	3.5/5.5/3.4/5	4	3	3	5	6.5	1		
Pph 43.2	? In Vaalharts			4.75	4.5	7	6.5	7.5	6	A	3 to 4
Pph 91.1.2	? In Cedara			0					6	C	4 to 5
Pph 92.3	? In Cedara			5	7	7	4	4	6	A, B, D	3 to 5
Pph 69.1	Pan9292 in Sarclet			3.75					6	B, C, D	4
Pph 46.3.3	? in Middelburg			3					6	B	1 to 4
Pph 61.2	PIC273 in Vaalharts			3.75					6	C	4 to 5
Pph 67.2	? In Sarclet								6	A,B,C	4 to 5
Pph 47.1.2	? In Middelburg			4					6	A	3 to 4
Pph 47.3.2	? In Middelburg			4.5					6	A	3 to 4
Pph 18.2	Kablanketi in Middelburg			4.5					6	A, B	4
Pph 18.3	Kablanketi in Middelburg			4					6	A, B	4
Pph 24.1	Lushala in Middelburg			4					6	A, B	3 to 4
Pph 2.2	Sodan in Middelburg			2.2					6	A, B, C, D	4 to 5
Pph 3.1	Maalasa in Middelburg								6	A, B	3 to 4
Pph 10.2	Blush in Middelburg								6	A, B, C, D	1 to 5
Pph 6.1	Black Wonder in Middelburg	4.1/5.6/3.5/4.8	4.3/5.8/3.7/4.8	5	4	6	3	6	8	B	1 to 4
Pph 80.2.2	Pan9292 in Petrus Steyn			4.25	5	1	3	2	8		
Pph 81.1	Sedeberg in Petrus Steyn			0	5	3	1	1	8		

5.3 Discussion

In South Africa, one of the main bean growing regions of the world, halo blight and brown spot are rampant. Unsurprisingly, most isolates of halo blight infecting bean fields these days are of race 6 (Fourie, 2002), the race that is able to infect all commercially important cultivars. This is indicative of genomic adaption to the crop environment. We asked i) if this is reflected in the phylogenetic relationship between modern isolates and representative isolates with curated genomes, and ii) which effectors are responsible for the success of these strains. In order to answer these questions, we had to custom build our own bioinformatic pipeline.

5.3.1 *Pseudomonas* classification is constantly evolving

Pseudomonas savastanoi pv *phaseolicola* was reclassified after being considered a part of the *Pseudomonas syringae* species for a large number of years, but this is not the first time the *Pseudomonas syringae species complex* has been modified. Phylogenetic trees for bacteria are often built using a small set of conserved genes, sometimes even just a single gene such as *gyrB*. Here I used the whole core genome of the *Pseudomonas syringae species complex*, allowing for more finetuned phylogenies. This data supports the reclassification of Pspph as a member of the species *Pseudomonas savastanoi*, as it clusters more closely with other *Pseudomonas savastanoi* strains (e.g. pv *glycinea*) than with representatives of *Pseudomonas syringae* (e.g. pv *syringae*). More importantly, all Pspph strains cluster closely together in a monophyletic clade., indicating the clade contains its most recent common ancestor (MRCA) and includes all descendants of that ancestor to the exclusion of any member of another group. Note that these phylogenetic trees based on full core genomes are not reconstructions

of clonal phylogeny but instead reflect population structure and the nonhomogeneous distribution of recombination rates in each lineage. To build a clonal phylogeny, sites of recombination would need to be removed from the analysis. However, identification of such sites requires a relatively recent MRCA in addition to low recombination rates, conditions which are not met by the datasets in figure 5.1 and 5.2. Recombination contributes significantly to whole genome phylogenies in bacteria and it is likely that there are essentially no loci that are unaffected by recombination in large datasets (Sakoparnig et al., 2021), such as those I consider in this chapter. New models are currently being built to take into account recombination rates in bacterial phylogenetic reconstructions (Steinberg et al., 2022, Baumdicker and Kupczok, 2023) but tools available to us as of now, e.g. ClonalFrameML (Didelot and Wilson, 2015), Gubbins (Croucher et al., 2015), do not allow us to isolate recombination rates from the clonal phylogeny in our dataset. My primary goal with phylogenetic analysis was to establish a robust placement for Pspph within Pseudomonas to enable and support further bioinformatic analysis, which can be achieved with the methodology used. The multigene trees presented here are derived from a model spanning over 200,000 informative sites drawn from the genomes involved in the tree, with each individual coding sequence being fit to a distinct substitution model. The resulting trees are likely to be representative of overall evolutionary history, even though an assumption of no recombination at all is unlikely to hold. Production of a detailed recombination model is beyond the scope of this DPhil, and is considered unlikely to modify the placement of this clade within Pseudomonas.

5.3.2 Refining bioinformatic approaches to T3SS effector identification

In order to improve the statistical power of bioinformatic based experiments, a large number of well annotated data is needed, in order to form a training set and a hold out set to validate bioinformatic pipelines (Pritchard & Broadhurst, 2014). In our case, we were unable to keep a hold-out set as to do so

would have made it difficult to have enough genetic diversity for a meaningful hmmer profile of each effector family. That being the case, the detection sensitivity of our approach was still subpar, as AvrPphB could not be detected reliably for instance. Optimisation could include relaxation of the threshold for effector belonging, and manual curation of effector sequences that are used to build the hmmer profiles of reference. In the future, more effector sequences will be reported and new tools will be made more easily accessible for effector identification. The recent rise of tools such as alpha fold (Jumper et al 2021) is promising as it could allow for detection of functional effectors based on their specific protein motifs rather than on sequence identity alone. Indeed, a stretch of nucleotide may not look conserved but may have identical protein folding structures. This is the case for AvrPphB and possibly the reason why our pipeline failed to identify AvrPphB accurately. Indeed, AvrPphB belongs to the papain superfamily of cysteine proteases. This family are characterized by the structurally conserved active site catalytic triad and the oxyanion hole. They share a few conserved residues but there is relatively low sequence identity among members of the YopT family of cysteine proteases. However, all members have very similar predicted secondary structure assignment (Zhu et al., 2004). This makes identification of AvrPphB from the genomic sequence alone particularly difficult, but tools such as Alpha Fold could make identification much more reliable.

5.3.3 Multiple independent evolutions of race 6

Interestingly, South-African strains belonging to race 6 clustered together but there were other separate clusters in the tree with other race 6 isolates (e.g. 1448A). This may be indicative of multiple independent evolutions of a race 6 “genotype”: a set of effectors that tune-down plant defences without triggering ETI. It is also possible that the race 6 “genotype” is ancestral but it is more likely that bacteria evolved to be pathogenic on more hosts than less. Regardless, we suspect that a substantial

amount of gene gain and loss is involved. Taken together with the large amounts of IS elements and phages found in PSSC genomes (Hockett et al., 2013), and the fact that many are transcriptionally active to this day (as seen in chapter 4), horizontal gene transfer and genomic recombinations of genomic islands is not unlikely. Pspph is capable of rapid evolution, as it has been described that strains passaged through resistant host plants can lose specific pathogenicity islands (e.g. containing AvrPphB) within a few generations (Pitman et al, 2005).

5.3.4 Thermoregulated and Oxidative stress responsive T3SS effectors

In chapter 4, we identified a number of genes that were differentially expressed in response to temperature and oxidative stress treatment, and this included some effectors and components of the T3SS. Notably, HopAH2, AvrE1 and HrpA are of special interest as they were differentially transcriptionally expressed in Pspph compared to Pss. Unfortunately, we were unable to obtain enough HopAH representative sequences to build a HMMer profile at the time of building the pipeline, so HopAH was excluded from the analysis. We were able to build profiles for AvrE1 and HrpA with varying levels of success. AvrE1 detection sensitivity needs improvement as we only found significant matches in a few strains, not in Pspph 1302A which is known to have a Avre1 sequence. We found multiple matches for genes belonging to the HrpA family in most strains. HrpA is an indispensable part of the type III secretion system in PSSC. Note that HrpA is not a T3SS effector but a component of the T3SS pilus. The majority of strains, including the model strains Pspph 1302A and 1448A had 3 matches for HrpA, one for each member of the family, however, a substantial number of strains had more than 3 statistically significant matches according to our pipeline. For instance, South-African strain Pph 61.2 had 4 matches. Members of the HrpA family (namely HrpA1, 2 and 3) have highly variable sequences (Ramos et al., 2007) which complicates profile building. We suspect that this is why our pipeline identified more

than 3 matches in many strains, but it is also possible that the *hrpA* genes have undergone gene duplication. We would like to note that where the pipeline analysis yielded substantially abnormal results (found no *hrpA* sequence or found more than 5 matches) were outgroup strains belonging to *P. amygdali* and *P. aeruginosa* (supplementary table S6), not Pspph, so we suspect our pipeline is more accurate for Pspph strains than other *Pseudomonas* as a result of biases in the training set.

5.3.5 AvrB4 may be accessory to Pspph virulence

Strains ICMP2740, 33.1, 4.1, 51.1.1 and 12.2.1 cluster together in the phylogenetic tree and share an identical effector set according to our analysis except for one effector family: Avrb4. AvrB4 suppresses the salicylic acid signalling pathway *in planta* (Zumaquero et al., 2010). It is possible that AvrB4 is accessory – helping to promote virulence in specific circumstances such as for instance when plants are experiencing abiotic stress such as nutrient starvation or water deficiency as the salicylic acid signalling pathway is affected by a multitude of cues in plants. It is also possible that our effector search pipeline is erroneous and was unable to accurately identify AvrB4 matches. In support of this idea, our pipeline did not find more than one match for AvrB4 effector family, where we know that there are at least two representatives in Pspph 1448A (Zumaquero et al., 2010). We suspect this may be caused by taxonomic confusion, as AvrB4-1 used to be called AvrB3. We also failed to find matches for the new AvrB3 family (previously named HopPsyC) and we suspect this may be due to inaccurate profiling caused by a mix of AvrB4-1 sequences incorrectly labelled as AvrB3, and true AvrB3 making up an erroneous HMMer profile.

5.3.6 HopF1 and HopF3 are required for race 1 phenotype

The race 1 South-African strains (33.1, 4.1, 51.1.1 and 12.2.1) are the only South-African strains we sequenced that have a significant match for effector families HopF1 and HopF3. HopF1 triggers ETI in bean plants carrying the R1 gene but contributes to virulence in bean plants lacking R1. HopF1 was first cloned from Pph race 5 and 7 (Tsiamis et al., 2000). It is not surprising that HopF1 is missing from the rest of the South-African strains since they are either race 6 or race 8 – so they are able to infect plants carrying R1 such as cultivar Red Mexican. Strains belonging to race1 are unable to infect Red Mexican which is consistent with our findings. Interestingly, mutants lacking hopF1 are unable to infect TenderGreen or Canadian Wonder (Tsiamis et al., 2000). HopF3 suppresses autophagy in plants to promote virulence in Pto DC3000 (Lal et al., 2020) but little is known about its specific role in race-typing because recombination of the locus is difficult to establish (Zumaquero et al., 2010). It is possible that HopF3 is also involved in race-typing for race 1. Altogether, this specific set of effectors further supports our previous suggestion that ICMP2740 is also a race 1 isolate as it also appears to carry *hopF1* and *hopF3*. This pipeline shows promise to predict effector set for races of Pspph but still needs improvements as evidenced by the AvrB4/AvrB3 and AvrPphB cases, in particular a better system for validating effector identity and avoiding confusions due to effector renaming. The absence of a hold-out set for validation will be easy to remedy in the future as it is likely that the greater ease of sequencing will lead to a large increase in sequence availability for future computational work and hypothesis testing.

5.3.7 Vertical transmission is more important in determining race structure of Pspph than horizontal transmission

Of all the phenotype differences we identified between Pspph strains, the only one that appeared to follow the phylogenetic tree is race typing. It is possible that this is an artefact caused by the low

resolution power, but it is also possible that race is one of the drivers of phylogenetic distance between Pspph strains along with other factors such as year of isolation. Altogether, this either suggests that i) loss and gain of effectors is an important driver of Pspph evolution or ii) vertical rather than horizontal transmission is the most important route for determining race structure in Pspph. Phenotyping of a larger diversity of Pspph strains for race would consolidate these findings and provide more resolution power for further investigations in this area.

Altogether, this suggests that despite displaying a range of phenotypes (different systemic infection scores, oxidative stress tolerance, race etc) the Pspph are a monophyletic group with low intraspecifc genetic variation in their core genome. Accessory genes and extranuclear genetic elements (such as plasmids) are likely to be largely responsible for intraspecific diversity in this clade.

5.4 Conclusions

In this chapter, we computed the phylogenetic relationship between all Pspph strains with sequenced genomes available. We found that Pspph are monophyletic and closely related to each other. We built the foundations of a pipeline to create profiles for the canonical set of effectors encoded in Pspph genomes and determine individual strain's effector set. Although this pipeline has some setbacks discussed in this chapter, it was able to identify key effectors for race-typing. In the future, the expansion of the genomic resources available as well as the rise of secondary structure prediction tools such as Alpha Fold will allow for more efficient and accurate effector prediction by our pipeline.

6.0 General discussion

In this thesis, we set out to investigate the effects of temperature on bacterial pathogens of common bean. We found that temperature affects virulence and oxidative stress tolerance of Pspph and Pss. Furthermore, we found that these two bean pathogens have opposite responses to temperature: Pspph is more virulent and more tolerant to H_2O_2 at 21°C than at 28°C whereas Pss is more virulent and more tolerant to H_2O_2 stress at 28°C than at 21°C. Having identified a striking cross-talk, we investigated the potential mechanisms underlying these responses. We found that hydrogen peroxide stability does not differ at 21°C and 28°C, and detoxification rates *in vitro* do not appear to be affected by temperature either. While Pss is more resilient to oxidative stress than Pspph and is able to withstand higher levels of exogenous hydrogen peroxide, medium composition and richness had large effects on the cross-talk response of both pathogens to oxidative stress and temperature.

We were interested in identifying candidate genes that may be involved in the interaction between temperature and oxidative stress. To do so, we performed a large *in vitro* transcriptomic screen of Pss and Pspph exposed to hydrogen peroxide or water at either 21°C or 28°C. We identified a number of differentially expressed genes, including genes involved in achromobactin biosynthesis and ROS detoxification and found that more genes were transcriptionally activated in response to hydrogen peroxide than in response to temperature. Overall, our transcriptomic screen results are mostly consistent with published results of transcriptomic screens in PSSC in response to temperature or oxidative stress, with a few exceptions but we strongly suspect that this is due to differences in medium used, as medium richness has large effects on the interaction between oxidative stress and temperature. Importantly, we found that many genes orthologous in Pss and Pspph did not share the

same transcriptional responses to temperature and oxidative stress. Of those, the master regulator rpoS and virulence factor hopAB1 are of special interest.

Finally, in chapter 5, we investigated the genetic potential of Pspph strains currently infecting bean fields. The majority of the strains currently infecting bean fields in South Africa are of race 6, which was expected. We found that the Pspph are monophyletic, and modern strains are very closely related to each other. We also found that strains of the same race often cluster together with a few exceptions, Interestingly, we found potential evidence for multiple independent evolutions of race 6 with T3SS and identified potential race-specific effectors although our effector mining pipeline was inconclusive. Most importantly, we find that vertical transmission is more important in determining race structure of Pspph than horizontal transmission.

Temperature is still largely understudied in phytopathology despite most predictions that it is one of the most important abiotic conditions in determining the outcome of plant-pathogen interactions (Velasquez et al., 2018, Huot et al., 2017). To the best of our knowledge, this is the first report of temperature differentially affecting virulence *in planta* in closely related plant pathogens, and it is also the first time the cross-talk between temperature and oxidative stress has been investigated formally via a transcriptomic approach. Many of our results are consistent with previous studies looking at the effects of temperature (Hockett et al., 2013, Ullrich et al., 2000, Arvizu-Gomez et al., 2013) and oxidative stress (Fones and Preston, 2012) separately in different members of the *Pseudomonas syringae species complex*.

In future studies, it would be interesting to expand investigations of the effect of temperature to other plant pathogens, and determine if indeed, temperature effects vary between pathogen species or if there is a general pattern in virulence response to temperature. We had attempted to build a mutant

library (TnSeq) of Pspph in order to determine which genes are important for temperature responses independent of post-transcriptional regulation, but we unfortunately met technical difficulties (see the Appendix). Whilst gene expression changes provide a valuable source of information, combining them with a TnSeq approach in the future would enhance our understanding of temperature effects and allow us to truly isolate temperature responses from temperature kinetics.

As we also found that metabolism plays a key role in both temperature and oxidative stress response, metabolic footprinting of the strains at different temperatures would be particularly interesting. From our results, we suspect that compounds related to sulfur metabolism, NADPH production and iron scavenging would be involved, as well as a number of antioxidants and other compounds important for stress resilience. Indeed, many of the temperature responses appear to be stress-related. This could be due to the medium they grew in, which is relatively nutrient poor (it is a minimal medium) but since we see cold-shock proteins and other chaperones amongst differentially expressed genes, this is unlikely to be the sole contributor to the stressed state of the bacteria. The temperatures we expose our pathogens to are common in bean-growing regions of the World, and not at all extreme, so it is puzzling that bacteria seem to be experiencing stress. Further investigations into this, would be particularly interesting. A common stress symptom of bacteria is ROS production so quantifying intracellular levels of ROS at different temperatures would be a first step to determine if indeed, some temperatures are more stressful to the bacteria than others. This could be achieved via the use of redox state reporters such as roGFP, a construct which has been successfully established in other *Pseudomonas* in our lab (personal statement).

Temperature changes in bean fields coincide with a range of other environmental shifts, including but not limited to changes in light intensity, daylight length and humidity. Unless otherwise stated, these factors were typically kept constant in the experiments described in this thesis, to reduce confounding

effects. Nonetheless, they may synergise together with temperature in affecting bacterial pathogens of common bean. Indeed, both humidity (Latorre et al., 2002) and light (Hua, 2013) have been described to affect disease development by plant pathogenic *Pseudomonas* and plant immunity. Stomata are an important point of entry for some members of the PSSC, and their opening is regulated by light, temperature and humidity (Zeng et al., 2010). A portion of the host plant ROS production is light dependent (Lu and Yao, 2018). Therefore, it is possible that light responses cross-talk with the aforementioned temperature-oxidative stress responses. Repeating some of the experiments described in chapter 3 of this thesis with different light regimes would be particularly interesting.

7.0 Acknowledgments

The research described in this thesis was graciously funded by UKRI-BBSRC and took place at Oxford University's Plant Sciences Department (now Biology South Park). We thank the staff at the department for their unending support: Rob Bryant, James Wisker, Ursula Pyzio, Tom King, Shane Hamp, and most importantly, our lab manager Sarah Rodgers.
Furthermore, Julianna would like to thank the members of her family and her labmates for their support, mentoring and feedback, specifically (but in no particular order): Alexandra Charavet-Piat, William Piat, Dr Lauren Chappell, Dr Nattapong Sanguankiattichai, Floren Scrafton, Morgan Wade, Ashleigh MacDonald, Dr William Kay, Brett Wadley, Alison Hochen, Chloe Harper, Dr Jaime Carrasco, John Dave Aquino, Dr Marcel Bach Pages, Jasmine Dodd, Marcella Cross, Megan Beattie, Rose Bourdon, Thomas Barnes, Dr Riccardo Soldan. Julianna gives her thanks to Dr Tyler C. Helmann, Dr Renier van der Hoorn, Dr Mark Fricker and Pedro Bota as well as the Plant Chemetics lab (especially Dr Renier van der Hoorn, Dr Judith Paulus, Dr Kyoko Morimoto, Dr Pierre Buscaill and Dr Jiorgos Kourelis) and the SIPBS-CompBiol group for sharing their expertise with me for troubleshooting purposes. And most importantly, thank you to my DPhil supervisors for their patient and thoughtful supervision, mentoring and guidance.

8.0 References

AGUILERA, S., ALVAREZ-MORALES, A., MURILLO, J., HERNANDEZ-FLORES, J. L., BRAVO, J. & DE LA TORRE-ZAVALA, S. 2017. Temperature-mediated biosynthesis of the phytotoxin phaseolotoxin by Pseudomonas syringae pv. phaseolicola depends on the autoregulated expression of the phtABC genes. *Plos One,* 12.

AGUILERA, S., DE LA TORRE-ZAVALA, S., HERNANDEZ-FLORES, J. L., MURILLO, J., BRAVO, J. & ALVAREZ-MORALES, A. 2012. Expression of the Gene for Resistance to Phaseolotoxin (argK) Depends on the Activity of Genes phtABC in Pseudomonas syringae pv. phaseolicola. *Plos One,* 7.

AGUILERA, S., LOPEZ-LOPEZ, K., NIETO, Y., GARCIDUENAS-PINA, R., HERNANDEZ-GUZMAN, G., HERNANDEZ-FLORES, J. L., MURILLO, J. & ALVAREZ-MORALES, A. 2007. Functional Characterization of the Gene Cluster from Pseudomonas syringae pv. phaseolicola NPS3121 Involved in Synthesis of Phaseolotoxin. *Journal of Bacteriology,* 189**,** 2834-2843.

AKHAVAN, A., BAHAR, M., ASKARIAN, H., LAK, M. R., NAZEMI, A. & ZAMANI, Z. 2013. Bean common bacterial blight: pathogen epiphytic life and effect of irrigation practices. *Springerplus,* 2.

ALVARADO-GUTIERREZ, A., DEL REAL-MONROY, M., RODRIGUEZ-GUERRA, R., ALMANZA-SANCHEZ, L., LOZOYA-GLORIA, E. & FRAIRE-VELAZQUEZ, S. 2008. A Phaseolus vulgaris EF-hand calcium-binding domain is induced early in the defense response against Colletotrichum lindemuthianum and by abiotic stress: Sequences shared between interacting partners. *Physiological and Molecular Plant Pathology,* 72**,** 111-121.

ARNOLD, D. L., LOVELL, H. C., JACKSON, R. W. & MANSFIELD, J. W. 2011. Pseudomonas syringae pv. phaseolicola: from 'has bean' to supermodel. *Molecular Plant Pathology,* 12**,** 617-627.

ARVIZU-GOMEZ, J. L., HERNANDEZ-MORALES, A., AGUILAR, J. R. P. & ALVAREZ-MORALES, A. 2013. Transcriptional profile of P. syringae pv. phaseolicola NPS3121 at low temperature: Physiology of phytopathogenic bacteria. *Bmc Microbiology,* 13.

ARVIZU-GOMEZ, J. L., HERNANDEZ-MORALES, A., JUAREZ-NAVARRO, R. A., PAREDES-TADEO, J. D., CAMPOS-GUILLEN, J., PACHECO-AGUILAR, J. R., MARTINEZ-RIZO, A. B. & GONZALEZ-REYES, C. 2022. OxyR Positively Influences Phaseolotoxin Synthesis and Pyoverdin Production in Pseudomonas savastanoi pv. phaseolicola NPS3121. *Microorganisms,* 10.

AZNAR, A., CHEN, N. W. G., THOMINE, S. & DELLAGI, A. 2015. Immunity to plant pathogens and iron homeostasis. *Plant Science,* 240**,** 90-97.

BALTRUS, D. A., MCCANN, H. C. & GUTTMAN, D. S. 2017. Evolution, genomics and epidemiology of Pseudomonas syringae: Challenges in Bacterial Molecular Plant Pathology. *Molecular Plant Pathology,* 18**,** 152-168.

BARNA, B., FODOR, J., HARRACH, B. D., POGANY, M. & KIRALY, Z. 2012. The Janus face of reactive oxygen species in resistance and susceptibility of plants to necrotrophic and biotrophic pathogens. *Plant Physiology and Biochemistry,* 59**,** 37-43.

BATTESTI, A., MAJDALANI, N. & GOTTESMAN, S. 2011. The RpoS-Mediated General Stress Response in Escherichia coli. *Annual Review of Microbiology, Vol 65,* 65**,** 189-213.

BAUMDICKER, F. & KUPCZOK, A. 2023. Tackling the Pangenome Dilemma Requires the Concerted Analysis of Multiple Population Genetic Processes. *Genome Biology and Evolution,* 15.

BAXTER, A., MITTLER, R. & SUZUKI, N. 2014. ROS as key players in plant stress signalling. *Journal of Experimental Botany,* 65**,** 1229-1240.
BELACHEW, K. Y., MAINA, N. H., DERSSEH, W. M., ZELEKE, B. & STODDARD, F. L. 2022. Yield Gaps of Major Cereal and Grain Legume Crops in Ethiopia: A Review. *Agronomy-Basel,* 12.
BENDER, C. L., ALARCON-CHAIDEZ, F. & GROSS, D. C. 1999. Pseudomonas syringae phytotoxins: Mode of action, regulation, and biosynthesis by peptide and polyketide synthetases. *Microbiology and Molecular Biology Reviews,* 63**,** 266-+.
BERGE, O., MONTEIL, C. L., BARTOLI, C., CHANDEYSSON, C., GUILBAUD, C., SANDS, D. C. & MORRIS, C. E. 2014. A User's Guide to a Data Base of the Diversity of Pseudomonas syringae and Its Application to Classifying Strains in This Phylogenetic Complex. *Plos One,* 9.
BERTANI, G. 1951. STUDIES ON LYSOGENESIS .1. THE MODE OF PHAGE LIBERATION BY LYSOGENIC ESCHERICHIA-COLI. *Journal of Bacteriology,* 62**,** 293-300.
BERTI, A. D. & THOMAS, M. G. 2009. Analysis of Achromobactin Biosynthesis by Pseudomonas syringae pv. syringae B728a. *Journal of Bacteriology,* 191**,** 4594-4604.
BIGEARD, J., COLCOMBET, J. & HIRT, H. 2015. Signaling Mechanisms in Pattern-Triggered Immunity (PTI). *Molecular Plant,* 8**,** 521-539.
BLANC, B., CLÉMANCEY, M., LATOUR, J. M., FONTECAVE, M. & DE CHOUDENS, S. O. 2014. Molecular Investigation of Iron Sulfur Cluster Assembly Scaffolds under Stress. *Biochemistry,* 53**,** 7867-7869.
BRAUN, Y., SMIRNOVA, A. V., WEINGART, H., SCHENK, A. & ULLRICH, M. S. 2007. A temperature-sensing histidine kinase - Function, genetics, and membrane topology. *Two-Component Signaling Systems, Pt B,* 423**,** 222-249.
BRAY, N. L., PIMENTEL, H., MELSTED, P. & PACHTER, L. 2016. Near-optimal probabilistic RNA-seq quantification. *Nature Biotechnology,* 34**,** 525-527.
BROUGHTON, W. J., HERNANDEZ, G., BLAIR, M., BEEBE, S., GEPTS, P. & VANDERLEYDEN, J. 2003. Beans (Phaseolus spp.) - model food legumes. *Plant and Soil,* 252**,** 55-128.
BROWN, I., TRETHOWAN, J., KERRY, M., MANSFIELD, J. & BOLWELL, G. P. 1998. Localization of components of the oxidative cross-linking of glycoproteins and of callose synthesis in papillae formed during the interaction between non-pathogenic strains of Xanthomonas campestris and French bean mesophyll cells. *Plant Journal,* 15**,** 333-343.
BUDDE, I. P., ROHDE, B. H., BENDER, C. L. & ULLRICH, M. S. 1998. Growth phase and temperature influence promoter activity, transcript abundance, and protein stability during biosynthesis of the Pseudomonas syringae phytotoxin coronatine. *Journal of Bacteriology,* 180**,** 1360-1367.
CAIN, A. K., BARQUIST, L., GOODMAN, A. L., PAULSEN, I. T., PARKHILL, J. & VAN OPIJNEN, T. 2020. A decade of advances in transposon-insertion sequencing. *Nature Reviews Genetics,* 21**,** 526-540.
CAMEJO, D., GUZMAN-CEDENO, A. & MORENO, A. 2016. Reactive oxygen species, essential molecules, during plant-pathogen interactions. *Plant Physiology and Biochemistry,* 103**,** 10-23.
CARTER, M. E., HELM, M., CHAPMAN, A. V. E., WAN, E., SIERRA, A. M. R., INNES, R. W., BOGDANOVE, A. J. & WISE, R. P. 2019. Convergent Evolution of Effector Protease Recognition by Arabidopsis and Barley. *Molecular Plant-Microbe Interactions,* 32**,** 550-565.
CHAN, J. & GOODWIN, P. H. 1999. Differentiation of Xanthomonas campestris pv. phaseoli from Xanthomonas campestris pv. phaseoli var. fuscans by PFGE and RFLP. *European Journal of Plant Pathology,* 105**,** 867-878.

CHANG, W., SMALL, D. A., TOGHROL, F. & BENTLEY, W. E. 2005. Microarray analysis of Pseudomonas aeruginosa reveals induction of pyocin genes in response to hydrogen peroxide. *Bmc Genomics,* 6**,** 1-14.

CHATNAPARAT, T., LI, Z., KORBAN, S. S. & ZHAO, Y. F. 2015. The bacterial alarmone (p)ppGpp is required for virulence and controls cell size and survival of Pseudomonas syringae on plants. *Environmental Microbiology,* 17**,** 4253-4270.

CHEN, L., LI, P., DENG, Z. X. & ZHAO, C. M. 2015. Ornithine Transcarbamylase ArgK Plays a Dual role for the Self-defense of Phaseolotoxin Producing Pseudomonas syringae pv. phaseolicola. *Scientific Reports,* 5.

CHEN, N. W. G., RUH, M., DARRASSE, A., FOUCHER, J., BRIAND, M., COSTA, J., STUDHOLME, D. J. & JACQUES, M. A. 2021. Common bacterial blight of bean: a model of seed transmission and pathological convergence. *Molecular Plant Pathology,* 22**,** 1464-1480.

CHENG, C., GAO, X. Q., FENG, B. M., SHEEN, J., SHAN, L. B. & HE, P. 2013. Plant immune response to pathogens differs with changing temperatures. *Nature Communications,* 4**,** 9.

CHISHOLM, S. T., COAKER, G., DAY, B. & STASKAWICZ, B. J. 2006. Host-microbe interactions: Shaping the evolution of the plant immune response. *Cell,* 124**,** 803-814.

CHOI, Y. S., SHIN, D. H., CHUNG, I. Y., KIM, S. H., HEO, Y. J. & CHO, Y. H. 2007. Identification of Pseudomonas aeruginosa genes crucial for hydrogen peroxide resistance. *Journal of Microbiology and Biotechnology,* 17**,** 1344-1352.

COHEN, S. P., LIU, H. X., ARGUES, C. T., PEREIRA, A., CRUZ, C. V., VERDIER, V. & LEACH, J. E. 2017. RNA-Seq analysis reveals insight into enhanced rice Xa7-mediated bacterial blight resistance at high temperature. *Plos One,* 12.

CORNELIS, P. & MATTHIJS, S. 2002. Diversity of siderophore-mediated iron uptake systems in fluorescent pseudomonads: not only pyoverdines. *Environmental Microbiology,* 4**,** 787-798.

CROUCHER, N. J., PAGE, A. J., CONNOR, T. R., DELANEY, A. J., KEANE, J. A., BENTLEY, S. D., PARKHILL, J. & HARRIS, S. R. 2015. Rapid phylogenetic analysis of large samples of recombinant bacterial whole genome sequences using Gubbins. *Nucleic Acids Research,* 43.

DE RON, A. M., RODINO, A. P., SANTALLA, M., GONZALEZ, A. M., LEMA, M. J., MARTIN, I. & KIGEL, J. 2016. Seedling Emergence and Phenotypic Response of Common Bean Germplasm to Different Temperatures under Controlled Conditions and in Open Field. *Frontiers in Plant Science,* 7.

DEGU, YAREGAL & GUDISA 2020. Status of Common Bean (Phaseolus vulgaris L.) Diseases in Metekel Zone, North West Ethiopia. *J Plant Pathol Microbiol*.

DELAFUENTEMARTINEZ, J. M., MOSQUEDACANO, G., ALVAREZMORALES, A. & HERRERAESTRELLA, L. 1992. EXPRESSION OF A BACTERIAL PHASEOLOTOXIN-RESISTANT ORNITHYL TRANSCARBAMYLASE IN TRANSGENIC TOBACCO CONFERS RESISTANCE TO PSEUDOMONAS-SYRINGAE PV PHASEOLICOLA. *Bio-Technology,* 10**,** 905-909.

DENG, X., WEERAPANA, E., ULANOVSKAYA, O., SUN, F., LIANG, H. H., JI, Q. J., YE, Y., FU, Y., ZHOU, L., LI, J. X., ZHANG, H. Y., WANG, C., ALVAREZ, S., HICKS, L. M., LAN, L. F., WU, M., CRAVATT, B. F. & HE, C. 2013. Proteome-wide Quantification and Characterization of Oxidation-Sensitive Cysteines in Pathogenic Bacteria. *Cell Host & Microbe,* 13**,** 358-370.

DIAZ-VALLE, A., LOPEZ-CALLEJA, A. C. & ALVAREZ-VENEGAS, R. 2019. Enhancement of Pathogen Resistance in Common Bean Plants by Inoculation With Rhizobium etli. *Frontiers in Plant Science,* 10.

DIDELOT, X. & WILSON, D. J. 2015. ClonalFrameML: Efficient Inference of Recombination in Whole Bacterial Genomes. *Plos Computational Biology,* 11.
DODDS, P. N. & RATHJEN, J. P. 2010. Plant immunity: towards an integrated view of plant-pathogen interactions. *Nature Reviews Genetics,* 11**,** 539-548.
DOKE, N. 1985. NADPH-DEPENDENT O-2- GENERATION IN MEMBRANE-FRACTIONS ISOLATED FROM WOUNDED POTATO-TUBERS INOCULATED WITH PHYTOPHTHORA-INFESTANS. *Physiological Plant Pathology,* 27**,** 311-322.
DOLAN, S. K., KOHLSTEDT, M., TRIGG, S., RAMIREZ, P. V., WITTMANN, C., KAMINSKI, C. & WELCH, M. 2020. Contextual Flexibility in Pseudomonas aeruginosa Central Carbon Metabolism during Growth in Single Carbon Sources. *Mbio,* 11.
EMMS, D. M. & KELLY, S. 2015. OrthoFinder: solving fundamental biases in whole genome comparisons dramatically improves orthogroup inference accuracy. *Genome Biology,* 16.
EMMS, D. M. & KELLY, S. 2019. OrthoFinder: phylogenetic orthology inference for comparative genomics. *Genome Biology,* 20.
EZRATY, B., GENNARIS, A., BARRAS, F. & COLLET, J. F. 2017. Oxidative stress, protein damage and repair in bacteria. *Nature Reviews Microbiology,* 15**,** 385-396.
FANG, F. C. 2011. Antimicrobial Actions of Reactive Oxygen Species. *Mbio,* 2.
FAO. 2019. *FAO STAT* [Online]. [Accessed 2019].
FASNACHT, M. & POLACEK, N. 2021. Oxidative Stress in Bacteria and the Central Dogma of Molecular Biology. *Frontiers in Molecular Biosciences,* 8.
FEIL, H., FEIL, W. S., CHAIN, P., LARIMER, F., DIBARTOLO, G., COPELAND, A., LYKIDIS, A., TRONG, S., NOLAN, M., GOLTSMAN, E., THIEL, J., MALFATTI, S., LOPER, J. E., LAPIDUS, A., DETTER, J. C., LAND, M., RICHARDSON, P. M., KYRPIDES, N. C., IVANOVA, N. & LINDOW, S. E. 2005. Comparison of the complete genome sequences of Pseudomonas syringae pv. syringae B728a and pv. tomato DC3000. *Proceedings of the National Academy of Sciences of the United States of America,* 102**,** 11064-11069.
FERLA, M. P. & PATRICK, W. M. 2014. Bacterial methionine biosynthesis. *Microbiology-Sgm,* 160**,** 1571-1584.
FONES, H. & PRESTON, G. M. 2012. Reactive oxygen and oxidative stress tolerance in plant pathogenic Pseudomonas. *Fems Microbiology Letters,* 327**,** 1-8.
FOURIE, D. 1998. Characterization of halo blight races on dry beans in South Africa. *Plant Disease,* 82**,** 307-310.
FOURIE, D. 2002. Distribution and severity of bacterial diseases on dry beans (Phaseolus vulgaris L.) in South Africa. *Journal of Phytopathology-Phytopathologische Zeitschrift,* 150**,** 220-226.
FRANZA, T. & EXPERT, D. 2013. Role of iron homeostasis in the virulence of phytopathogenic bacteria: an "a la carte' menu. *Molecular Plant Pathology,* 14**,** 429-438.
GADGIL, M., KAPUR, V. & HU, W. S. 2005. Transcriptional response of Escherichia coli to temperature shift. *Biotechnology Progress,* 21**,** 689-699.
GANGULY, A. & BAURI, B. 2014. Parametric and performance analysis of a naturally ventilated floriculture greenhouse using a thermal model. *10th International Conference on Mechanical Engineering (Icme 2013),* 90**,** 485-490.
GARDAN, L., SHAFIK, H., BELOUIN, S., BROCH, R., GRIMONT, F. & GRIMONT, P. A. D. 1999. DNA relatedness among the pathovars of Pseudomonas syringae and description of Pseudomonas tremae sp. nov. and Pseudomonas cannabina sp. nov. (ex Sutic and Dowson 1959). *International Journal of Systematic Bacteriology,* 49**,** 469-478.
GENNARIS, A., EZRATY, B., HENRY, C., AGREBI, R., VERGNES, A., OHEIX, E., BOS, J., LEVERRIER, P., ESPINOSA, L., SZEWCZYK, J., VERTOMMEN, D., IRANZO, O., COLLET, J. F. & BARRAS, F. 2015. Repairing oxidized proteins in the bacterial envelope using respiratory chain electrons. *Nature,* 528**,** 409-+.

GOMILA, M., BUSQUETS, A., MULET, M., GARCIA-VALDES, E. & LALUCAT, J. 2017. Clarification of Taxonomic Status within the Pseudomonas syringae Species Group Based on a Phylogenomic Analysis. *Frontiers in Microbiology,* 8.
GONZALEZ-VILLANUEVA, L., ARVIZU-GOMEZ, J. L., HERNANDEZ-MORALES, A., AGUILERA-AGUIRRE, S. & ALVAREZ-MORALES, A. 2014. The PhtL protein of Pseudomonas syringae pv. phaseolicola NPS3121 affects the expression of both phaseolotoxin cluster (Pht) and Non-Pht encoded genes. *Microbiological Research,* 169**,** 221-231.
GOSS, R. W. 1940. The relation of temperature to common and halo blight of beans. *Phytopathology,* 30**,** 258-264.
GRIFFIN, A. S., WEST, S. A. & BUCKLING, A. 2004. Cooperation and competition in pathogenic bacteria. *Nature,* 430**,** 1024-1027.
GROSS, H. & LOPER, J. E. 2009. Genomics of secondary metabolite production by Pseudomonas spp. *Natural Product Reports,* 26**,** 1408-1446.
GUO, M., BLOCK, A., BRYAN, C. D., BECKER, D. F. & ALFANO, J. R. 2012. Pseudomonas syringae Catalases Are Collectively Required for Plant Pathogenesis. *Journal of Bacteriology,* 194**,** 5054-5064.
GUTTMAN, D. S., VINATZER, B. A., SARKAR, S. F., RANALL, M. V., KETTLER, G. & GREENBERG, J. T. 2002. A functional screen for the type III (Hrp) secretome of the plant pathogen Pseudomonas syringae. *Science,* 295**,** 1722-1726.
HEALTH, E. P. O. P. 2014. Scientific Opinion on the pest categorisation of Xanthomonas axonopodis pv. phaseoli and Xanthomonas fuscans subsp. fuscans. 12.
HELMANN, T. C., DEUTSCHBAUER, A. M. & LINDOW, S. E. 2019. Genome-wide identification of Pseudomonas syringae genes required for fitness during colonization of the leaf surface and apoplast. *Proceedings of the National Academy of Sciences of the United States of America,* 116**,** 18900-18910.
HERNANDEZ-MORALES, A., ROJAS-MORALES, J. A., REYNOSO-LOPEZ, M., MARTINEZ-RIZO, A. B., VELAZQUEZ-FERNANDEZ, J. B. & ARVIZU-GOMEZ, J. L. 2018. Oxidative stress regulates the expression of the Pht cluster genes involved in phaseolotoxin synthesis in Pseudomonas syringae pv. phaseolicola NPS3121. *Journal of General Plant Pathology,* 84**,** 137-141.
HILDEBRAND 1988. Laboratory Guide for Identification of Plant Pathogenic Bacteria.
HNATUSZKO-KONKA, K., KOWALCZYK, T., GERSZBERG, A., GLINSKA, S. & GRZEGORCZYK-KAROLAK, I. 2019. Regeneration of Phaseolus vulgaris from epicotyls and hypocotyls via direct organogenesis. *Scientific Reports,* 9.
HOCKETT, K. L., BURCH, A. Y. & LINDOW, S. E. 2013. Thermo-Regulation of Genes Mediating Motility and Plant Interactions in Pseudomonas syringae. *Plos One,* 8**,** 12.
HONDORP, E. R. & MATTHEWS, R. G. 2004. Oxidative stress inactivates cobalamin-independent methionine synthase (MetE) in Escherichia coli. *Plos Biology,* 2**,** 1738-1753.
HUA, J. 2013. Modulation of plant immunity by light, circadian rhythm, and temperature. *Current Opinion in Plant Biology,* 16**,** 406-413.
HUECK, C. J. 1998. Type III protein secretion systems in bacterial pathogens of animals and plants. *Microbiology and Molecular Biology Reviews,* 62**,** 379-+.
HUGOUVIEUX-COTTE-PATTAT, N., DES-COMBES, C. J., BRIOLAY, J. & PRITCHARD, L. 2021. Proposal for the creation of a new genus Musicola gen. nov., reclassification of Dickeya paradisiaca (Samson et al. 2005) as Musicola paradisiaca comb. nov. and description of a new species Musicola keenii sp. nov. *International Journal of Systematic and Evolutionary Microbiology,* 71.

HUMAIR, B., GONZALEZ, N., MOSSIALOS, D., REIMMANN, C. & HAAS, D. 2009. Temperature-responsive sensing regulates biocontrol factor expression in Pseudomonas fluorescens CHA0. *Isme Journal,* 3**,** 955-965.

HUOT, B., CASTROVERDE, C. D. M., VELASQUEZ, A. C., HUBBARD, E., PULMAN, J. A., YAO, J., CHILDS, K. L., TSUDA, K., MONTGOMERY, B. L. & HE, S. Y. 2017. Dual impact of elevated temperature on plant defence and bacterial virulence in Arabidopsis. *Nature Communications,* 8**,** 12.

INAMULLAH & ISODA, A. 2005. Adaptive responses of soybean and cotton to water stress - I. Transpiration changes in relation to stomatal area and stomatal conductance. *Plant Production Science,* 8**,** 16-26.

ISHIGA, Y. & ICHINOSE, Y. 2016. Pseudomonas syringae pv. tomato OxyR Is Required for Virulence in Tomato and Arabidopsis. *Molecular Plant-Microbe Interactions,* 29**,** 119-131.

JAYARAMAN, J., CHATTERJEE, A., HUNTER, S., CHEN, R., STROUD, E. A., SAEI, H., HOYTE, S., DEROLES, S., TAHIR, J., TEMPLETON, M. D. & BRENDOLISE, C. 2021. Rapid Methodologies for Assessing Pseudomonas syringae pv. actinidiae Colonization and Effector-Mediated Hypersensitive Response in Kiwifruit. *Molecular Plant-Microbe Interactions,* 34**,** 880-890.

JENNER, C., HITCHIN, E., MANSFIELD, J., WALTERS, K., BETTERIDGE, P., TEVERSON, D. & TAYLOR, J. 1991. GENE-FOR-GENE INTERACTIONS BETWEEN PSEUDOMONAS-SYRINGAE PV PHASEOLICOLA AND PHASEOLUS. *Molecular Plant-Microbe Interactions,* 4**,** 553-562.

JOARDAR, V., LINDEBERG, M., JACKSON, R. W., SELENGUT, J., DODSON, R., BRINKAC, L. M., DAUGHERTY, S. C., DEBOY, R., DURKIN, A. S., GIGLIO, M. G., MADUPU, R., NELSON, W. C., ROSOVITZ, M. J., SULLIVAN, S., CRABTREE, J., CREASY, T., DAVIDSEN, T., HAFT, D. H., ZAFAR, N., ZHOU, L. W., HALPIN, R., HOLLEY, T., KHOURI, H., FELDBLYUM, T., WHITE, O., FRASER, C. M., CHATTERJEE, A. K., CARTINHOUR, S., SCHNEIDER, D. J., MANSFIELD, J., COLLMER, A. & BUELL, C. R. 2005. Whole-genome sequence analysis of Pseudomonas syringae pv. phaseolicola 1448A reveals divergence among pathovars in genes involved in virulence and transposition. *Journal of Bacteriology,* 187**,** 6488-6498.

JONES, J. D. G. & DANGL, J. L. 2006. The plant immune system. *Nature,* 444**,** 323-329.

JOSE, M. S., RODICIO, M. R., ARGUDIN, M. A., MENDOZA, M. C. & GONZALEZ, A. J. 2010. Regional variations in the population structure of Pseudomonas syringae pathovar phaseolicola from Spain are revealed by typing with PmeI pulsed-field gel electrophoresis, plasmid profiling and virulence gene complement. *Microbiology-Sgm,* 156**,** 1795-1804.

KATOH, K., MISAWA, K., KUMA, K. & MIYATA, T. 2002. MAFFT: a novel method for rapid multiple sequence alignment based on fast Fourier transform. *Nucleic Acids Research,* 30**,** 3059-3066.

KEANE, P. J., KERR, A. & NEW, P. B. 1970. CROWN GALL OF STONE FRUIT .2. IDENTIFICATION AND NOMENCLATURE OF AGROBACTERIUM ISOLATES. *Australian Journal of Biological Sciences,* 23**,** 585-&.

KEITH, L. M. W. & BENDER, C. L. 1999. A1gT (sigma(22)) controls alginate production and tolerance to environmental stress in Pseudomonas syringae. *Journal of Bacteriology,* 181**,** 7176-7184.

KEITH, L. M. W., PARTRIDGE, J. E. & BENDER, C. L. 1999. dnaK and the heat stress response of Pseudomonas syringae pv. glycinea. *Molecular Plant-Microbe Interactions,* 12**,** 563-574.

KERSTERS, K., LUDWIG, W., VANCANNEYT, M., DEVOS, P., GILLIS, M. & SCHLEIFER, K. H. 1996. Recent changes in the classification of the pseudomonads: An overview. *Systematic and Applied Microbiology,* 19**,** 465-477.

KHAKIMOVA, M., AHLGREN, H. G., HARRISON, J. J., ENGLISH, A. M. & NGUYEN, D. 2013. The Stringent Response Controls Catalases in Pseudomonas aeruginosa and Is Required for Hydrogen Peroxide and Antibiotic Tolerance. *Journal of Bacteriology,* 195**,** 2011-2020.

KIM, J. & PARK, W. 2014. Oxidative stress response in Pseudomonas putida. *Applied Microbiology and Biotechnology,* 98**,** 6933-6946.

KIM, Y. C., MILLER, C. D. & ANDERSON, A. J. 1999. Transcriptional regulation by iron and role during plant pathogenesis of genes encoding iron- and manganese-superoxide dismutases of Pseudomonas syringae pv. syringae B728a. *Physiological and Molecular Plant Pathology,* 55**,** 327-339.

KING, E. O., WARD, M. K. & RANEY, D. E. 1954. 2 SIMPLE MEDIA FOR THE DEMONSTRATION OF PYOCYANIN AND FLUORESCIN. *Journal of Laboratory and Clinical Medicine,* 44**,** 301-307.

KISSOUDIS, C., VAN DE WIEL, C., VISSER, R. G. F. & VAN DER LINDEN, G. 2014. Enhancing crop resilience to combined abiotic and biotic stress through the dissection of physiological and molecular crosstalk. *Frontiers in Plant Science,* 5.

KLOTZ, M. G. & HUTCHESON, S. W. 1992. MULTIPLE PERIPLASMIC CATALASES IN PHYTOPATHOGENIC STRAINS OF PSEUDOMONAS-SYRINGAE. *Applied and Environmental Microbiology,* 58**,** 2468-2473.

KNOKE, L. R., ZIMMERMANN, J., LUPILOV, N., SCHNEIDER, J. F., CELEBI, B., MORGAN, B. & LEICHERT, L. I. 2023. The role of glutathione in periplasmic redox homeostasis and oxidative protein folding in Escherichia coli. *Redox Biology,* 64.

LAFLAMME, B., DILLON, M. M., MARTEL, A., ALMEIDA, R. N. D., DESVEAUX, D. & GUTTMAN, D. S. 2020. The pan-genome effector-triggered immunity landscape of a host-pathogen interaction. *Science,* 367**,** 763-+.

LAGUERRE, G., NOUR, S. M., MACHERET, V., SANJUAN, J., DROUIN, P. & AMARGER, N. 2001. Classification of rhizobia based on nodC and nifH gene analysis reveals a close phylogenetic relationship among Phaseolus vulgaris symbionts. *Microbiology-Sgm,* 147**,** 981-993.

LAL, N. K., THANASUWAT, B., HUANG, P. J., CAVANAUGH, K. A., CARTER, A., MICHELMORE, R. W. & DINESH-KUMAR, S. P. 2020. Phytopathogen Effectors Use Multiple Mechanisms to Manipulate Plant Autophagy. *Cell Host & Microbe,* 28**,** 558-+.

LAM, H. N., CHAKRAVARTHY, S., WEI, H. L., BUINGUYEN, H., STODGHILL, P. V., COLLMER, A., SWINGLE, B. M. & CARTINHOUR, S. W. 2014. Global Analysis of the HrpL Regulon in the Plant Pathogen Pseudomonas syringae pv. tomato DC3000 Reveals New Regulon Members with Diverse Functions. *Plos One,* 9.

LANGLEY, D. B., TEMPLETON, M. D., FIELDS, B. A., MITCHELL, R. E. & COLLYER, C. A. 2000. Mechanism of inactivation of ornithine transcarbamoylase by N-delta-(N '-sulfodiaminophosphinyl)-L-ornithine, a true transition state analogue? Crystal structure and implications for catalytic mechanism. *Journal of Biological Chemistry,* 275**,** 20012-20019.

LATORRE, B. A., LILLO, C. & RIOJA, M. E. 2002. Effects of temperature, free moisture duration and inoculum concentration on infection of sweet cherry by Pseudomonas syringae pv. syringae. *Phytoparasitica,* 30**,** 410-419.

LEICHERT, L. I. & JAKOB, U. 2004. Protein thiol modifications visualized in vivo. *Plos Biology,* 2**,** 1723-1737.

LINDEBERG, M., CUNNAC, S. & COLLMER, A. 2009. The evolution of Pseudomonas syringae host specificity and type III effector repertoires. *Molecular Plant Pathology,* 10**,** 767-775.

LINDEBERG, M., STAVRINIDES, J., CHANG, J. H., ALFANO, J. R., COLLMER, A., DANGL, J. L., GREENBERG, J. T., MANSFIELD, J. W. & GUTTMAN, D. S. 2005. Proposed guidelines for a unified nomenclature and phylogenetic analysis of type III Hop effector proteins in the plant pathogen Pseudomonas syringae. *Molecular Plant-Microbe Interactions,* 18**,** 275-282.

LIU, J., YU, M. H., GE, Y. X., TIAN, Y. L., HU, B. S. & ZHAO, Y. F. 2021. The RsmA RNA-Binding Proteins in Pseudomonas syringae Exhibit Distinct and Overlapping Roles in Modulating Virulence and Survival Under Different Nutritional Conditions. *Frontiers in Plant Science,* 12.

LOVE, M. I., HUBER, W. & ANDERS, S. 2014. Moderated estimation of fold change and dispersion for RNA-seq data with DESeq2. *Genome Biology,* 15.

LU, Y. & YAO, J. 2018. Chloroplasts at the Crossroad of Photosynthesis, Pathogen Infection and Plant Defense. *International Journal of Molecular Sciences,* 19.

MACHO, A. P., ZUMAQUERO, A., GONZALEZ-PLAZA, J. J., ORTIZ-MARTIN, I., RUFIAN, J. S. & BEUZON, C. R. 2012. Genetic Analysis of the Individual Contribution to Virulence of the Type III Effector Inventory of Pseudomonas syringae pv. phaseolicola. *Plos One,* 7**,** 12.

MAES, A., GRACIA, E., INNOCENTI, N., ZHANG, K. Y., AURELL, E. & HAJNSDORF, E. 2017. Landscape of RNA polyadenylation in E-coli. *Nucleic Acids Research,* 45**,** 2746-2756.

MANSILLA, M. C. & DE MENDOZA, D. 2005. The Bacillus subtilis desaturase: a model to understand phospholipid modification and temperature sensing. *Archives of Microbiology,* 183**,** 229-235.

MARGISPINHEIRO, M., MARIVET, J. & BURKARD, G. 1994. BEAN CLASS-IV CHITINASE GENE - STRUCTURE, DEVELOPMENTAL EXPRESSION AND INDUCTION BY HEAT-STRESS. *Plant Science,* 98**,** 163-173.

MARKEL, E., STODGHILL, P., BAO, Z. M., MYERS, C. R. & SWINGLE, B. 2016. AlgU Controls Expression of Virulence Genes in Pseudomonas syringae pv. tomato DC3000. *Journal of Bacteriology,* 198**,** 2330-2344.

MARQUES, A. S. D. & SAMSON, R. 2016. Population dynamics of Pseudomonas savastanoi pv. phaseolicola in bean, throughout the epiphytic and pathogenic phases. *Pesquisa Agropecuaria Brasileira,* 51**,** 623-630.

MASIP, L., VEERAVALLI, K. & GEORGIOUI, G. 2006. The many faces of glutathione in bacteria. *Antioxidants & Redox Signaling,* 8**,** 753-762.

MATERN, S., PESKAN-BERGHOEFER, T., GROMES, R., KIESEL, R. V. & RAUSCH, T. 2015. Imposed glutathione-mediated redox switch modulates the tobacco wound-induced protein kinase and salicylic acid-induced protein kinase activation state and impacts on defence against Pseudomonas syringae. *Journal of Experimental Botany,* 66**,** 1935-1950.

MCCRAW, S. L. A. & PRESTON, G. D. S. 2014. *The metabolic context for virulence in Pseudomonas syringae.* Thesis (Ph.D.), University of Oxford.

MCMULLAN, M., GARDINER, A., BAILEY, K., KEMEN, E., WARD, B. J., CEVIK, V., ROBERT-SEILANIANTZ, A., SCHULTZ-LARSEN, T., BALMUTH, A., HOLUB, E., VAN OOSTERHOUT, C. & JONES, J. D. G. 2015. Evidence for suppression of immunity as a driver for genomic introgressions and host range expansion in races of Albugo candida, a generalist parasite. *eLife,* 4**,** e04550.

MENNA, A., NGUYEN, D., GUTTMAN, D. S. & DESVEAUX, D. 2015. Elevated Temperature Differentially Influences Effector-Triggered Immunity Outputs in Arabidopsis. *Frontiers in Plant Science,* 6**,** 7.

MEZIADI, C., LINTZ, J., NADERPOUR, M., GAUTIER, C., BLANCHET, S., NOLY, A., GRATIAS-WEILL, A., GEFFROY, V. & PFLIEGER, S. 2021. R-BPMV-Mediated Resistance to Bean pod mottle virus in Phaseolus vulgaris L. Is Heat-Stable but

Elevated Temperatures Boost Viral Infection in Susceptible Genotypes. *Viruses-Basel,* 13.
MILLER 1972. *Experiments in molecular genetics*.
MIURA, K. & TADA, Y. 2014. Regulation of water, salinity, and cold stress responses by salicylic acid. *Frontiers in Plant Science,* 5.
MORRIS, C. E., LAMICHHANE, J. R., NIKOK, I., STANKOVIC, S. & MOURY, B. 2019. The overlapping continuum of host range among strains in the Pseudomonas syringae complex. *Phytopathology Research,* 1.
MORRIS, C. E., SANDS, D. C., VINATZER, B. A., GLAUX, C., GUILBAUD, C., BUFFIERE, A., YAN, S. C., DOMINGUEZ, H. & THOMPSON, B. M. 2008. The life history of the plant pathogen Pseudomonas syringae is linked to the water cycle. *Isme Journal,* 2**,** 321-334.
MUEDI, H. T. H., FOURIE, D. & MCLAREN, N. W. 2015. Distribution and severity of bacterial brown spot on dry beans in South Africa: An update. *South African Journal of Science,* 111**,** 52-57.
MURILLO, J., BARDAJI, L., DE LA FUENTE, L. N., FUHRER, M. E., AGUILERA, S. & ALVAREZ-MORALES, A. 2011. Variation in conservation of the cluster for biosynthesis of the phytotoxin phaseolotoxin in Pseudomonas syringae suggests at least two events of horizontal acquisition. *Research in Microbiology,* 162**,** 253-261.
MYERS, J. R. & KMIECIK, K. 2017. Common Bean: Economic Importance and Relevance to Biological Science Research. *Common Bean Genome***,** 1-20.
NGOU, B. P. M., DING, P. T. & JONES, J. D. G. 2022a. Thirty years of resistance: Zig-zag through the plant immune system. *Plant Cell,* 34**,** 1447-1478.
NGOU, B. P. M., JONES, J. D. G. & DING, P. T. 2022b. Plant immune networks. *Trends in Plant Science,* 27**,** 255-273.
NIKEL, P. I., FUHRER, T., CHAVARRIA, M., SANCHEZ-PASCUALA, A., SAUER, U. & DE LORENZO, V. 2021. Reconfiguration of metabolic fluxes in Pseudomonas putida as a response to sub-lethal oxidative stress. *Isme Journal,* 15**,** 1751-1766.
NIZER, W. S. D., INKOVSKIY, V., VERSEY, Z., STREMPEL, N., CASSOL, E. & OVERHAGE, J. 2021. Oxidative Stress Response in Pseudomonas aeruginosa. *Pathogens,* 10.
NOCTOR, G., LELARGE-TROUVERIE, C. & MHAMDI, A. 2015. The metabolomics of oxidative stress. *Phytochemistry,* 112**,** 33-53.
NOMAN, A., LIU, Z. Q., YANG, S., SHEN, L., HUSSAIN, A., ASHRAF, M. F., KHAN, M. I. & HE, S. L. 2018. Expression and functional evaluation of CaZNF830 during pepper response to Ralstonia solanacearum or high temperature and humidity. *Microbial Pathogenesis,* 118**,** 336-346.
NOTREDAME, C., HIGGINS, D. G. & HERINGA, J. 2000. T-Coffee: A novel method for fast and accurate multiple sequence alignment. *Journal of Molecular Biology,* 302**,** 205-217.
NOWOGORSKA, A. & PATYKOWSKI, J. 2015. Selected reactive oxygen species and antioxidant enzymes in common bean after Pseudomonas syringae pv. phaseolicola and Botrytis cinerea infection. *Acta Physiologiae Plantarum,* 37.
NUSKE, J. & FRITSCHE, W. 1989. PHASEOLOTOXIN PRODUCTION BY PSEUDOMONAS-SYRINGAE PV PHASEOLICOLA - THE INFLUENCE OF TEMPERATURE. *Journal of Basic Microbiology,* 29**,** 441-447.
O'LEARY, B. M., RICO, A., MCCRAW, S., FONES, H. N. & PRESTON, G. M. 2014. The Infiltration-centrifugation Technique for Extraction of Apoplastic Fluid from Plant Leaves Using Phaseolus vulgaris as an Example. *Jove-Journal of Visualized Experiments*.
OH, H. S., PARK, D. H. & COLLMER, A. 2010. Components of the Pseudomonas syringae Type III Secretion System Can Suppress and May Elicit Plant Innate Immunity. *Molecular Plant-Microbe Interactions,* 23**,** 727-739.

OPIO, A. F., ALLEN, D. J. & TERI, J. M. 1996. Pathogenic variation in Xanthomonas campestris pv phaseoli, the causal agent of common bacterial blight in Phaseolus beans. *Plant Pathology,* 45**,** 1126-1133.
PALMA, M., DELUCA, D., WORGALL, S. & QUADRI, L. E. N. 2004. Transcriptome analysis of the response of Pseudomonas aeruginosa to hydrogen peroxide. *Journal of Bacteriology,* 186**,** 248-252.
PALMER, D. A. & BENDER, C. L. 1993. EFFECTS OF ENVIRONMENTAL AND NUTRITIONAL FACTORS ON PRODUCTION OF THE POLYKETIDE PHYTOTOXIN CORONATINE BY PSEUDOMONAS-SYRINGAE PV GLYCINEA. *Applied and Environmental Microbiology,* 59**,** 1619-1626.
PANOPOULOS, N. J. & SCHROTH, M. N. 1974. ROLE OF FLAGELLAR MOTILITY IN INVASION OF BEAN-LEAVES BY PSEUDOMONAS-PHASEOLICOLA. *Phytopathology,* 64**,** 1389-1397.
PARKINSON, N., BRYANT, R., BEW, J. & ELPHINSTONE, J. 2011. Rapid phylogenetic identification of members of the Pseudomonas syringae species complex using the rpoD locus. *Plant Pathology,* 60**,** 338-344.
PATIL, S. S., ROWLEY, K. B., KAMDAR, H. V., CLEMENTS, D., MANDEL, M. & HUMPHREYS, T. 1991. MOLECULAR ANALYSIS OF PHASEOLOTOXIN PRODUCTION IN PSEUDOMONAS-SYRINGAE PV PHASEOLICOLA. *Molecular Strategies of Pathogens and Host Plants***,** 95-104.
PAVANKUMAR, T. L., MITTAL, P. & HALLSWORTH, J. E. 2021. Molecular insights into the ecology of a psychrotolerant Pseudomonas syringae. *Environmental Microbiology,* 23**,** 3665-3681.
PLENER, L., BOISTARD, P., GONZALEZ, A., BOUCHER, C. & GENIN, S. 2012. Metabolic Adaptation of Ralstonia solanacearum during Plant Infection: A Methionine Biosynthesis Case Study. *Plos One,* 7.
POOLE, L. B. 2015. The basics of thiols and cysteines in redox biology and chemistry. *Free Radical Biology and Medicine,* 80**,** 148-157.
PRESTON, G. M. 2017. Profiling the extended phenotype of plant pathogens: Challenges in Bacterial Molecular Plant Pathology. *Molecular Plant Pathology,* 18**,** 443-456.
PRITCHARD, L., GLOVER, R. H., HUMPHRIS, S., ELPHINSTONE, J. G. & TOTH, I. K. 2016. Genomics and taxonomy in diagnostics for food security: soft-rotting enterobacterial plant pathogens. *Analytical Methods,* 8**,** 12-24.
QUINONES, B., DULLA, G. & LINDOW, S. E. 2005. Quorum sensing regulates exopolysaccharide production, motility, and virulence in Pseudomonas syringae. *Molecular Plant-Microbe Interactions,* 18**,** 682-693.
RAMIREZ-ZAPATA, D., RAMOS, C., AGUILERA, S., BARDAJI, L., MARTINEZ-GIL, M. & MURILLO, J. 2020. Two Homologues of the Global Regulator Csr/Rsm Redundantly Control Phaseolotoxin Biosynthesis and Virulence in the Plant Pathogen Pseudomonas amygdali pv. phaseolicola 1448A. *Microorganisms,* 8.
RAMOS, A. R., MORELLO, J. E., RAVINDRAN, S., DENG, W. L., HUANG, H. C. & COLLMER, A. 2007. Identification of Pseudomonas syringae pv. syringae 61 type III secretion system Hrp proteins that can travel the type III pathway and contribute to the translocation of effector proteins into plant cells. *Journal of Bacteriology,* 189**,** 5773-5778.
RHEE, S. G., BAE, Y. S., LEE, S.-R. & KWON, J. 2000. Hydrogen Peroxide: A Key Messenger That Modulates Protein Phosphorylation Through Cysteine Oxidation. *Science's STKE,* 2000**,** pe1-pe1.
RICO, A., LOPEZ, R., ASENSIO, C., AIZPUN, M. T., ASENSIO-S-MANZANERA, M. C. & MURILLO, J. 2003. Nontoxigenic strains of Pseudomonas syringae pv. phaseolicola are

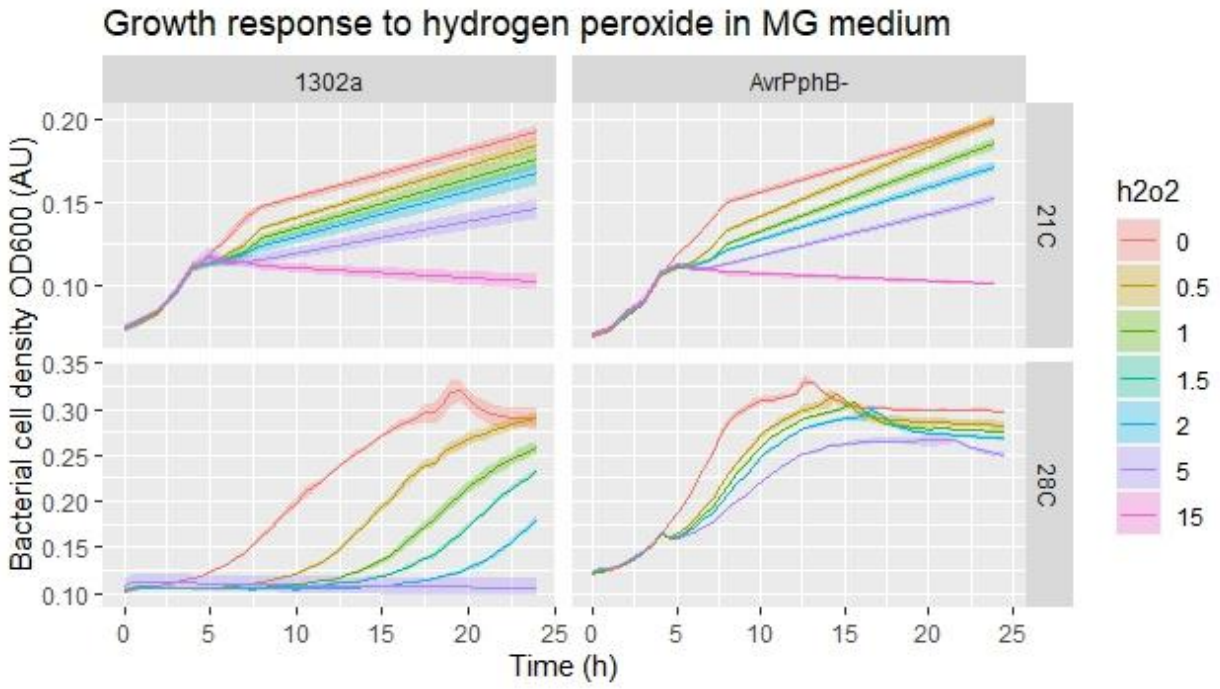
a main cause of halo blight of beans in Spain and escape current detection methods. *Phytopathology,* 93**,** 1553-1559.
ROTH, M., JAQUET, V., LEMEILLE, S., BONETTI, E. J., CAMBET, Y., FRANCOIS, P. & KRAUSE, K. H. 2022. Transcriptomic Analysis of E. coli after Exposure to a Sublethal Concentration of Hydrogen Peroxide Revealed a Coordinated Up-Regulation of the Cysteine Biosynthesis Pathway. *Antioxidants,* 11.
ROWLEY, K. B., CLEMENTS, D. E., MANDEL, M., HUMPHREYS, T. & PATIL, S. S. 1993. MULTIPLE COPIES OF A DNA-SEQUENCE FROM PSEUDOMONAS-SYRINGAE PATHOVAR PHASEOLICOLA ABOLISH THERMOREGULATION OF PHASEOLOTOXIN PRODUCTION. *Molecular Microbiology,* 8**,** 625-635.
ROWLEY, K. B., XU, R. H. & PATIL, S. S. 2000. Molecular analysis of thermoregulation of phaseolotoxin-resistant ornithine carbamoyltransferase (argK) from Pseudomonas syringae pv. phaseolicola. *Molecular Plant-Microbe Interactions,* 13**,** 1071-1080.
SAETTLER 1989. *Bean production problems in the tropics*.
SAHA, C. K., PIRES, R. S., BROLIN, H., DELANNOY, M. & ATKINSON, G. C. 2021. FlaGs and webFlaGs: discovering novel biology through the analysis of gene neighbourhood conservation. *Bioinformatics,* 37**,** 1312-1314.
SAKOPARNIG, T., FIELD, C. & VAN NIMWEGEN, E. 2021. Whole genome phylogenies reflect the distributions of recombination rates for many bacterial species. *Elife,* 10.
SALUNKHE, P., TOPFER, T., BUER, J. & TUMMLER, B. 2005. Genome-wide transcriptional profiling of the steady-state response of Pseudomonas aeruginosa to hydrogen peroxide. *Journal of Bacteriology,* 187**,** 2565-2572.
SANINJUK, K., ROMSANG, A., DUANG-NKERN, J., VATTANAVIBOON, P. & MONGKOLSUK, S. 2019. Transcriptional regulation of the Pseudomonas aeruginosa iron-sulfur cluster assembly pathway by binding of IscR to multiple sites. *Plos One,* 14.
SARRIS, P. F., GAO, S., KARADEMIRIS, K., JIN, H. L., KALANTIDIS, K. & PANOPOULOS, N. J. 2011. Phytobacterial Type III Effectors HopX1, HopAB1 and HopF2 Enhance Sense-Post-Transcriptional Gene Silencing Independently of Plant R Gene-Effector Recognition. *Molecular Plant-Microbe Interactions,* 24**,** 907-917.
SCHOLZ-SCHROEDER, B. K., HUTCHISON, M. L., GRGURINA, I. & GROSS, D. C. 2001. The contribution of syringopeptin and syringomycin to virulence of Pseudomonas syringae pv. syringae strain B301D on the basis of sypA and syrB1 biosynthesis mutant analysis. *Molecular Plant-Microbe Interactions,* 14**,** 336-348.
SERFONTEIN, J. J. 1994. OCCURRENCE OF BACTERIAL BROWN SPOT OF DRY BEANS IN THE TRANSVAAL PROVINCE OF SOUTH-AFRICA. *Plant Pathology,* 43**,** 597-599.
SEWELAM, N., KAZAN, K. & SCHENK, P. M. 2016. Global Plant Stress Signaling: Reactive Oxygen Species at the Cross-Road. *Frontiers in Plant Science,* 7.
SHIVAJI, S., RAO, N. S., SAISREE, L., SHETH, V., REDDY, G. S. N. & BHARGAVA, P. M. 1989. ISOLATION AND IDENTIFICATION OF PSEUDOMONAS SPP FROM SCHIRMACHER OASIS, ANTARCTICA. *Applied and Environmental Microbiology,* 55**,** 767-770.
SIEVERS, F. & HIGGINS, D. G. 2018. Clustal Omega for making accurate alignments of many protein sequences. *Protein Science,* 27**,** 135-145.
SIEVERS, F., WILM, A., DINEEN, D., GIBSON, T. J., KARPLUS, K., LI, W. Z., LOPEZ, R., MCWILLIAM, H., REMMERT, M., SODING, J., THOMPSON, J. D. & HIGGINS, D. G. 2011. Fast, scalable generation of high-quality protein multiple sequence alignments using Clustal Omega. *Molecular Systems Biology,* 7.
SINDEN, S. L., DEVAY, J. E. & BACKMAN, P. A. 1971. PROPERTIES OF SYRINGOMYCIN, A WIDE SPECTRUM ANTIBIOTIC AND PHYTOTOXIN PRODUCED BY PSEUDOMONAS-SYRINGAE, AND ITS ROLE IN BACTERIAL CANKER DISEASE OF PEACH TREES. *Physiological Plant Pathology,* 1**,** 199-+.

SINGH, G. M., VAILLANCOURT, F. H., YIN, J. & WALSH, C. T. 2007. Characterization of SyrC, an aminoacyltransferase shuttling threonyl and chlorothreonyl residues in the syringomycin biosynthetic assembly line. *Chemistry & Biology,* 14**,** 31-40.
STAMATAKIS, A. 2014. RAxML version 8: a tool for phylogenetic analysis and post-analysis of large phylogenies. *Bioinformatics,* 30**,** 1312-1313.
STEINBERG, A. P., LIN, M. Z. & KUSSELL, E. 2022. Core genes can have higher recombination rates than accessory genes within global microbial populations. *Elife,* 11.
STEWART, T. M., DUNSTON, T. T., WOSTER, P. M. & CASERO, R. A. 2018. Polyamine catabolism and oxidative damage. *Journal of Biological Chemistry,* 293**,** 18736-18745.
STOCK, A. M., ROBINSON, V. L. & GOUDREAU, P. N. 2000. Two-component signal transduction. *Annual Review of Biochemistry,* 69**,** 183-215.
STOCK, J. B., NINFA, A. J. & STOCK, A. M. 1989. PROTEIN-PHOSPHORYLATION AND REGULATION OF ADAPTIVE RESPONSES IN BACTERIA. *Microbiological Reviews,* 53**,** 450-490.
SYDENHAM, G. M., MCSORLEY, R. & DUNN, R. A. 1997. Effects of temperature on resistance in Phaseolus vulgaris genotypes and on development of Meloidogyne species. *Journal of Nematology,* 29**,** 90-103.
TAYLOR, J. D., TEVERSON, D. M., ALLEN, D. J. & PASTORCORRALES, M. A. 1996. Identification and origin of races of Pseudomonas syringae pv phaseolicola from Africa and other bean growing areas. *Plant Pathology,* 45**,** 469-478.
THAKUR, S., WEIR, B. S. & GUTTMAN, D. S. 2016. Phytopathogen Genome Announcement: Draft Genome Sequences of 62 Pseudomonas syringae Type and Pathotype Strains. *Molecular Plant-Microbe Interactions,* 29**,** 243-246.
TORRES, M. A. & DANGL, J. L. 2005. Functions of the respiratory burst oxidase in biotic interactions, abiotic stress and development. *Current Opinion in Plant Biology,* 8**,** 397-403.
TORRES, M. A., JONES, J. D. G. & DANGL, J. L. 2006. Reactive oxygen species signaling in response to pathogens. *Plant Physiology,* 141**,** 373-378.
TSIAMIS, G., MANSFIELD, J. W., HOCKENHULL, R., JACKSON, R. W., SESMA, A., ATHANASSOPOULOS, E., BENNETT, M. A., STEVENS, C., VIVIAN, A., TAYLOR, J. D. & MURILLO, J. 2000. Cultivar-specific avirulence and virulence functions assigned to avrPphF in Pseudomonas syringae pv. phaseolicola, the cause of bean halo-blight disease. *Embo Journal,* 19**,** 3204-3214.
ULLRICH, M., PENALOZAVAZQUEZ, A., BAILEY, A. M. & BENDER, C. L. 1995. A MODIFIED 2-COMPONENT REGULATORY SYSTEM IS INVOLVED IN TEMPERATURE-DEPENDENT BIOSYNTHESIS OF THE PSEUDOMONAS-SYRINGAE PHYTOTOXIN CORONATINE. *Journal of Bacteriology,* 177**,** 6160-6169.
ULLRICH, M. S., SCHERGAUT, M., BOCH, J. & ULLRICH, B. 2000. Temperature-responsive genetic loci in the plant pathogen Pseudomanas syringae pv. glycinea. *Microbiology-Sgm,* 146**,** 2457-2468.
VALVERDE, C., HEEB, S., KEEL, C. & HAAS, D. 2003. RsmY, a small regulatory RNA, is required in concert with RsmZ for GacA-dependent expression of biocontrol traits in Pseudomonas fluorescens CHA0. *Molecular Microbiology,* 50**,** 1361-1379.
VAN ACKER, H. & COENYE, T. 2017. The Role of Reactive Oxygen Species in Antibiotic-Mediated Killing of Bacteria. *Trends in Microbiology,* 25**,** 456-466.
VELASQUEZ, A. C., CASTROVERDE, C. D. M. & HE, S. Y. 2018. Plant-Pathogen Warfare under Changing Climate Conditions. *Current Biology,* 28**,** R619-R634.
VENCATO, M., TIAN, F., ALFANO, J. R., BUELL, C. R., CARTINHOUR, S., DECLERCK, G. A., GUTTMAN, D. S., STAVRINIDES, J., JOARDAR, V., LINDEBERG, M., BRONSTEIN, P. A., MANSFIELD, J. W., MYERS, C. R., COLLMER, A. & SCHNEIDER, D. J. 2006. Bioinformatics-enabled identification of the HrpL regulon and type III secretion system

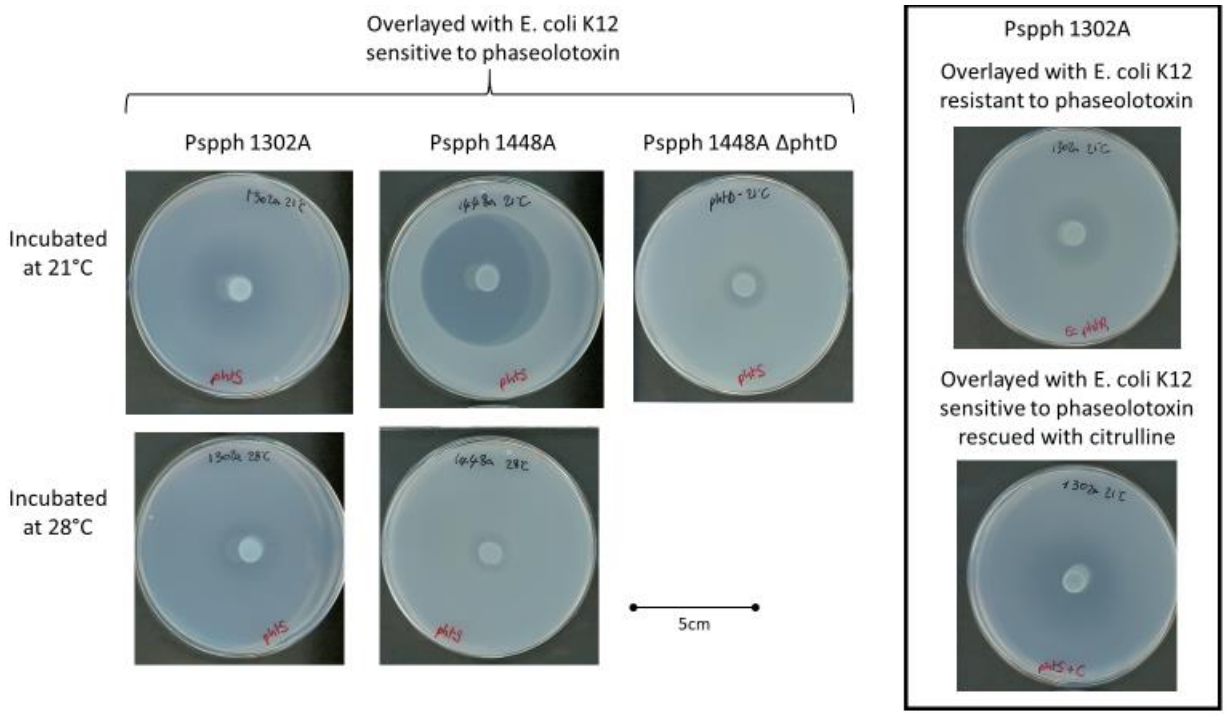
effector proteins of Pseudomonas syringae pv. phaseolicola 1448A. *Molecular Plant-Microbe Interactions,* 19**,** 1193-1206.
VENERO, E. C. S., RICARDI, M. M., GOMEZ-LOZANO, M., MOLIN, S., TRIBELLI, P. M. & LOPEZ, N. I. 2019. Oxidative stress under low oxygen conditions triggers hyperflagellation and motility in the Antarctic bacterium Pseudomonas extremaustralis. *Extremophiles,* 23**,** 587-597.
VIDAVER, A. K., THOMAS, M. E., SCHUSTER, M. L. & MATHYS, M. L. 1972. BACTERIOCINS OF PHYTOPATHOGENS PSEUDOMONAS-SYRINGAE, P GLYCINEA, AND P PHASEOLICOLA. *Canadian Journal of Microbiology,* 18**,** 705-&.
VILAS, J. M., ROMERO, F. M., ROSSI, F. R., MARINA, M., MAIALE, S. J., CALZADILLA, P. I., PIECKENSTAIN, F. L., RUIZ, O. A. & GARRIZ, A. 2018. Modulation of plant and bacterial polyamine metabolism during the compatible interaction between tomato and Pseudomonas syringae. *Journal of Plant Physiology,* 231**,** 281-290.
VINATZER, B. A., TEITZEL, G. M., LEE, M. W., JELENSKA, J., HOTTON, S., FAIRFAX, K., JENRETTE, J. & GREENBERG, J. T. 2006. The type III effector repertoire of Pseudomonas syringae pv. syringae B728a and its role in survival and disease on host and non-host plants. *Molecular Microbiology,* 62**,** 26-44.
WAITE, C., SCHUMACHER, J., JOVANOVIC, M., BENNETT, M. & BUCK, M. 2017. Evading plant immunity: feedback control of the T3SS in Pseudomonas syringae. *Microbial Cell,* 4**,** 137-139.
WALLEN, V. R. & JACKSON, H. R. 1975. MODEL FOR YIELD LOSS DETERMINATION OF BACTERIAL BLIGHT OF FIELD BEANS UTILIZING AERIAL INFRARED PHOTOGRAPHY COMBINED WITH FIELD PLOT STUDIES. *Phytopathology,* 65**,** 942-948.
WANG, H. B., SMITH, A., LOVELACE, A. & KVITKO, B. H. 2022. In planta transcriptomics reveals conflicts between pattern-triggered immunity and the AlgU sigma factor regulon. *Plos One,* 17.
WANG, L., BENDER, C. L. & ULLRICH, M. S. 1999. The transcriptional activator CorR is involved in biosynthesis of the phytotoxin coronatine and binds to the cmaABT promoter region in a temperature-dependent manner. *Molecular and General Genetics,* 262**,** 250-260.
WANG, Y. J., ZHANG, Q., SUN, M. A. & GUO, D. J. 2011. High-accuracy prediction of bacterial type III secreted effectors based on position-specific amino acid composition profiles. *Bioinformatics,* 27**,** 777-784.
WASKOM, M. L. 2021. seaborn: statistical data visualization. *Journal of Open Source Software,* 6**,** 3021.
WEINSTEIN-FISCHER, D., ELGRABLY-WEISS, M. & ALTUVIA, S. 2000. Escherichia coli response to hydrogen peroxide:: a role for DNA supercoiling, topoisomerase I and Fis. *Molecular Microbiology,* 35**,** 1413-1420.
WETMORE, K. M., PRICE, M. N., WATERS, R. J., LAMSON, J. S., HE, J., HOOVER, C. A., BLOW, M. J., BRISTOW, J., BUTLAND, G., ARKIN, A. P. & DEUTSCHBAUER, A. 2015. Rapid Quantification of Mutant Fitness in Diverse Bacteria by Sequencing Randomly Bar-Coded Transposons. *Mbio,* 6.
WICKHAM, AVERICK, M., J, B., W, C., LD, M., R, F., G, G., A, H., L, H., J, H., M, K., TL, P., E, M., SM, B., K, M., J, O., D, R., DP, S., V, S., K, T., D, V., C, W., K, W. & H, Y. 2019. Welcome to the tidyverse. *Journal of Open Source Software*.
WICKHAM, H. 2009. ggplot2: Elegant Graphics for Data Analysis. *Ggplot2: Elegant Graphics for Data Analysis***,** 1-212.
WINSOR, G. L., GRIFFITHS, E. J., LO, R., DHILLON, B. K., SHAY, J. A. & BRINKMAN, F. S. L. 2016. Enhanced annotations and features for comparing thousands of Pseudomonas

genomes in the Pseudomonas genome database. *Nucleic Acids Research,* 44**,** D646-D653.
WONGSAROJ, L., SANINJUK, K., ROMSANG, A., DUANG-NKERN, J., TRINACHARTVANIT, W., VATTANAVIBOON, P. & MONGKOLSUK, S. 2018. Pseudomonas aeruginosa glutathione biosynthesis genes play multiple roles in stress protection, bacterial virulence and biofilm formation. *Plos One,* 13.
WORTMANN & ALLEN 1994. AFRICAN BEAN PRODUCTION ENVIRONMENTS: THEIR DEFINITION, CHARACTERISTICS AND CONSTRAINTS. *Network on Bean Research in Africa, Occasional Paper Series*.
XIAO, Y. X., LU, Y., HEU, S. G. & HUTCHESON, S. W. 1992. ORGANIZATION AND ENVIRONMENTAL-REGULATION OF THE PSEUDOMONAS-SYRINGAE PV SYRINGAE-61 HRP CLUSTER. *Journal of Bacteriology,* 174**,** 1734-1741.
YANG, S. M., TANG, F., GAO, M. Q., KRISHNAN, H. B. & ZHU, H. Y. 2010. R gene-controlled host specificity in the legume-rhizobia symbiosis. *Proceedings of the National Academy of Sciences of the United States of America,* 107**,** 18735-18740.
YOUNG, LUKETINA & MARSHALL 1977. The Effects on Temperature on Growth in vitro of Pseudomonas syringae and Xanthomonas pruni. *Journal of Applied Bacteriology,* 42**,** 345-354.
YOUNG, J. M. 1991. PATHOGENICITY AND IDENTIFICATION OF THE LILAC PATHOGEN, PSEUDOMONAS-SYRINGAE PV SYRINGAE VAN HALL 1902. *Annals of Applied Biology,* 118**,** 283-298.
YU, G. C., WANG, L. G., HAN, Y. Y. & HE, Q. Y. 2012. clusterProfiler: an R Package for Comparing Biological Themes Among Gene Clusters. *Omics-a Journal of Integrative Biology,* 16**,** 284-287.
YU, X. L., LUND, S. P., GREENWALD, J. W., RECORDS, A. H., SCOTT, R. A., NETTLETON, D., LINDOW, S. E., GROSS, D. C. & BEATTIE, G. A. 2014. Transcriptional Analysis of the Global Regulatory Networks Active in Pseudomonas syringae during Leaf Colonization. *Mbio,* 5.
YU, X. L., LUND, S. P., SCOTT, R. A., GREENWALD, J. W., RECORDS, A. H., NETTLETON, D., LINDOW, S. E., GROSS, D. C. & BEATTIE, G. A. 2013. Transcriptional responses of Pseudomonas syringae to growth in epiphytic versus apoplastic leaf sites. *Proceedings of the National Academy of Sciences of the United States of America,* 110**,** E425-E434.
YUAN, M. H., NGOU, B. P. M., DING, P. T. & XIU-FAN, X. 2021. PTI-ETI crosstalk: an integrative view of plant immunity. *Current Opinion in Plant Biology,* 62.
ZENG, W. Q., MELOTTO, M. & HE, S. Y. 2010. Plant stomata: a checkpoint of host immunity and pathogen virulence. *Current Opinion in Biotechnology,* 21**,** 599-603.
ZHU, M. F., SHAO, F., INNES, R. W., DIXON, J. E. & XU, Z. H. 2004. The crystal structure of Pseudomonas avirulence protein AvrPphB: A papain-like fold with a distinct substrate-binding site. *Proceedings of the National Academy of Sciences of the United States of America,* 101**,** 302-307.
ZUMAQUERO, A., MACHO, A. P., RUFIAN, J. S. & BEUZON, C. R. 2010. Analysis of the Role of the Type III Effector Inventory of Pseudomonas syringae pv. phaseolicola 1448a in Interaction with the Plant. *Journal of Bacteriology,* 192**,** 4474-4488.

Supplementary material



Supplementary figure S1
The AvrPphB- mutant of 1302A does not behave differently than the wild type in the face of oxidative stress and temperature. The wild type growth rate is a little slower than the mutant which can be attributed to the cost of producing the AvrPphB- product. Indeed, this experiment was conducted in MG which is a minimal medium which induces expression of the T3SS. The MG medium was chosen because it would be more biologically relevant since AvrPphB- is used for infections *in planta*.



Supplementary figure S2
Strain 1302A does not produce phaseolotoxin *in vitro*. Pspph strains 1302A (wt), 1448A (wt) and 1448A ΔphtD (an essential gene to phaseolotoxin production; this mutant was obtained from the Murillo lab (Aguilera et al., 2007)) were grown as a single colony in the center of plates containing M9-glucose medium solidified with agar at either 21°C or 28°C overnight to allow growth and phaseolotoxin production. Water-agar mixed with *E.coli* was then overlayed on each plate. The *E. coli* was either wt K12 (to which phaseolotoxin is lethal) or phaseolotoxin-resistant. Optionally, phaseolotoxin sensitivity could be rescued by adding citrulline to the overlay (see chapter 2: Materials and Methods for more detail). Phaseolotoxin only causes an inhibition halo at permissive temperature 21°C, in the absence of citrulline, by strains capable of production, as exemplified by 1448A. There is a faint halo surrounding 1302A but it is not diminished at 28C° or by citrulline rescue, and it is also displayed by the phaseolotoxin-resistant *E. coli*, suggesting that the faint halo is not caused by phaseolotoxin but some other inhibitory factor. This means that 1302A does not produce detectable levels of phaseolotoxin *in vitro*. Photos are representative of n=3 replicates and N=2 repeat experiments.

Supplementary table S1
GO term enrichment analysis (GOTEA) of the transcriptomic data for strain Pspph 1302A. A Fisher and a Kolmogorov-Smirnov test were performed to identify GO terms significantly enriched among transcriptionally responsive genes to treatment (P-value < 0.05).

GO.ID	Annotated	Significant	Expected	weight_ks	weight_fisher	weight_ks (adjusted)	weight_fisher (adjusted)	treatment
GO:0051539	18	3	1.01	0.078	0.075	0.784	1.000	h2o2effectsat21C
GO:1901607	55	7	3.01	0.004	0.014	0.284	1.000	h2o2effectsat21C
GO:1901607	55	6	3.17	0.003	0.314	0.218	1.000	h2o2effectsat28C
GO:1901606	16	5	0.88	0.017	0.197	0.530	1.000	h2o2effectsat21C
GO:1901606	16	4	0.92	0.028	0.208	0.571	1.000	h2o2effectsat28C
GO:1901606	16	3	0.91	0.018	1.000	1.000	1.000	temperatureeffectsinwater
GO:1901605	81	9	4.66	0.069	1.000	0.739	1.000	h2o2effectsat28C
GO:0009063	19	6	1.04	0.003	0.049	0.246	1.000	h2o2effectsat21C
GO:0009063	19	5	1.09	0.004	0.055	0.218	1.000	h2o2effectsat28C
GO:0009063	19	4	1.08	0.027	0.330	1.000	1.000	temperatureeffectsinwater
GO:0006520	141	15	7.73	0.009	0.804	0.503	1.000	h2o2effectsat21C
GO:0015171	19	2	0.98	0.003	0.411	0.156	1.000	temperatureeffectsinwater
GO:0006040	5	1	0.27	0.031	0.246	0.644	1.000	h2o2effectsat21C
GO:0006040	5	1	0.26	0.078	0.236	0.990	1.000	interactionterm
GO:0006040	5	1	0.24	0.023	0.215	0.542	1.000	temperatureeffectsin20mMh2O2
GO:0002161	7	1	0.39	0.084	0.332	0.784	1.000	h2o2effectsat21C
GO:0006526	8	1	0.38	0.009	0.322	0.387	1.000	temperatureeffectsin20mMh2O2
GO:0006526	8	1	0.45	0.034	0.374	1.000	1.000	temperatureeffectsinwater
GO:0009072	17	1	0.93	0.094	1.000	0.912	1.000	h2o2effectsat21C

GO:0009072	17	1	0.96	0.024	1.000	1.000	1.000	temperatureeffectsinwater
GO:0019439	25	2	1.37	0.087	0.402	0.912	1.000	h2o2effectsat21C
GO:0019439	25	2	1.44	0.094	0.427	0.797	1.000	h2o2effectsat28C
GO:0009066	17	2	0.96	0.052	0.057	1.000	1.000	temperatureeffectsinwater
GO:0140662	7	2	0.39	0.042	0.054	0.705	1.000	h2o2effectsat21C
GO:0140662	7	1	0.4	0.080	0.338	0.778	1.000	h2o2effectsat28C
GO:0140662	7	2	0.36	0.091	0.047	0.696	1.000	temperatureeffectsinwater
GO:0044780	9	1	0.49	0.012	0.398	0.504	1.000	h2o2effectsat21C
GO:0044780	9	2	0.52	0.004	0.091	0.218	1.000	h2o2effectsat28C
GO:0044780	9	2	0.47	0.059	0.077	0.990	1.000	interactionterm
GO:0044780	9	3	0.43	0.001	0.007	0.288	0.634	temperatureeffectsin20mMh2O2
GO:0009425	11	4	0.57	0.006	0.259	0.062	1.000	h2o2effectsat28C
GO:0009425	10	5	0.42	0.000	0.001	0.000	0.025	interactionterm
GO:0009425	10	4	0.38	0.000	0.012	0.017	0.312	temperatureeffectsin20mMh2O2
GO:0030694	5	1	0.23	0.013	0.210	0.104	1.000	h2o2effectsat21C
GO:0030694	5	3	0.26	0.003	0.001	0.041	0.058	h2o2effectsat28C
GO:0030694	5	2	0.21	0.025	0.016	0.423	0.365	interactionterm
GO:0071973	19	3	1.04	0.044	0.082	0.712	1.000	h2o2effectsat21C
GO:0071973	18	7	1.04	0.000	0.000	0.014	0.009	h2o2effectsat28C
GO:0071973	17	7	0.89	0.000	0.000	0.059	0.006	interactionterm
GO:0071973	17	6	0.8	0.007	0.000	0.387	0.042	temperatureeffectsin20mMh2O2
GO:0005488	1122	53	52.06	0.009	1.000	0.541	1.000	interactionterm
GO:0005488	1167	56	52.18	0.001	0.542	0.153	1.000	temperatureeffectsin20mMh2O2

GO:0042401	11	2	0.6	0.023	1.000	0.530	1.000	h2o2effectsat21C
GO:0042401	11	2	0.63	0.021	1.000	0.465	1.000	h2o2effectsat28C
GO:0009082	9	3	0.49	0.066	0.011	0.834	1.000	h2o2effectsat21C
GO:0009082	9	2	0.52	0.095	0.091	0.797	1.000	h2o2effectsat28C
GO:0005509	6	1	0.27	0.013	0.240	0.419	1.000	temperatureeffectsin20mMh2O2
GO:0016051	29	2	1.37	0.002	0.403	0.387	1.000	temperatureeffectsin20mMh2O2
GO:0097367	356	21	20.32	0.014	0.232	0.568	1.000	h2o2effectsat28C
GO:0034219	7	2	0.38	0.041	0.052	0.712	1.000	h2o2effectsat21C
GO:0008643	13	1	0.75	0.063	1.000	0.719	1.000	h2o2effectsat28C
GO:0008643	13	1	0.74	0.046	1.000	1.000	1.000	temperatureeffectsinwater
GO:0019752	226	17	13.01	0.058	1.000	0.719	1.000	h2o2effectsat28C
GO:0046942	36	2	1.7	0.052	0.355	0.702	1.000	temperatureeffectsin20mMh2O2
GO:0046942	36	3	2.04	0.087	0.253	1.000	1.000	temperatureeffectsinwater
GO:0016831	15	1	0.67	0.000	0.497	0.048	1.000	temperatureeffectsin20mMh2O2
GO:0016831	15	2	0.77	0.002	0.180	0.128	1.000	temperatureeffectsinwater
GO:0004096	5	3	0.28	0.028	0.002	0.705	0.320	h2o2effectsat21C
GO:0004096	5	3	0.29	0.032	0.002	0.755	0.267	h2o2effectsat28C
GO:0004096	5	3	0.23	0.032	0.001	0.837	0.142	interactionterm
GO:0004096	5	3	0.22	0.034	0.001	0.536	0.087	temperatureeffectsin20mMh2O2
GO:0022402	7	1	0.33	0.040	0.288	0.651	1.000	temperatureeffectsin20mMh2O2
GO:0009279	17	2	0.81	0.013	0.194	0.127	1.000	temperatureeffectsinwater
GO:0044036	11	1	0.58	0.007	0.448	0.363	1.000	interactionterm
GO:0044036	11	1	0.52	0.009	0.414	0.387	1.000	temperatureeffectsin20mMh2O2

GO:0006081	8	1	0.45	0.068	0.374	1.000	1.000	temperatureeffectsinwater
GO:0110165	788	34	32.79	0.077	1.000	0.682	1.000	interactionterm
GO:0044248	70	10	3.84	0.024	0.383	0.530	1.000	h2o2effectsat21C
GO:0044248	70	8	4.03	0.011	0.527	0.361	1.000	h2o2effectsat28C
GO:0022607	48	7	2.27	0.012	1.000	0.421	1.000	temperatureeffectsin20mMh2O2
GO:0019725	9	1	0.51	0.092	1.000	1.000	1.000	temperatureeffectsinwater
GO:0044255	57	3	2.99	0.052	0.802	0.980	1.000	interactionterm
GO:0009987	1811	106	104.24	0.065	1.000	0.719	1.000	h2o2effectsat28C
GO:0051716	255	15	14.68	0.016	0.112	0.417	1.000	h2o2effectsat28C
GO:0015267	22	2	0.98	0.083	0.306	0.674	1.000	temperatureeffectsin20mMh2O2
GO:0015267	22	4	1.14	0.029	0.341	0.371	1.000	temperatureeffectsinwater
GO:0006935	57	8	3.28	0.056	0.015	0.719	1.000	h2o2effectsat28C
GO:0006935	56	11	2.94	0.000	0.000	0.078	0.018	interactionterm
GO:0006935	56	10	2.65	0.019	0.000	0.542	0.057	temperatureeffectsin20mMh2O2
GO:0006935	57	7	3.23	0.075	0.039	1.000	1.000	temperatureeffectsinwater
GO:0003774	8	3	0.46	0.002	0.008	0.182	0.528	h2o2effectsat28C
GO:0003774	7	5	0.32	0.001	0.000	0.114	0.001	interactionterm
GO:0003774	7	4	0.31	0.003	0.000	0.216	0.038	temperatureeffectsin20mMh2O2
GO:0005829	6	1	0.28	0.013	0.250	0.104	1.000	h2o2effectsat21C
GO:0005829	6	1	0.31	0.044	0.273	0.263	1.000	h2o2effectsat28C
GO:0005829	6	1	0.29	0.026	0.256	0.211	1.000	temperatureeffectsinwater
GO:0098754	5	2	0.27	0.008	0.027	0.490	1.000	h2o2effectsat21C
GO:0098754	5	3	0.29	0.000	0.002	0.109	0.313	h2o2effectsat28C

GO:0098754	5	1	0.26	0.033	0.236	0.803	1.000	interactionterm
GO:0015074	25	3	1.31	0.083	0.140	0.990	1.000	interactionterm
GO:0003899	6	1	0.34	0.033	0.297	0.755	1.000	h2o2effectsat28C
GO:0006352	15	3	0.86	0.032	0.051	0.626	1.000	h2o2effectsat28C
GO:0006352	15	1	0.71	0.082	0.518	0.839	1.000	temperatureeffectsin20mMh2O2
GO:0004175	32	2	1.83	0.078	1.000	0.778	1.000	h2o2effectsat28C
GO:0051649	9	1	0.51	0.029	0.409	1.000	1.000	temperatureeffectsinwater
GO:0008238	17	1	0.79	0.019	1.000	0.657	1.000	interactionterm
GO:0008238	17	2	0.88	0.087	1.000	0.696	1.000	temperatureeffectsinwater
GO:0140352	54	5	3.11	0.005	0.111	0.218	1.000	h2o2effectsat28C
GO:0140352	34	2	1.78	0.003	0.103	0.264	1.000	interactionterm
GO:0005576	9	1	0.35	0.010	1.000	0.194	1.000	temperatureeffectsin20mMh2O2
GO:0005615	6	1	0.23	0.072	0.210	0.397	1.000	temperatureeffectsin20mMh2O2
GO:0006633	21	2	1.1	0.060	0.303	0.990	1.000	interactionterm
GO:0006631	28	2	1.61	0.004	1.000	0.218	1.000	h2o2effectsat28C
GO:0006006	7	2	0.33	0.003	0.040	0.387	1.000	temperatureeffectsin20mMh2O2
GO:0006006	7	1	0.4	0.039	0.336	1.000	1.000	temperatureeffectsinwater
GO:0006536	6	2	0.33	0.066	0.039	0.834	1.000	h2o2effectsat21C
GO:0006536	6	1	0.35	0.015	0.300	0.417	1.000	h2o2effectsat28C
GO:0004356	5	1	0.22	0.030	0.205	0.536	1.000	temperatureeffectsin20mMh2O2
GO:0006542	5	1	0.24	0.037	0.215	0.632	1.000	temperatureeffectsin20mMh2O2
GO:0009065	7	2	0.38	0.002	0.052	0.241	1.000	h2o2effectsat21C
GO:0009065	7	1	0.4	0.009	0.340	0.322	1.000	h2o2effectsat28C

GO:0006546	5	2	0.27	0.020	0.027	0.530	1.000	h2o2effectsat21C
GO:0006546	5	2	0.28	0.004	0.028	0.364	1.000	temperatureeffectsinwater
GO:0006544	8	2	0.46	0.062	1.000	0.719	1.000	h2o2effectsat28C
GO:0006096	8	1	0.38	0.006	0.322	0.387	1.000	temperatureeffectsin20mMh2O2
GO:0006096	8	1	0.45	0.020	0.374	1.000	1.000	temperatureeffectsinwater
GO:0005525	20	2	1.14	0.065	0.318	0.778	1.000	h2o2effectsat28C
GO:0003924	14	3	0.78	0.030	0.040	0.705	0.887	h2o2effectsat21C
GO:0003924	14	2	0.8	0.062	0.188	0.778	1.000	h2o2effectsat28C
GO:0000105	10	2	0.58	0.061	0.109	0.719	1.000	h2o2effectsat28C
GO:0000105	10	3	0.57	0.033	0.016	1.000	1.000	temperatureeffectsinwater
GO:0016798	31	5	1.44	0.053	1.000	0.871	1.000	interactionterm
GO:0016798	31	3	1.39	0.031	0.393	0.536	1.000	temperatureeffectsin20mMh2O2
GO:0004553	21	4	1.17	0.052	0.027	0.705	0.887	h2o2effectsat21C
GO:0004553	20	2	0.89	0.063	0.224	0.600	1.000	temperatureeffectsin20mMh2O2
GO:0016836	34	3	1.9	0.000	0.296	0.023	1.000	h2o2effectsat21C
GO:0016836	34	2	1.94	0.002	0.587	0.182	1.000	h2o2effectsat28C
GO:0098661	7	1	0.4	0.016	0.340	0.417	1.000	h2o2effectsat28C
GO:0098661	7	2	0.37	0.002	0.048	0.219	1.000	interactionterm
GO:0098661	7	2	0.33	0.002	0.040	0.387	1.000	temperatureeffectsin20mMh2O2
GO:0022890	41	6	2.12	0.094	0.098	0.702	1.000	temperatureeffectsinwater
GO:0005622	172	11	8.25	0.004	0.007	0.054	0.166	temperatureeffectsinwater
GO:0055082	6	1	0.34	0.095	1.000	1.000	1.000	temperatureeffectsinwater
GO:0006886	9	2	0.49	0.046	1.000	0.712	1.000	h2o2effectsat21C

GO:0006826	27	4	1.53	0.058	0.404	1.000	1.000	temperatureeffectsinwater
GO:0016226	10	2	0.52	0.012	0.093	0.502	1.000	interactionterm
GO:0016226	10	4	0.47	0.071	0.001	0.812	0.145	temperatureeffectsin20mMh2O2
GO:0015934	7	1	0.32	0.000	0.280	0.008	1.000	h2o2effectsat21C
GO:0015934	7	1	0.36	0.001	0.310	0.022	1.000	h2o2effectsat28C
GO:0016879	37	2	1.65	0.008	0.758	0.384	1.000	temperatureeffectsin20mMh2O2
GO:0016879	37	2	1.91	0.073	1.000	0.646	1.000	temperatureeffectsinwater
GO:0009057	23	2	1.21	0.021	1.000	0.589	1.000	interactionterm
GO:0046872	133	11	7.44	0.066	0.176	0.709	1.000	h2o2effectsat21C
GO:0004222	12	1	0.67	0.057	0.499	0.705	1.000	h2o2effectsat21C
GO:0008235	8	1	0.46	0.070	0.375	0.778	1.000	h2o2effectsat28C
GO:0008235	8	2	0.41	0.033	0.060	0.391	1.000	temperatureeffectsinwater
GO:0140104	5	2	0.23	0.053	0.019	0.871	0.757	interactionterm
GO:0140104	5	2	0.22	0.008	0.018	0.384	1.000	temperatureeffectsin20mMh2O2
GO:0098772	7	1	0.31	0.048	0.274	0.600	1.000	temperatureeffectsin20mMh2O2
GO:0022839	7	1	0.31	0.038	0.274	0.545	1.000	temperatureeffectsin20mMh2O2
GO:0022839	7	1	0.36	0.028	0.311	0.371	1.000	temperatureeffectsinwater
GO:0072329	12	1	0.66	0.023	0.492	0.530	1.000	h2o2effectsat21C
GO:0072329	12	1	0.69	0.014	0.510	0.417	1.000	h2o2effectsat28C
GO:0032787	68	4	3.73	0.064	0.323	0.834	1.000	h2o2effectsat21C
GO:0032787	68	6	3.91	0.008	0.116	0.322	1.000	h2o2effectsat28C
GO:0004497	14	4	0.8	0.057	0.007	0.778	0.520	h2o2effectsat28C
GO:0004497	12	1	0.56	0.047	0.435	0.853	1.000	interactionterm

GO:0016071	7	1	0.37	0.048	0.315	0.953	1.000	interactionterm
GO:0051287	36	3	1.61	0.046	0.216	0.600	1.000	temperatureeffectsin20mMh2O2
GO:0019184	7	2	0.33	0.007	0.040	0.387	1.000	temperatureeffectsin20mMh2O2
GO:0019184	7	1	0.4	0.084	0.336	1.000	1.000	temperatureeffectsinwater
GO:0047429	7	1	0.32	0.098	0.283	1.000	1.000	interactionterm
GO:0009225	7	1	0.33	0.014	0.288	0.472	1.000	temperatureeffectsin20mMh2O2
GO:0016779	40	2	1.79	0.066	0.789	0.600	1.000	temperatureeffectsin20mMh2O2
GO:0006082	231	17	13.3	0.027	1.000	0.571	1.000	h2o2effectsat28C
GO:1901575	98	10	5.37	0.024	0.679	0.530	1.000	h2o2effectsat21C
GO:1901575	98	9	5.64	0.009	0.703	0.322	1.000	h2o2effectsat28C
GO:0019867	42	4	2.01	0.059	0.327	0.325	1.000	temperatureeffectsinwater
GO:0016705	21	4	1.2	0.006	0.028	0.356	1.000	h2o2effectsat28C
GO:0016702	7	1	0.39	0.038	0.332	0.705	1.000	h2o2effectsat21C
GO:0016620	25	6	1.4	0.000	0.002	0.023	0.320	h2o2effectsat21C
GO:0016903	28	7	1.57	0.096	0.154	0.808	1.000	h2o2effectsat21C
GO:0016620	25	7	1.43	0.000	0.000	0.019	0.109	h2o2effectsat28C
GO:0016638	7	3	0.39	0.050	0.005	0.705	0.384	h2o2effectsat21C
GO:0016638	7	2	0.4	0.049	0.056	0.778	1.000	h2o2effectsat28C
GO:0043436	228	17	12.49	0.025	1.000	0.530	1.000	h2o2effectsat21C
GO:0003755	13	1	0.58	0.027	0.449	0.530	1.000	temperatureeffectsin20mMh2O2
GO:0003755	13	4	0.67	0.016	0.003	0.304	0.469	temperatureeffectsinwater
GO:0004601	15	2	0.77	0.014	0.410	0.304	1.000	temperatureeffectsinwater
GO:0031177	7	1	0.31	0.064	0.274	0.600	1.000	temperatureeffectsin20mMh2O2

GO:0031177	7	1	0.36	0.021	0.311	0.354	1.000	temperatureeffectsinwater
GO:0016773	98	6	5.48	0.056	0.432	0.705	1.000	h2o2effectsat21C
GO:0098797	72	4	3.45	0.061	1.000	0.325	1.000	temperatureeffectsinwater
GO:0006596	7	2	0.4	0.048	0.057	0.719	1.000	h2o2effectsat28C
GO:0006596	7	1	0.33	0.005	0.288	0.387	1.000	temperatureeffectsin20mMh2O2
GO:0006596	7	2	0.4	0.004	0.056	0.364	1.000	temperatureeffectsinwater
GO:0034308	6	2	0.34	0.006	0.056	0.480	1.000	temperatureeffectsinwater
GO:0005515	136	9	6.31	0.023	0.774	0.725	1.000	interactionterm
GO:0046983	9	1	0.46	0.037	0.380	0.426	1.000	temperatureeffectsinwater
GO:0006457	24	5	1.36	0.001	0.010	0.182	1.000	temperatureeffectsinwater
GO:0044183	8	3	0.41	0.009	0.051	0.259	1.000	temperatureeffectsinwater
GO:0008320	5	1	0.28	0.034	0.250	0.705	1.000	h2o2effectsat21C
GO:0008320	5	1	0.29	0.046	0.255	0.778	1.000	h2o2effectsat28C
GO:0065003	12	1	0.63	0.014	0.477	0.502	1.000	interactionterm
GO:0015986	8	4	0.45	0.000	0.001	0.063	0.317	temperatureeffectsinwater
GO:0015078	16	4	0.83	0.004	0.105	0.156	1.000	temperatureeffectsinwater
GO:0046933	5	2	0.26	0.001	0.024	0.074	0.956	temperatureeffectsinwater
GO:0045259	7	3	0.34	0.000	0.003	0.008	0.149	temperatureeffectsinwater
GO:0034032	9	1	0.52	0.090	0.414	0.797	1.000	h2o2effectsat28C
GO:0009168	11	1	0.6	0.022	1.000	0.530	1.000	h2o2effectsat21C
GO:0030170	45	4	2.57	0.035	0.253	0.755	1.000	h2o2effectsat28C
GO:0072593	5	2	0.27	0.063	0.027	0.834	1.000	h2o2effectsat21C
GO:0072593	5	2	0.29	0.098	0.029	0.797	1.000	h2o2effectsat28C

GO:0010468	292	14	13.82	0.086	0.356	0.843	1.000	temperatureeffectsin20mMh2O2
GO:0060255	291	16	15.27	0.019	1.000	0.571	1.000	interactionterm
GO:0019219	279	15	14.64	0.005	1.000	0.325	1.000	interactionterm
GO:0022904	9	1	0.52	0.038	0.414	0.640	1.000	h2o2effectsat28C
GO:0009605	67	13	3.52	0.080	1.000	0.990	1.000	interactionterm
GO:0031667	5	1	0.27	0.089	0.246	0.912	1.000	h2o2effectsat21C
GO:0006979	13	7	0.71	0.001	0.000	0.129	0.001	h2o2effectsat21C
GO:0006979	13	7	0.75	0.001	0.000	0.109	0.001	h2o2effectsat28C
GO:0006979	13	5	0.68	0.003	0.000	0.264	0.044	interactionterm
GO:0006979	13	4	0.62	0.087	0.002	0.843	0.330	temperatureeffectsin20mMh2O2
GO:1901700	5	1	0.26	0.046	0.236	0.937	1.000	interactionterm
GO:0043021	5	2	0.26	0.028	0.024	0.371	0.956	temperatureeffectsinwater
GO:0033875	9	1	0.52	0.090	0.414	0.797	1.000	h2o2effectsat28C
GO:0005840	52	4	2.39	0.000	0.260	0.010	1.000	h2o2effectsat21C
GO:0005840	52	5	2.49	0.000	0.108	0.000	1.000	temperatureeffectsinwater
GO:0019843	6	1	0.31	0.000	0.273	0.016	1.000	temperatureeffectsinwater
GO:0008115	5	2	0.28	0.052	0.028	0.705	0.887	h2o2effectsat21C
GO:0008115	5	1	0.26	0.012	0.233	0.304	1.000	temperatureeffectsinwater
GO:0019748	7	1	0.4	0.072	1.000	0.741	1.000	h2o2effectsat28C
GO:0019748	7	3	0.33	0.030	0.091	0.576	1.000	temperatureeffectsin20mMh2O2
GO:0044550	5	1	0.27	0.082	0.246	0.912	1.000	h2o2effectsat21C
GO:0044550	5	2	0.24	0.052	0.020	0.702	1.000	temperatureeffectsin20mMh2O2
GO:0015343	12	2	0.62	0.030	0.125	0.371	1.000	temperatureeffectsinwater

GO:0016987	14	3	0.8	0.023	0.042	0.755	1.000	h2o2effectsat28C
GO:0016987	14	1	0.63	0.092	0.474	0.692	1.000	temperatureeffectsin20mMh2O2
GO:0007165	191	15	10.02	0.008	0.009	0.389	0.762	interactionterm
GO:0007165	194	13	11	0.012	0.040	0.830	1.000	temperatureeffectsinwater
GO:0038023	42	5	1.95	0.098	1.000	1.000	1.000	interactionterm
GO:0038023	42	8	2.17	0.029	0.118	0.371	1.000	temperatureeffectsinwater
GO:0036094	516	31	29.45	0.074	0.531	0.778	1.000	h2o2effectsat28C
GO:0044283	172	11	9.75	0.050	0.556	1.000	1.000	temperatureeffectsinwater
GO:0044281	385	26	21.83	0.100	1.000	1.000	1.000	temperatureeffectsinwater
GO:0015935	6	1	0.23	0.015	0.210	0.194	1.000	temperatureeffectsin20mMh2O2
GO:0015081	5	1	0.26	0.024	0.233	0.371	1.000	temperatureeffectsinwater
GO:0030527	5	1	0.29	0.077	0.255	0.778	1.000	h2o2effectsat28C
GO:0030527	5	1	0.23	0.093	0.212	1.000	1.000	interactionterm
GO:0030527	5	3	0.22	0.001	0.001	0.153	0.087	temperatureeffectsin20mMh2O2
GO:0030527	5	1	0.26	0.048	0.233	0.480	1.000	temperatureeffectsinwater
GO:0003735	52	4	2.91	0.000	0.331	0.007	1.000	h2o2effectsat21C
GO:0003735	52	5	2.69	0.000	0.128	0.000	1.000	temperatureeffectsinwater
GO:0008272	5	1	0.29	0.001	0.257	0.122	1.000	h2o2effectsat28C
GO:0008272	5	4	0.26	0.001	0.000	0.119	0.009	interactionterm
GO:0008272	5	2	0.24	0.021	0.020	0.542	1.000	temperatureeffectsin20mMh2O2
GO:0000097	13	1	0.75	0.059	1.000	0.719	1.000	h2o2effectsat28C
GO:0006790	49	4	2.57	0.033	0.474	0.803	1.000	interactionterm
GO:0015293	9	2	0.46	0.084	0.146	0.696	1.000	temperatureeffectsinwater

GO:0046653	9	1	0.52	0.062	0.414	0.719	1.000	h2o2effectsat28C
GO:0008483	23	4	1.31	0.074	0.039	0.778	1.000	h2o2effectsat28C
GO:0008483	22	1	0.98	0.023	0.636	0.519	1.000	temperatureeffectsin20mMh2O2
GO:0008483	22	5	1.14	0.090	0.004	0.696	0.469	temperatureeffectsinwater
GO:0008134	20	5	0.93	0.091	0.002	1.000	0.180	interactionterm
GO:0008134	20	5	0.89	0.064	0.001	0.600	0.117	temperatureeffectsin20mMh2O2
GO:0006412	90	6	4.93	0.000	0.371	0.009	1.000	h2o2effectsat21C
GO:0006412	90	6	5.1	0.000	0.403	0.000	1.000	temperatureeffectsinwater
GO:0008135	11	2	0.62	0.067	0.123	0.709	1.000	h2o2effectsat21C
GO:0008135	11	1	0.57	0.047	0.443	0.480	1.000	temperatureeffectsinwater
GO:0004888	30	5	1.39	0.003	0.011	0.249	0.740	interactionterm
GO:0004888	30	4	1.34	0.062	0.042	0.600	1.000	temperatureeffectsin20mMh2O2
GO:0004888	30	6	1.55	0.004	0.004	0.156	0.469	temperatureeffectsinwater
GO:1902495	61	4	2.54	0.059	0.118	0.682	1.000	interactionterm
GO:1902495	72	4	3.45	0.039	1.000	0.267	1.000	temperatureeffectsinwater
GO:0008033	35	2	1.84	0.097	0.478	1.000	1.000	interactionterm
GO:0051082	10	1	0.52	0.006	0.412	0.192	1.000	temperatureeffectsinwater
GO:0042908	6	2	0.35	0.017	0.042	0.417	1.000	h2o2effectsat28C

Supplementary table S2
GO term enrichment analysis (GOTEA) of the transcriptomic data for strain Pss B728a. A Fisher and a Kolmogorov-Smirnov test were performed to identify GO terms significantly enriched among transcriptionally responsive genes to treatment (P-value < 0.05).

GO.ID	Annotated	Significant	Expected	weight_ks	weight_fisher	weight_ks (adjusted)	weight_fisher (adjusted)	treatment
GO:0000902	8	2	0.43	0.007	0.064	0.478	1.000	temperatureeffectsin80mMh2O2
GO:0000902	8	1	0.42	0.002	0.353	0.543	1.000	interactionterm
GO:0003676	444	27	19.14	0.044	0.892	0.540	1.000	h2o2effectsat21C
GO:0003723	69	6	2.97	0.032	0.074	0.525	1.000	h2o2effectsat21C
GO:0003723	69	7	3.47	0.000	0.378	0.066	1.000	temperatureeffectsin80mMh2O2
GO:0003735	53	8	2.28	0.000	0.002	0.000	0.517	h2o2effectsat21C
GO:0003735	53	14	2.48	0.000	0.000	0.000	0.000	temperatureeffectsinwater
GO:0003735	53	16	2.67	0.000	0.000	0.000	0.000	temperatureeffectsin80mMh2O2
GO:0003755	13	1	0.68	0.025	0.504	0.499	1.000	h2o2effectsat28C
GO:0003755	13	1	0.61	0.014	0.465	0.321	1.000	temperatureeffectsinwater
GO:0003755	13	3	0.65	0.094	0.025	0.988	1.000	temperatureeffectsin80mMh2O2
GO:0003774	8	4	0.42	0.013	0.000	0.499	0.139	h2o2effectsat28C
GO:0003774	8	1	0.4	0.027	0.339	0.876	1.000	temperatureeffectsin80mMh2O2
GO:0003774	8	4	0.42	0.012	0.000	0.584	0.138	interactionterm
GO:0003899	6	1	0.26	0.017	0.233	0.428	1.000	h2o2effectsat21C
GO:0003924	15	2	0.65	0.024	0.134	0.452	1.000	h2o2effectsat21C
GO:0004096	5	2	0.22	0.006	0.017	0.422	0.910	h2o2effectsat21C
GO:0004096	5	2	0.26	0.023	0.025	0.499	1.000	h2o2effectsat28C
GO:0004175	33	3	1.73	0.009	0.193	0.499	1.000	h2o2effectsat28C

GO:0004252	15	6	0.7	0.011	0.000	0.310	0.003	temperatureeffectsinwater
GO:0004497	13	3	0.56	0.058	0.016	0.540	0.910	h2o2effectsat21C
GO:0004497	13	2	0.68	0.044	0.146	0.549	1.000	h2o2effectsat28C
GO:0004497	12	4	0.56	0.086	0.002	0.779	0.134	temperatureeffectsinwater
GO:0004519	11	2	0.47	0.046	0.079	0.540	1.000	h2o2effectsat21C
GO:0004888	32	4	1.68	0.069	0.083	0.586	1.000	h2o2effectsat28C
GO:0004888	32	3	1.68	0.002	0.235	0.268	1.000	interactionterm
GO:0005198	63	10	2.72	0.021	0.188	0.452	1.000	h2o2effectsat21C
GO:0005509	11	2	0.52	0.025	0.091	0.431	1.000	temperatureeffectsinwater
GO:0005525	20	2	0.86	0.075	0.212	0.540	1.000	h2o2effectsat21C
GO:0005576	11	1	0.5	0.059	0.399	0.236	1.000	h2o2effectsat21C
GO:0005576	11	1	0.59	0.065	0.455	0.389	1.000	temperatureeffectsin80mMh2O2
GO:0005615	7	2	0.43	0.071	0.063	0.415	0.565	temperatureeffectsinwater
GO:0005622	175	14	10.67	0.001	1.000	0.005	1.000	temperatureeffectsinwater
GO:0005622	178	18	9.51	0.028	0.330	0.270	1.000	temperatureeffectsin80mMh2O2
GO:0005737	108	7	5.09	0.067	0.673	0.384	1.000	h2o2effectsat28C
GO:0005829	7	3	0.33	0.082	0.003	0.384	0.072	h2o2effectsat28C
GO:0005829	7	2	0.38	0.021	0.051	0.253	0.612	interactionterm
GO:0005840	53	8	2.39	0.000	0.078	0.000	0.752	h2o2effectsat21C
GO:0005840	53	14	3.23	0.000	0.000	0.000	0.000	temperatureeffectsinwater
GO:0005840	53	16	2.83	0.000	0.000	0.000	0.000	temperatureeffectsin80mMh2O2
GO:0006006	8	2	0.37	0.036	0.050	0.980	1.000	temperatureeffectsinwater
GO:0006006	8	3	0.43	0.015	0.007	0.623	1.000	temperatureeffectsin80mMh2O2

GO:0006040	5	1	0.24	0.025	0.221	0.668	1.000	h2o2effectsat21C
GO:0006090	12	2	0.64	0.062	1.000	0.970	1.000	temperatureeffectsin80mMh2O2
GO:0006096	9	1	0.44	0.051	0.362	0.825	1.000	h2o2effectsat21C
GO:0006096	9	2	0.48	0.008	0.080	0.478	1.000	temperatureeffectsin80mMh2O2
GO:0006099	16	1	0.89	0.014	0.602	0.499	1.000	h2o2effectsat28C
GO:0006119	6	1	0.33	0.013	0.291	0.499	1.000	h2o2effectsat28C
GO:0006188	9	3	0.48	0.080	1.000	1.000	1.000	temperatureeffectsin80mMh2O2
GO:0006188	9	2	0.48	0.078	1.000	1.000	1.000	interactionterm
GO:0006189	8	3	0.43	0.060	0.007	0.970	1.000	temperatureeffectsin80mMh2O2
GO:0006189	8	2	0.42	0.099	0.063	1.000	1.000	interactionterm
GO:0006351	308	17	14.96	0.038	0.255	0.766	1.000	h2o2effectsat21C
GO:0006351	308	21	17.16	0.088	1.000	0.994	1.000	h2o2effectsat28C
GO:0006396	66	4	3.68	0.014	0.498	0.499	1.000	h2o2effectsat28C
GO:0006412	92	10	4.47	0.000	0.012	0.000	1.000	h2o2effectsat21C
GO:0006412	92	14	4.27	0.000	0.000	0.000	0.029	temperatureeffectsinwater
GO:0006412	92	17	4.92	0.000	0.000	0.000	0.004	temperatureeffectsin80mMh2O2
GO:0006414	6	1	0.32	0.064	0.281	0.970	1.000	temperatureeffectsin80mMh2O2
GO:0006457	25	2	1.39	0.024	0.410	0.625	1.000	h2o2effectsat28C
GO:0006457	21	3	0.97	0.005	0.070	0.427	1.000	temperatureeffectsinwater
GO:0006508	60	5	3.34	0.002	0.240	0.298	1.000	h2o2effectsat28C
GO:0006508	60	8	2.78	0.034	0.006	0.980	1.000	temperatureeffectsinwater
GO:0006508	60	4	3.17	0.072	0.392	1.000	1.000	interactionterm
GO:0006520	152	10	7.38	0.005	1.000	0.347	1.000	h2o2effectsat21C

GO:0006526	8	1	0.43	0.028	0.356	0.776	1.000	temperatureeffectsin80mMh2O2
GO:0006536	6	1	0.33	0.030	0.291	0.700	1.000	h2o2effectsat28C
GO:0006541	7	1	0.39	0.071	0.331	0.943	1.000	h2o2effectsat28C
GO:0006541	7	2	0.37	0.017	0.104	0.623	1.000	temperatureeffectsin80mMh2O2
GO:0006541	7	1	0.37	0.031	0.316	0.820	1.000	interactionterm
GO:0006546	5	1	0.28	0.002	0.249	0.301	1.000	h2o2effectsat28C
GO:0006568	5	2	0.24	0.021	0.021	0.640	1.000	h2o2effectsat21C
GO:0006568	5	2	0.28	0.096	0.028	1.000	1.000	h2o2effectsat28C
GO:0006596	7	2	0.32	0.039	0.038	1.000	1.000	temperatureeffectsinwater
GO:0006596	7	1	0.37	0.057	0.320	0.970	1.000	temperatureeffectsin80mMh2O2
GO:0006605	7	2	0.34	0.073	0.042	0.873	1.000	h2o2effectsat21C
GO:0006605	7	2	0.39	0.061	0.054	0.943	1.000	h2o2effectsat28C
GO:0006605	7	1	0.37	0.081	0.320	1.000	1.000	temperatureeffectsin80mMh2O2
GO:0006886	9	2	0.44	0.028	1.000	0.690	1.000	h2o2effectsat21C
GO:0006886	9	2	0.48	0.059	0.104	0.970	1.000	temperatureeffectsin80mMh2O2
GO:0006935	61	6	3.4	0.085	0.120	0.994	1.000	h2o2effectsat28C
GO:0006935	61	8	3.22	0.003	0.013	0.543	1.000	interactionterm
GO:0006974	58	4	3.23	0.074	0.331	0.943	1.000	h2o2effectsat28C
GO:0006974	57	3	2.64	0.087	0.039	1.000	1.000	temperatureeffectsinwater
GO:0006979	13	5	0.63	0.011	0.000	0.522	0.130	h2o2effectsat21C
GO:0006979	13	6	0.72	0.003	0.000	0.301	0.009	h2o2effectsat28C
GO:0007165	201	11	10.62	0.012	0.149	0.543	1.000	interactionterm
GO:0008135	11	2	0.47	0.071	0.079	0.540	1.000	h2o2effectsat21C

GO:0008186	5	1	0.23	0.014	0.214	0.321	1.000	temperatureeffectsinwater
GO:0008186	5	1	0.25	0.087	0.228	0.988	1.000	temperatureeffectsin80mMh2O2
GO:0008199	7	1	0.37	0.038	0.314	0.545	1.000	h2o2effectsat28C
GO:0008233	75	8	3.52	0.046	1.000	0.516	1.000	temperatureeffectsinwater
GO:0008235	8	1	0.42	0.042	0.350	0.549	1.000	h2o2effectsat28C
GO:0008236	24	6	1.13	0.079	1.000	0.760	1.000	temperatureeffectsinwater
GO:0008236	24	3	1.21	0.052	0.185	0.876	1.000	temperatureeffectsin80mMh2O2
GO:0008237	34	2	1.59	0.028	1.000	0.431	1.000	temperatureeffectsinwater
GO:0008238	16	1	0.84	0.068	1.000	0.842	1.000	interactionterm
GO:0008270	37	2	1.59	0.042	0.479	0.540	1.000	h2o2effectsat21C
GO:0008270	37	4	1.94	0.025	0.126	0.499	1.000	h2o2effectsat28C
GO:0008272	5	1	0.28	0.071	0.249	0.943	1.000	h2o2effectsat28C
GO:0008272	5	1	0.23	0.006	0.212	0.427	1.000	temperatureeffectsinwater
GO:0008272	5	2	0.27	0.001	0.026	0.255	1.000	temperatureeffectsin80mMh2O2
GO:0008272	5	1	0.26	0.079	0.238	1.000	1.000	interactionterm
GO:0008299	9	1	0.5	0.075	0.404	0.943	1.000	h2o2effectsat28C
GO:0008320	5	1	0.22	0.016	0.198	0.428	1.000	h2o2effectsat21C
GO:0009055	39	2	1.68	0.034	0.507	0.525	1.000	h2o2effectsat21C
GO:0009058	763	41	35.39	0.005	0.030	0.427	1.000	temperatureeffectsinwater
GO:0009058	788	52	42.16	0.016	0.581	0.623	1.000	temperatureeffectsin80mMh2O2
GO:0009060	24	2	1.34	0.095	1.000	1.000	1.000	h2o2effectsat28C
GO:0009063	23	3	1.28	0.023	0.400	0.619	1.000	h2o2effectsat28C
GO:0009065	9	1	0.5	0.005	0.404	0.406	1.000	h2o2effectsat28C

GO:0009066	20	2	1.06	0.019	1.000	0.652	1.000	interactionterm
GO:0009072	16	3	0.89	0.067	1.000	0.943	1.000	h2o2effectsat28C
GO:0009073	11	2	0.61	0.033	0.122	0.700	1.000	h2o2effectsat28C
GO:0009073	11	1	0.58	0.010	0.450	0.543	1.000	interactionterm
GO:0009081	12	4	0.67	0.052	0.055	0.943	1.000	h2o2effectsat28C
GO:0009081	12	1	0.63	0.062	1.000	1.000	1.000	interactionterm
GO:0009082	11	3	0.53	0.007	0.014	0.415	1.000	h2o2effectsat21C
GO:0009082	11	1	0.51	0.002	0.408	0.285	1.000	temperatureeffectsin water
GO:0009082	11	1	0.59	0.003	0.455	0.283	1.000	temperatureeffectsin 80mMh2O2
GO:0009082	11	1	0.58	0.067	0.450	1.000	1.000	interactionterm
GO:0009086	8	1	0.42	0.067	0.353	1.000	1.000	interactionterm
GO:0009152	26	4	1.39	0.055	1.000	0.970	1.000	temperatureeffectsin 80mMh2O2
GO:0009152	26	4	1.37	0.019	0.381	0.652	1.000	interactionterm
GO:0009156	13	3	0.7	0.064	1.000	0.970	1.000	temperatureeffectsin 80mMh2O2
GO:0009156	13	3	0.69	0.068	0.102	1.000	1.000	interactionterm
GO:0009165	51	4	2.73	0.075	1.000	1.000	1.000	temperatureeffectsin 80mMh2O2
GO:0009168	11	1	0.53	0.062	1.000	0.825	1.000	h2o2effectsat21C
GO:0009168	11	3	0.59	0.024	1.000	0.764	1.000	temperatureeffectsin 80mMh2O2
GO:0009168	11	2	0.58	0.047	1.000	0.937	1.000	interactionterm
GO:0009225	7	1	0.37	0.041	0.316	0.856	1.000	interactionterm
GO:0009260	29	4	1.55	0.016	1.000	0.623	1.000	temperatureeffectsin 80mMh2O2
GO:0009260	29	5	1.53	0.018	0.147	0.652	1.000	interactionterm
GO:0009279	20	4	1.22	0.003	0.029	0.027	0.419	temperatureeffectsin water

GO:0009288	19	5	0.86	0.003	0.042	0.040	0.500	h2o2effectsat21C
GO:0009288	19	8	0.9	0.000	0.281	0.007	1.000	h2o2effectsat28C
GO:0009288	19	2	1.01	0.095	0.354	0.421	1.000	temperatureeffectsin80mMh2O2
GO:0009425	11	7	0.52	0.017	0.023	0.138	0.368	h2o2effectsat28C
GO:0009425	11	1	0.59	0.039	1.000	0.309	1.000	temperatureeffectsin80mMh2O2
GO:0009425	11	6	0.6	0.004	0.000	0.206	0.005	interactionterm
GO:0010558	10	1	0.49	0.060	1.000	0.825	1.000	h2o2effectsat21C
GO:0010605	16	2	0.78	0.097	0.257	0.967	1.000	h2o2effectsat21C
GO:0015074	25	3	1.21	0.002	0.118	0.347	1.000	h2o2effectsat21C
GO:0015343	12	3	0.56	0.006	0.016	0.261	0.640	temperatureeffectsinwater
GO:0015891	12	3	0.56	0.007	0.016	0.428	1.000	temperatureeffectsinwater
GO:0015934	7	2	0.32	0.000	0.036	0.001	0.500	h2o2effectsat21C
GO:0015934	7	3	0.43	0.000	0.006	0.002	0.148	temperatureeffectsinwater
GO:0015934	7	1	0.37	0.000	0.320	0.004	1.000	temperatureeffectsin80mMh2O2
GO:0015935	6	2	0.27	0.007	0.027	0.058	0.500	h2o2effectsat21C
GO:0015935	6	1	0.32	0.000	0.281	0.003	1.000	temperatureeffectsin80mMh2O2
GO:0015980	31	2	1.73	0.019	1.000	0.563	1.000	h2o2effectsat28C
GO:0015986	8	1	0.43	0.005	0.356	0.388	1.000	temperatureeffectsin80mMh2O2
GO:0016226	10	3	0.53	0.073	0.014	1.000	1.000	temperatureeffectsin80mMh2O2
GO:0016226	10	3	0.53	0.029	0.013	0.820	1.000	interactionterm
GO:0016620	30	3	1.29	0.088	0.137	0.565	1.000	h2o2effectsat21C
GO:0016620	30	2	1.57	0.001	0.472	0.210	1.000	h2o2effectsat28C
GO:0016627	31	3	1.63	0.039	0.220	0.545	1.000	h2o2effectsat28C

GO:0016705	21	4	0.91	0.047	0.011	0.540	0.910	h2o2effectsat21C
GO:0016705	21	4	1.1	0.051	0.022	0.560	1.000	h2o2effectsat28C
GO:0016705	20	4	0.94	0.010	0.012	0.310	0.640	temperatureeffectsinwater
GO:0016742	10	1	0.53	0.066	0.417	0.842	1.000	interactionterm
GO:0016790	10	1	0.52	0.012	0.417	0.499	1.000	h2o2effectsat28C
GO:0016798	30	2	1.57	0.084	1.000	0.654	1.000	h2o2effectsat28C
GO:0016831	18	2	0.84	0.061	0.205	0.625	1.000	temperatureeffectsinwater
GO:0016831	18	1	0.91	0.003	0.606	0.240	1.000	temperatureeffectsin80mMh2O2
GO:0016836	35	3	1.51	0.007	0.190	0.422	1.000	h2o2effectsat21C
GO:0016836	35	5	1.84	0.054	0.034	0.560	1.000	h2o2effectsat28C
GO:0016860	8	1	0.34	0.090	1.000	0.565	1.000	h2o2effectsat21C
GO:0016860	8	1	0.42	0.087	1.000	0.654	1.000	h2o2effectsat28C
GO:0016861	6	1	0.28	0.033	0.251	0.431	1.000	temperatureeffectsinwater
GO:0016861	7	2	0.35	0.071	0.045	0.945	1.000	temperatureeffectsin80mMh2O2
GO:0016866	20	2	0.86	0.054	0.327	0.540	1.000	h2o2effectsat21C
GO:0016879	38	4	1.91	0.028	0.214	0.876	1.000	temperatureeffectsin80mMh2O2
GO:0016903	33	3	1.73	0.008	0.149	0.499	1.000	h2o2effectsat28C
GO:0019219	306	21	17.05	0.070	1.000	0.943	1.000	h2o2effectsat28C
GO:0019290	5	3	0.23	0.030	0.001	0.980	0.244	temperatureeffectsinwater
GO:0019318	10	2	0.46	0.099	1.000	1.000	1.000	temperatureeffectsinwater
GO:0019725	10	1	0.49	0.076	0.393	0.873	1.000	h2o2effectsat21C
GO:0019842	76	4	3.28	0.081	1.000	0.559	1.000	h2o2effectsat21C
GO:0019843	6	3	0.3	0.004	0.002	0.240	0.237	temperatureeffectsin80mMh2O2

GO:0019856	6	1	0.32	0.020	0.278	0.652	1.000	interactionterm
GO:0020037	25	3	1.08	0.014	0.090	0.428	1.000	h2o2effectsat21C
GO:0020037	25	2	1.31	0.071	0.380	0.586	1.000	h2o2effectsat28C
GO:0022607	48	5	2.57	0.099	0.661	1.000	1.000	temperatureeffectsin80mMh2O2
GO:0022607	47	6	2.48	0.079	0.379	1.000	1.000	interactionterm
GO:0022857	358	18	16.79	0.027	0.670	0.431	1.000	temperatureeffectsinwater
GO:0030163	7	1	0.39	0.010	0.331	0.499	1.000	h2o2effectsat28C
GO:0030554	345	20	16.18	0.044	0.752	0.516	1.000	temperatureeffectsinwater
GO:0030554	358	19	18.8	0.011	0.579	0.584	1.000	interactionterm
GO:0030694	5	3	0.23	0.003	0.001	0.040	0.038	h2o2effectsat21C
GO:0030694	5	5	0.24	0.000	0.000	0.000	0.000	h2o2effectsat28C
GO:0030694	5	2	0.27	0.015	0.026	0.253	0.612	interactionterm
GO:0031177	21	7	0.98	0.000	0.000	0.077	0.003	temperatureeffectsinwater
GO:0031177	21	4	1.06	0.038	0.019	0.876	1.000	temperatureeffectsin80mMh2O2
GO:0031324	12	2	0.58	0.080	1.000	0.873	1.000	h2o2effectsat21C
GO:0031324	12	1	0.64	0.100	1.000	1.000	1.000	temperatureeffectsin80mMh2O2
GO:0031327	10	1	0.49	0.060	1.000	0.825	1.000	h2o2effectsat21C
GO:0032784	6	1	0.33	0.100	0.291	1.000	1.000	h2o2effectsat28C
GO:0032784	6	1	0.32	0.073	0.281	1.000	1.000	temperatureeffectsin80mMh2O2
GO:0033875	9	1	0.5	0.033	0.404	0.700	1.000	h2o2effectsat28C
GO:0034032	9	1	0.5	0.033	0.404	0.700	1.000	h2o2effectsat28C
GO:0038023	44	5	2.06	0.006	0.016	0.261	0.640	temperatureeffectsinwater
GO:0042401	11	1	0.53	0.048	0.422	0.824	1.000	h2o2effectsat21C

GO:0042401	11	2	0.51	0.088	1.000	1.000	1.000	temperatureeffectsinwater
GO:0042578	26	2	1.31	0.062	1.000	0.910	1.000	temperatureeffectsin80mMh2O2
GO:0042578	26	2	1.37	0.037	0.578	0.756	1.000	interactionterm
GO:0042626	54	4	2.53	0.030	0.318	0.431	1.000	temperatureeffectsinwater
GO:0044036	10	1	0.46	0.012	0.379	0.646	1.000	temperatureeffectsinwater
GO:0044183	8	1	0.42	0.086	1.000	0.654	1.000	h2o2effectsat28C
GO:0044183	8	2	0.38	0.021	0.047	0.423	1.000	temperatureeffectsinwater
GO:0044248	73	5	4.07	0.069	1.000	0.943	1.000	h2o2effectsat28C
GO:0044271	560	29	27.2	0.013	1.000	0.539	1.000	h2o2effectsat21C
GO:0044272	27	4	1.43	0.038	0.192	0.856	1.000	interactionterm
GO:0044275	7	1	0.32	0.018	0.283	0.725	1.000	temperatureeffectsinwater
GO:0044550	6	1	0.29	0.014	0.259	0.539	1.000	h2o2effectsat21C
GO:0045259	7	1	0.37	0.007	0.320	0.083	1.000	temperatureeffectsin80mMh2O2
GO:0045892	9	1	0.44	0.060	0.362	0.825	1.000	h2o2effectsat21C
GO:0045892	9	3	0.5	0.001	0.011	0.249	1.000	h2o2effectsat28C
GO:0045892	9	1	0.48	0.065	0.391	0.970	1.000	temperatureeffectsin80mMh2O2
GO:0045934	10	2	0.49	0.044	0.048	0.795	1.000	h2o2effectsat21C
GO:0045934	10	3	0.56	0.082	1.000	0.994	1.000	h2o2effectsat28C
GO:0046112	9	1	0.48	0.044	0.391	0.970	1.000	temperatureeffectsin80mMh2O2
GO:0046112	9	1	0.48	0.023	1.000	0.712	1.000	interactionterm
GO:0046914	92	4	3.97	0.090	1.000	0.565	1.000	h2o2effectsat21C
GO:0046914	92	6	4.63	0.016	1.000	0.653	1.000	temperatureeffectsin80mMh2O2
GO:0046914	90	8	4.73	0.020	1.000	0.628	1.000	interactionterm

GO:0046983	9	1	0.42	0.093	0.351	0.820	1.000	temperatureeffectsinwater
GO:0050661	22	1	0.95	0.054	0.622	0.540	1.000	h2o2effectsat21C
GO:0050661	22	2	1.11	0.014	0.305	0.636	1.000	temperatureeffectsin80mMh2O2
GO:0051082	10	1	0.52	0.021	0.417	0.499	1.000	h2o2effectsat28C
GO:0051172	12	2	0.58	0.097	1.000	0.967	1.000	h2o2effectsat21C
GO:0051539	19	2	0.82	0.079	0.196	0.554	1.000	h2o2effectsat21C
GO:0051539	19	2	1	0.070	0.263	0.586	1.000	h2o2effectsat28C
GO:0065003	13	1	0.6	0.033	0.462	0.980	1.000	temperatureeffectsinwater
GO:0070566	5	1	0.26	0.078	0.237	0.865	1.000	interactionterm
GO:0070887	5	2	0.28	0.061	0.028	0.943	1.000	h2o2effectsat28C
GO:0071704	1285	71	68.75	0.087	0.381	1.000	1.000	temperatureeffectsin80mMh2O2
GO:0071973	18	4	0.87	0.037	0.010	0.766	1.000	h2o2effectsat21C
GO:0071973	18	8	1	0.001	0.000	0.249	0.001	h2o2effectsat28C
GO:0071973	18	6	0.95	0.008	0.000	0.543	0.117	interactionterm
GO:0072522	41	5	2.19	0.058	0.194	0.970	1.000	temperatureeffectsin80mMh2O2
GO:0072593	5	2	0.24	0.012	0.021	0.522	1.000	h2o2effectsat21C
GO:0072593	5	2	0.28	0.021	0.028	0.588	1.000	h2o2effectsat28C
GO:0097159	914	47	39.4	0.012	1.000	0.428	1.000	h2o2effectsat21C
GO:0098661	7	1	0.39	0.011	0.331	0.499	1.000	h2o2effectsat28C
GO:0098661	7	1	0.32	0.078	0.283	1.000	1.000	temperatureeffectsinwater
GO:0098661	7	2	0.37	0.002	0.050	0.255	1.000	temperatureeffectsin80mMh2O2
GO:0098661	7	1	0.37	0.014	0.316	0.617	1.000	interactionterm
GO:0098754	8	2	0.45	0.026	0.069	0.630	1.000	h2o2effectsat28C

GO:0098772	7	1	0.33	0.008	0.286	0.294	1.000	temperatureeffectsinwater
GO:0098772	7	1	0.35	0.043	0.304	0.876	1.000	temperatureeffectsin80mMh2O2
GO:0098772	7	2	0.37	0.002	0.048	0.268	1.000	interactionterm
GO:0140104	5	3	0.25	0.044	0.001	0.876	0.194	temperatureeffectsin80mMh2O2
GO:0140104	5	1	0.26	0.091	0.237	0.907	1.000	interactionterm
GO:0140110	179	12	7.72	0.049	1.000	0.540	1.000	h2o2effectsat21C
GO:0140110	179	12	9.39	0.020	0.052	0.499	1.000	h2o2effectsat28C
GO:0140359	39	2	1.83	0.029	0.752	0.431	1.000	temperatureeffectsinwater
GO:0140535	18	3	0.85	0.014	0.049	0.134	0.470	h2o2effectsat28C
GO:0140662	7	1	0.33	0.024	0.286	0.431	1.000	temperatureeffectsinwater
GO:0140694	11	1	0.51	0.018	0.408	0.725	1.000	temperatureeffectsinwater
GO:1901135	111	6	5.39	0.019	0.273	0.623	1.000	h2o2effectsat21C
GO:1901135	108	9	5.7	0.081	0.718	1.000	1.000	interactionterm
GO:1901363	914	47	39.4	0.012	1.000	0.428	1.000	h2o2effectsat21C
GO:1901576	741	50	39.64	0.039	0.383	0.967	1.000	temperatureeffectsin80mMh2O2
GO:1901607	59	6	2.87	0.004	0.131	0.347	1.000	h2o2effectsat21C
GO:1901607	59	5	3.29	0.005	0.192	0.406	1.000	h2o2effectsat28C
GO:1901700	7	2	0.39	0.050	0.054	0.943	1.000	h2o2effectsat28C
GO:1902494	52	6	2.45	0.009	0.037	0.104	0.444	h2o2effectsat28C
GO:1990204	11	1	0.5	0.006	0.399	0.058	1.000	h2o2effectsat21C
GO:1990204	11	1	0.52	0.002	0.414	0.034	1.000	h2o2effectsat28C
GO:1990904	14	3	0.75	0.051	0.052	0.349	0.864	temperatureeffectsin80mMh2O2
GO:1990904	14	1	0.76	0.056	1.000	0.541	1.000	interactionterm

Supplementary Table S3
Full results of the transcriptomic screen from chapter 4.

http://dx.doi.org/10.5287/ora-mzjqbogqm

Supplementary Table S4
T3SS effector name aliases, reproduced from https://guttman.csb.utoronto.ca/resources-software/type-iii-effector-aliases/

NEW NAME	OLD NAME
avrA	avrA
avrB1	avrB
avrB2	avrC
avrB2	avrPphC
avrB3	hopPsyC
avrB3	hopPsyC2
avrB4-1	avrB3
avrD1	avrD
avrD1	avrDg0
avrD1	avrDg1
avrD1	avrDg3/6
avrD1	avrg3/6
avrD1	avrDp2
avrE1	avrE
avrPto1	avrPto
avrPto1	avrP
avrPto1	avrPro
avrRpm1	avrRpm1
avrRpm1	avrPmaA1
avrRpm1	avrRpm1
avrRpm1	avrPpiA2.R2
avrRpm1	avrPpiA1
avrRps4	avrRps4

avrRps4	hopK (1)
avrRpt2	avrRpt2
hopA1	hrmA
hopA1	hopPsyA(Pto)
hopA1	hopPsyA
hopA1	ORF2 (2)
hopA2	hopPsyB1
hopA2	ORF2 (2)
hopA2'	hopPsyA (premature stop)
hopAA1	hopPtoA1
hopAA1-1	CEL ORF5
hopAA1-2	hopPtoA2
hopAB1	virPphA
hopAB1	avrPtoB
hopAB2	avrPtoB
hopAB2	virPtoA
hopAB3-1	hopPmaL
hopAB3-2	holPmaN
hopAC::ISPsy5	holPtoAC
hopAC::ISPsy5	hopPtoB2
hopAC::ISPsy5	EEL ORF1-like
hopAC1	holPsyAC
hopAD1	holPtoS
hopAD1	hopPtoI
hopAE1	holPsyAE
hopAF1	holPtoN

hopAF1	hopPtoJ
hopAG::ISPssy	ORF28
hopAG1	holPsyAG
hopAH1	holPsyAH
hopAH1	holPtoAH
hopAH2	holPsyAH2
hopAH2-1	holPsyAH2
hopAI1	holPtoAI
hopAI1'	holPsyAI
hopAJ1	hopPmaG
hopAK1	hopPmaH
hopAL1	hopPmaK
hopAM1	avrPpiB
hopAM1-1	avrPpiB1
hopAM1-2	avrPpiB2
hopAN1	ipx53
hopAO1	avrPphD2
hopAP1	hopPtoH2
hopAQ1	holPtoAA
hopAR1	avrPphB
hopAR1	avrPph3
hopAS1'	ORF01152 (premature stop)
hopAX1	hopPsyL/hopL
hopB1	hopPtoB2
hopB1	EEL ORF1
hopB1	hopPtoB2

hopB1	hopPsyG
hopC1	avrPpiC2
hopC1	hopPtoC
hopD::IS52	hopPtoD1-related
hopD1	avrPphD
hopD1	hopPtoD1
hopE1	hopPtoE
hopE1	holPtoV
hopF1	avrPphF-orf2
hopF2	hopPtoF
hopF2	holPtoAD
hopF3	HopF2 (1)
hopG1	hopPtoG
hopG1	holPtoW
hopH1	hopPtoH
hopI1	hopPmaI
hopJ1	hopPmaJ
hopK1	holPtoAB
hopK1	hopPtoK
hopL1	hopPtoL
hopL1	ORF29
hopM1	hopPtoM
hopM1	holPtoX
hopM1	CEL ORF3
hopN1	hopPtoN
hopN1	holPtoT

hopN1	CEL ORF7
hopO1-1	hopPtoO
hopO1-1	hopPtoS1
hopO1-2	hopPtoO2
hopO1-2	hopPtoS3
hopO1-3'	hopPtoO-related (premature stop)
hopP1	hopPtoP
hopP1	hrpW-related
hopQ1-1	holPtoQ
hopQ1-1	ORF19
hopQ1-2	holPtoQ2
hopQ1-2	holPtoQ-like
hopR1	holPtoR
hopS1'	holPtoZ
hopS1'	hopPtoS4
hopS1'	ORF26
hopS2	holPtoZ2
hopS2	ORF15
hopT1-1	holPtoU
hopT1-1	hopPtoT1
hopT1-2	holPtoU2
hopT2	holPtoU3 (premature stop)
hopT2	holPtoU-related
hopU1	hopPtoS2
hopV1	hopPtoV
hopW1-1	hopPmaA

hopW1-2	hopPmaA
hopX1	avrPphE
hopX1	hopPsyE
hopX1	EEL ORF2
hopX1	avrPphE8
hopX1	hopPsyE2
hopX2	hopPmaB
hopY1	holPtoY
hopY1	hrpA-like
hopZ1	hopPmaD
hopZ1	hopPsyH
hopZ2	avrPpiG1
hopZ3	hopPsyV
hopZ3	EEL ORF5
hrpA1	hrpA
hrpA2	hrpA
hrpA3	hrpA
hrpK1	hrpK
hrpK1	hrpY
hrpW1	hrpW
hrpZ1	hrpZ

Supplementary table S5
List of *P. savastanoi* candidate strains with >95% genome identity and 50% coverage to Pspph 1302A. These 262 strains were used for analysis in chapter 5 (phylogeny building and effector mining).

ID	NCBI description
GCA_001723935.1_ASM172393v1	MCRW01000001.1 Pseudomonas sp. BDAL1 Bakken_S3_L001_R1_001_trimmed_contig_1, whole genome shotgun sequence
GCA_003700865.1_ASM370086v1	RBQI01000839.1 Pseudomonas amygdali pv. lachrymans strain ICMP 826 PlaICMP826_Contig_1, whole genome shotgun sequence
GCA_003701325.1_ASM370132v1	RBRR01001242.1 Pseudomonas savastanoi pv. glycinea strain ICMP 3482 PgyICMP3482_Contig_1, whole genome shotgun sequence
GCA_003701635.1_ASM370163v1	RBSP01000591.1 Pseudomonas amygdali pv. photiniae strain ICMP 7847 PhoICMP7847_Contig_1, whole genome shotgun sequence
GCA_003703215.1_ASM370321v1	RBVA01000487.1 Pseudomonas amygdali pv. tabaci strain ICMP 4525 PtaICMP4525_Contig_1, whole genome shotgun sequence
GCA_014653325.1_ASM1465332v1	JACADI010000001.1 Pseudomonas amygdali pv. morsprunorum strain ICMP 3676 utg000001c, whole genome shotgun sequence
GCF_000012205.1_ASM1220v1	NC_005773.3 Pseudomonas savastanoi pv. phaseolicola 1448A, complete sequence
GCF_000143005.1_ASM14300v1	NZ_GL376639.1 Pseudomonas syringae pv. glycinea str. race 4 genomic scaffold Scaffold_1, whole genome shotgun sequence
GCF_000145685.1_ASM14568v1	NZ_GL384620.1 Pseudomonas amygdali pv. aesculi str. 0893_23 Scaffold_1, whole genome shotgun sequence
GCF_000145765.1_ASM14576v1	NZ_GL384773.1 Pseudomonas syringae pv. mori str. 301020 genomic scaffold Scaffold_1, whole genome shotgun sequence
GCF_000145945.1_ASM14594v1	NZ_GL385365.1 Pseudomonas amygdali pv. tabaci str. ATCC 11528 Scaffold_1, whole genome shotgun sequence
GCF_000145945.2_ASM14594v2	NZ_CP042804.1 Pseudomonas amygdali pv. tabaci str. ATCC 11528 chromosome, complete genome
GCF_000146005.1_ASM14600v1	NZ_GG775127.1 Pseudomonas amygdali pv. lachrymans str. M301315 Scaffold_2, whole genome shotgun sequence
GCF_000146005.2_ASM14600v2	NZ_CP031225.1 Pseudomonas amygdali pv. lachrymans str. M301315 chromosome, complete genome
GCF_000159835.1_ASM15983v1	NZ_GG699514.1 Pseudomonas syringae pv. tabaci ATCC 11528 genomic scaffold supercontig_1160.1, whole genome shotgun sequence
GCF_000159835.2_ASM15983v2	NZ_ACHU02000001.1 Pseudomonas amygdali pv. tabaci str. ATCC 11528 contig_8_1.1, whole genome shotgun sequence
GCF_000163255.1_ASM16325v1	NZ_GG700071.1 Pseudomonas amygdali pv. aesculi str. NCPPB 3681 scf_4912_6059, whole genome shotgun sequence
GCF_000163275.1_ASM16327v1	NZ_GG700435.1 Pseudomonas amygdali pv. aesculi str. 2250 scf_4865_3047, whole genome shotgun sequence
GCF_000164015.2_PsavNCPPB3335v2	NZ_CM001834.1 Pseudomonas savastanoi pv. savastanoi NCPPB 3335 chromosome, whole genome shotgun sequence
GCF_000164015.3_ASM16401v3	NZ_CP008742.1 Pseudomonas savastanoi pv. savastanoi NCPPB 3335 chromosome, complete genome
GCF_000187045.1_ASM18704v2	NZ_AEGG01000104.1 Pseudomonas savastanoi pv. glycinea str. B076 Contig104, whole genome shotgun sequence

GCF_000187065.1_ASM18706v2	NZ_AEGH01000108.1 Pseudomonas savastanoi pv. glycinea str. race 4 Contig108, whole genome shotgun sequence
GCF_000225805.1_ASM22580v1	NZ_JH137509.1 Pseudomonas savastanoi pv. phaseolicola 1644R Scaffold_1, whole genome shotgun sequence
GCF_000275945.1_ASM27594v1	NZ_AJXI01000001.1 Pseudomonas amygdali pv. tabaci str. 6605 contig00001_contig_1, whole genome shotgun sequence
GCF_000732035.1_PSV1.0	NZ_JOJV01000001.1 Pseudomonas savastanoi pv. savastanoi strain DAPP-PG722 contig001, whole genome shotgun sequence
GCF_000751155.1_PSV1.0	NZ_CCMP01000001.1 Pseudomonas savastanoi pv. savastanoi, whole genome shotgun sequence
GCF_000934645.1_ASM93464v1	NZ_JWJF01000022.1 Pseudomonas amygdali pv. tabaci strain yuexi-1 contig_1, whole genome shotgun sequence
GCF_000935645.1_PSAVPseNe107-G1	NZ_JYHB01000001.1 Pseudomonas amygdali strain CFBP 3205 CFBP3205001, whole genome shotgun sequence
GCF_000935665.1_PDCFBP4219-G1	NZ_JYHD01000001.1 Pseudomonas syringae pv. daphniphylli strain CFBP 4219 CFBP4219001, whole genome shotgun sequence
GCF_000935675.1_PMCFBP3225-G1	NZ_JYHE01000001.1 Pseudomonas meliae strain CFBP 3225 CFBP3225001, whole genome shotgun sequence
GCF_000935695.1_PSAVPseNe107-G1	NZ_JYHF01000001.1 Pseudomonas savastanoi pv. savastanoi strain PseNe107 PseNe107001, whole genome shotgun sequence
GCF_000935735.1_PSDCFBP3226-G1	NZ_JYHG01000001.1 Pseudomonas amygdali pv. dendropanacis strain CFBP 3226 CFBP3226001, whole genome shotgun sequence
GCF_001006445.1_PSl_v01	NZ_LCWT01000001.1 Pseudomonas amygdali pv. lachrymans strain 98A-744 scaffold1, whole genome shotgun sequence
GCF_001006455.1_PSt_v01	NZ_LCWS01000001.1 Pseudomonas amygdali pv. tabaci str. ATCC 11528 scaffold1.1, whole genome shotgun sequence
GCF_001293725.1_Psv4352	NZ_LGKR01000034.1 Pseudomonas savastanoi strain 4352 Psv4352_Scaffold004, whole genome shotgun sequence
GCF_001293765.1_PgyLN10	NZ_LGLM01000105.1 Pseudomonas savastanoi pv. glycinea strain LN10 PgyLN10_Scaffold001, whole genome shotgun sequence
GCF_001293825.1_Pla107	NZ_LGLK01000044.1 Pseudomonas amygdali pv. lachrymans strain 107 Pla107_Scaffold001, whole genome shotgun sequence
GCF_001293845.1_PlaYM7902	NZ_LGLI01000037.1 Pseudomonas amygdali pv. lachrymans strain YM7902 PlaYM7902_Scaffold001, whole genome shotgun sequence
GCF_001293975.1_PmeN6801	NZ_LGLB01000051.1 Pseudomonas amygdali pv. mellea strain N6801 PmeN6801_Scaffold003, whole genome shotgun sequence
GCF_001293985.1_PmyAZ84488	NZ_LGLA01000055.1 Pseudomonas amygdali pv. myricae strain AZ84488 PmyAZ84488_Scaffold001, whole genome shotgun sequence
GCF_001294025.1_Pph1302A	NZ_LGKY01000072.1 Pseudomonas savastanoi pv. phaseolicola strain 1302A Pph1302A_Scaffold001, whole genome shotgun sequence
GCF_001294035.1_PphHB10Y	NZ_LGKX01000021.1 Pseudomonas savastanoi pv. phaseolicola strain HB10Y PphHB10Y_Scaffold002, whole genome shotgun sequence
GCF_001294065.1_PphY5_2	NZ_LGKV01000019.1 Pseudomonas savastanoi pv. phaseolicola strain Y5_2 PphY52_Scaffold005, whole genome shotgun sequence

GCF_001294105.1_PphNPS3121	NZ_LGKW01000041.1 Pseudomonas savastanoi pv. phaseolicola strain NPS3121 PphNPS3121_Scaffold001, whole genome shotgun sequence
GCF_001294115.1_PseHC_1	NZ_LGKS01000126.1 Pseudomonas amygdali pv. sesami strain HC_1 PseHC1_Scaffold002, whole genome shotgun sequence
GCF_001294185.1_PmaKN91	NZ_LGLF01000021.1 Pseudomonas syringae pv. maculicola strain KN91 PmaKN91_Scaffold005, whole genome shotgun sequence
GCF_001294195.1_PgyKN44	NZ_LGLP01000039.1 Pseudomonas savastanoi pv. glycinea strain KN44 PgyKN44_Scaffold003, whole genome shotgun sequence
GCF_001294215.1_PmpFTRS_U7805	NZ_LGLQ01000180.1 Pseudomonas amygdali pv. morsprunorum strain FTRS_U7805 PmpFTRSU7_Scaffold001, whole genome shotgun sequence
GCF_001294265.1	NZ_LGLO01000006.1 Pseudomonas savastanoi pv. glycinea strain BR1 PgyBR1_Scaffold001, whole genome shotgun sequence
GCF_001294275.1_PgyUnB647	NZ_LGLL01000085.1 Pseudomonas savastanoi pv. glycinea strain UnB647 PgyUnB647_Scaffold001, whole genome shotgun sequence
GCF_001400115.1_PamICMP3918	NZ_LJPQ01000188.1 Pseudomonas amygdali strain ICMP3918 PamICMP3918_Contig_1, whole genome shotgun sequence
GCF_001400215.1_PceICMP17524	NZ_LJQA01000320.1 Pseudomonas syringae pv. cerasicola strain ICMP 17524 PceICMP17524_Contig_1, whole genome shotgun sequence
GCF_001400275.1_PdaICMP9757	NZ_LJQF01000168.1 Pseudomonas syringae pv. daphniphylli strain ICMP9757 PdaICMP9757_Contig_1, whole genome shotgun sequence
GCF_001400285.1_PcsICMP9419	NZ_LJQD01000333.1 Pseudomonas syringae pv. castaneae strain ICMP 9419 PcsICMP9419_Contig_1, whole genome shotgun sequence
GCF_001400375.1_PgyICMP2189	NZ_LJQL01000037.1 Pseudomonas savastanoi pv. glycinea strain ICMP 2189 PgyICMP2189_Contig_1, whole genome shotgun sequence
GCF_001400395.1_PhiICMP9623	NZ_LJQN01000015.1 Pseudomonas amygdali pv. hibisci strain ICMP 9623 PhiICMP9623_Contig_1, whole genome shotgun sequence
GCF_001400415.1_PhoICMP7840	NZ_LJQO01000136.1 Pseudomonas amygdali pv. photiniae strain ICMP 7840 PhoICMP7840_Contig_1, whole genome shotgun sequence
GCF_001400435.1_PdeICMP9150	NZ_LJQG01000154.1 Pseudomonas amygdali pv. dendropanacis strain ICMP 9150 PdeICMP9150_Contig_1, whole genome shotgun sequence
GCF_001400455.1_PerICMP4455	NZ_LJQI01000307.1 Pseudomonas amygdali pv. eriobotryae strain ICMP 4455 PerICMP4455_Contig_1, whole genome shotgun sequence
GCF_001400475.1_PlaICMP3507	NZ_LJQP01000010.1 Pseudomonas amygdali pv. lachrymans strain ICMP 3507 PlaICMP3507_Contig_1, whole genome shotgun sequence
GCF_001400515.1_PmlICMP6289	NZ_LJQT01000414.1 Pseudomonas meliae strain ICMP 6289 PmlICMP6289_Contig_1, whole genome shotgun sequence
GCF_001400525.1_PmoICMP4331	NZ_LJQU01000538.1 Pseudomonas amygdali pv. mori strain ICMP 4331 PmoICMP4331_Contig_1, whole genome shotgun sequence
GCF_001400555.1_PmyICMP7118	NZ_LJQV01000225.1 Pseudomonas amygdali pv. myricae strain ICMP 7118 PmyICMP7118_Contig_1, whole genome shotgun sequence
GCF_001400575.1_PneICMP16943	NZ_LJQW01000304.1 Pseudomonas savastanoi pv. nerii strain ICMP 16943 PneICMP16943_Contig_1, whole genome shotgun sequence
GCF_001400605.1_PphICMP2740	NZ_LJQZ01000130.1 Pseudomonas savastanoi pv. phaseolicola strain ICMP 2740 PphICMP2740_Contig_1, whole genome shotgun sequence
GCF_001400675.1_PaeICMP8947	NZ_LJPN01000418.1 Pseudomonas amygdali pv. aesculi strain ICMP 8947 PaeICMP8947_Contig_1, whole genome shotgun sequence

GCF_001400715.1_PbrICMP13650	NZ_LJPV01000168.1 Pseudomonas syringae pv. broussonetiae strain ICMP 13650 PbrICMP13650_Contig_1, whole genome shotgun sequence
GCF_001400755.1_PccICMP5710	NZ_LJPY01000030.1 Pseudomonas amygdali pv. ciccaronei strain ICMP 5710 PccICMP5710_Contig_1, whole genome shotgun sequence
GCF_001400795.1_PcuICMP11894	NZ_LJQE01000368.1 Pseudomonas syringae pv. cunninghamiae strain ICMP11894 PcuICMP11894_Contig_1, whole genome shotgun sequence
GCF_001400815.1_PfiICMP7848	NZ_LJQJ01000543.1 Pseudomonas ficuserectae strain ICMP 7848 PfiICMP7848_Contig_1, whole genome shotgun sequence
GCF_001400875.1_PmeICMP5711	NZ_LJQS01000233.1 Pseudomonas amygdali pv. mellea strain ICMP 5711 PmeICMP5711_Contig_1, whole genome shotgun sequence
GCF_001400935.1_PreICMP16945	NZ_LJRD01000493.1 Pseudomonas savastanoi pv. retacarpa strain ICMP 16945 PreICMP16945_Contig_1, whole genome shotgun sequence
GCF_001400995.1_PrhICMP9756	NZ_LJRE01000255.1 Pseudomonas syringae pv. rhaphiolepidis strain ICMP9756 PrhICMP9756_Contig_1, whole genome shotgun sequence
GCF_001401095.1_PtaICMP2835	NZ_LJRL01000008.1 Pseudomonas amygdali pv. tabaci strain ICMP 2835 PtaICMP2835_Contig_1, whole genome shotgun sequence
GCF_001401165.1_PumICMP3962	NZ_LJRQ01000258.1 Pseudomonas amygdali pv. ulmi strain ICMP 3962 PumICMP3962_Contig_1, whole genome shotgun sequence
GCF_001401265.1_PseICMP763	NZ_LJRG01000235.1 Pseudomonas amygdali pv. sesami strain ICMP 763 PseICMP763_Contig_1, whole genome shotgun sequence
GCF_001401285.1_PsvICMP4352	NZ_LJRJ01000054.1 Pseudomonas savastanoi pv. savastanoi strain ICMP 4352 PsvICMP4352_Contig_1, whole genome shotgun sequence
GCF_001466905.1_ASM146690v1	NZ_LKEK01000001.1 Pseudomonas sp. ICMP 3272 scaffold1, whole genome shotgun sequence
GCF_001467105.1_ASM146710v1	NZ_LKCH01000001.1 Pseudomonas syringae ICMP 19498 scaffold1, whole genome shotgun sequence
GCF_001467115.1_ASM146711v1	NZ_LKCI01000001.1 Pseudomonas savastanoi strain ICMP 19499 scaffold1, whole genome shotgun sequence
GCF_001483545.1_PfrICMP7711	NZ_LLJL01000403.1 Pseudomonas savastanoi pv. fraxini strain ICMP 7711 PfrICMP7711_Contig_1, whole genome shotgun sequence
GCF_001535735.1_ASM153573v1	NZ_LIIB01000001.1 Pseudomonas amygdali pv. morsprunorum strain 2341 mors2341_contig_1, whole genome shotgun sequence
GCF_001535785.1_ASM153578v1	NZ_LIHZ01000001.1 Pseudomonas amygdali pv. morsprunorum strain HRI-W 5269 mors5269_contig_1, whole genome shotgun sequence
GCF_001535805.1_ASM153580v1	NZ_LIHY01000001.1 Pseudomonas amygdali pv. myricae strain CFBP 2897 myri2897_contig_1, whole genome shotgun sequence
GCF_001535815.1_ASM153581v1	NZ_LIHX01000001.1 Pseudomonas savastanoi pv. nerii strain CFBP 5067 neri5067_contig_1, whole genome shotgun sequence
GCF_001535835.1_ASM153583v1	NZ_LIHV01000001.1 Pseudomonas syringae pv. rhaphiolepidis strain CFBP 4220 rhap4220_contig_1, whole genome shotgun sequence
GCF_001535915.1_ASM153591v1	NZ_LIHQ01000001.1 Pseudomonas amygdali pv. ulmi strain CFBP 1407 ulmi1407_contig_1, whole genome shotgun sequence
GCF_001537945.1_ASM153794v1	NZ_LIIG01000001.1 Pseudomonas syringae pv. cerasicola strain CFBP 6109 cera6109_contig_1, whole genome shotgun sequence
GCF_001537955.1_ASM153795v1	NZ_LILK01000001.1 Pseudomonas amygdali pv. aesculi strain 2329 aesc2329_contig_1, whole genome shotgun sequence

GCF_001537965.1_ASM153796v1	NZ_LIKY01000001.1 Pseudomonas amygdali pv. aesculi strain 2113 aesc2113_contig_1, whole genome shotgun sequence
GCF_001537985.1_ASM153798v1	NZ_LILI01000001.1 Pseudomonas amygdali pv. aesculi strain 2306 aesc2306_contig_1, whole genome shotgun sequence
GCF_001538045.1_ASM153804v1	NZ_LILH01000001.1 Pseudomonas amygdali pv. aesculi strain 2279 aesc2279_contig_1, whole genome shotgun sequence
GCF_001538055.1_ASM153805v1	NZ_LIID01000001.1 Pseudomonas amygdali pv. eriobotryae strain CFBP 2343 erio2343_contig_1, whole genome shotgun sequence
GCF_001538085.1_ASM153808v1	NZ_LILL01000001.1 Pseudomonas amygdali pv. aesculi strain 2336 aesc2336_contig_1, whole genome shotgun sequence
GCF_001538145.1_ASM153814v1	NZ_LIIE01000001.1 Pseudomonas amygdali pv. dendropanacis strain CFBP 3226 dend3226_contig_1, whole genome shotgun sequence
GCF_001538155.1_ASM153815v1	NZ_LIIC01000001.1 Pseudomonas savastanoi pv. fraxini strain CFBP 5062 frax5062_contig_1, whole genome shotgun sequence
GCF_001538185.1_ASM153818v1	NZ_LILJ01000001.1 Pseudomonas amygdali pv. aesculi strain 2315 aesc2315_contig_1, whole genome shotgun sequence
GCF_001538205.1_ASM153820v1	NZ_LIII01000001.1 Pseudomonas syringae pv. broussonetiae strain CFBP 5140 brou5140_contig_1, whole genome shotgun sequence
GCF_001538245.1_ASM153824v1	NZ_LIIH01000001.1 Pseudomonas syringae pv. castaneae strain CFBP 4217 cast4217_contig_1, whole genome shotgun sequence
GCF_001538255.1_ASM153825v1	NZ_LIIF01000001.1 Pseudomonas syringae pv. daphniphylli strain CFBP 4219 daph4219_contig_1, whole genome shotgun sequence
GCF_002068135.1_ASM206813v1	NZ_CP020351.1 Pseudomonas amygdali pv. lachrymans strain NM002 chromosome, complete genome
GCF_002115545.1_ASM211554v1	NZ_NBYW01000001.1 Pseudomonas savastanoi pv. retacarpa strain CECT 4861 pvRetacarpaCECT4861R1.adapter_paired_contig1, whole genome shotgun sequence
GCF_002269785.1_ASM226978v1	NZ_NIAW01000001.1 Pseudomonas savastanoi pv. fraxini strain NCPPB 1006 pv_Fraxini_NCPPB_R1.adapter__paired__contig_1, whole genome shotgun sequence
GCF_002269885.1_ASM226988v1	NZ_NIAX01000001.1 Pseudomonas savastanoi strain Ph3 Mandevilla_B203_R1.adapter__paired__contig_1, whole genome shotgun sequence
GCF_002270015.1_ASM227001v1	NZ_NIAY01000001.1 Pseudomonas savastanoi pv. nerii strain ESC 23 pv_Nerii_ESC_23_R1.adapter__paired__contig_1, whole genome shotgun sequence
GCF_002699855.1_ASM269985v1	NZ_LKBW01000001.1 Pseudomonas amygdali strain ICMP 3918 scaffold1, whole genome shotgun sequence
GCF_002699945.1_ASM269994v1	NZ_LKCC01000001.1 Pseudomonas syringae pv. cerasicola strain ICMP 17525 scaffold1, whole genome shotgun sequence
GCF_002700065.1_ASM270006v1	NZ_LKCB01000001.1 Pseudomonas syringae pv. cerasicola strain ICMP 13929 scaffold1, whole genome shotgun sequence
GCF_002736925.1_ASM273692v1	NZ_LKCD01000001.1 Pseudomonas amygdali pv. morsprunorum strain NZIPFR-PS6 scaffold1, whole genome shotgun sequence
GCF_002837595.1_ASM283759v1	NZ_NBLF01000001.1 Pseudomonas amygdali pv. lachrymans strain 814/98 Scaffold1, whole genome shotgun sequence

GCF_002905685.1_ASM290568v1	NZ_MLEB01000001.1 Pseudomonas amygdali pv. morsprunorum strain R15244 contig_1, whole genome shotgun sequence
GCF_002905685.2_ASM290568v2	NZ_CP026558.1 Pseudomonas amygdali pv. morsprunorum strain R15244 chromosome, complete genome
GCF_002905735.1_ASM290573v1	NZ_MLEE01000001.1 Pseudomonas amygdali pv. morsprunorum strain R19646 contig_1, whole genome shotgun sequence
GCF_002905755.1_ASM290575v1	NZ_MLEF01000001.1 Pseudomonas amygdali pv. morsprunorum strain R19657 contig_1, whole genome shotgun sequence
GCF_002905875.1_ASM290587v1	NZ_MLEN01000001.1 Pseudomonas amygdali pv. morsprunorum strain R15300 contig_1, whole genome shotgun sequence
GCF_002905875.2_ASM290587v2	NZ_MLEN02000002.1 Pseudomonas amygdali pv. morsprunorum strain R15300 plasmid p1_tig46 tig00000046_pilon, whole genome shotgun sequence
GCF_002905895.1_ASM290589v1	NZ_MLEO01000001.1 Pseudomonas amygdali pv. morsprunorum strain R19326 contig_1, whole genome shotgun sequence
GCF_002905915.1_ASM290591v1	NZ_MLEP01000001.1 Pseudomonas amygdali pv. morsprunorum strain R19629 contig_1, whole genome shotgun sequence
GCF_002916395.1_5270	NZ_NBAN01000001.1 Pseudomonas amygdali pv. morsprunorum strain 5270 contig_1, whole genome shotgun sequence
GCF_002939205.1_ASM293920v1	NZ_MTAE01000001.1 Pseudomonas amygdali pv. morsprunorum strain FTRS_U6602 Psmor301448_contig_1, whole genome shotgun sequence
GCF_002939225.1_ASM293922v1	NZ_MTAD01000001.1 Pseudomonas amygdali pv. morsprunorum strain FTRS_U8017 Psmor301437_contig_1, whole genome shotgun sequence
GCF_002939245.1_ASM293924v1	NZ_MTAF01000001.1 Pseudomonas amygdali pv. morsprunorum strain FTRS_U6603 Psmor301610_contig_1, whole genome shotgun sequence
GCF_003205945.1_ASM320594v1	NZ_QJTT01000100.1 Pseudomonas savastanoi pv. glycinea strain 2411 NODE_100_length_15209_cov_227.304_ID_24390, whole genome shotgun sequence
GCF_003412855.1_ASM341285v1	NZ_QPBO01000001.1 Pseudomonas savastanoi pv. phaseolicola strain 535 Contig_1, whole genome shotgun sequence
GCF_003412865.1_ASM341286v1	NZ_QPBN01000001.1 Pseudomonas savastanoi pv. phaseolicola strain 533 Contig_1, whole genome shotgun sequence
GCF_003412905.1_ASM341290v1	NZ_QPBM01000001.1 Pseudomonas savastanoi pv. phaseolicola strain 532 Contig_1, whole genome shotgun sequence
GCF_003412915.1_ASM341291v1	NZ_QPBL01000001.1 Pseudomonas savastanoi pv. phaseolicola strain 531 Contig_1, whole genome shotgun sequence
GCF_003412965.1_ASM341296v1	NZ_QPBH01000001.1 Pseudomonas savastanoi pv. phaseolicola strain 527 Contig_1, whole genome shotgun sequence
GCF_003412985.1_ASM341298v1	NZ_QPBF01000001.1 Pseudomonas savastanoi pv. phaseolicola strain 525 Contig_1, whole genome shotgun sequence
GCF_003412995.1_ASM341299v1	NZ_QPBE01000001.1 Pseudomonas savastanoi pv. phaseolicola strain 524 Contig_1, whole genome shotgun sequence
GCF_003413015.1_ASM341301v1	NZ_QPBD01000001.1 Pseudomonas savastanoi pv. phaseolicola strain 523 Contig_1, whole genome shotgun sequence
GCF_003413035.1_ASM341303v1	NZ_QPBC01000001.1 Pseudomonas savastanoi pv. phaseolicola strain 522 Contig_1, whole genome shotgun sequence
GCF_003413065.1_ASM341306v1	NZ_QPBB01000001.1 Pseudomonas savastanoi pv. phaseolicola strain 521 Contig_1, whole genome shotgun sequence

GCF_003413075.1_ASM341307v1	NZ_QPAZ01000001.1 Pseudomonas savastanoi pv. phaseolicola strain 519 Contig_1, whole genome shotgun sequence
GCF_003413095.1_ASM341309v1	NZ_QPAW01000001.1 Pseudomonas savastanoi pv. phaseolicola strain 516 Contig_1, whole genome shotgun sequence
GCF_003413115.1_ASM341311v1	NZ_QPAV01000001.1 Pseudomonas savastanoi pv. phaseolicola strain 515 Contig_1, whole genome shotgun sequence
GCF_003413145.1_ASM341314v1	NZ_QPAT01000001.1 Pseudomonas savastanoi pv. phaseolicola strain 513 Contig_1, whole genome shotgun sequence
GCF_003413155.1_ASM341315v1	NZ_QPAS01000001.1 Pseudomonas savastanoi pv. phaseolicola strain 512 Contig_1, whole genome shotgun sequence
GCF_003413175.1_ASM341317v1	NZ_QPAR01000001.1 Pseudomonas savastanoi pv. phaseolicola strain 511 Contig_1, whole genome shotgun sequence
GCF_003413195.1_ASM341319v1	NZ_QPAQ01000001.1 Pseudomonas savastanoi pv. phaseolicola strain 510 Contig_1, whole genome shotgun sequence
GCF_003413225.1_ASM341322v1	NZ_QPAP01000001.1 Pseudomonas savastanoi pv. phaseolicola strain 509 Contig_1, whole genome shotgun sequence
GCF_003413235.1_ASM341323v1	NZ_QPAO01000001.1 Pseudomonas savastanoi pv. phaseolicola strain 508 Contig_1, whole genome shotgun sequence
GCF_003413245.1_ASM341324v1	NZ_QPAN01000001.1 Pseudomonas savastanoi pv. phaseolicola strain 507 Contig_1, whole genome shotgun sequence
GCF_003413305.1_ASM341330v1	NZ_QPBK01000001.1 Pseudomonas savastanoi pv. phaseolicola strain 530 Contig_1, whole genome shotgun sequence
GCF_003413325.1_ASM341332v1	NZ_QPBA01000001.1 Pseudomonas savastanoi pv. phaseolicola strain 520 Contig_1, whole genome shotgun sequence
GCF_003413345.1_ASM341334v1	NZ_QPAY01000001.1 Pseudomonas savastanoi pv. phaseolicola strain 518 Contig_1, whole genome shotgun sequence
GCF_003413365.1_ASM341336v1	NZ_QPBI01000001.1 Pseudomonas savastanoi pv. phaseolicola strain 528 Contig_1, whole genome shotgun sequence
GCF_003413375.1_ASM341337v1	NZ_QPBG01000001.1 Pseudomonas savastanoi pv. phaseolicola strain 526 Contig_1, whole genome shotgun sequence
GCF_003413385.1_ASM341338v1	NZ_QPAX01000001.1 Pseudomonas savastanoi pv. phaseolicola strain 517 Contig_1, whole genome shotgun sequence
GCF_003413425.1_ASM341342v1	NZ_QPAU01000001.1 Pseudomonas savastanoi pv. phaseolicola strain 514 Contig_1, whole genome shotgun sequence
GCF_003413445.1_ASM341344v1	NZ_QPAM01000001.1 Pseudomonas savastanoi pv. phaseolicola strain 506 Contig_1, whole genome shotgun sequence
GCF_003415755.1_ASM341575v1	NZ_QPDX01000001.1 Pseudomonas amygdali pv. tabaci strain 478 Contig_1, whole genome shotgun sequence
GCF_003415785.1_ASM341578v1	NZ_QPDP01000001.1 Pseudomonas amygdali pv. tabaci strain 469 Contig_1, whole genome shotgun sequence
GCF_003416145.1_ASM341614v1	NZ_QPDZ01000001.1 Pseudomonas amygdali pv. tabaci strain 480 Contig_1, whole genome shotgun sequence
GCF_003416165.1_ASM341616v1	NZ_QPDY01000001.1 Pseudomonas amygdali pv. tabaci strain 479 Contig_1, whole genome shotgun sequence
GCF_003416255.1_ASM341625v1	NZ_QPDO01000001.1 Pseudomonas coronafaciens pv. garcae strain 467 Contig_1, whole genome shotgun sequence

GCF_003416585.1_ASM341658v1	NZ_QPCR01000001.1 Pseudomonas amygdali pv. tabaci strain 440 Contig_1, whole genome shotgun sequence
GCF_003699045.1_ASM369904v1	NZ_RBOH01000327.1 Pseudomonas amygdali pv. lachrymans strain YM8003 PlaYM8003_Contig_1, whole genome shotgun sequence
GCF_003699095.1_ASM369909v1	NZ_RBOL01000350.1 Pseudomonas savastanoi pv. glycinea strain ICMP 4402 PgyICMP4402_Contig_1, whole genome shotgun sequence
GCF_003699125.1_ASM369912v1	NZ_RBOT01000781.1 Pseudomonas savastanoi pv. glycinea strain ICMP 10449 PgyICMP10449_Contig_1, whole genome shotgun sequence
GCF_003699215.1_ASM369921v1	NZ_RBPF01000190.1 Pseudomonas savastanoi pv. savastanoi strain ICMP 1411 PsvICMP1411_Contig_1, whole genome shotgun sequence
GCF_003699255.1_ASM369925v1	NZ_RBNM01000403.1 Pseudomonas savastanoi pv. retacarpa strain ICMP 16947 PreICMP16947_Contig_1, whole genome shotgun sequence
GCF_003699315.1_ASM369931v1	NZ_RBNP01000406.1 Pseudomonas savastanoi pv. glycinea strain ICMP 9589 PgyICMP9589_Contig_1, whole genome shotgun sequence
GCF_003699365.1_ASM369936v1	NZ_RBNW01000134.1 Pseudomonas savastanoi pv. savastanoi strain ICMP 13519 PsvICMP13519_Contig_1, whole genome shotgun sequence
GCF_003699395.1_ASM369939v1	NZ_RBNY01000535.1 Pseudomonas savastanoi strain 0485_9 Psv0485_9_Contig_1, whole genome shotgun sequence
GCF_003699405.1_ASM369940v1	NZ_RBNX01000242.1 Pseudomonas amygdali pv. tabaci strain ICMP 2851 PtaICMP2851_Contig_1, whole genome shotgun sequence
GCF_003699425.1_ASM369942v1	NZ_RBNZ01000315.1 Pseudomonas savastanoi pv. glycinea strain ICMP 807 PgyICMP807_Contig_1, whole genome shotgun sequence
GCF_003699445.1_ASM369944v1	NZ_RBOA01000314.1 Pseudomonas amygdali pv. eriobotryae strain ICMP 8636 PerICMP8636_Contig_1, whole genome shotgun sequence
GCF_003699565.1_ASM369956v1	NZ_RBOM01000136.1 Pseudomonas savastanoi pv. glycinea strain ICMP 4332 PgyICMP4332_Contig_1, whole genome shotgun sequence
GCF_003699605.1_ASM369960v1	NZ_RBON01000214.1 Pseudomonas savastanoi pv. glycinea strain ICMP 4324 PgyICMP4324_Contig_1, whole genome shotgun sequence
GCF_003699675.1_ASM369967v1	NZ_RBOQ01000119.1 Pseudomonas savastanoi pv. glycinea strain ICMP 5928 PgyICMP5928_Contig_1, whole genome shotgun sequence
GCF_003699685.1_ASM369968v1	NZ_RBOR01001296.1 Pseudomonas savastanoi pv. glycinea strain ICMP 10451 PgyICMP10451_Contig_1, whole genome shotgun sequence
GCF_003699695.1_ASM369969v1	NZ_RBOS01000890.1 Pseudomonas savastanoi pv. glycinea strain ICMP 10450 PgyICMP10450_Contig_1, whole genome shotgun sequence
GCF_003699735.1_ASM369973v1	NZ_RBOU01001066.1 Pseudomonas savastanoi pv. glycinea strain ICMP 10448 PgyICMP10448_Contig_1, whole genome shotgun sequence
GCF_003699855.1_ASM369985v1	NZ_RBPD01000097.1 Pseudomonas amygdali pv. hibisci strain ICMP 9314 PhiICMP9314_Contig_1, whole genome shotgun sequence
GCF_003700005.1_ASM370000v1	NZ_RBPS01000194.1 Pseudomonas savastanoi pv. glycinea strain ICMP 6372 PgyICMP6372_Contig_1, whole genome shotgun sequence
GCF_003700095.1_ASM370009v1	NZ_RBQD01000020.1 Pseudomonas amygdali pv. morsprunorum strain ICMP 3897 PmpICMP3897_Contig_1, whole genome shotgun sequence
GCF_003700145.1_ASM370014v1	NZ_RBQM01000278.1 Pseudomonas savastanoi pv. retacarpa strain ICMP 16946 PreICMP16946_Contig_1, whole genome shotgun sequence
GCF_003700195.1_ASM370019v1	NZ_RBQN01000413.1 Pseudomonas savastanoi pv. glycinea strain ICMP 4180 PgyICMP4180_Contig_1, whole genome shotgun sequence

GCF_003700245.1_ASM370024v1	NZ_RBQV01000141.1 Pseudomonas savastanoi pv. glycinea strain ICMP 5560 PgyICMP5560_Contig_1, whole genome shotgun sequence
GCF_003700295.1_ASM370029v1	NZ_RBRG01000090.1 Pseudomonas savastanoi pv. phaseolicola strain ICMP 637 PphICMP637_Contig_1, whole genome shotgun sequence
GCF_003700305.1_ASM370030v1	NZ_RBRK01000090.1 Pseudomonas viridiflava strain ICMP 11296 PvrICMP11296_Contig_1, whole genome shotgun sequence
GCF_003700335.1_ASM370033v1	NZ_RBQZ01000110.1 Pseudomonas viridiflava strain ICMP 3272 PvrICMP3272_Contig_1, whole genome shotgun sequence
GCF_003700395.1_ASM370039v1	NZ_RBRM01000557.1 Pseudomonas savastanoi pv. glycinea strain ICMP 4631 PgyICMP4631_Contig_1, whole genome shotgun sequence
GCF_003700405.1_ASM370040v1	NZ_RBRZ01000042.1 Pseudomonas syringae pv. actinidiae strain ICMP 19198 PsaICMP19198_Contig_1, whole genome shotgun sequence
GCF_003700425.1_ASM370042v1	NZ_RBRW01000279.1 Pseudomonas amygdali pv. mori strain ICMP 4468 PmoICMP4468_Contig_1, whole genome shotgun sequence
GCF_003700445.1_ASM370044v1	NZ_RBSA01000336.1 Pseudomonas savastanoi pv. fraxini strain ICMP 9129 PfrICMP9129_Contig_1, whole genome shotgun sequence
GCF_003700495.1_ASM370049v1	NZ_RBSL01000502.1 Pseudomonas savastanoi strain ICMP 13685 PbrICMP13685_Contig_1, whole genome shotgun sequence
GCF_003700505.1_ASM370050v1	NZ_RBSE01000004.1 Pseudomonas amygdali pv. tabaci strain ICMP 2812 PtaICMP2812_Contig_1, whole genome shotgun sequence
GCF_003700615.1_ASM370061v1	NZ_RBPP01000074.1 Pseudomonas amygdali pv. morsprunorum strain ICMP 568 PmpICMP568_Contig_1, whole genome shotgun sequence
GCF_003700625.1_ASM370062v1	NZ_RBPO01000311.1 Pseudomonas savastanoi pv. phaseolicola strain ICMP 5059 PphICMP5059_Contig_1, whole genome shotgun sequence
GCF_003700655.1_ASM370065v1	NZ_RBPT01000337.1 Pseudomonas savastanoi pv. glycinea strain ICMP 867 PgyICMP867_Contig_1, whole genome shotgun sequence
GCF_003700695.1_ASM370069v1	NZ_RBPR01000078.1 Pseudomonas savastanoi pv. glycinea strain ICMP 6373 PgyICMP6373_Contig_1, whole genome shotgun sequence
GCF_003700715.1_ASM370071v1	NZ_RBPV01000429.1 Pseudomonas amygdali pv. eriobotryae strain ICMP 4316 PerICMP4316_Contig_1, whole genome shotgun sequence
GCF_003700805.1_ASM370080v1	NZ_RBQE01000408.1 Pseudomonas syringae pv. persicae strain ICMP 3706 PpeICMP3706_Contig_1, whole genome shotgun sequence
GCF_003700985.1_ASM370098v1	NZ_RBQU01000269.1 Pseudomonas savastanoi pv. glycinea strain ICMP 5562 PgyICMP5562_Contig_1, whole genome shotgun sequence
GCF_003701015.1_ASM370101v1	NZ_RBQT01000029.1 Pseudomonas syringae pv. actinidiae strain ICMP 19589 PsaICMP19589_Contig_1, whole genome shotgun sequence
GCF_003701035.1_ASM370103v1	NZ_RBQW01000372.1 Pseudomonas savastanoi pv. glycinea strain ICMP 5559 PgyICMP5559_Contig_1, whole genome shotgun sequence
GCF_003701045.1_ASM370104v1	NZ_RBQY01000031.1 Pseudomonas savastanoi pv. glycinea strain ICMP 4181 PgyICMP4181_Contig_1, whole genome shotgun sequence
GCF_003701095.1_ASM370109v1	NZ_RBQX01000111.1 Pseudomonas savastanoi pv. glycinea strain ICMP 4182 PgyICMP4182_Contig_1, whole genome shotgun sequence
GCF_003701155.1_ASM370115v1	NZ_RBRH01000256.1 Pseudomonas savastanoi pv. glycinea strain ICMP 2185 PgyICMP2185_Contig_1, whole genome shotgun sequence
GCF_003701185.1_ASM370118v1	NZ_RBRD01000236.1 Pseudomonas amygdali pv. mori strain ICMP 535 PmoICMP535_Contig_1, whole genome shotgun sequence

GCF_003701195.1_ASM370119v1	NZ_RBRF01000209.1 Pseudomonas savastanoi pv. glycinea strain ICMP 5378 PgyICMP5378_Contig_1, whole genome shotgun sequence
GCF_003701265.1_ASM370126v1	NZ_RBRN01000296.1 Pseudomonas savastanoi pv. glycinea strain ICMP 4630 PgyICMP4630_Contig_1, whole genome shotgun sequence
GCF_003701335.1_ASM370133v1	NZ_RBRS01000185.1 Pseudomonas amygdali pv. ulmi strain ICMP 5931 PumICMP5931_Contig_1, whole genome shotgun sequence
GCF_003701385.1_ASM370138v1	NZ_RBRU01000029.1 Pseudomonas savastanoi pv. glycinea strain ICMP 2400 PgyICMP2400_Contig_1, whole genome shotgun sequence
GCF_003701475.1_ASM370147v1	NZ_RBSB01000011.1 Pseudomonas savastanoi pv. fraxini strain ICMP 9132 PfrICMP9132_Contig_1, whole genome shotgun sequence
GCF_003701485.1_ASM370148v1	NZ_RBSC01000183.1 Pseudomonas savastanoi pv. fraxini strain ICMP 7712 PfrICMP7712_Contig_1, whole genome shotgun sequence
GCF_003701515.1_ASM370151v1	NZ_RBSF01000068.1 Pseudomonas savastanoi pv. glycinea strain ICMP 9923 PgyICMP9923_Contig_1, whole genome shotgun sequence
GCF_003701585.1_ASM370158v1	NZ_RBSN01000066.1 Pseudomonas ficuserectae strain ICMP 7850 PfiICMP7850_Contig_1, whole genome shotgun sequence
GCF_003701615.1_ASM370161v1	NZ_RBSO01000342.1 Pseudomonas ficuserectae strain ICMP 7849 PfiICMP7849_Contig_1, whole genome shotgun sequence
GCF_003701695.1_ASM370169v1	NZ_RBSV01000277.1 Pseudomonas savastanoi strain ICMP 13927 PceICMP13927_Contig_1, whole genome shotgun sequence
GCF_003701705.1_ASM370170v1	NZ_RBSW01000164.1 Pseudomonas savastanoi strain ICMP 9421 PcsICMP9421_Contig_1, whole genome shotgun sequence
GCF_003701725.1_ASM370172v1	NZ_RBSU01000132.1 Pseudomonas savastanoi strain ICMP 13928 PceICMP13928_Contig_1, whole genome shotgun sequence
GCF_003701775.1_ASM370177v1	NZ_RBSX01000259.1 Pseudomonas savastanoi strain ICMP 9420 PcsICMP9420_Contig_1, whole genome shotgun sequence
GCF_003701815.1_ASM370181v1	NZ_RBTB01000096.1 Pseudomonas amygdali pv. lachrymans strain N7512 PlaN7512_Contig_1, whole genome shotgun sequence
GCF_003701825.1_ASM370182v1	NZ_RBTC01000076.1 Pseudomonas savastanoi pv. phaseolicola strain KN86 PphKN86_Contig_1, whole genome shotgun sequence
GCF_003701865.1_ASM370186v1	NZ_RBTE01000204.1 Pseudomonas savastanoi strain ICMP 13684 PbrICMP13684_Contig_1, whole genome shotgun sequence
GCF_003701915.1_ASM370191v1	NZ_RBTI01000034.1 Pseudomonas savastanoi strain ICMP 17525 PceICMP17525_Contig_1, whole genome shotgun sequence
GCF_003701955.1_ASM370195v1	NZ_RBTJ01000074.1 Pseudomonas amygdali pv. myricae strain ICMP 7120 PmyICMP7120_Contig_1, whole genome shotgun sequence
GCF_003701975.1_ASM370197v1	NZ_RBTN01000340.1 Pseudomonas savastanoi pv. nerii strain ICMP 13786 PneICMP13786_Contig_1, whole genome shotgun sequence
GCF_003702035.1_ASM370203v1	NZ_RBTO01000205.1 Pseudomonas savastanoi pv. nerii strain ICMP 13781 PneICMP13781_Contig_1, whole genome shotgun sequence
GCF_003702085.1_ASM370208v1	NZ_RBTS01000168.1 Pseudomonas amygdali pv. sesami strain ICMP 4995 PseICMP4995_Contig_1, whole genome shotgun sequence
GCF_003702125.1_ASM370212v1	NZ_RBTU01000277.1 Pseudomonas savastanoi pv. glycinea strain ICMP 9026 PgyICMP9026_Contig_1, whole genome shotgun sequence
GCF_003702145.1_ASM370214v1	NZ_RBTV01000661.1 Pseudomonas savastanoi pv. glycinea strain ICMP 9025 PgyICMP9025_Contig_1, whole genome shotgun sequence

GCF_003702155.1_ASM370215v1	NZ_RBTW01000212.1 Pseudomonas amygdali pv. lachrymans strain ICMP 3402 PlaICMP3402_Contig_1, whole genome shotgun sequence
GCF_003702205.1_ASM370220v1	NZ_RBTY01000035.1 Pseudomonas amygdali pv. morsprunorum strain ICMP 4983 PmpICMP4983_Contig_1, whole genome shotgun sequence
GCF_003702255.1_ASM370225v1	NZ_RBTD01000306.1 Pseudomonas amygdali pv. mori strain ICMP 6941 PmoICMP6941_Contig_1, whole genome shotgun sequence
GCF_003702295.1_ASM370229v1	NZ_RBTR01000036.1 Pseudomonas amygdali pv. sesami strain ICMP 3386 PseICMP3386_Contig_1, whole genome shotgun sequence
GCF_003702335.1_ASM370233v1	NZ_RBUB01000065.1 Pseudomonas savastanoi pv. nerii strain ICMP 16944 PneICMP16944_Contig_1, whole genome shotgun sequence
GCF_003702375.1_ASM370237v1	NZ_RBUC01000207.1 Pseudomonas savastanoi pv. glycinea strain ICMP 5027 PgyICMP5027_Contig_1, whole genome shotgun sequence
GCF_003702805.1_ASM370280v1	NZ_RBUW01000636.1 Pseudomonas savastanoi pv. glycinea strain ICMP 4333 PgyICMP4333_Contig_1, whole genome shotgun sequence
GCF_003702845.1_ASM370284v1	NZ_RBUD01001073.1 Pseudomonas savastanoi pv. glycinea strain ICMP 4966 PgyICMP4966_Contig_1, whole genome shotgun sequence
GCF_003702925.1_ASM370292v1	NZ_RBUL01000056.1 Pseudomonas amygdali pv. myricae strain ICMP 11510 PmyICMP11510_Contig_1, whole genome shotgun sequence
GCF_003702965.1_ASM370296v1	NZ_RBUM01000451.1 Pseudomonas savastanoi strain ICMP 11899 PcuICMP11899_Contig_1, whole genome shotgun sequence
GCF_003702975.1_ASM370297v1	NZ_RBUO01000374.1 Pseudomonas savastanoi strain ICMP 11895 PcuICMP11895_Contig_1, whole genome shotgun sequence
GCF_003702985.1_ASM370298v1	NZ_RBUN01000603.1 Pseudomonas savastanoi strain ICMP 11897 PcuICMP11897_Contig_1, whole genome shotgun sequence
GCF_003703025.1_ASM370302v1	NZ_RBUP01000255.1 Pseudomonas amygdali pv. myricae strain ICMP 11123 PmyICMP11123_Contig_1, whole genome shotgun sequence
GCF_003703035.1_ASM370303v1	NZ_RBUR01000158.1 Pseudomonas savastanoi pv. phaseolicola strain K4 PphK4_Contig_1, whole genome shotgun sequence
GCF_003703085.1_ASM370308v1	NZ_RBUU01000250.1 Pseudomonas amygdali pv. lachrymans strain ICMP 1448 PlaICMP1448_Contig_1, whole genome shotgun sequence
GCF_003703175.1_ASM370317v1	NZ_RBUZ01000002.1 Pseudomonas amygdali pv. sesami strain ICMP 7459 PseICMP7459_Contig_1, whole genome shotgun sequence
GCF_003703335.1_ASM370333v1	NZ_RBVH01000333.1 Pseudomonas savastanoi pv. glycinea strain ICMP 7082 PgyICMP7082_Contig_1, whole genome shotgun sequence
GCF_005937945.1_ASM593794v1	NZ_VCCG01000001.1 Pseudomonas sp. KBS0707 FCE86_1, whole genome shotgun sequence
GCF_005937945.2_ASM593794v2	NZ_CP041754.1 Pseudomonas sp. KBS0707 chromosome, complete genome
GCF_007352665.1_ASM735266v1	NZ_VKOF01000001.1 Pseudomonas sp. ST1 1, whole genome shotgun sequence
GCF_008502015.1_ASM850201v1	NZ_QUSH01000001.1 Pseudomonas savastanoi strain SBV_12848 Scaffold1, whole genome shotgun sequence
GCF_013911125.1_ASM1391112v1	NZ_JACERS010000001.1 Pseudomonas savastanoi pv. savastanoi strain UPN912 UPN912_1_(paired)_trimmed_(paired)_contig_1, whole genome shotgun sequence
GCF_014652995.1_ASM1465299v1	NZ_BMZW01000001.1 Pseudomonas amygdali pv. eriobotryae strain AM001 sequence001, whole genome shotgun sequence

GCF_014653015.1_ASM1465301v1	NZ_BMZX01000001.1 Pseudomonas amygdali pv. eriobotryae strain BM001 sequence001, whole genome shotgun sequence
GCF_014653035.1_ASM1465303v1	NZ_BMZY01000001.1 Pseudomonas amygdali pv. eriobotryae strain CG001 sequence001, whole genome shotgun sequence
GCF_014855475.1_ASM1485547v1	NZ_CP032456.1 Pseudomonas savastanoi strain CAS03 chromosome, complete genome
GCF_016307865.1_ASM1630786v1	NZ_JAEIKH010000001.1 Pseudomonas amygdali strain Kayisi_1_Pss_Erzin YA0086_1, whole genome shotgun sequence
GCF_016308165.1_ASM1630816v1	NZ_JAEIJR010000001.1 Pseudomonas amygdali strain Kaysi_meyve3 YA0032_1, whole genome shotgun sequence
GCF_017009525.1_ASM1700952v1	NZ_JAAFOY010000001.1 Pseudomonas savastanoi pv. phaseolicola strain T11544 T11544_000001, whole genome shotgun sequence
GCF_017009545.1_ASM1700954v1	NZ_JAAFOZ010000001.1 Pseudomonas savastanoi pv. phaseolicola strain K4287 K4287_000001, whole genome shotgun sequence
GCF_017140835.1_ASM1714083v1	NZ_JAANQA010000001.1 Pseudomonas savastanoi pv. phaseolicola strain race 5 R5_1, whole genome shotgun sequence
GCF_017140875.1_ASM1714087v1	NZ_JAANPZ010000001.1 Pseudomonas savastanoi pv. phaseolicola strain race 8 R8_1, whole genome shotgun sequence
GCF_900235815.1_CFBP3840	NZ_LT963409.1 Pseudomonas syringae isolate CFBP3840 chromosome 1, complete sequence
GCF_900235885.1_CFBP6109	NZ_LT963391.1 Pseudomonas syringae pv. cerasicola isolate CFBP6109 chromosome 1, complete sequence
GCF_900289125.1_CFBP2116	NZ_LT985192.1 Pseudomonas syringae strain CFBP 2116 chromosome 1, complete sequence
GCF_900289135.1_CFBP6110chr	NZ_OLMP01000002.1 Pseudomonas syringae pv. cerasicola strain CFBP 6110, whole genome shotgun sequence

Supplementary table S6
Number of statistically significant matches for each effector/effector family where more than 2 matches were found in at least one of the genomes queried. (-1 = no match found, = no statistically significant match found).

	Hrpa	hrpk1	hopw	hopw1	hopab2	hopab3	hopac1	hrpb	hopaf1	shcf	hopf3	hopq1	hopg1	avre	avre1	hopr1
1302A	3	1	1	2	2	2	2	2	1	1	1	1	1	1	1	1
14290_2159Pspp hisolate61race8	3	1	1	2	2	2	2	2	1	1	1	1	1	1	1	1
14291_2160Pspp hisolate432race6	3	1	1	2	2	2	2	2	-1	1	1	1	1	1	1	1
14292_2213Pspp hisolate9112race6	3	1	1	2	2	2	2	2	-1	1	1	1	1	1	1	1
14293_2214Pspp hisolate923race6	3	1	1	2	2	2	2	2	-1	1	1	1	1	1	1	1
14300_2239Pspp hisolate331race1	3	1	1	2	2	2	2	2	1	2	2	1	1	1	1	1
14301_2244Pspp hisolate41race1	3	1	1	2	2	2	2	2	1	2	2	1	1	1	1	1
14302_2248Pspp hisolate1221race1	3	1	1	2	2	2	2	2	1	2	2	1	1	1	1	1
14303_2163Pspp hisolate5111race1	3	1	1	2	2	2	2	2	1	2	2	1	1	1	1	1
14304_2169Pspp hisolate8022race8	3	1	1	2	2	2	2	2	1	1	1	1	1	1	1	1
14305_2170Pspp hisolate811race8	3	1	1	2	2	2	2	2	1	1	1	1	1	1	1	1
14306_2218Pspp hisolate691race6	3	1	1	2	2	2	2	2	-1	1	1	1	1	1	1	1
14307_2226Pspp hisolate4633race6	3	1	1	2	2	2	2	2	-1	1	1	1	1	1	1	1
14308_2230Pspp hisolate612race6	3	1	1	2	2	2	2	2	-1	1	1	1	1	1	1	1
14309_2217Pspp hisolate672race6	4	1	0	1	2	0	2	5	-1	-1	-1	1	1	3	3	3
14310_2227Pspp hisolate4712race6	3	1	1	2	2	2	2	2	-1	1	1	1	1	1	1	1
14311_2228Pspp hisolate4732race6	3	1	1	2	2	2	2	2	-1	1	1	1	1	1	1	1

14312_2231Pspp hisolate182race6	3	1	1	2	2	2	2	2	-1	1	1	1	1	1	1	1
14313_2232Pspp hisolate183race6	3	1	1	2	2	2	2	2	-1	1	1	1	1	1	1	1
14314_2233Pspp hisolate241race6	3	1	1	2	2	2	2	2	-1	1	1	1	1	1	1	1
14315_2241Pspp hisolate22race6	3	1	1	2	2	2	2	2	-1	1	1	1	1	1	1	1
14316_2242Pspp hisolate23race6	3	1	1	2	2	2	2	2	-1	1	1	1	1	1	1	1
14317_2243Pspp hisolate31race6	3	1	1	2	2	2	2	2	-1	1	1	1	1	1	1	1
14318_2247Pspp hisolate102race6	3	1	1	2	2	2	2	2	-1	1	1	1	1	1	1	1
14319_2178	3	1	1	2	2	2	2	2	-1	1	1	1	1	1	1	1
1448A	3	1	1	3	2	2	2	2	1	1	1	1	1	1	1	1
7840_Pph2709a	3	1	1	2	2	2	2	2	1	2	2	1	1	1	1	1
7841_Pph2656a	3	1	1	2	2	2	2	2	1	1	1	1	1	1	1	1
7843_Pph1375a	3	1	1	1	1	1	1	2	1	2	2	1	1	1	1	1
7844_Pph1301a	3	1	1	2	2	1	2	2	1	1	1	1	1	1	1	1
7845_Pph1281a	3	1	1	2	2	2	2	2	1	2	2	1	1	1	1	1
GCA_001723935.1	3	1	1	1	1	1	2	2	-1	0	-1	-1	-1	1	1	1
GCA_003700865.1	8	1	1	2	1	1	2	8	1	1	1	-1	-1	2	2	-1
GCA_003701325.1	8	1	1	3	1	1	2	7	1	1	-1	1	0	3	3	2
GCA_003701635.1	4	1	1	1	1	1	1	3	2	3	2	1	2	3	3	1
GCA_003703215.1	11	1	1	1	1	1	3	10	-1	1	1	-1	-1	3	3	4
GCA_004351915.1	-1	0	-1	-1	-1	-1	-1	0	-1	-1	-1	-1	-1	-1	-1	-1
GCA_004352025.1	2	0	-1	-1	-1	-1	-1	1	-1	-1	-1	-1	-1	-1	-1	-1
GCA_004352155.1	1	-1	-1	-1	-1	-1	-1	1	-1	-1	-1	-1	-1	-1	-1	-1
GCA_004352245.1	2	-1	0	-1	-1	-1	-1	2	0	-1	-1	-1	-1	-1	-1	-1
GCA_004352255.1	3	-1	0	-1	-1	-1	-1	2	-1	-1	-1	-1	-1	-1	-1	-1
GCA_004352425.1	1	-1	-1	-1	-1	-1	-1	1	-1	-1	-1	-1	-1	-1	-1	-1
GCA_014653325.1	3	3	1	3	-1	-1	5	3	2	2	1	1	-1	3	6	6

GCF_000012205.1	3	1	1	3	2	2	2	2	1	1	1	1	1	1	1	1
GCF_000143005.1	9	1	1	2	1	1	2	6	-1	4	-1	1	1	1	1	2
GCF_000145685.1	5	1	1	1	1	1	1	4	0	2	1	1	1	1	1	1
GCF_000145765.1	8	1	1	1	3	3	2	7	2	3	3	1	2	2	2	1
GCF_000145945.1	3	1	2	2	1	1	1	2	-1	1	1	-1	-1	1	1	2
GCF_000145945.2	3	1	5	5	1	1	1	2	-1	1	1	-1	-1	1	1	1
GCF_000146005.1	5	1	1	2	1	1	1	4	1	0	-1	-1	-1	1	1	-1
GCF_000146005.2	5	1	1	2	1	1	1	4	2	0	-1	-1	-1	1	1	-1
GCF_000159835.1	4	1	2	2	1	1	1	3	-1	1	1	-1	-1	2	2	1
GCF_000159835.2	4	1	2	2	1	1	1	3	-1	1	1	-1	-1	2	2	3
GCF_000163255.1	5	1	1	1	1	1	2	4	1	2	2	1	1	1	1	1
GCF_000163275.1	3	1	1	4	1	1	2	2	1	1	1	1	1	1	1	1
GCF_000164015.2	3	1	1	3	1	1	1	2	2	1	0	1	1	1	1	1
GCF_000164015.3	3	1	1	3	1	1	1	2	2	1	0	1	1	1	1	1
GCF_000187045.1	4	1	1	1	1	1	2	3	1	0	-1	1	1	1	1	1
GCF_000187065.1	4	1	1	2	1	1	2	3	-1	0	-1	1	1	1	1	1
GCF_000225805.1	3	1	1	1	1	1	2	3	2	2	1	1	1	2	2	2
GCF_000275945.1	3	1	2	2	2	1	2	2	-1	0	-1	-1	-1	1	2	2
GCF_000732035.1	5	1	1	3	2	2	2	4	2	2	0	1	1	1	1	1
GCF_000751155.1	5	1	1	3	2	2	2	4	2	2	0	1	1	1	1	1
GCF_000934645.1	4	1	2	2	1	1	1	3	-1	2	2	-1	-1	1	1	2
GCF_000935645.1	3	1	1	1	1	1	2	2	0	2	3	1	-1	1	1	1
GCF_000935665.1	3	1	1	1	0	0	1	2	3	3	1	1	1	1	1	1

GCF_000935675.1	4	1	1	1	1	1	2	3	0	1	-1	1	1	1	1	1
GCF_000935695.1	5	1	1	3	3	1	2	4	1	2	0	1	1	1	1	1
GCF_000935735.1	3	1	1	1	1	1	1	2	1	4	2	1	1	1	1	2
GCF_001006445.1	3	1	1	2	1	1	1	2	1	1	1	-1	-1	1	1	-1
GCF_001006455.1	3	1	2	2	1	1	1	2	-1	1	1	-1	-1	1	1	1
GCF_001293725.1	5	1	1	3	2	1	2	4	1	2	0	1	1	1	1	1
GCF_001293765.1	4	1	1	1	1	1	2	3	1	0	0	1	1	1	1	1
GCF_001293825.1	5	1	1	2	1	1	1	4	1	0	-1	-1	-1	2	2	-1
GCF_001293845.1	3	1	1	2	1	1	1	2	1	1	1	-1	-1	1	1	-1
GCF_001293975.1	3	1	1	2	2	2	2	2	1	1	1	1	1	1	1	1
GCF_001293985.1	4	1	1	1	1	1	3	3	1	2	-1	1	1	1	1	1
GCF_001294025.1	6	2	2	4	4	4	4	4	2	2	2	2	2	2	2	2
GCF_001294035.1	3	1	1	2	2	2	2	2	1	1	1	1	1	1	1	1
GCF_001294065.1	3	1	1	1	2	2	2	2	1	3	2	-1	2	2	2	1
GCF_001294105.1	3	1	1	2	2	2	2	2	1	1	1	1	1	2	2	1
GCF_001294115.1	3	1	1	1	1	1	2	2	-1	2	1	1	-1	1	1	1
GCF_001294185.1	3	1	1	1	1	1	1	2	1	1	1	-1	2	1	1	1
GCF_001294195.1	4	1	1	1	1	1	2	3	1	0	-1	1	1	2	2	1
GCF_001294215.1	4	1	1	1	-1	-1	1	3	0	1	0	1	-1	1	1	1
GCF_001294265.1	4	1	1	1	1	1	2	3	1	0	-1	1	1	1	1	1
GCF_001294275.1	4	1	1	1	1	1	2	3	1	1	-1	1	1	2	2	1
GCF_001400115.1	3	1	1	1	1	1	1	2	-1	1	1	-1	-1	1	1	-1
GCF_001400215.1	3	1	1	2	-1	-1	3	2	4	2	3	-1	-1	1	1	1

GCF_001400275.1	3	1	1	1	-1	-1	1	2	2	3	0	1	1	1	1	2
GCF_001400285.1	3	1	1	1	1	1	1	2	1	3	1	1	-1	1	1	2
GCF_001400375.1	4	1	1	2	1	1	2	3	1	1	-1	1	1	1	1	1
GCF_001400395.1	3	1	2	3	1	1	1	2	-1	1	1	-1	-1	1	1	-1
GCF_001400415.1	2	1	1	1	1	1	1	2	2	3	2	1	2	1	1	1
GCF_001400435.1	3	1	1	1	1	1	1	2	1	4	2	1	1	1	1	1
GCF_001400455.1	5	1	1	1	1	1	2	4	2	1	1	1	-1	2	2	2
GCF_001400475.1	6	1	1	3	2	1	2	5	-1	0	-1	-1	-1	3	3	2
GCF_001400515.1	2	1	1	1	1	1	2	2	0	1	-1	1	1	1	1	2
GCF_001400525.1	4	1	1	1	2	2	1	4	1	1	1	1	2	1	1	1
GCF_001400555.1	5	1	1	1	1	1	3	4	4	3	0	1	2	1	1	1
GCF_001400575.1	4	1	1	3	1	1	2	3	2	1	0	1	1	1	1	2
GCF_001400605.1	3	1	1	2	2	2	2	2	1	2	2	1	1	1	1	1
GCF_001400675.1	4	1	1	1	1	1	3	4	1	2	2	1	1	2	2	1
GCF_001400715.1	1	1	1	2	1	1	1	1	-1	0	-1	1	-1	1	1	3
GCF_001400755.1	3	1	1	2	1	1	1	2	2	0	0	0	1	1	1	1
GCF_001400795.1	3	1	1	1	1	1	2	2	1	0	-1	1	1	2	2	1
GCF_001400815.1	2	1	1	1	2	2	2	2	-1	0	-1	1	2	1	1	2
GCF_001400875.1	3	1	1	1	1	1	1	3	-1	1	1	-1	-1	1	1	-1
GCF_001400935.1	4	1	1	3	1	1	1	4	2	2	2	1	-1	1	1	1
GCF_001400995.1	3	1	2	2	0	0	1	2	2	1	-1	-1	2	1	1	2
GCF_001401095.1	3	1	2	2	1	1	1	2	-1	1	1	-1	-1	1	1	1
GCF_001401165.1	5	1	2	2	1	1	3	4	2	-1	0	1	1	1	1	1

GCF_001401265.1	3	1	1	1	1	1	2	2	-1	2	1	1	-1	1	1	1
GCF_001401285.1	5	1	1	4	2	2	2	4	1	2	0	1	1	1	1	1
GCF_001466905.1	3	1	0	0	-1	-1	1	2	-1	0	-1	-1	-1	1	1	-1
GCF_001467105.1	3	1	0	0	-1	-1	1	2	-1	0	-1	-1	-1	1	1	-1
GCF_001467115.1	3	1	0	0	-1	-1	1	2	-1	0	-1	-1	-1	1	1	-1
GCF_001483545.1	5	1	1	3	1	1	1	4	1	2	1	1	1	1	1	1
GCF_001535735.1	3	1	1	1	0	0	2	2	2	3	3	1	-1	1	1	1
GCF_001535785.1	3	1	1	1	0	0	1	2	2	5	4	1	-1	1	1	1
GCF_001535805.1	4	1	1	1	1	1	3	3	3	3	0	1	2	1	1	1
GCF_001535815.1	4	1	1	3	1	1	1	3	2	1	0	1	1	1	1	2
GCF_001535835.1	3	1	2	2	0	0	1	2	2	1	-1	-1	2	1	1	2
GCF_001535915.1	5	1	2	2	1	1	3	4	2	-1	0	2	1	1	1	1
GCF_001537945.1	3	1	1	1	-1	-1	2	2	2	1	3	-1	-1	1	1	1
GCF_001537955.1	3	1	1	4	1	1	2	2	1	1	1	1	1	1	1	1
GCF_001537965.1	3	1	1	4	1	1	2	2	1	1	1	1	1	1	1	1
GCF_001537985.1	3	1	1	4	1	1	2	2	1	1	1	1	1	1	1	1
GCF_001538045.1	3	1	1	4	1	1	3	2	1	1	1	1	1	1	1	1
GCF_001538055.1	3	1	1	1	1	1	1	2	2	1	1	1	-1	1	1	1
GCF_001538085.1	3	1	1	4	1	1	2	2	1	1	1	1	1	1	1	1
GCF_001538145.1	3	1	1	1	1	1	1	2	1	4	2	1	1	1	1	2
GCF_001538155.1	5	1	1	3	1	1	1	4	1	2	1	1	1	1	1	1
GCF_001538185.1	3	1	1	4	1	1	2	2	1	1	1	1	1	1	1	1
GCF_001538205.1	2	1	1	1	1	1	1	1	-1	1	2	1	-1	1	1	1

GCF_001538245.1	3	1	1	1	1	1	1	2	1	3	1	1	-1	1	1	1
GCF_001538255.1	3	1	1	1	0	0	1	2	2	2	0	1	1	1	1	1
GCF_002068135.1	3	1	1	2	1	1	2	2	-1	0	-1	-1	-1	1	1	-1
GCF_002115545.1	4	1	1	3	1	1	1	3	2	1	2	1	-1	1	1	1
GCF_002269785.1	5	1	1	3	1	1	1	4	1	1	-1	1	1	1	1	1
GCF_002269885.1	3	1	1	3	1	1	1	2	1	2	0	1	1	1	1	1
GCF_002270015.1	4	1	1	3	1	1	1	3	1	2	0	1	1	1	1	1
GCF_002699855.1	4	1	1	1	1	1	2	3	1	2	2	1	-1	1	1	1
GCF_002699945.1	3	1	1	1	-1	-1	1	2	2	3	3	-1	-1	1	1	1
GCF_002700065.1	3	1	1	1	-1	-1	1	2	2	3	2	-1	-1	1	1	1
GCF_002736925.1	3	1	1	1	-1	-1	1	2	2	4	3	1	-1	1	1	1
GCF_002837595.1	4	1	1	2	1	1	1	3	2	0	-1	-1	-1	1	1	-1
GCF_002905685.1	3	1	1	1	0	0	1	2	2	4	2	1	-1	1	1	1
GCF_002905685.2	3	1	1	1	0	0	1	2	2	5	3	1	-1	1	1	1
GCF_002905735.1	3	1	1	1	0	0	1	2	2	5	3	1	-1	1	1	1
GCF_002905755.1	3	1	3	3	1	1	1	2	1	4	2	2	1	1	1	1
GCF_002905875.1	3	1	2	2	1	1	1	2	1	4	2	1	1	1	1	1
GCF_002905875.2	3	1	2	2	1	1	1	2	1	4	2	2	1	1	1	1
GCF_002905895.1	3	1	3	3	1	1	1	2	1	4	2	2	1	1	1	1
GCF_002905915.1	3	1	3	3	1	1	1	2	1	4	2	2	1	1	1	1
GCF_002916395.1	3	1	1	1	0	0	1	2	2	4	3	1	-1	1	1	1
GCF_002939205.1	7	1	1	2	1	1	2	6	1	4	3	1	-1	3	3	1
GCF_002939225.1	5	1	1	1	-1	-1	1	4	0	3	4	1	-1	1	1	1

GCF_002939245.1	3	1	2	2	1	1	2	2	1	4	3	1	-1	1	1	1
GCF_003205945.1	4	1	1	1	1	1	2	3	1	1	0	1	1	1	1	2
GCF_003412855.1	3	1	2	3	2	2	2	2	2	1	1	1	1	1	1	1
GCF_003412865.1	3	1	1	2	2	2	2	2	1	1	1	1	1	1	1	2
GCF_003412905.1	2	1	1	2	2	2	2	2	1	1	1	1	1	2	2	2
GCF_003412915.1	3	1	1	2	2	2	2	2	1	1	1	1	1	2	2	2
GCF_003412965.1	3	1	1	2	2	2	2	2	1	1	1	1	1	1	1	1
GCF_003412985.1	3	1	1	2	2	2	2	2	1	1	1	1	1	1	1	1
GCF_003412995.1	3	1	1	2	2	2	2	2	1	1	1	1	1	1	1	1
GCF_003413015.1	3	1	1	2	2	2	2	2	1	1	1	1	1	1	1	1
GCF_003413035.1	3	1	1	2	2	2	2	2	1	1	1	1	1	1	1	1
GCF_003413065.1	3	1	1	2	2	2	3	2	1	1	1	1	1	1	1	3
GCF_003413075.1	2	1	1	2	2	2	2	2	1	1	1	1	1	1	1	1
GCF_003413095.1	3	1	1	3	2	2	2	2	1	1	1	1	1	1	1	2
GCF_003413115.1	3	1	2	3	2	2	2	2	2	1	1	1	1	1	1	1
GCF_003413145.1	3	1	2	3	2	2	2	2	2	1	1	1	1	1	1	1
GCF_003413155.1	3	1	2	3	2	2	2	2	2	1	1	1	1	1	1	1
GCF_003413175.1	3	1	2	3	2	2	2	2	2	1	1	1	1	1	1	1
GCF_003413195.1	3	1	2	3	2	2	2	2	2	1	1	1	1	1	1	1
GCF_003413225.1	3	1	2	3	2	2	2	2	1	1	1	1	1	1	1	1
GCF_003413235.1	3	1	2	3	2	2	2	2	1	1	1	1	1	1	1	1
GCF_003413245.1	3	1	2	3	2	2	2	2	2	1	1	1	1	1	1	1
GCF_003413305.1	3	1	2	3	2	2	2	2	2	1	1	1	1	1	1	1

GCF_003413325.1	3	1	1	2	2	2	3	2	1	1	1	1	1	1	1	2
GCF_003413345.1	3	1	2	3	2	2	2	2	2	1	1	1	1	2	2	1
GCF_003413365.1	3	1	2	3	2	2	2	2	2	1	1	1	1	1	1	1
GCF_003413375.1	3	1	1	2	2	2	2	2	1	1	1	1	1	1	1	1
GCF_003413385.1	3	1	1	2	2	2	2	2	1	1	1	1	1	1	1	2
GCF_003413425.1	3	1	2	3	2	2	2	2	2	1	1	1	1	1	1	1
GCF_003413445.1	3	1	1	2	2	2	2	2	1	1	1	1	1	1	1	1
GCF_003415755.1	3	1	1	1	1	1	1	2	-1	0	-1	-1	-1	1	1	1
GCF_003415785.1	3	1	1	1	1	1	1	2	-1	0	-1	-1	-1	1	1	1
GCF_003416145.1	3	1	1	1	1	1	1	2	-1	0	-1	-1	-1	1	1	1
GCF_003416165.1	3	1	1	1	1	1	1	2	-1	0	-1	-1	-1	1	1	1
GCF_003416255.1	3	1	1	1	1	1	1	2	-1	0	-1	-1	-1	1	1	1
GCF_003416585.1	3	1	1	1	1	1	1	2	-1	0	-1	1	-1	1	1	1
GCF_003699045.1	3	1	1	2	1	1	1	2	1	1	1	-1	-1	1	1	-1
GCF_003699095.1	4	1	1	3	2	1	3	3	1	1	0	1	1	1	1	2
GCF_003699125.1	5	1	1	3	-1	-1	3	4	-1	1	-1	1	1	2	2	1
GCF_003699215.1	3	1	1	4	1	1	1	2	2	1	0	1	1	1	1	1
GCF_003699255.1	5	1	1	4	1	1	1	4	2	2	2	1	-1	1	1	1
GCF_003699315.1	3	1	1	2	1	1	2	2	1	3	1	1	1	2	2	2
GCF_003699365.1	5	1	1	5	2	2	2	4	2	2	0	1	1	1	1	1
GCF_003699395.1	5	1	1	4	2	1	2	4	1	2	0	1	1	3	3	2
GCF_003699405.1	3	1	2	2	1	1	1	2	-1	0	-1	-1	-1	1	1	1
GCF_003699425.1	3	1	1	1	1	1	2	2	1	2	1	1	1	1	1	1

GCF_003699445.1	3	1	1	1	1	1	1	2	2	1	1	1	-1	1	1	1
GCF_003699565.1	3	1	1	2	2	2	2	2	1	2	2	1	1	2	2	2
GCF_003699605.1	3	1	1	1	1	1	1	2	1	2	2	1	2	1	1	1
GCF_003699675.1	4	1	1	1	1	1	2	3	1	1	-1	1	1	1	1	1
GCF_003699685.1	6	1	1	2	1	1	2	5	1	1	-1	1	1	2	2	2
GCF_003699695.1	7	1	1	3	1	1	2	6	1	1	0	1	1	1	1	1
GCF_003699735.1	4	1	1	3	1	1	2	3	1	1	-1	1	1	3	3	1
GCF_003699855.1	3	1	2	3	1	1	1	2	-1	1	1	-1	-1	1	1	-1
GCF_003700005.1	4	1	1	2	-1	-1	2	3	1	1	-1	-1	1	1	1	1
GCF_003700095.1	3	1	2	2	-1	-1	1	2	1	3	2	1	-1	1	1	1
GCF_003700145.1	5	1	1	3	1	1	1	4	1	2	2	1	-1	2	2	2
GCF_003700195.1	4	1	1	2	1	1	2	3	1	0	0	1	1	1	1	1
GCF_003700245.1	4	1	1	2	1	1	2	3	1	1	0	1	1	1	1	1
GCF_003700295.1	3	1	1	2	2	2	2	2	1	2	2	1	1	1	1	1
GCF_003700305.1	3	1	0	0	-1	-1	1	2	-1	0	-1	-1	-1	1	1	-1
GCF_003700335.1	3	1	0	0	-1	-1	1	2	-1	0	-1	-1	-1	1	1	-1
GCF_003700395.1	4	1	1	2	1	1	2	3	1	0	-1	1	1	1	1	1
GCF_003700405.1	3	1	0	0	-1	-1	1	2	-1	0	-1	-1	-1	1	1	-1
GCF_003700425.1	4	1	1	1	3	2	1	3	1	1	1	2	2	1	1	2
GCF_003700445.1	5	1	1	3	1	1	1	4	1	1	1	1	1	1	1	2
GCF_003700495.1	1	2	1	1	1	1	1	1	-1	1	1	1	-1	2	2	2
GCF_003700505.1	3	1	2	2	1	1	1	2	-1	0	-1	-1	-1	1	1	1
GCF_003700615.1	3	1	1	1	0	0	1	2	2	4	3	1	-1	1	1	1

GCF_003700625.1	2	1	1	1	1	0	1	1	2	2	1	1	1	1	1	2
GCF_003700655.1	4	1	1	2	1	1	2	3	-1	1	-1	1	1	1	1	1
GCF_003700695.1	3	1	1	2	-1	-1	2	3	1	1	-1	-1	1	1	1	1
GCF_003700715.1	4	1	1	1	1	1	1	4	2	1	1	1	-1	1	1	3
GCF_003700805.1	3	1	0	0	1	0	1	2	-1	0	1	-1	-1	1	1	-1
GCF_003700985.1	4	1	1	2	1	1	2	3	1	1	-1	1	1	1	1	1
GCF_003701015.1	3	1	0	-1	-1	-1	1	2	-1	0	-1	-1	-1	1	1	-1
GCF_003701035.1	4	1	1	2	1	1	2	3	1	1	-1	1	1	1	1	1
GCF_003701045.1	4	1	1	2	1	1	2	3	1	1	-1	1	1	1	1	1
GCF_003701095.1	4	1	1	2	1	1	2	3	1	1	-1	1	1	1	1	1
GCF_003701155.1	2	1	1	2	2	2	2	2	1	1	1	1	1	1	1	1
GCF_003701185.1	4	1	1	1	3	2	1	3	1	1	1	1	2	1	1	1
GCF_003701195.1	4	1	1	1	1	1	2	3	1	1	-1	1	1	1	1	1
GCF_003701265.1	4	1	1	1	1	1	2	3	1	1	-1	1	1	2	2	1
GCF_003701335.1	5	1	2	3	1	1	3	4	3	-1	0	1	1	1	1	1
GCF_003701385.1	4	1	1	1	1	1	2	4	1	1	-1	1	1	3	3	1
GCF_003701475.1	5	1	1	3	1	1	1	4	1	2	1	1	1	1	1	1
GCF_003701485.1	5	1	1	3	1	1	1	4	1	2	0	1	1	1	1	1
GCF_003701515.1	3	1	1	1	1	1	1	2	1	2	2	1	3	1	1	2
GCF_003701585.1	4	1	1	1	2	2	2	3	-1	0	-1	1	2	1	1	2
GCF_003701615.1	3	1	1	1	2	2	2	2	-1	0	-1	1	2	1	1	1
GCF_003701695.1	4	1	1	2	-1	-1	3	3	3	2	3	-1	-1	2	2	2
GCF_003701705.1	3	1	1	1	1	1	1	3	2	1	1	1	-1	1	1	1

GCF_003701725.1	3	1	1	1	-1	-1	2	2	3	2	3	-1	-1	1	1	1
GCF_003701775.1	3	1	1	1	1	1	1	2	1	3	1	1	-1	1	1	2
GCF_003701815.1	5	1	1	2	1	1	1	4	1	0	-1	-1	-1	1	1	-1
GCF_003701825.1	2	1	1	2	2	2	2	2	1	2	2	1	1	1	1	1
GCF_003701865.1	2	1	1	2	1	1	1	1	-1	1	1	1	-1	2	2	1
GCF_003701915.1	4	1	1	1	-1	-1	1	3	2	2	1	1	-1	1	1	1
GCF_003701955.1	4	1	1	1	1	1	3	3	2	2	-1	1	2	1	1	1
GCF_003701975.1	5	1	1	3	1	1	2	4	1	2	0	1	1	1	1	1
GCF_003702035.1	4	1	1	3	1	1	1	3	2	2	0	1	1	2	2	2
GCF_003702085.1	3	1	1	1	1	1	2	2	-1	2	1	1	-1	1	1	2
GCF_003702125.1	8	1	1	2	1	1	3	7	1	1	-1	1	1	1	1	2
GCF_003702145.1	5	1	1	3	1	1	3	4	1	1	-1	1	1	1	1	2
GCF_003702155.1	3	1	1	2	1	1	1	2	1	1	1	-1	-1	1	1	-1
GCF_003702205.1	3	1	1	2	0	0	1	2	2	4	3	1	-1	2	2	2
GCF_003702255.1	4	1	1	1	3	2	1	3	2	1	1	2	2	1	1	1
GCF_003702295.1	3	1	1	1	1	1	2	2	-1	2	1	-1	-1	1	1	1
GCF_003702335.1	3	1	1	3	1	1	2	2	2	2	0	1	1	1	1	1
GCF_003702375.1	4	1	1	2	1	1	2	3	1	1	-1	1	1	1	1	1
GCF_003702805.1	3	1	1	2	2	2	2	2	1	2	2	1	1	2	2	1
GCF_003702845.1	6	1	1	3	1	1	2	5	-1	1	-1	1	1	2	2	1
GCF_003702925.1	4	1	1	2	1	1	3	3	2	2	-1	1	2	1	1	1
GCF_003702965.1	2	1	1	1	1	1	1	2	1	0	-1	1	1	1	1	1
GCF_003702975.1	3	1	1	1	1	1	1	2	1	0	-1	1	1	2	2	2

GCF_003702985.1	4	1	1	2	1	1	4	3	1	0	-1	1	1	1	1	3
GCF_003703025.1	4	1	1	1	1	1	3	3	2	2	0	1	2	1	1	1
GCF_003703035.1	3	1	1	2	2	2	2	2	1	3	2	0	2	1	1	1
GCF_003703085.1	3	1	1	2	1	1	1	2	-1	0	-1	-1	-1	1	1	-1
GCF_003703175.1	3	1	1	1	1	1	2	2	-1	2	1	1	-1	2	2	1
GCF_003703335.1	3	1	1	2	1	1	2	3	1	1	-1	1	1	1	1	2
GCF_005937945.1	3	1	1	3	2	2	2	2	1	1	1	1	1	1	1	1
GCF_005937945.2	3	1	1	3	2	2	2	2	1	1	1	1	1	1	1	1
GCF_007352665.1	5	1	1	3	2	2	2	4	1	2	0	1	1	1	1	1
GCF_008502015.1	5	1	1	4	2	1	2	4	2	2	0	1	1	1	1	1
GCF_013911125.1	3	1	1	3	1	1	1	2	2	1	0	1	1	1	1	1
GCF_014652995.1	3	1	1	1	1	1	1	2	2	1	1	1	-1	1	1	2
GCF_014653015.1	3	1	1	1	1	1	2	2	1	1	-1	1	1	1	1	2
GCF_014653035.1	3	1	1	1	1	1	1	2	2	1	1	1	-1	1	1	1
GCF_014855475.1	3	1	2	2	1	1	1	2	2	0	-1	-1	-1	1	1	1
GCF_016307865.1	3	1	2	2	-1	-1	1	2	1	3	2	3	-1	1	1	1
GCF_016308165.1	3	1	2	2	-1	-1	1	2	1	3	2	2	-1	1	1	1
GCF_017009525.1	2	1	1	1	2	1	1	1	2	3	2	1	1	1	1	1
GCF_017009545.1	2	1	1	1	2	1	1	1	2	3	2	1	-1	1	1	1
GCF_017140835.1	3	1	1	1	1	1	1	2	1	2	2	1	1	1	1	1
GCF_017140875.1	3	1	1	3	2	2	2	2	1	1	1	1	1	1	1	1
GCF_900235815.1	3	1	1	1	0	0	1	2	2	5	4	1	-1	1	1	1
GCF_900235885.1	3	1	1	1	-1	-1	2	2	2	2	4	-1	-1	1	1	1

GCF_900289125.1	3	1	1	1	0	0	1	2	2	4	3	1	-1	1	1	1
GCF_900289135.1	3	1	1	1	-1	-1	1	2	1	-1	-1	-1	-1	1	1	1
savastanoi_savastanoiASM146711v1	3	1	0	0	-1	-1	1	2	-1	0	-1	-1	-1	1	1	-1

Supplementary table S7
Gene Set enrichment analysis (GSEA) analysis using KEGG annotations for strain Pss B728a. In the context of hydrogen peroxide effects (treatments "h2o2effectsat21C" and "h2o2effectsat28C"), a positive enrichment score indicates that most genes of this pathway were activated, whilst a negative value indicates that they were suppressed. In the context of temperature effects (treatments "temperatureeffectsinwater" and "temperatureeffectsin80mMh2o2"), a positive value indicates that most genes belonging to this group were more expressed at 28 than at 21°C and vice versa for negative values. Only KEGG categories with P-values below 0.05 are shown. R package ClusterProfiler was used to perform this analysis with default settings on KEGG gene sets with more than 3 genes (Yu et al., 2012).

KEGG ID	Description	Enrichment Score	P-value	Treatment
psb03010	Ribosome	-0.594	1.55E-09	temperatureeffectsinwater
psb00920	Sulfur metabolism	0.726	5.83E-07	temperatureeffectsinwater
psb02010	ABC transporters	0.463	0.00016255	temperatureeffectsinwater
psb00670	One carbon pool by folate	0.905	0.002139759	temperatureeffectsinwater
psb01230	Biosynthesis of amino acids	-0.346	0.005247399	temperatureeffectsinwater
psb00260	Glycine, serine and threonine metabolism	0.549	0.008049055	temperatureeffectsinwater
psb00190	Oxidative phosphorylation	-0.490	0.008208772	temperatureeffectsinwater
psb01110	Biosynthesis of secondary metabolites	-0.247	0.025304032	temperatureeffectsinwater
psb04626	Plant-pathogen interaction	-0.804	0.025660308	temperatureeffectsinwater
psb03018	RNA degradation	-0.594	0.027519213	temperatureeffectsinwater
psb01200	Carbon metabolism	-0.384	0.031263636	temperatureeffectsinwater
psb03060	Protein export	-0.529	0.041920554	temperatureeffectsinwater
psb03010	Ribosome	-0.593	1.00E-10	temperatureeffectsin80mMh2O2

psb01110	Biosynthesis of secondary metabolites	-0.308	4.44E-09	temperatureeffectsin80mMh2O2
psb00920	Sulfur metabolism	0.615	1.19E-06	temperatureeffectsin80mMh2O2
psb01230	Biosynthesis of amino acids	-0.342	1.71E-05	temperatureeffectsin80mMh2O2
psb01100	Metabolic pathways	-0.170	0.001384278	temperatureeffectsin80mMh2O2
psb00230	Purine metabolism	-0.361	0.002292003	temperatureeffectsin80mMh2O2
psb01240	Biosynthesis of cofactors	-0.272	0.002486477	temperatureeffectsin80mMh2O2
psb01200	Carbon metabolism	-0.302	0.003348012	temperatureeffectsin80mMh2O2
psb03070	Bacterial secretion system	-0.438	0.004370404	temperatureeffectsin80mMh2O2
psb01232	Nucleotide metabolism	-0.367	0.007992847	temperatureeffectsin80mMh2O2
psb03060	Protein export	-0.539	0.009531539	temperatureeffectsin80mMh2O2
psb04626	Plant-pathogen interaction	-0.634	0.010094585	temperatureeffectsin80mMh2O2
psb00240	Pyrimidine metabolism	-0.396	0.012823 88	temperatureeffectsin80mMh2O2
psb00540	Lipopolysaccharide biosynthesis	-0.452	0.014868526	temperatureeffectsin80mMh2O2
psb00020	Citrate cycle (TCA cycle)	-0.509	0.015885744	temperatureeffectsin80mMh2O2
psb00010	Glycolysis / Gluconeogenesis	-0.415	0.018797915	temperatureeffectsin80mMh2O2
psb00030	Pentose phosphate pathway	-0.409	0.020810202	temperatureeffectsin80mMh2O2
psb00770	Pantothenate and CoA biosynthesis	-0.455	0.022887806	temperatureeffectsin80mMh2O2
psb00400	Phenylalanine, tyrosine and tryptophan biosynthesis	-0.427	0.026027134	temperatureeffectsin80mMh2O2
psb00550	Peptidoglycan biosynthesis	-0.459	0.029813063	temperatureeffectsin80mMh2O2
psb00310	Lysine degradation	0.606	0.032514454	temperatureeffectsin80mMh2O2
psb00970	Aminoacyl-tRNA biosynthesis	-0.382	0.035123513	temperatureeffectsin80mMh2O2
psb00270	Cysteine and methionine metabolism	-0.333	0.038522822	temperatureeffectsin80mMh2O2
psb03018	RNA degradation	-0.462	0.045837449	temperatureeffectsin80mMh2O2

psb00280	Valine, leucine and isoleucine degradation	0.566	0.046712803	temperatureeffectsin80mMh2O2
psb01100	Metabolic pathways	0.316	1.00E-10	h2o2effectsat21C
psb01120	Microbial metabolism in diverse environments	0.418	2.52E-08	h2o2effectsat21C
psb01200	Carbon metabolism	0.477	8.17E-07	h2o2effectsat21C
psb00920	Sulfur metabolism	0.694	4.29E-06	h2o2effectsat21C
psb01110	Biosynthesis of secondary metabolites	0.309	5.00E-06	h2o2effectsat21C
psb01230	Biosynthesis of amino acids	0.395	0.000264019	h2o2effectsat21C
psb00380	Tryptophan metabolism	0.685	0.000278673	h2o2effectsat21C
psb00310	Lysine degradation	0.625	0.00047089	h2o2effectsat21C
psb00280	Valine, leucine and isoleucine degradation	0.582	0.000499932	h2o2effectsat21C
psb00620	Pyruvate metabolism	0.532	0.000596977	h2o2effectsat21C
psb00260	Glycine, serine and threonine metabolism	0.474	0.001967613	h2o2effectsat21C
psb00640	Propanoate metabolism	0.575	0.002006151	h2o2effectsat21C
psb01210	2-Oxocarboxylic acid metabolism	0.512	0.002372815	h2o2effectsat21C
psb00650	Butanoate metabolism	0.537	0.002474917	h2o2effectsat21C
psb00020	Citrate cycle (TCA cycle)	0.547	0.003924565	h2o2effectsat21C
psb00630	Glyoxylate and dicarboxylate metabolism	0.500	0.004673109	h2o2effectsat21C
psb00625	Chloroalkane and chloroalkene degradation	0.723	0.006159116	h2o2effectsat21C
psb00250	Alanine, aspartate and glutamate metabolism	0.474	0.009392371	h2o2effectsat21C
psb00730	Thiamine metabolism	0.878	0.009618211	h2o2effectsat21C
psb00071	Fatty acid degradation	0.588	0.013337799	h2o2effectsat21C
psb00970	Aminoacyl-tRNA biosynthesis	0.461	0.013956777	h2o2effectsat21C
psb01212	Fatty acid metabolism	0.480	0.015206458	h2o2effectsat21C

psb02040	Flagellar assembly	0.375	0.018129067	h2o2effectsat21C
psb00270	Cysteine and methionine metabolism	0.447	0.018524664	h2o2effectsat21C
psb00350	Tyrosine metabolism	0.624	0.020431814	h2o2effectsat21C
psb00330	Arginine and proline metabolism	0.498	0.02134818	h2o2effectsat21C
psb00785	Lipoic acid metabolism	0.541	0.027449409	h2o2effectsat21C
psb00480	Glutathione metabolism	0.519	0.035966695	h2o2effectsat21C
psb00010	Glycolysis / Gluconeogenesis	0.419	0.042405548	h2o2effectsat21C
psb02010	ABC transporters	0.270	0.044994324	h2o2effectsat21C
psb00543	Exopolysaccharide biosynthesis	0.650	0.046440372	h2o2effectsat21C
psb02040	Flagellar assembly	0.571	3.38E-05	h2o2effectsat28C
psb00920	Sulfur metabolism	0.642	5.93E-05	h2o2effectsat28C
psb00280	Valine, leucine and isoleucine degradation	0.640	6.19E-05	h2o2effectsat28C
psb00310	Lysine degradation	0.590	0.000679905	h2o2effectsat28C
psb01120	Microbial metabolism in diverse environments	0.339	0.000782237	h2o2effectsat28C
psb00380	Tryptophan metabolism	0.647	0.001986017	h2o2effectsat28C
psb03070	Bacterial secretion system	-0.473	0.002382138	h2o2effectsat28C
psb01100	Metabolic pathways	0.244	0.003652725	h2o2effectsat28C
psb00071	Fatty acid degradation	0.624	0.006286057	h2o2effectsat28C
psb00640	Propanoate metabolism	0.535	0.011355651	h2o2effectsat28C
psb00290	Valine, leucine and isoleucine biosynthesis	0.670	0.017170308	h2o2effectsat28C
psb00630	Glyoxylate and dicarboxylate metabolism	0.444	0.019499123	h2o2effectsat28C
psb00650	Butanoate metabolism	0.492	0.028671944	h2o2effectsat28C
psb01200	Carbon metabolism	0.335	0.039455782	h2o2effectsat28C

psb00625	Chloroalkane and chloroalkene degradation	0.631	0.049822064	h2o2effectsat28C
psb00540	Lipopolysaccharide biosynthesis	-0.458	0.049861814	h2o2effectsat28C

Supplementary table S8
Gene Set enrichment analysis (GSEA) analysis using KEGG annotations for Pspph strain 1448A (representative for 1302A). In the context of hydrogen peroxide effects (treatments "h2o2effectsat21C" and "h2o2effectsat28C"), a positive enrichment score indicates that most genes of this pathway were activated, whilst a negative value indicates that they were suppressed. In the context of temperature effects (treatments "temperatureeffectsinwater" and "temperatureeffectsin20mMh2o2"), a positive value indicates that most genes belonging to this group were more expressed at 28 than at 21°C and vice versa for negative values. Only KEGG categories with P-values below 0.05 are shown. R package ClusterProfiler was used to perform this analysis with default settings on KEGG gene sets with more than 3 genes (Yu et al., 2012).

KEGG ID	Description	Enrichment Score	P-value	Treatment
psp02030	Bacterial chemotaxis	0.586	1.84E-06	temperatureeffectsinwater
psp02020	Two-component system	0.354	0.00074215	temperatureeffectsinwater
psp03010	Ribosome	-0.469	0.001538521	temperatureeffectsinwater
psp01100	Metabolic pathways	-0.242	0.001705709	temperatureeffectsinwater
psp02025	Biofilm formation	0.439	0.009895692	temperatureeffectsinwater
psp01110	Biosynthesis of secondary metabolites	-0.276	0.011634236	temperatureeffectsinwater
psp04626	Plant-pathogen interaction	0.560	0.017480569	temperatureeffectsinwater
psp00260	Glycine, serine and threonine metabolism	-0.442	0.018733254	temperatureeffectsinwater
psp00970	Aminoacyl-tRNA biosynthesis	0.714	0.029472598	temperatureeffectsinwater
psp00340	Histidine metabolism	-0.539	0.031519912	temperatureeffectsinwater
psp00330	Arginine and proline metabolism	-0.484	0.042687588	temperatureeffectsinwater
psp01200	Carbon metabolism	-0.332	0.044217687	temperatureeffectsinwater
psp00500	Starch and sucrose metabolism	-0.576	0.049335863	temperatureeffectsinwater

psp01110	Biosynthesis of secondary metabolites	-0.428	1.26E-05	temperatureeffectsin20mMh2O2
psp01230	Biosynthesis of amino acids	-0.506	0.000151858	temperatureeffectsin20mMh2O2
psp01100	Metabolic pathways	-0.307	0.000259329	temperatureeffectsin20mMh2O2
psp00500	Starch and sucrose metabolism	-0.716	0.002018178	temperatureeffectsin20mMh2O2
psp02040	Flagellar assembly	0.502	0.014836148	temperatureeffectsin20mMh2O2
psp00270	Cysteine and methionine metabolism	-0.599	0.016020989	temperatureeffectsin20mMh2O2
psp00010	Glycolysis / Gluconeogenesis	-0.552	0.024157135	temperatureeffectsin20mMh2O2
psp00330	Arginine and proline metabolism	-0.644	0.025651727	temperatureeffectsin20mMh2O2
psp03010	Ribosome	-0.546	0.026410958	temperatureeffectsin20mMh2O2
psp02030	Bacterial chemotaxis	0.450	0.042662116	temperatureeffectsin20mMh2O2
psp01100	Metabolic pathways	0.391	1.00E-10	h2o2effectsat21C
psp01120	Microbial metabolism in diverse environments	0.458	8.49E-10	h2o2effectsat21C
psp00920	Sulfur metabolism	0.713	1.86E-07	h2o2effectsat21C
psp01200	Carbon metabolism	0.490	2.34E-06	h2o2effectsat21C
psp01110	Biosynthesis of secondary metabolites	0.338	9.72E-06	h2o2effectsat21C
psp00260	Glycine, serine and threonine metabolism	0.588	3.09E-05	h2o2effectsat21C
psp00630	Glyoxylate and dicarboxylate metabolism	0.592	4.87E-05	h2o2effectsat21C
psp00310	Lysine degradation	0.710	5.36E-05	h2o2effectsat21C
psp00280	Valine, leucine and isoleucine degradation	0.636	0.000194651	h2o2effectsat21C
psp00380	Tryptophan metabolism	0.725	0.000229181	h2o2effectsat21C
psp00650	Butanoate metabolism	0.620	0.000308885	h2o2effectsat21C
psp00250	Alanine, aspartate and glutamate metabolism	0.602	0.000664851	h2o2effectsat21C
psp02010	ABC transporters	0.361	0.00092198	h2o2effectsat21C

psp01230	Biosynthesis of amino acids	0.408	0.000988544	h2o2effectsat21C
psp00620	Pyruvate metabolism	0.507	0.001759078	h2o2effectsat21C
psp00330	Arginine and proline metabolism	0.587	0.001789096	h2o2effectsat21C
psp01210	2-Oxocarboxylic acid metabolism	0.553	0.002351226	h2o2effectsat21C
psp00020	Citrate cycle (TCA cycle)	0.567	0.003847375	h2o2effectsat21C
psp00360	Phenylalanine metabolism	0.791	0.00883544	h2o2effectsat21C
psp00660	C5-Branched dibasic acid metabolism	0.841	0.010115317	h2o2effectsat21C
psp00040	Pentose and glucuronate interconversions	0.819	0.015985173	h2o2effectsat21C
psp00350	Tyrosine metabolism	0.668	0.017737071	h2o2effectsat21C
psp00643	Styrene degradation	0.812	0.018778617	h2o2effectsat21C
psp00340	Histidine metabolism	0.604	0.019252098	h2o2effectsat21C
psp00640	Propanoate metabolism	0.496	0.019520253	h2o2effectsat21C
psp00290	Valine, leucine and isoleucine biosynthesis	0.644	0.026682537	h2o2effectsat21C
psp00410	beta-Alanine metabolism	0.675	0.027215459	h2o2effectsat21C
psp00625	Chloroalkane and chloroalkene degradation	0.680	0.031733201	h2o2effectsat21C
psp00785	Lipoic acid metabolism	0.576	0.032786928	h2o2effectsat21C
psp00362	Benzoate degradation	0.598	0.033708795	h2o2effectsat21C
psp00071	Fatty acid degradation	0.590	0.03967481	h2o2effectsat21C
psp01100	Metabolic pathways	0.304	5.18E-07	h2o2effectsat28C
psp00920	Sulfur metabolism	0.644	9.42E-06	h2o2effectsat28C
psp00260	Glycine, serine and threonine metabolism	0.588	4.06E-05	h2o2effectsat28C
psp00630	Glyoxylate and dicarboxylate metabolism	0.605	0.000228815	h2o2effectsat28C
psp01120	Microbial metabolism in diverse environments	0.365	0.000286372	h2o2effectsat28C

psp02040	Flagellar assembly	0.489	0.000994577	h2o2effectsat28C
psp01200	Carbon metabolism	0.424	0.001115215	h2o2effectsat28C
psp00380	Tryptophan metabolism	0.667	0.00125534	h2o2effectsat28C
psp00310	Lysine degradation	0.600	0.002521368	h2o2effectsat28C
psp00280	Valine, leucine and isoleucine degradation	0.582	0.00379278	h2o2effectsat28C
psp00250	Alanine, aspartate and glutamate metabolism	0.563	0.007238673	h2o2effectsat28C
psp00330	Arginine and proline metabolism	0.535	0.011121912	h2o2effectsat28C
psp00650	Butanoate metabolism	0.564	0.011626572	h2o2effectsat28C
psp00625	Chloroalkane and chloroalkene degradation	0.700	0.021851259	h2o2effectsat28C
psp00660	C5-Branched dibasic acid metabolism	0.858	0.024594979	h2o2effectsat28C
psp00640	Propanoate metabolism	0.559	0.025665353	h2o2effectsat28C
psp00020	Citrate cycle (TCA cycle)	0.552	0.029291781	h2o2effectsat28C
psp01110	Biosynthesis of secondary metabolites	0.263	0.034709981	h2o2effectsat28C
psp00643	Styrene degradation	0.719	0.038844177	h2o2effectsat28C
psp02010	ABC transporters	0.291	0.040787623	h2o2effectsat28C
psp02030	Bacterial chemotaxis	0.369	0.045676998	h2o2effectsat28C
psp00620	Pyruvate metabolism	0.415	0.047619048	h2o2effectsat28C
psp00670	One carbon pool by folate	0.563	0.048956075	h2o2effectsat28C

[1] Aguilera, S. et al. Functional Characterization of the Gene Cluster from Pseudomonas syringae pv. phaseolicola NPS3121 Involved in Synthesis of Phaseolotoxin. Journal of Bacteriology 189, 2834-2843, doi:10.1128/jb.01845-06 (2007).

Appendix

RB-TnSeq Optimisation

Introduction

Having identified a cross-talk between temperature and oxidative stress responses in bacterial phytopathogens Pspph and Pss, we were interested in determining the genetic mechanisms underlying this phenomenon. Typically, single gene mutants are constructed and phenotyped. However, temperature is an understudied environmental factor and there were very few published results to choose candidate genes in Pspph. We were interested in conducting a TnSeq screen instead, which would allow bulk screening of almost all genes in the Pspph genome at the same time and give us candidate genes. Furthermore, this screen would complement the transcriptomic screen results described in this thesis in chapter 4.

Background

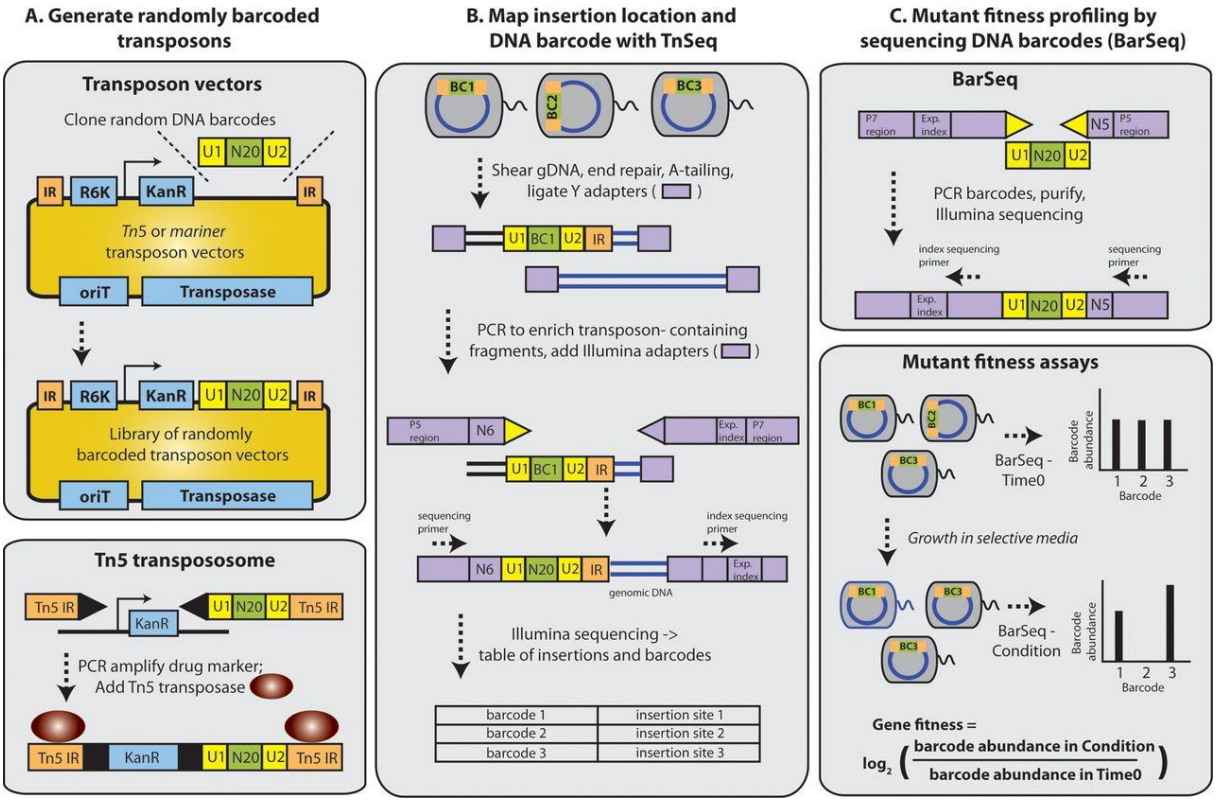
TnSeq is an emerging technique in the field of bacteriology (Cain et al., 2020). Also referred to as InSeq (Insertion Sequence) or RB-TnSeq (Randomly Barcoded TnSeq), it is essentially a method for bulk transposon mutagenesis. A library of a pool of mutants covering each gene of a bacterial genome at least once is generated, and in the case of RB-Tnseq, each mutant has a specific random sequence of nucleotides (a 'barcode') which allows easer tracking of mutant fitness (appendix figure A[1]). The abundance of each barcode before and after the library is challenged (for instance by exogenous application of hydrogen peroxide) is used as a proxy for gene fitness.

This technique has a few caveats:

i) As with all mutagenesis, some genes are essential and cultivable bacteria cannot be retrieved when the gene is inactivated by transposon insertion. Therefore, each library does not contain mutants for every single gene in the genome.

ii) Genetic redundancy between genes can hide gene involvement in fitness, as each mutant only contains a single transposon insertion.

iii) Social interactions between bacteria can hide gene involvement in fitness during mutant screens, as bacteria that carry a functional gene for a trait may be able to support the growth of mutants that lack a trait.



Appendix figure A1: Pipeline for RB-TnSeq (reproduced from Wetmore et al., 2015)
Overview of RB-TnSeq. (A) (Top) Tn5 or mariner transposon delivery vectors introduced into RB-TnSeq vectors by cloning millions of unique DNA bar codes (N20) flanked by common PCR priming sites (U1 and U2) near the edge of the transposon's inverted repeat (IR). (A) (Bottom) Generation of the mar or Tn5

barcoded transposome by attaching the kanamycin resistance gene to the random DNA bar code region and Tn5 transposase. The goal is to generate a large transposon mutant population such that each strain contains a unique DNA bar code. (B) The resulting randomly bar-coded transposon mutant library is purified and sequenced. Both the DNA bar code and the transposon insertion site are identified in a single 150-nucleotide Illumina sequencing read. The TnSeq results are a table of bar codes and associated transposon insertion locations. (C) (Top) Once the TnSeq results are established, the barcode sequence alone can be sequenced (BarSeq). Furthermore, the barcode sequence contains an experiment index and enables multiplexing of multiple experiments on a single lane of Illumina sequencing. (C) (Bottom) Competitive mutant fitness assays are performed by comparing the abundance of the DNA bar codes with BarSeq before (time zero) and after (condition) selective growth.

Wetmore et al (2015) first established two barcode vector libraries in *E. coli*, one using Tn5, and the other using mariner as the transposon. This *E. coli* vector strain was chosen to be DAP-auxotrophic, allowing for easy negative selection. They then showed proof of concept by using this library to make multiple RB-TnSeq library of various bacterial strains, including *E. coli* and *Pseudomonas stutzeri*. Their protocol was adapted and RB-TnSeq was recently successfully established in Pss B728a by Tyler Helmann (Helmann et al., 2019), and so it seemed likely that building a TnSeq library of Pspph would also be possible.

Having observed that temperature and oxidative stress response form a cross-talk in Pspph and Pss (as described in chapter 3 of this thesis), we hoped to identify candidate genes that may be responsible for this. The TnSeq screen was an attractive experimental strategy to do this that would complement the RNAseq data in Chapter 4, as transcriptomic screens do not capture post-transcriptional regulation effects. Here I describe progress made towards creation of a Tnseq library for Pspph 1302A, including the protocol developed and preliminary results.

Protocol

This protocol was adapted from Tyler Helmann (personal communication).

1) Library preparation

i) Day 1-3: Culture preparations

Streak Luria's Broth-agar (LBA) plates containing 50µg/mL nitrofurantoin with Pspph 1302A from glycerol stock. Incubate for 2 days at 28°C.

Pick 3 Pspph colonies and inoculate 100 ml sterile LB. Distribute this inoculum between 12 50ml falcon tubes, and incubate at 28°C for ca. 24h. On the same day, make a fresh solution of 60 mM diaminopimelic acid (DAP) and filter-sterilise it. Make up 25 ml LB supplemented with final concentration 300µM DAP and 50µg/ml kanamycin. Inoculate with a whole frozen aliquot of the *E. coli mariner* barcoded library (Wetmore et al., 2015). Transfer to a 250ml flat-bottom flask and incubate at 37°C for ca. 12h.

ii) Day 4: Conjugation

Pool the Pspph 1302A cultures together and measure the OD_{600} using a spectrophotometer (100 µl is sampled and discarded to prevent contamination). The OD_{600} of the *E. coli* culture is also measured. Use these values to calculate how much *E. coli* culture needs to be used to achieve the desired ratio of 1:3 (*E. coli*:Pspph) when using the entirety of Pspph culture available. Before mixing, the cultures are cleaned up separately: the cultures are split into 5-10 ml aliquots and spun down in a centrifuge set at room temperature, at 2000xg rcf for 5 min. The supernatant is discarded, and each pellet is resuspended in 20 ml warm LB kept at 50°C. These centrifugation and resuspension steps are repeated another 2 times, before the cells are mixed in 1:3 ratio. The conjugation mix is then centrifuged at room temperature at 2000xg rcf, for 5min. The supernatant is carefully discarded and the pellet is resuspended in 10-12 ml warm LB by gentle pipetting. This dense conjugation mix is then plated on 50 conjugation plates containing LBA with 300 µM DAP (no antibiotics): 8 spots per plate or ca. 25 µl conjugation mix per conjugation spot. The plates were left to dry completely at room temperature under a flow hood (ca. 30 min) and they were then incubated at 28°C overnight.

iii) Day 5-6: Selection

Scrape up the conjugation spots and resuspend in 200 µl PBS per plate (so a total of 10ml PBS is added). 200ul of this mixture is then spread on each selection plate – LBA with 50µg/ml kanamycin (no DAP), on a total of 200 square 120mmx120mm plates, using sterile glass beads. The plates are allowed to completely dry (ca. 30min) before they are transferred to an incubator and incubated at 28°C for 2 days.

iv) Day 7: Colony count

Plates are examined for number of colonies per 1 cm^2, to estimate the overall number of recombinants observed. If the predicted number is over 220,000 colonies, we can expect that there is at least 1 mutant for each gene in the genome, and the library is then saved. Scrape up all the colonies off the plates and transfer them to 200ml LB containing 50µg/ml kanamycin (no DAP). We measure the OD_{600} and adjust the OD to ca. 0.2 by adding LB-kanamycin if necessary. The culture is transferred to a flat-bottom 1L flask and incubated at 28°C, 300rpm until it reaches OD_{600}>1. An appropriate amount of glycerol is added to reach 25% glycerol content, and the mixture is thoroughly mixed. It is then aliquoted into 1 ml portions in safelock Eppendorf tubes which are then flash-frozen in liquid nitrogen and stored at -80°C.

2) Library sequencing

i) DNA purification

Dethaw an aliquot of the library generated above and centrifuge at 3000xg at room temperature for 3 min. Discard the supernatant. Isolate genomic DNA with the DNeasy kit (Qiagen) using the manufacturer's instructions:

Resuspend the cell pellet in 180ul DNEasy kit Buffer ATL. Add 20 ul proteinase K to each tube, mix by vortexing for at least 5s and incubate at 56°C for 10 min. Vortex occasionally and place in a shaking

thermomixer. Once the 10 minutes are over, vortex continuously for 15s and add 200ul buffer AL to the sample. Vortex for 5s. Add 200ul pure ethanol and vortex immediately for 5-10s. Pipet the mixture into a DNeasy mini spin column placed in a 2ml collection tube. Centrifuge at > 6000xg for 1 min. Discard flow through and collection tube. Place the mini spin column in a new 2ml collection tube, add 500ul buffer AW1. Centrifuge for 1 min at > 6000 xg. Discard flow through and collection tube. Place the mini spin column in a new 2ml collection tube, add 500ul buffer AW2. Centrifuge for 3min at 20 000 xg to dry the DNEAsy membrane. Discard flow through and collection tube. Place the mini spin column in a clean tube and add 200 ul buffer 50°C sterile milliQ. Incubate at room temperature for 3 min. Centrifuge for 1 min at 6000 x g. The eluate contains the DNA of interest.

ii) Prepare “Splinkerette” Adapter.

Resuspend primers oAD570 and oAD571 to a concentration of 100µM in 1X TE buffer.

oAD570: /5Phos/G*ATCGGAAGAGCACACGTCTGGGttttttttttcaaaaaaa*a

oAD571: G*AGATCGGTCTCGGCATTCCCAGACGTGTGCTCTTCCGATC*T

Mix 5 µl of each in a PCR tube and run the following thermocycler program:

Heated lid ON.

Step type	Temperature	Time
Hold	37˚C	Preheat block
Hold	37˚C	30 min
Ramp to 97˚C	+0.5˚C / second	-
Hold	97.5˚C	2:35

Gradient	-0.1˚C / second	-
Hold	4˚C	-

Dilute 10 µl prepared primer mix to 15 µM by adding 23.5 µl 1X TE buffer pH8. Prepared adapter can be stored at -20˚C.

iii) Fragmentation

Bring 500 ng purified genomic DNA to a total volume of 26 µl by adding 1X TE buffer. Place all components on ice. Add the following components to a 0.2 ml PCR tube:

DNA (500ng)	26 µl
NEBNext Ultra II FS buffer	7 µl
NEBNext Ultra II FS enzyme mix	2 µl
Total	35 µl

Vortex the reaction for 5 seconds and briefly spin down. Place in thermocycler and run the following program:

Heated lid set to 75˚C.

Step type	Temperature	Time
Hold	37˚C	Preheat block
Hold	37˚C	12 min
Hold	65˚C	30 min

Hold	4˚C	Inf

iv) Adapter Ligation.

As soon as the fragmentation step is over, add the following components directly to the fragmentation mixture:

FS reaction mixture (previous step)	35µl
NEBNext Ultra II Ligation MM	30µl
NEBNext Ligation Enhancer	1µl
15µM “Splinkerette” Adapter	2.5µl
Total	68.5µl

Set a 100 or 200 µl pipette to 50 µl and pipette gently up and down at least 10 times to mix the ligation reaction. Incubate at 20˚C on a thermocycler for 15 minutes with the heated lid off.

v) Clean-up and Size Selection with AMPure XP Beads.

Bring the total volume to 100 µl by adding 31.5 µl 1X TE buffer. Add 40 µl AMPure XP Beads, mix well by pipetting up and down 10 times. Incubate 5 minutes at room temperature. Place tube on magnetic stand to separate beads from supernatant, for ca. 5 minutes. Transfer the supernatant (~140 µl) containing the DNA to a new tube. Discard the beads that contain large unwanted DNA fragments. Add 20 µl AMPure XP Beads, mix well by pipetting up and down at least 10 times. Incubate 5 minutes at room temperature. Place tube on magnetic stand to separate beads from supernatant for ca. 5 minutes.

Remove and discard the supernatant, containing small unwanted DNA fragments. Add 200µl freshly prepared 80% ethanol to the tube while on the magnetic stand. Incubate at room temperature for 30 seconds, then carefully remove and discard the supernatant. Repeat the ethanol wash step for a total of two washes. Remove all visible liquid using a P10 pipette tip. Air dry the beads for up to 5 minutes while the tube is on the magnetic stand with the lid open. Remove the tube from the magnetic stand. Elute the DNA targets by adding 17µl 0.1X TE (diluted in milliQ H_2O), mix well, and incubate for 2 minutes at room temperature. Place the tube on the magnetic stand. After 5 minutes or when solution is clear, transfer 15 µl to a new tube.

vi) First round of PCR Enrichment of Adapter-Ligated DNA

Add the following components to a 0.2ml PCR tube:

Adapter Ligated DNA fragments	15µl
NEBNext Ultra II Q5 master mix	25µl
Premixed primers oAD454+oAD493	10µl
Total volume	50µl

Run the following thermocycler program:

Heated lid ON.

Step type	Temperature	Time
Hold 0	98˚C	Preheat block
Hold 1	98˚C	45 sec

Hold 2	98˚C	15 sec
Hold 3	60˚C	30 sec
Hold 4	72˚C	30 sec
Repeat steps 2-4		15 cycles
Hold	72˚C	60 sec
Hold	4˚C	Inf.

vii) Cleanup with AMPure XP Beads.

In a 0.2 ml PCR tube, add 45 µl (0.9X) AMPure XP Beads to the PCR product, mix well by pipetting up and down 10 times. Incubate 5 minutes at room temperature. Place tube on magnetic stand to separate beads from supernatant, approximately 5 minutes. Remove and discard the supernatant. Add 200 µl freshly prepared 80% ethanol to the tube while on the magnetic stand. Incubate at room temperature for 30 seconds, then carefully remove and discard the supernatant. Repeat the ethanol wash step for a total of two washes. Remove all visible liquid using a P10 pipette tip. Air dry the beads for up to 5 minutes while the tube is on the magnetic stand with the lid open. Remove the tube from the magnetic stand. Elute the DNA targets by adding 17 µl 0.1X TE (diluted in milliQ H_2O), mix well, and incubate for 2 minutes at room temperature. Place the tube on the magnetic stand. After 5 minutes, transfer 15 µl to a new tube.

viii) Second round of PCR Enrichment of Adapter-Ligated DNA

Add the following components to a 0.2 ml PCR tube:

Purified DNA 15 µl

5X Q5 Buffer	10 µl
10mM dNTPs	1 µl
dH2O	13.5 µl
Premixed primers oAD492+oAD572	10 µl
Q5 DNA polymerase	0.5 µl
Total volume	50 µl

Run the following thermocycler program on this mixture:

Heated lid ON.

Step type	Temperature	Time
Hold 0	98˚C	Preheat block
Hold 1	98˚C	45 sec
Hold 2	98˚C	15 sec
Hold 3	55˚C	30 sec
Hold 4	72˚C	30 sec
Repeat steps 2-4		8 cycles
Hold	72˚C	60 sec
Hold	4˚C	Inf.

ix) Cleanup with AMPure XP Beads.

Add 45 µl (0.9X) AMPure XP Beads to the PCR product, mix well by pipetting up and down 10 times. Incubate 5 minutes at room temperature. Place tube on magnetic stand to separate beads from supernatant for ca. 5 minutes. Remove and discard the supernatant. Add 200 µl freshly prepared 80% ethanol to the tube while on the magnetic stand. Incubate at room temperature for 30 seconds, then carefully remove and discard the supernatant. Repeat the ethanol wash step for a total of two washes. Remove all visible liquid using a P10 pipette tip. Air dry the beads for up to 5 minutes while the tube is on the magnetic stand with the lid open. Remove the tube from the magnetic stand. Elute the DNA targets by adding 33 µl 0.1X TE (diluted in milliQ H_2O), mix well, and incubate for 2 minutes at room temperature. Place the tube on the magnetic stand. After 5 minutes (or when solution is clear), transfer 30 µl to a new tube.

x) DNA quantification

Quantify genomic DNA with a Qubit dsDNA assay kit (Qiagen) according to the manufacturer's instructions, and independently with a DNA1000 chip on an Agilent Bioanalyser. At least 200ng DNA were needed for sequencing and fragment size should be clustering around 150 bp.

xi) Sequencing

Sequencing was performed by Novogene, on a NovaSeq pair-ended PE150 (but only the forward strand reads were used for data analysis purposes).

3) Data analysis

Mapping reads to the Pspph target genome and assigning barcodes to each gene mutation can be achieved by following the custom pipeline built by Tyler Helmann, which can be found here: https://github.com/tylerhelmann/dickeya-barseq-2021/blob/main/lib_mapping.md. We also used this pipeline to determine whether the data was mapping on the *E. coli* donor.

Optimisation and discussion

We attempted conjugation a total of 5 times, with varying levels of success. In order to optimise this process for Pspph, we tested different conjugation mix ratios. After adjusting both *E.coli* and Pspph cultures to OD = 2, we mixed them in these ratios (n=2 replicates / ratio):

- 2:1 (67 µl *E. coli* + 33 µl Pspph)
- 1:1 (50µl + 50 µl) – this is the ratio that Tyler Helmann used for Pss B728a
- 1:2 (33µl *E. coli* + 67 µl Pspph)
- 1:3 (25 µl + 75 µl)
- 1:4 (20 µl + 80 µl)

These were left to incubate and streaked on selection plates as described above. I attempted to count the number of colonies in a 1 cm^2 area for each selection plate, but bacterial growth covered most of the plate in all treatments, although to a slightly lesser extent in the 1:1 ratio treatment. At the time, I assumed this meant that conjugation was successful in all treatments except 1:1, and proceeded to use ratio 1:3. In hindsight, this was an indication that the selection agent was not sufficient to prevent *E. coli* breakthrough.

This was indeed, the case, as when I scaled up this test and followed the protocol described above until the end, sequencing revealed that the vast majority of the reads (>98.7%) mapped to the *E. coli* genome rather than the Pspph genome. This could be potentially due to external contamination of the medium, but the overwhelming amount of bacterial growth observed on selection plates containing kanamycin suggests that the donor *E. coli* (which is resistant to kanamycin unlike wild-type *E. coli*) is responsible. The *E. coli* should not have been able to grow on the selection plates, as the donor is DAP auxotrophic, and the plates consisted of LBA without DAP supplementation. We hypothesised that LB may contain trace amounts of DAP as it is not a minimal medium. To test whether our LBA medium contains enough

DAP to allow the *E. coli* donor library to grow, I streaked the *E. coli* library, as well as a new conjugation mix and Pspph 1302A alone on the following plates:

- LBA with kanamycin 50
- LBA with kanamycin 50 and nitrofurantoin 50
- LBA with kanamycin 100
- LBA with kanamycin 100 and nitrofurantoin 50
- KBA (minimal medium) with kanamycin 50

I found that while neither the *E. coli* library or Pspph 1302A fresh from glycerol stock grew alone on any of the plates listed above, the same large amount of bacterial growth forming a smear over the plate overnight appeared following streaking with conjugation mix. This smear is potentially indicative of breakthrough by the donor *E. coli*. This may mean that in the time it takes to make the conjugation mix (a day and a half approximately) the *E. coli* is reverting to DAP autotrophy or that it is obtaining DAP through other means (from Pspph perhaps).

We were not able to investigate this further due to time constraints, but in the future, including additional methods of selection against the donor library may be important. The levels of nitrofurantoin used here were not able to selectively remove *E. coli* from conjugation mixes, but a higher level may. Alternatively, we could consider using the *Pseudomonas*-specific CFC (Cetrimide, Fucidin and Cephalothin) antibiotic cocktail. Furthermore, we suspect that streaking plates with a lower volume of conjugate may help reduce crowding and therefore reduce plate-wide decay of selection agents (antibiotics). It is possible that *E. coli* simply outgrows Pspph, and considering Pss displays strong broad-spectrum antibacterial activity *in vitro* (Sinden et al., 1971), this is possibly why Pss conjugation was more successful. Considering Pspph antibacterial activity (through phaseolotoxin production) is restricted to temperatures below 28°C (Bender et al., 1999), it is possible that incubating conjugation mixes at 21°C instead of 28°C would benefit Pspph.

In the future, once the TnSeq library for 1302A is successfully established, we would first want to screen gene fitness using the same experimental setup as the transcriptomic screen described in chapter 4 of this thesis: growing bacteria *in vitro* in minimal medium at 21°C and 28°C and applying exogenous hydrogen peroxide or water. It would also be interesting to use the TnSeq library of both B728a and 1302A *in planta* during infection in plants growing at 21°C or 28°C. An advantage of TnSeq is that host plant contamination is not much of an issue thanks to the unique barcode sequences used. Furthermore, Tyler Helmann successfully used the B728a library *in planta*, in bean (Helmann et al., 2019).

Appendix references

BENDER, C. L., ALARCON-CHAIDEZ, F. & GROSS, D. C. 1999. Pseudomonas syringae phytotoxins: Mode of action, regulation, and biosynthesis by peptide and polyketide synthetases. Microbiology and Molecular Biology Reviews, 63, 266-+.
CAIN, A. K., BARQUIST, L., GOODMAN, A. L., PAULSEN, I. T., PARKHILL, J. & VAN OPIJNEN, T. 2020. A decade of advances in transposon-insertion sequencing. Nature Reviews Genetics, 21, 526-540.
HELMANN, T. C., DEUTSCHBAUER, A. M. & LINDOW, S. E. 2019. Genome-wide identification of Pseudomonas syringae genes required for fitness during colonization of the leaf surface and apoplast. Proceedings of the National Academy of Sciences of the United States of America, 116, 18900-18910.
SINDEN, S. L., DEVAY, J. E. & BACKMAN, P. A. 1971. PROPERTIES OF SYRINGOMYCIN, A WIDE SPECTRUM ANTIBIOTIC AND PHYTOTOXIN PRODUCED BY PSEUDOMONAS-SYRINGAE, AND ITS ROLE IN BACTERIAL CANKER DISEASE OF PEACH TREES. Physiological Plant Pathology, 1, 199-+.
WETMORE, K. M., PRICE, M. N., WATERS, R. J., LAMSON, J. S., HE, J., HOOVER, C. A., BLOW, M. J., BRISTOW, J., BUTLAND, G., ARKIN, A. P. & DEUTSCHBAUER, A. 2015. Rapid Quantification of Mutant Fitness in Diverse Bacteria by Sequencing Randomly Bar-Coded Transposons. Mbio, 6.